UNIVERSITY OF SOUTHAMPTON

FACULTY OF MEDICINE

Institute of Developmental Sciences

The Pharmacokinetics of Medical Countermeasures Against Nerve Agents

by

Stuart Jon Armstrong

Thesis for the degree of Doctor of Philosophy

November 2014

UNIVERSITY OF SOUTHAMPTON

ABSTRACT

FACULTY OF MEDICINE

Institute of Developmental Sciences

Thesis for the degree of Doctor of Philosophy

THE PHARMACOKINETICS OF MEDICAL COUNTERMEASURES AGAINST NERVE AGENTS

Stuart Jon Armstrong

Nerve agents are organophosphorus compounds that irreversibly inhibit acetylcholinesterase, causing accumulation of the neurotransmitter acetylcholine and this excess leads to an overstimulation of acetylcholine receptors. Inhalation exposure to nerve agent can be lethal in minutes and conversely, skin exposure may be lethal over longer durations. Medical Countermeasures (MedCM) are fielded in response to the threat posed by nerve agents. MedCM with improved efficacy are being developed but the efficacy of these cannot be tested in humans, so their effectiveness is proven in animals. It is UK Government policy that all MedCM are licensed for human use.

The aim of this study was to test the hypothesis that the efficacy of MedCM against nerve agent exposure by different routes could be better understood and rationalised through knowledge of the MedCM pharmacokinetics (PK). The PK of MedCM was determined in naïve and nerve agent poisoned guinea pigs. PK interactions between individual MedCM drugs when administered in combination were also investigated. *In silico* simulations to predict the concentration-time profiles of different administration regimens of the MedCM were completed using the PK parameters determined *in vivo*. These simulations were used to design subsequent *in vivo* PK studies and to explain or predict the efficacy or lack thereof for the MedCM.

The PK data generated in this study are the first such data in conscious guinea pigs, the small animal species of choice for determination of MedCM efficacy. These data show how PK can improve the understanding of MedCM efficacy. PK studies such as those reported here should be integrated into the development programmes of future MedCM.

Contents

List of tables

List of figures

List of accompanying materials

DECLARATION OF AUTHORSHIP

I, Stuart Jon Armstrong declare that this thesis and the work presented in it are my own and has been generated by me as the result of my own original research.

The Pharmacokinetics of Medical Countermeasures Against Nerve Agents:

1. This work was done wholly or mainly while in candidature for a research degree at this University;
2. Where any part of this thesis has previously been submitted for a degree or any other qualification at this University or any other institution, this has been clearly stated;
3. Where I have consulted the published work of others, this is always clearly attributed;
4. Where I have quoted from the work of others, the source is always given. With the exception of such quotations, this thesis is entirely my own work;
5. I have acknowledged all main sources of help;
6. Where the thesis is based on work done by myself jointly with others, I have made clear exactly what was done by others and what I have contributed myself;
7. Parts of this work have been published as:

    Mumford, H., Docx, C.J., Price, M.E., Green, A.C., Tattersall, J.E.H., Armstrong, S.J. *Chemico-Biological Interactions* 2013; 203(1): 160–166.

Signed:.....

Date:.....

Acknowledgements

The completion of this thesis has only been possible through the guidance of several people who have contributed their valuable assistance on many occasions. In particular, to my supervisors: Dr Chris Green, for his unselfish and unfailing support throughout the duration of my work, in his own time. Prof. Geraldine Clough, for the guidance and encouragement she has provided to me on every occasion.

For their practical advice and assistance, many thanks to Cerys Docx, Louise Thompsett, Vicky Wood, Kendra Cummins, Dr Matt Price, Helen Rice and Dr Belinda Farnfield.

Thanks also to May Irwin, a fantastic technician who ensured equipment was always prepared and within reach, exactly when required and who, without fail, throughout the time we worked together, provided a smile and friendly face.

My gratitude also goes to Janet Wetherell for ensuring that I had this opportunity to complete my postgraduate education.

I am grateful to all my colleagues who have supported me one way or another over the duration of my studies.

Last but by no means least my family, whom I cannot thank enough. In particular, my wife Nicola. Without her unstinting love, strength and support I would simply not have been able to complete my studies. Nicola amazes me, during the tenure of my studentship she has given me two healthy children, between which she overcame cancer.

Finally to my two boys, Luca and Noah, who were not even twinkles in my eye when I first started my studies. Their bright eyed smiles have revitalised me every day, I hope that I have made them as proud of me as I am of them.

Thank you.

1. INTRODUCTION

1.1 Background

The organophosphorus compounds, commonly known as nerve agents are designated as chemical warfare agents [1] and pose a significant risk to the UK and its Armed Forces [2]. It is therefore essential that the Military have an effective response to counter the threat posed by these compounds. Medical countermeasures (MedCM) are part of an integrated approach (which includes physical means of protection such as respirators and collective protection) to defend against nerve agent poisoning. In addition to saving lives, MedCM act as deterrents to aggressors and also have a positive impact on morale of the Military personnel.

Developing MedCM that are effective, practicable, acceptable and affordable is a challenge, as is their subsequent licensing for human use. Unlike the development of many other drugs by the mainstream pharmaceutical industry, there is no clinical population in which efficacy can be demonstrated. Although human volunteers have been exposed to nerve agents in both clinical and military trials in the past [3;4], it is not now considered ethical to expose people to nerve agent in order to prove the efficacy of MedCM. The extrapolation of efficacy from animal studies is therefore critical to the development of MedCM. The pharmacokinetics (PK) and pharmacodynamics (PD) of drugs are accepted as standard data for these purposes.

The PK or PD of MedCM have not been systematically determined in the animal species used to study efficacy, so they have not been considered in the interpretation of MedCM effectiveness. The lack of PK and PD data makes extrapolation of efficacious doses from animals to humans more difficult. The research detailed in this thesis investigated the PK of MedCM in guinea pigs, providing key data to aid the interpretation and extrapolation of efficacy data. The PK and PD of the nerve agents sarin and VX were also determined in guinea pigs, data which can also be used in the interpretation of MedCM efficacy. The project described here is part of a larger programme of work researching and developing MedCM against nerve agents.

The introduction of this thesis provides information on normal cholinergic function and how this is disrupted by nerve agents. The routes of exposure of the nerve agents are briefly discussed to highlight the challenges they pose for MedCM. The mechanisms of action of the MedCM are described, enabling the reader to understand later discussion of the impact of nerve agents on the body and how MedCM help to restore or protect function. Justification is provided for the use of the guinea pig as the animal species in which the studies reported here were carried out. Information on methods used as well as PK and PD parameters are provided. Finally, the aims of the studies and hypotheses tested are presented.

1.2 Normal cholinergic function

During normal function, cholinergic transmission is initiated by an action potential arriving at the synapse or neuromuscular junction (Figure 1.1). This action potential triggers the release of the neurotransmitter acetylcholine from vesicles through the terminal membrane by exocytosis into the synaptic cleft. The acetylcholine crosses the synaptic cleft and binds to receptors, eliciting a response from the post-synaptic nerve or muscle. Two types of post-synaptic receptor are activated by acetylcholine, nicotinic and muscarinic. Nicotinic receptors are ligand-gated ion channels, causing increased permeability to cations and therefore depolarisation. Muscarinic receptors are G protein-coupled receptors, which are linked to effectors such as adenylate cyclase and phospholipase C that induce changes of cellular biochemistry and physiology [5]. The action of acetylcholine is terminated when it is hydrolysed to choline and acetate; this reaction is catalysed by the enzyme acetylcholinesterase (Section 1.3, Figure 1.2).

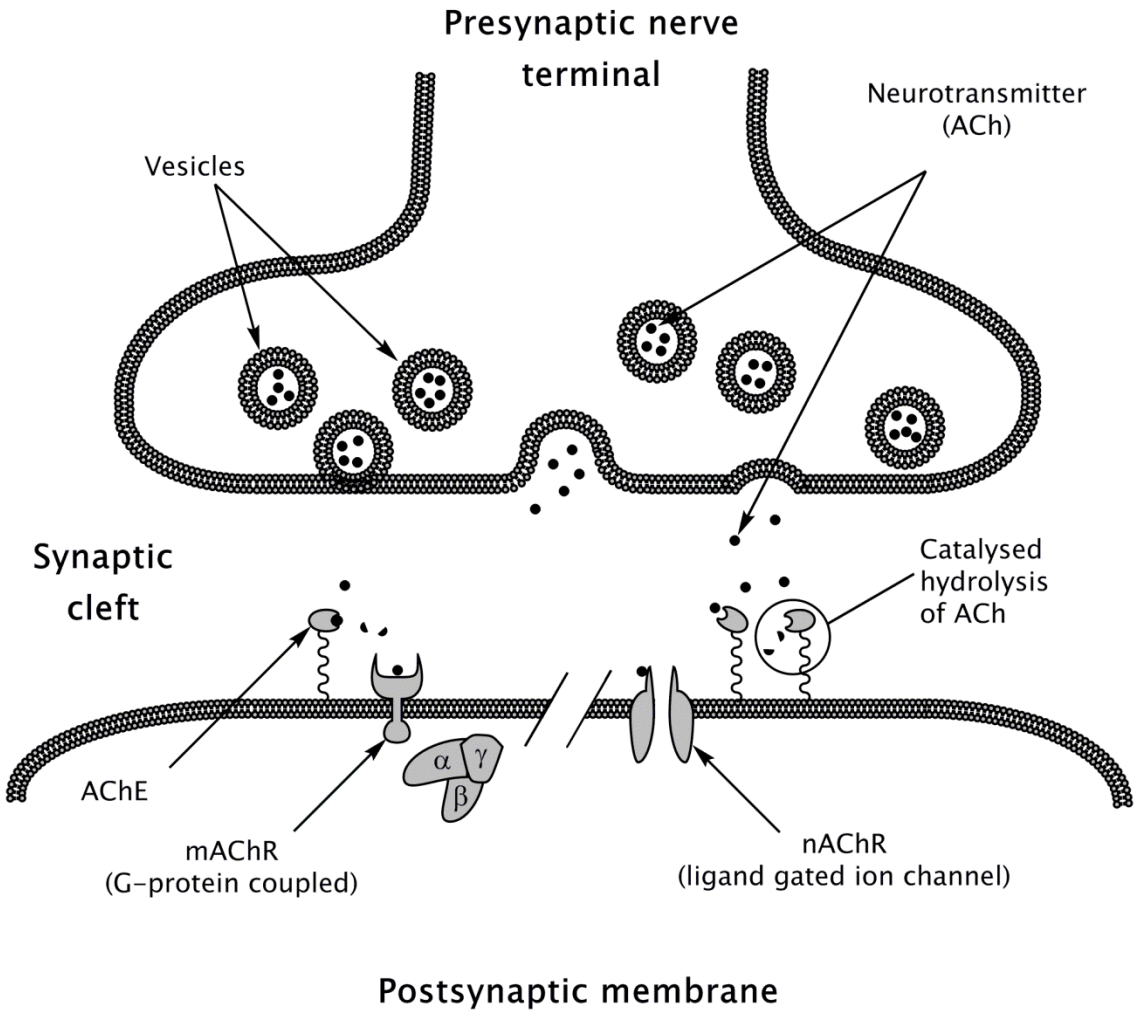

Figure 1.1. Schematic diagram of a cholinergic neuronal synapse or neuromuscular junction.

An action potential arriving at the terminal membrane activates the release of acetylcholine from the vesicles into the synaptic cleft. The acetylcholine crosses the cleft and binds to post-synaptic receptors eliciting a response. The action of acetylcholine on the receptors is terminated when hydrolysed into acetate and choline by acetylcholinesterase.

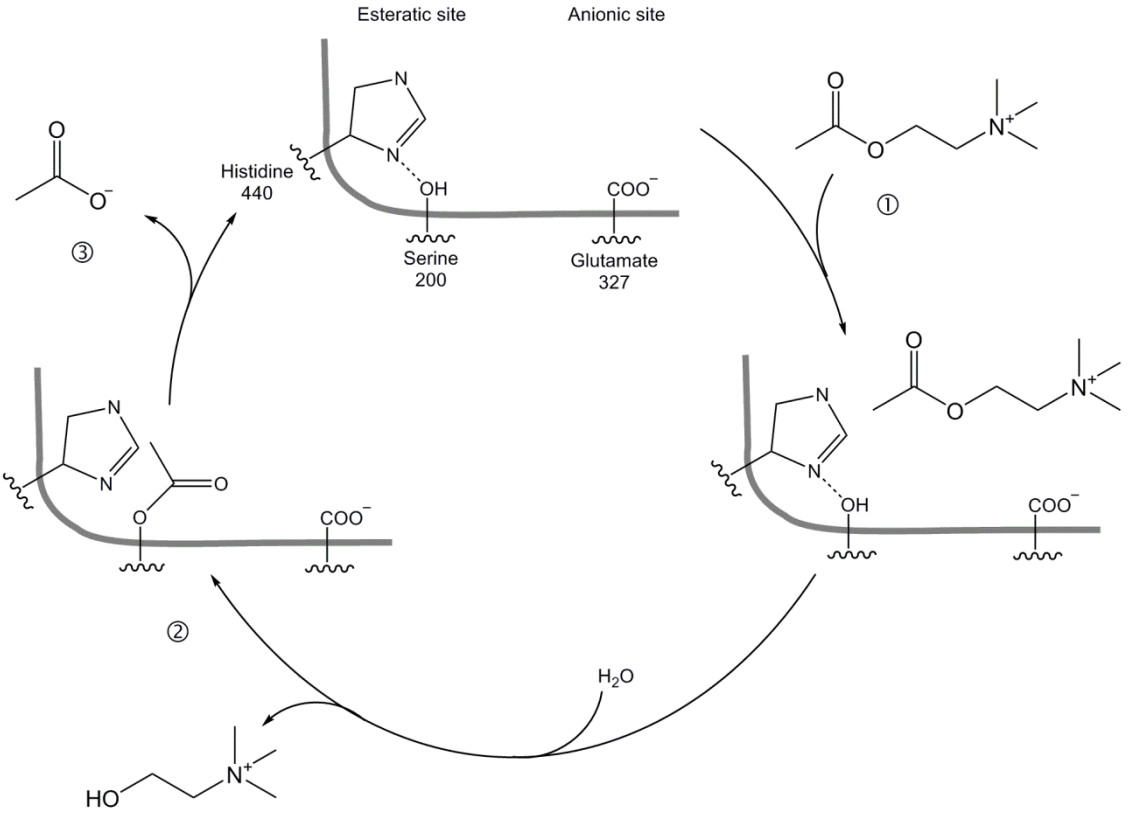

Figure 1.2. Steps involved in acetylcholinesterase catalysed hydrolysis of acetylcholine.

Acetylcholine enters the active site of the acetylcholinesterase enzyme, binding to the esteratic and anionic sites ①. It is hydrolysed into choline ② and acetate ③, terminating its action at nicotinic and/or muscarinic receptors. Figure adapted from Moore *et al* [6], Eyer [7] and Rang *et al* [5].

1.3 Cholinesterases

Acetylcholinesterase (EC 3.1.1.7) is a very efficient enzyme, responsible for terminating the action of acetylcholine at cholinergic synapses. It is capable of hydrolysing 6×10^5 molecules of acetylcholine per minute [8]. The time taken to hydrolyse one molecule of acetylcholine is approximately 100 μs [9]. This high turnover rate is essential for the rapid termination of chemical signalling at cholinergic synapses, allowing the maintenance of a high temporal fidelity of transmission. Acetylcholinesterase (AChE) has been found to exist in either globular or asymmetric forms. The globular form can be monomeric, dimeric and tetrameric, whereas the asymmetric forms exist as homomeric versions of the tetramer (A_4, A_8 or A_{12}) [10]. Tetramers also exist linked by disulphide bonds to collagen like strands [8;10], which tether the enzyme in place at the synapse. AChE is also present in the blood, on erythrocyte membranes. It is this readily accessible erythrocyte cholinesterase that is utilized as a marker of synaptic or neuromuscular acetylcholinesterase activity in animal efficacy studies and is employed in studies described in this thesis. The related enzyme butyrylcholinesterase (BChE; EC 3.1.1.8), which is also able to hydrolyse acetylcholine, is present in the plasma. The physiological function of BChE is unclear but has been suggested as detoxification of ester-containing poisons [11].

1.4 Nerve agents

Nerve agents are organophosphate compounds which are extremely toxic: for example, the estimated human lethal dose of sarin is 1 mg [12] (estimated lethal concentration of 60 mg□min/m³ [12] and minute volume of 0.015 m³/min, Figure 1.3). Organophosphates such as tabun, sarin, soman and cyclosarin were first synthesised during research to identify pesticides in the 1930s. The toxic properties of these compounds was reported to the Military and the research was subverted to investigate their use as weapons [4]. The nerve agent VX was discovered in the UK during the 1950s [13], again through research investigating insecticides. The structures, chemical formulae and formula masses of acetylcholine, muscarine, nicotine and nerve agents are presented in Table 1.1. Nerve agents continue to pose a threat to the United Kingdom and its Armed Forces, as stated in the National Security Strategy [2]. Nerve agents have been deployed in military conflicts and by terrorist organisations (Aum Shinrikyo) [13], with the most recent use of nerve agents occurring in August 2013 in Syria [14].

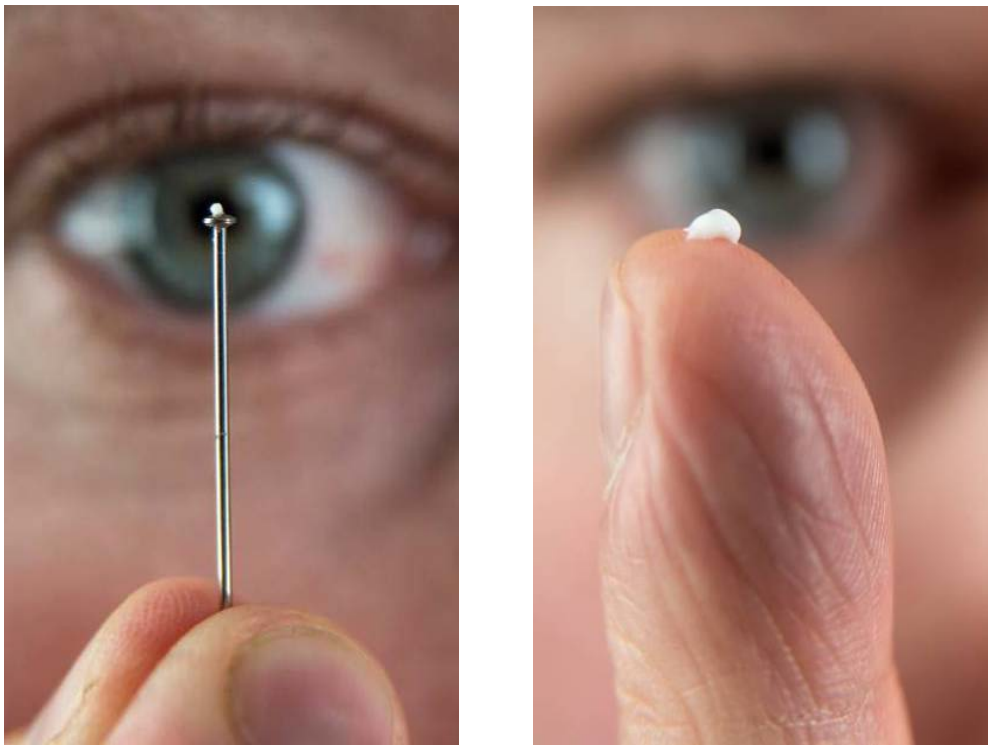

Figure 1.3. Photographs illustrating the approximate amount of nerve agent estimated to be lethal by the inhalation (left) and percutaneous (right) routes, being approximately 0.25 mg and 5 mg, respectively. [†]

[†] The liquid used for this photograph was not nerve agent.

	Volatility at 25 ˚C (mg/m³)	Structure	Formula	Mass
Acetylcholine	n/a	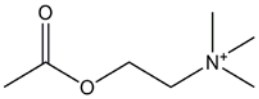	$C_7H_{16}NO_2^+$	146.21
Muscarine	n/a	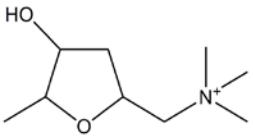	$C_9H_{20}NO_2^+$	174.26
Nicotine	n/a	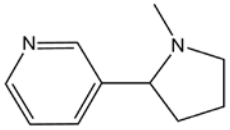	$C_{10}H_{14}N_2$	162.24
Tabun	490 [15]	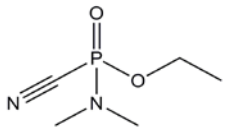	$C_5H_{11}N_2O_2P$	162.13
Sarin	22,000 [15]	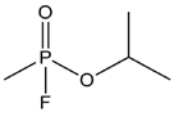	$C_4H_{10}FO_2P$	140.09
Soman	3,900 [15]	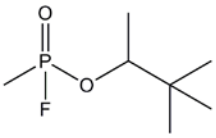	$C_7H_{16}FO_2P$	182.18
Cyclosarin	817 [16]	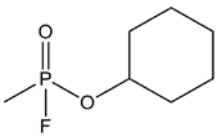	$C_7H_{14}FO_2P$	180.16
VX	10.5 [15]	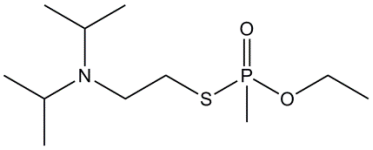	$C_{11}H_{26}NO_2PS$	267.37

Table 1.1. Nerve agent structures, chemical formulae and formula masses.

Acetylcholine structure, formula and mass are included for reference.

Nerve agents exert their effect by inhibition of acetylcholinesterase (Figure 1.4), the enzyme that terminates the action of the neurotransmitter acetylcholine. Inhibition of this enzyme leads to an accumulation of acetylcholine, so the rate of hydrolysis of acetylcholine into acetate and choline is greatly reduced. The excess neurotransmitter then causes overstimulation of synaptic ACh receptors and aberrant responses.

There are two main types of acetylcholine receptors, muscarinic and nicotinic. Overstimulation of these receptors disturbs the normal inhibitory and excitatory balance in the nervous system [17]. The symptoms of cholinergic syndrome are a mixture of muscarinic and nicotinic effects (see Figure 1.5). In severe cases of nerve agent exposure, overstimulation can lead to depolarising block at the nicotinic receptor, with paralysis ensuing. Likewise, overstimulation of muscarinic receptors in the central nervous system induces seizure activity, which in turn increases excitatory tone of the central nervous system and recruitment of other neurotransmitter systems to propagate the seizure [17]. If the seizure is sustained, brain damage will occur. The overstimulation of muscarinic and/or nicotinic receptors causes death by respiratory failure either at the neuromuscular junction of the respiratory muscles, or the respiratory centre in the central nervous system [18,19]. As a result of these effects death may occur within minutes of exposure to nerve agents [20]. For example, this was demonstrated dramatically when the Japanese cult Aum Shinrikyo released sarin on the Tokyo underground system in 1995 and several people were killed very rapidly following their exposure to sarin [21].

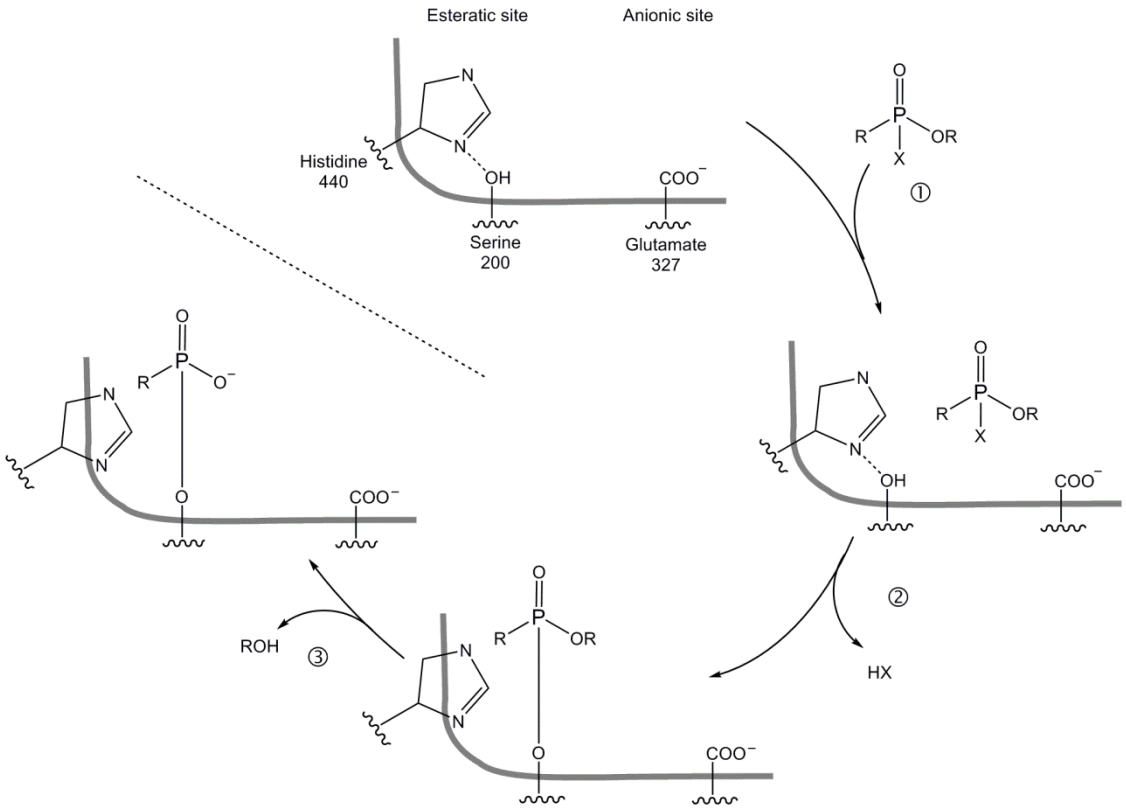

Figure 1.4. Steps involved in inhibition of acetylcholinesterase by nerve agents.

Nerve agent enters the active site of acetylcholine ①, phosphorylating the enzyme, irreversibly inactivating it ②, loss of an alkyl group (ageing) makes the nerve agent-enzyme complex resistant to reactivation by oximes ③. Figure adapted from Moore *et al* [6], Eyer [7] and Rang *et al* [5].

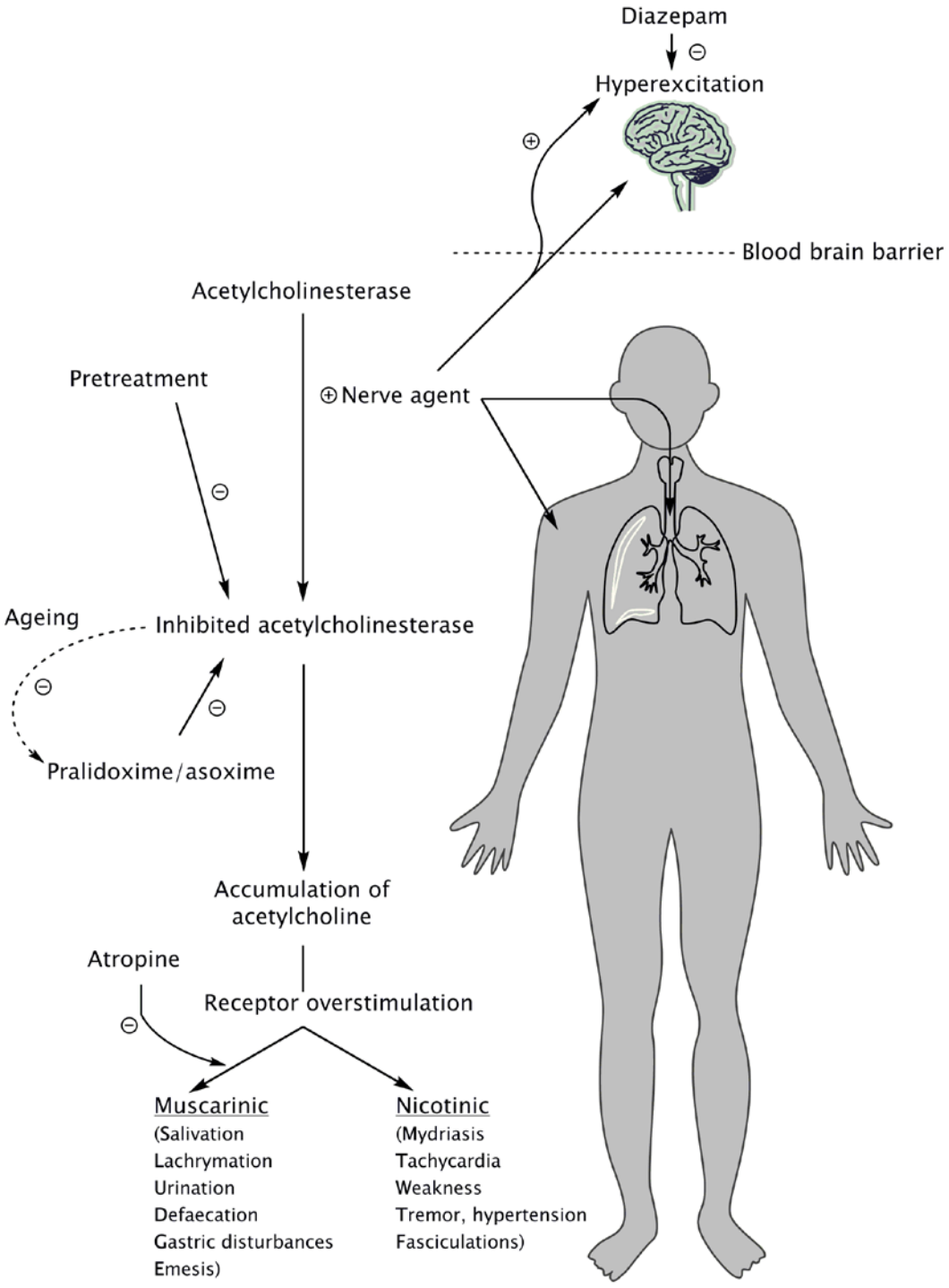

Figure 1.5. Schematic representation of nerve agent effects on the body and MedCM remedial mechanisms of action.

Muscarinic and nicotinic symptoms of cholinergic syndrome can be remembered by the mnemonics SLUDGE and MTWThF (days of the week). Figure adapted from Gearhart *et al* [22].

1.4.1 Routes of exposure

Nerve agents have similar chemical structures and the same mechanism of action. However, they can have very different physico-chemical properties and are classed as either persistent or volatile. The volatile agents (for example sarin, Table 1.1) readily form vapour and therefore the primary route of exposure for these agents is by inhalation. Agents such as VX have lower propensity to form vapours (Table 1.1) and therefore persist in the liquid state. Aerosols of these persistent agents can also pose an inhalation threat. However, if these agents contaminate the skin they persist as liquids and can be absorbed into the body. Therefore, percutaneous absorption is also a major route of entry into the body for persistent agents. The estimated human lethal dose of VX by the percutaneous route of exposure is 5 mg [12,13].

The rate of uptake of nerve agent into the body differs depending on the route, duration and amount of nerve agent to which the person is exposed. Therefore, the signs of poisoning which develop and their rate of onset also differ [3]. The effects of exposure by inhalation occur rapidly, with death occurring within minutes [21,23,24]. Conversely, exposure by percutaneous absorption is slow. The deleterious effects occur over a protracted period as the nerve agent continues to be absorbed through the skin, with death occurring several hours after exposure [25-27]. There have only been two medical cases of human exposure to VX, one of which was by parenteral administration and was lethal. The second was by percutaneous exposure and following treatment this individual made a full recovery [28,29].

These two exposure scenarios pose different challenges for MedCM. The rapid onset of signs of poisoning associated with inhalation exposure means that there is a limited opportunity for intervention, thus necessitating MedCM which can be administered quickly. In response many Armed Forces developed autoinjectors for their personnel. These devices are self or buddy administered First Aid, enabling individuals to take action quickly in the event of inhalation exposure. The current Military doctrine for administration of the autoinjectors (3 autoinjectors at 15 minute intervals [30]) is not optimal for protection against

percutaneous exposure to nerve agents [31]. Continuous administration of MedCM is required to achieve maximum efficacy against exposure to nerve agent by the percutaneous route [31]. The reduced efficacy of MedCM is most likely due to the nerve agent being absorbed from the skin and slowly inhibiting the AChE prior to manifestation of signs of poisoning. These signs trigger the administration of MedCM, as per the doctrine. The nerve agent continues to be absorbed, thus continuing to poison the individual throughout the treatment period.

Regardless of the route of exposure all nerve agents are lethal by the same mechanism of action and it is these actions or effects that MedCM oppose. The effectiveness of MedCM is governed by which route of entry into the body the nerve agent passed. Understanding these routes of exposure by determining the PK and PD for nerve agents will enable optimised administration of MedCM (once their PK and/or PD have also been determined).

1.5 Medical countermeasures

MedCM are part of an integrated approach to mitigating or preventing the deleterious and lethal effects of exposure to nerve agents. This includes assessment, disablement, deterrence and physical protection. The UK in-service MedCM consist of pretreatment tablets (pyridostigmine bromide tablets taken at 8 h intervals) supported by up to three self or buddy-administered autoinjection devices (containing atropine sulphate, avizafone hydrochloride and pralidoxime methane sulphonate) (Figure 1.6). The latter enable rapid treatment in the event of inhalation exposure to nerve agent. This combination of pretreatment and post-exposure therapy does not prevent nerve agent induced incapacitation [32-34]. That is, the MedCM are expected to prevent lethality but casualties may still require significant medical management. Therefore, several new MedCM have been identified that show improved efficacy against the incapacitating effects of nerve agent in animals [32-35]. These studies have led to proposed replacement MedCM, which comprise a pretreatment patch and modified autoinjection devices. The patch contains physostigmine and hyoscine and the autoinjector contains HI-6 dimethanesulphonate as a replacement for pralidoxime methane sulphonate.

A

B

C

Figure 1.6. Photographs of the current in-service pretreatment, the proposed replacement and the current in-service autoinjectors.

(A) Pyridostigmine bromide tablets [36], (B) physostigmine and hyoscine prototype patch, and (C) autoinjectors containing atropine sulphate, avizafone and pralidoxime methane sulphonate [37].

1.5.1 Post-poisoning therapy

The current post-poisoning therapy provided to the UK Armed Forces contains atropine sulphate (2 mg), avizafone hydrochloride (10 mg) and pralidoxime methane sulphonate (500 mg) [30], the mechanisms of action for each of these drugs are detailed below. The aim of the autoinjectors is to oppose the effects of cholinergic overstimulation rapidly in the event of exposure.

1.5.1.1 Atropine

Atropine (Table 1.2) a muscarinic antagonist competitively antagonises acetylcholine at muscarinic receptors, so it counteracts the accumulated acetylcholine. Atropine has been the mainstay of nerve agent MedCM, having been the standard treatment for nerve agent poisoning since the 1940s [27]. Atropine has proven efficacy as the sole therapeutic agent against nerve agent [34 :38]. In animal models, if sufficiently high doses of atropine are administered, the requirement for avizafone/diazepam or oxime as adjunct therapeutic agents is reduced [39]. Atropine has the ability to prevent or stop nerve agent-induced seizures, but this effectiveness is time dependent, reducing when administration is delayed [17]. Atropine is toxic under normal circumstances (a minimal lethal dose can be 1 – 2 mg/kg [40], with hallucinations, delirium and coma occurring at doses of 10 mg and above [41]) but the mutual antagonism of atropine and the nerve agent means that a much larger amount of atropine can be tolerated by organophosphate poisoned patients [42 :43]. Typically large amounts of atropine are required to treat anticholinesterase poisoning (e.g. 60 - 480 mg [42]).

Even though large amounts of atropine are required in the treatment of anticholinesterase poisoned patients the dose of atropine used in animal efficacy studies is considered to be high [32 :44]. This is particularly apparent when relative doses in immediate therapies are compared between animals and man. For example, the standard guinea pig dose of atropine originated from studies completed in 1952 and reported as;

> *"a convenient dose which was well in excess of the minimum amount required to give the maximum degree of protection obtainable, under the conditions of the test"* [45].

The above dose of atropine was considered a protective pretreatment (atropinisation) against an LD_{99} of sarin in the absence of other MedCM. It has since been used in animal studies to preserve life, enabling the efficacy of other drugs to be determined. Subsequent studies have adopted this dose of atropine as the standard, in conjunction with the other drugs that are combined in the MedCM regimen [46-49].

The use of other muscarinic antagonists such as caramiphen [50] or biperiden [51-53] that have specificity for one of the receptor subtypes, or that have reduced ability to penetrate into the CNS (leading to increased activity at peripheral sites of action compared to less specific antagonists), may improve efficacy against nerve agents [54]. However, caution must be exercised when interpreting efficacy of such drugs to ensure the receptor subtype expression in specific tissues is comparable between animals and humans.

acetylcholine	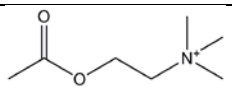	$C_7H_{16}NO_2^+$	146.21
muscarine	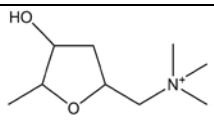	$C_9H_{20}NO_2^+$	174.26
nicotine	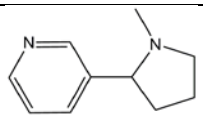	$C_{10}H_{14}N_2$	162.24
atropine (sulphate)	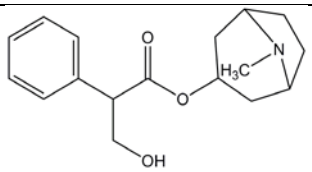	$C_{17}H_{23}NO_3$	289.38 (694.83)
hyoscine (hydrobromide)	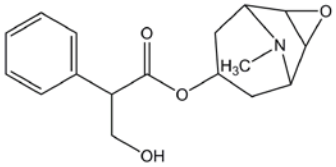	$C_{17}H_{21}NO_4$	303.36 (438.31)
pralidoxime (methane sulphonate)	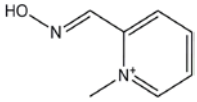	$C_7H_9N_2O^+$	137.16 (232.26)
HI-6 (dimethanesulphonate)	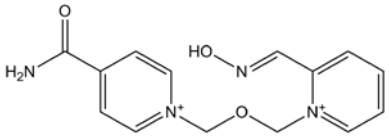	$C_{14}H_{16}N_4O_3^{2+}$	288.31 (478.5)
pyridostigmine (bromide)	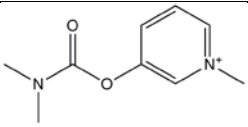	$C_9H_{13}N_2O_2^+$	181.21 (261.12)
physostigmine (salicylate)	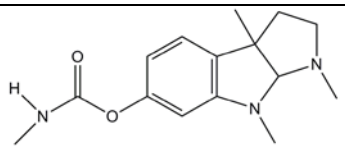	$C_{15}H_{21}N_3O_2$	275.35 (413.47)
diazepam (avizafone hydrochloride)	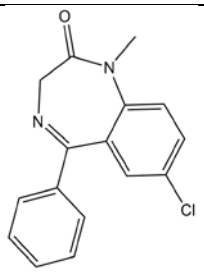	$C_{16}H_{13}ClN_2O$	284.74 (503.85)

Table 1.2. Chemical structures and formula mass for the neurotransmitter acetylcholine, acetylcholine receptor agonists and MedCM.

1.5.1.2 Avizafone

Avizafone is a water soluble pro-drug of diazepam. It is included in the in-service UK therapy MedCM to prevent seizures, which can otherwise result in subsequent neuropathology [17,55]. Avizafone is rapidly metabolised in the blood to diazepam and lysine (Figure 1.7) within 0.5 minutes and 5 minutes in guinea pigs and humans, respectively [56]. The water solubility of avizafone enables more rapid availability of diazepam (through improved absorption and rapid conversion to the active drug) than following administration of diazepam [57], thus providing better protection against seizure activity and lethality [39,58,59]. Diazepam, a benzodiazepine, is an allosteric modulator of gamma aminobutyric acid (GABA) at the $GABA_A$ receptor, enhancing the hyperpolarisation of the neuron produced by GABA [17].The efficacy of diazepam is most likely related to its PK profile in the brain [17]. Diazepam prevents or stops nerve agent induced seizures and the associated brain damage by increasing inhibitory tone in the CNS. Avizafone was approved for human use in combination with atropine sulphate and pralidoxime methane sulphonate in 1996 [60].

Other benzodiazepines have been considered for treatment of nerve agent induced seizures. These include lorazepam [15] and midazolam [61], with the latter stopping seizures more rapidly and at lower doses than diazepam in a guinea pig seizure model [44]. Supported by antimuscarinic drugs (e.g. atropine), benzodiazepines have demonstrated the ability to stop seizures 40 minutes after they were established [62]. However, concern has been raised regarding the respiratory depressant effects associated with benzodiazepines, so antimuscarinics with N-methyl-D-aspartate (NMDA) receptor antagonistic activity, such as biperiden or benactyzine have been suggested [55]. Glutamate receptors, of which NMDA receptor is a subtype, have been implicated in having a key role in nerve agent induced seizure and subsequent neuropathology [17,55]. Thus treatment with antagonists of these receptors, such as ketamine, may prove beneficial.

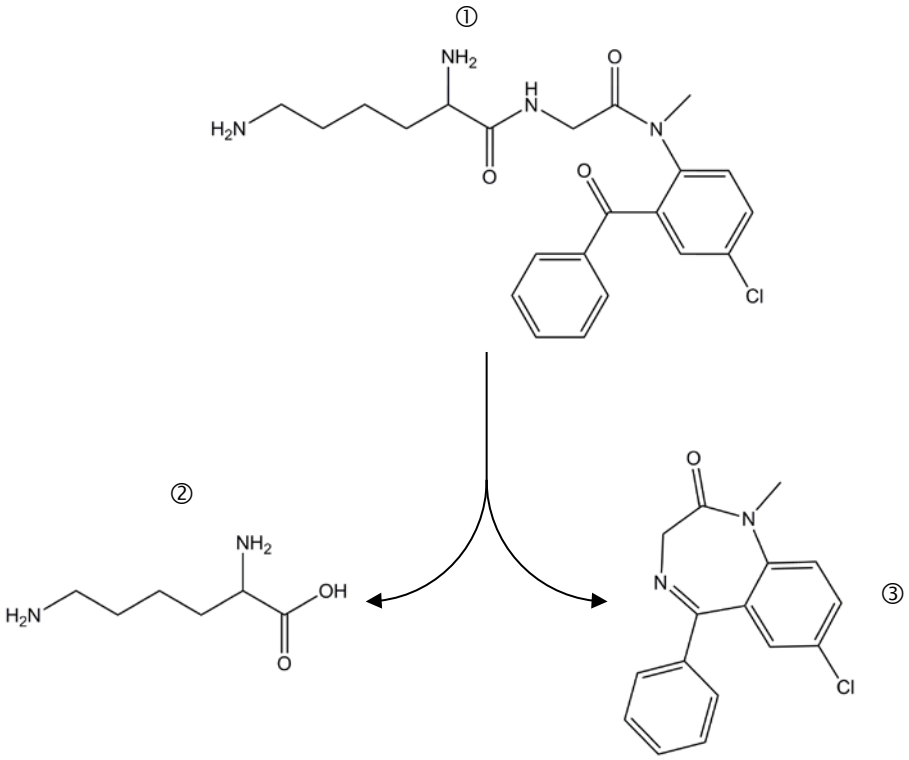

Figure 1.7. The metabolic conversion of avizafone ① into lysine ② and diazepam ③.

This reaction is rapid and extensive in the blood[57], especially in guinea pigs [56].

1.5.1.3 Oxime

Oximes are able to reactivate nerve agent inhibited acetylcholinesterase through nucleophilic attack of the phosphorus in the nerve agent-enzyme complex, cleaving the nerve agent from the enzyme (Figure 1.8). Pralidoxime (also known as P2S, pralidoxime methane sulphonate or 2PAM, pralidoxime chloride) is the current oxime therapy in many countries (including the UK) and is used as a standard against which other oximes are compared [63]. Pralidoxime in combination with atropine provides greater protection against nerve agent than either compound alone [34 :48]. However, pralidoxime is not efficacious in preventing incapacitation or lethality when administered alone [34].

The efficacy of treatment against nerve agent inhibition with oximes is time dependent. Some nerve agents can become refractory to nucleophilic attack, due to the loss of an alkyl group from the nerve agent-enzyme complex [8 :18 :64 :65] (Figure 1.4). This process is known as ageing. The rate at which an agent ages varies depending on the agent and the animal species studied [66-69]. Some agents are particularly prone to ageing (e.g. soman), whereas others age more slowly and are readily reactivated (e.g. VX). Furthermore, the ability of an oxime to reactivate inhibited acetylcholinesterase is agent specific, due to the chemical and steric differences with each nerve agent-enzyme complex. For example, whilst pralidoxime and HI-6 reactivate sarin inhibited AChE efficiently they are very poor reactivators of tabun inhibited AChE [70]. Obidoxime has greater effectiveness for reactivating tabun inhibited AChE [71]. This problem may be overcome with a diagnostic technique suggested by Worek *et al* [72], which is able to identify the best oxime and dose required.

The oxime HI-6 (also known as asoxime) is in advanced development to replace pralidoxime in the UK autoinjector. Animal studies have demonstrated the improved efficacy of HI-6 when compared to pralidoxime, in multiple species, against multiple nerve agents [73-76]. This improved efficacy compared to pralidoxime has been attributed not only to its reactivating properties but also to a direct pharmacological action. Several mechanisms have been proposed,

including general ganglion blocking properties [77], nicotinic receptor blocking [78] and reduction of pre-junctional acetylcholine release [79].

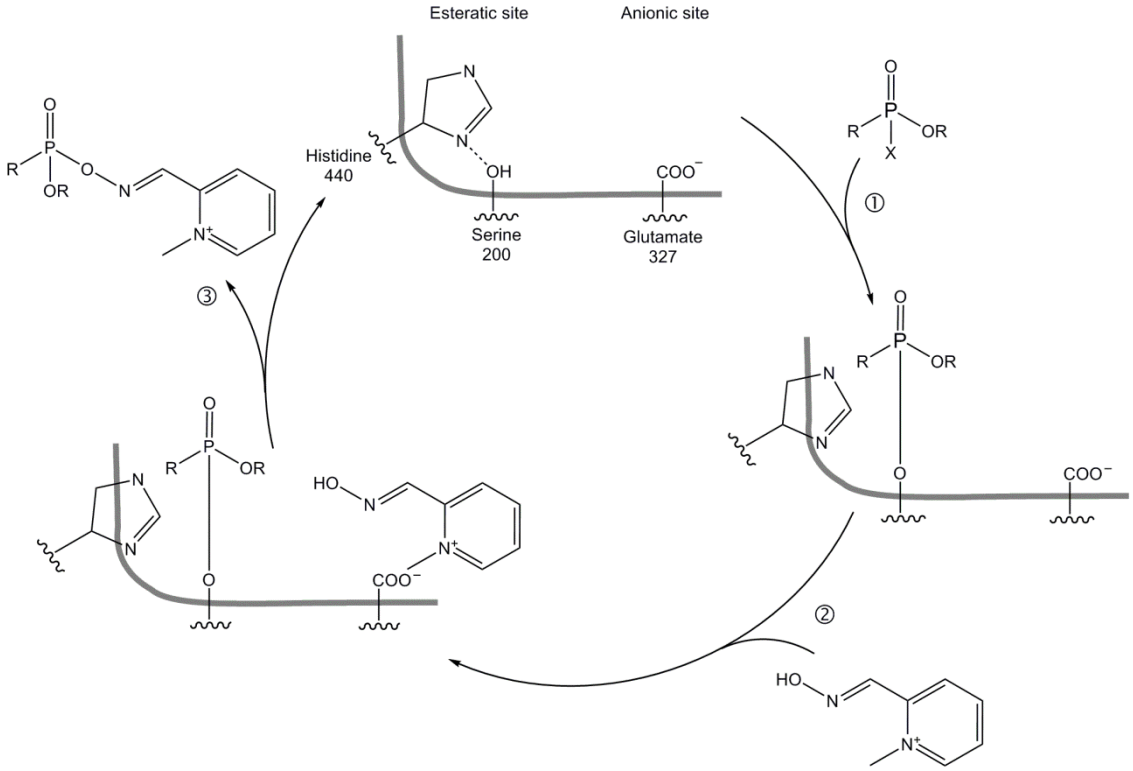

Figure 1.8. Steps involved in the reactivation of nerve agent inhibited acetylcholinesterase by oximes.

Acetylcholinesterase inhibited by nerve agent ① can be reactivated by oximes such as pralidoxime, which subject the nerve agent-enzyme complex to nucleophilic attack ②, generating a phosphorylated oxime ③. Figure adapted from Rang *et al* [5].

1.5.2 Pretreatment

1.5.2.1 Pyridostigmine bromide

Pretreatment with pyridostigmine bromide was introduced as a supplement to post-poisoning MedCM in response to the rapid ageing of soman and its consequent resistance to therapy with an oxime [47 :80 :81]. The in-service and proposed replacement pretreatments are both carbamates, which reversibly inhibit cholinesterase (Figure 1.9), protecting a portion of the enzyme from being irreversibly bound by nerve agent [32 :82]. The spontaneous process of decarbamoylation of the cholinesterase hydrolyses the carbamate, whilst reversing the inhibition. This happens at a much slower rate than the hydrolysis of acetylcholine. The carbamate therefore inhibits a proportion of AChE and the remaining active AChE is sufficient to support normal synaptic function. In the event of nerve agent poisoning the carbamoylated AChE is protected from inhibition by the nerve agent. Decarbamoylation of this AChE then recovers sufficient activity to support some synaptic function [47].

Pretreatment is dependent upon supportive therapy, which includes atropine and an oxime. In the absence of supporting therapy pretreatment with carbamate alone fails to provide protection [48]. Pretreatments provide maximal protection at high doses, protecting large amounts of AChE. However, due to the adverse effects associated with high doses and the resulting inhibition of AChE activity, lower doses that are tolerated by healthy individuals must be used [83]. Knowledge of the carbamate concentration required to inhibit a target amount of AChE is critical for the determination of efficacious doses of pretreatment. Typically the target of 20 – 40 % inhibition of AChE is used in animal efficacy studies [84 :85]. The UK Armed Forces in-service pretreatment is pyridostigmine bromide, more commonly known as Nerve Agent Pretreatment Set (NAPS, Figure 1.6). Pyridostigmine bromide is provided in tablet form (31.5 mg), to be taken 3 times a day at 8 hour intervals [36] and was shown to inhibit AChE by a minimum of 15 % when taken by humans [86].

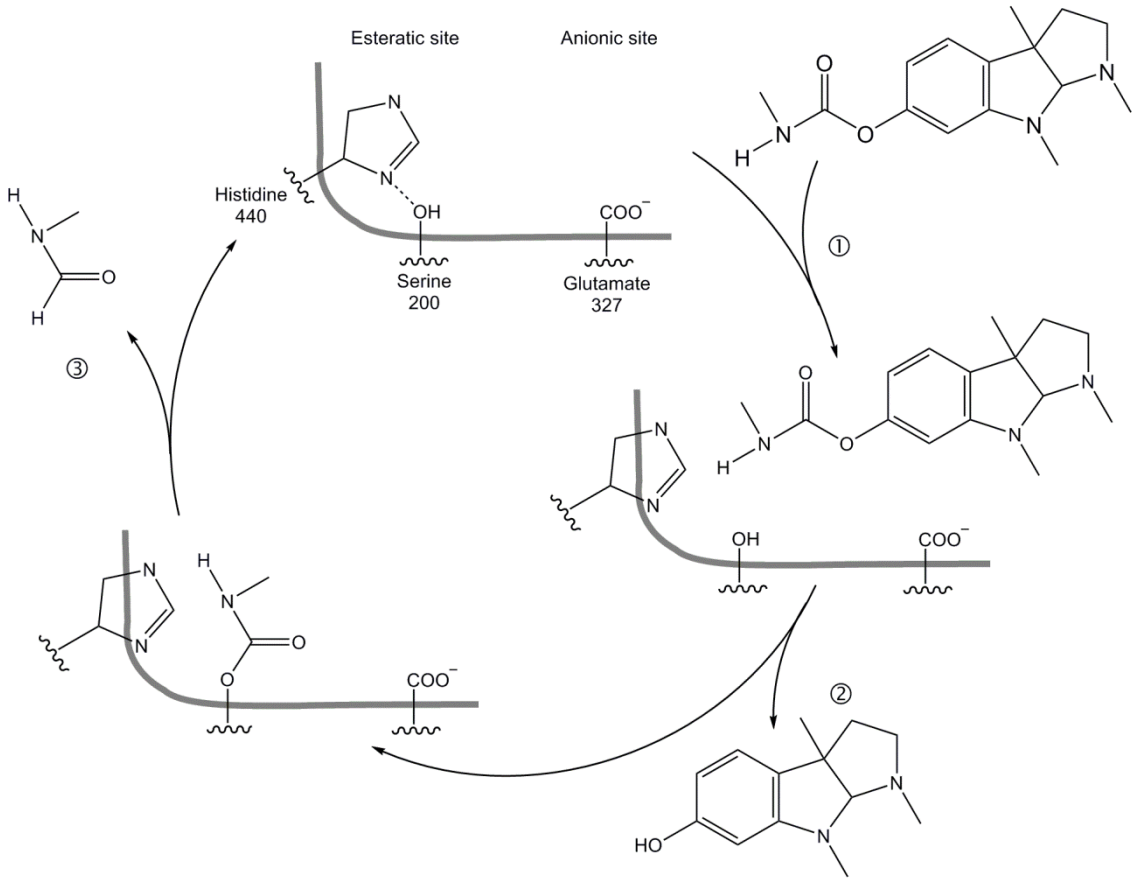

Figure 1.9. Steps involved in inhibition of acetylcholinesterase by carbamates such as physostigmine.

Carbamates enter the active site of acetylcholinesterase ①, inhibiting activity by carbamoylating the enzyme ②. Hydrolysis of the remaining carbamoyl ③ is much slower than the hydrolysis of acetylcholine, sequestering a pool of acetylcholinesterase and preventing it from being irreversibly inhibited by nerve agent. Adapted from Rang *et al* [5].

1.5.2.2 Hyoscine and physostigmine

Hyoscine and physostigmine, formulated in a transdermal patch (Figure 1.6), are in advanced development to replace the pyridostigmine bromide tablets, as the pretreatment against nerve agent exposure. Unlike pyridostigmine, physostigmine (also a carbamate) is able to cross the blood brain barrier [8 :87] and can inhibit central AChE. As a result physostigmine is able to protect against nerve agent induced incapacitation [33]. Physostigmine has also been shown to have an agonist action on nicotinic receptors, similar to that of galantamine [88]. This action has not been implicated in physostigmine's protective efficacy against nerve agents. The combination of hyoscine and physostigmine has proven efficacy as a nerve agent pretreatment in proof-of-concept studies that used guinea pigs [35 :84 :89] and marmosets [90]. Evidence suggests that recovery from nerve agent poisoning is quicker following pre-treatment with physostigmine compared to pyridostigmine [48]. High doses of physostigmine in the absence of supporting therapy have also demonstrated efficacy against the lethality of both soman and sarin [33].

Hyoscine, a muscarinic antagonist akin to atropine, is more potent but shorter acting than atropine [91]. Addition of a muscarinic antagonist to physostigmine has been demonstrated to be more effective as a pretreatment for nerve agent poisoning than physostigmine alone [33 :89 :92]. Hyoscine in combination with physostigmine was found to provide greater protection against nerve agent than other antimuscarinic drugs, including atropine and caramiphen [93]. Subsequent studies have shown physostigmine and hyoscine improve nerve agent induced cognitive effects, changes in neurochemistry, incapacitation and lethality [35 :84 :85 :90 :94 :95]. Physostigmine and hyoscine are ideally suited for co-administration as they have complimentary pharmacological activities [91 :96]. Hyoscine reduces the adverse effects caused by physostigmine, enabling greater doses of physostigmine to be administered, which protect sufficient central AChE (typically 20 - 40 % [35 :84 :97]) to provide improved protection against nerve agent induced incapacitation compared to physostigmine alone [84].

1.5.2.3 Other pretreatments

Other anticholinesterases have also been investigated as pretreatments, for example, huperzine and galantamine [98,99]. Huperzine has demonstrated improved efficacy over pyridostigmine bromide when supported by atropine [98], but has also been shown to be toxic at therapeutic doses [100]. Galantamine has demonstrated benefit as a pretreatment to nerve agent exposure with and without atropine [99] and also has a neuroprotective action [88]. However, galantamine has not demonstrated efficacy against nerve agents at the high a challenge dose at which pyridostigmine has proven efficacious.

1.5.3 Bioscavengers

A different approach to providing protection against exposure to nerve agent has been investigated, using exogenous butyrylcholinesterase (BChE) as a bioscavenger. This enzyme is similar to the target AChE molecule. Administration of large amounts of BChE can inactivate nerve agent by irreversibly binding with and preventing it from inhibiting endogenous AChE. Wolfe *et al* were the first to report the protective efficacy of exogenous cholinesterase administration [101]. Bioscavengers have been investigated as pretreatments, with human plasma-derived BChE (huBChE) and a recombinant human BChE (rBChE) progressing to advanced development for this indication [102]. However, the development of the most promising source of rBChE (transgenic goats) has stopped, due to the prohibitive costs, the sub-optimal PK profile and decreasing yields of rBChE [103]. This recombinant enzyme had successfully completed a Phase I Clinical Trial [104]. Alternative recombinant sources of huBChE include plants [105], animal cells [106], and human cells[107] . The majority of recombinant huBChE produced in these expression systems remain at the proof-of-concept stage of development. Recombinant bioscavengers must overcome a series of challenges associated with recombinant proteins, including more rapid rate of clearance than the native huBChE. These issues were the subject of a solicitation for proposals to develop recombinant huBChE, published by the US Defense Threat Reduction Agency. This solicitation aimed not only to address these issues but also scale up of the production systems, to manufacture the amount of bioscavenger required [108].

In the UK, the focus has been on the post-exposure use of BChE, for effective treatment of percutaneous exposure to nerve agent [109,110]. BChE based bioscavengers are stoichiometric (bind in a 1:1 ratio), requiring large doses to be administered to effectively neutralise the nerve agent. These large doses of stoichiometric bioscavengers have implications for scale of production, costs and feasibility of administration, as the main source is from outdated human blood products. The amount of the enzyme in the human body is low at approximately 700 nmol [111]. Large volumes of blood are therefore required to produce the bioscavenger. The maximum amount of bioscavenger that could be produced annually is expected to be 1 – 2 kg, from 1,200,000 L of outdated plasma [112]. This annual amount is equivalent to 4,000 – 8,000 doses of *circa* 250 mg [113], thus making the use of plasma derived huBChE prohibitively expensive [108].

Catalytic bioscavengers increase the rate at which nerve agents are broken down into inactive products [114] and require lower doses to be administered. Unlike stoichiometric bioscavengers such as BChE, catalytic scavengers are not expended when inactivating the nerve agent. Site directed mutagenesis of several enzymes has been investigated, with the aim of improving their catalytic efficiency. However, the transgenic production systems from which they originate may cause the bioscavengers to induce an immunologic response in humans, as well as potentially leading to unfavourable PK profiles [114]. The immunological response may be overcome by gene therapy approaches, in which the bioscavenger can be introduced by a viral vector [115], although more work is required to ensure these vectors do not produce toxic proteins or other immune responses [100]. The PK profile of bioscavengers may be improved by fusing the recombinant molecules with human serum albumin, prolonging the residence time of the bioscavengers [116]. These latter bioscavenger approaches are still at the proof-of-concept stage of development. HuBChE remains the most advanced bioscavenger, with studies proving its efficacy in animals [100] and completed Phase I Clinical Trials in man.

MedCM have mechanisms of action that either directly oppose the mechanism of action of nerve agent or oppose/alleviate the deleterious effects of nerve agents (Figure 1.5). Determination of the efficacy of MedCM against nerve agents is not ethically possible in human clinical trials. Therefore, it is of utmost importance to fully understand the efficacy in animals, to enable effective extrapolation to the clinical scenario. The period of the pharmacological effects or concentrations of MedCM has not systematically been studied in animals. Addressing this knowledge gap through PK studies will help to understand efficacy and enable extrapolation of effective doses/concentrations to man.

1.6 Choice of animal species

The choice of animal species in which efficacy is demonstrated is key. Variation in efficacy between species and experimental protocols creates uncertainty when extrapolating efficacy to humans. Thus, developing a logical procedure with which to do so is important [117]. PK and PD (discussed in section 1.7) are integral to the development of drugs by the pharmaceutical industry [118]. To date, the PK and PD studies in this field of research have concentrated on investigating nerve agents. There has been no systematic determination of MedCM PK in animals, with studies being completed in different species. The majority of animal studies of MedCM have primarily investigated efficacy.

The research presented in this thesis aims to address the paucity of PK and PD data in animal species. Guinea pigs were chosen as the appropriate species for these studies, due their sensitivity to nerve agents and their response to treatment, which is closer to non-human primates than either rats or mice [76]. Rats and mice have been reported to not respond well to post-poisoning treatment [119]. The difference in response to nerve agent between these species is due to the amount of carboxylesterase in the blood. Carboxylesterase (CaE; EC 3.1.1.1) is an enzyme that catalyses the hydrolysis of a variety of different compounds containing esters and amides. CaE detoxifies nerve agents. Rats and mice have large amounts of CaE in their blood, whereas guinea pigs have less and humans none [11,120]. The greater the amount of CaE the greater the

dose of nerve agent required to achieve lethality. This CaE theory to explain species differences in nerve agent toxicity was first proposed by Sterri and Fonnum [121]. Recent studies using CaE-knockout mice support this theory, as these mice were more sensitive to soman coumarin (a nerve agent simulant) than wild type mice [122]. The influence of CaE on nerve agent toxicity has previously been reduced through the use of specific CaE inhibitors [120]. However, this may further complicate interpretation of the data generated, especially with MedCM, as oximes have been shown to reactivate this enzyme (increasing the detoxification of the nerve agent) [119].

Whilst there is no CaE expressed in human plasma there are considerable amounts in the tissues, particularly the liver. Evidence in the literature has shown that inhibition of CaE by di-isopropyl fluorophosphate (an organophosphate insecticide) affects atropine metabolism [123]. Therefore it is possible that inhibition of CaE by nerve agent could alter the PK profile of MedCM. As such, using guinea pigs, a species in which the CaE effect is minimal, is preferable. Furthermore, the majority of MedCM efficacy studies in small animals have used guinea pigs. It is this wealth of existing efficacy data from guinea pigs which must be understood in terms of concentration-time and concentration-effect, hence guinea pigs were used in the studies described in this thesis.

1.7 Pharmacokinetics and pharmacodynamics

Pharmacokinetics (PK) is the study of drug concentration over time in plasma or tissues following administration. It can in essence be considered as what the body does to the drug. Determination of the concentration-time profile for a drug enables many parameters to be calculated. The primary parameters are: apparent volume of distribution (the volume into which the drug appears to distribute), clearance (the volume of blood cleared of drug per unit time) and absorption/elimination rate constants (the rates at which drug concentrations change). From these primary parameters many other secondary parameters can be calculated, including (but not exclusively), the elimination half-life (duration over which the concentration of drug decreases by a factor of 2), area under

the curve (total exposure to the drug), mean residence time (average time a molecule of drug remains in the body). Integration of many of these parameters with physiological parameters or processes aids the interpretation of the PK data. For example, drugs *x* and *y* have apparent volumes of distribution of 5 L and 43 L, respectively. These values correspond approximately to blood volume and total body water in an adult, indicating that drug *x* remains in the systemic circulation, whereas drug *y* is distributed extensively in the body.

Pharmacodynamics (PD) is the study of concentration or time dependent effect of a drug. It can be thought of as what the drug does to the body. In a similar manner to PK, a concentration-effect profile or effect-time profile can be determined and parameters calculated from the data. Parameters include, maximum response, concentration required to achieve 50 % of the maximal response, threshold concentration (minimum concentration required to elicit an efficacious response) and duration of response. The PD can be linked to the PK, i.e. drug concentration is correlated to response at a specific time-point. Hysteresis loops may also be identified, to account for lags in response at a measured concentration [124].

The determination of MedCM efficacy in humans is not ethical. Therefore, providing evidence of efficacy of MedCM for inclusion in a Marketing Authority Application to the drug licensing authorities is dependent on non-clinical animal data. In “first in human” clinical trials of new drugs the doses are proposed on the basis of *in vitro* and non-clinical data [125,126]. The approach of using animal PK parameters can be used for this purpose [126] and should be used for MedCM. Indeed, this has been suggested for HI-6 [127] but for no other MedCM.

To date the extrapolation of efficacious MedCM doses from animals to humans has been scaled on body mass or body surface area [32]. These arbitrary methods do not account for the absorption, distribution, metabolism or excretion (ADME) of each component drug and how these differ for each drug. Other

MedCM (pyridostigmine and physostigmine) have been scaled on a specific PD endpoint (erythrocyte AChE inhibition). This is an empirical method, which is more accurate than scaling by body mass or surface area but does not provide a correlation to blood concentration in a PKPD relationship. Knowledge of such a relationship can improve the understanding of efficacy in the different species. To enable scaling of MedCM doses using PK parameters, as is the norm in the pharmaceutical industry, these PK parameters must first be determined.

Whilst the PK or PD of physostigmine [128], avizafone/diazepam [57], HI-6 [129] and bioscavengers [130] have been studied individually in guinea pigs, extensive characterisation of their PK and the effect of interactions that may or may not occur following combined administration [5 :113-115] have not been determined. Surprisingly, given that it is the mainstay of nerve agent therapy, the PK of atropine has not been described previously in the guinea pig. This lack of PK data from systematic studies means that its efficacy is not well understood in terms of concentration-time profiles or concentration-effect relationships.

An example of the lack of PK knowledge and its implication for efficacy is provided by the high dose of atropine used in guinea pigs, which could result in either an overestimation or a masking of the efficacy of the drugs that are administered in combination with atropine [58 :131 :132]. The putative existence of atropinesterase (EC 3.1.1.10), an enzyme that metabolises atropine, in guinea pig plasma has been claimed to necessitate the use of this high atropine dose [46]. However, investigation of guinea pig atropinesterase activity by Harrison *et al,* found none to be present in plasma [133]. Therefore, CaE in guinea pig liver or tissues may account for a rapid elimination of atropine in this species. In general, the doses of MedCM used in proof-of-concept efficacy studies are not well correlated with the doses that can be administered to humans or *vice versa*.

The PK of nerve agent MedCM in animals has been determined in unpoisoned animals. It is conceivable that nerve agent exposure may have an effect on the

MedCM PK [134,135], through disrupted physiology and therefore altered ADME processes. However, there has only been one study that has determined the PK of MedCM in nerve agent poisoned animals [134]. That study suggested the brain bioavailability of HI-6 was reduced in soman poisoned animals [134]. The PK of MedCM following nerve agent exposure can only be determined in animals. Knowing and quantifying these differences in PK from unpoisoned animals will allow appropriate scaling of doses to humans, ensuring the doses are efficacious.

Knowledge of the PK and PD of nerve agents will also improve the understanding of MedCM efficacy, by determining the period during which they are present at toxicologically relevant concentrations. Several studies have investigated nerve agent PK (or toxicokinetics: the study of the concentration-time profile of toxic doses) but these studies used anaesthetised, artificially ventilated and/or atropinised guinea pigs [136-139]. These experimental conditions are in themselves likely to affect the data obtained, especially as they are designed to prevent nerve agent lethality in the guinea pigs. To date, only one study has investigated the PK and PD of nerve agent in conscious untreated guinea pigs [140].

The kinetic studies of percutaneous nerve agent have, to date, been short term studies of 6 – 8 hours [136,141], whereas guinea pigs exposed to percutaneous VX in efficacy studies died between 24 and 48 hours after exposure [31,110,142]. In those studies the signs of poisoning occurred on average 6.5 hours after exposure [110]. Therefore, a requirement exists for longer duration PK studies of percutaneous VX.

There is little PK/PD data for nerve agent MedCM in guinea pigs but this is the key species in which the efficacy of these MedCM is determined. Therefore, it is difficult to link efficacy with PK/PD and subsequently to define pharmacologically effective plasma and tissue concentrations. This information is required for the extrapolation of efficacious doses of nerve agent MedCM to

humans, in support of the advanced development and licensing of these MedCM.

1.8 Microdialysis

The PK of drugs is generally measured in blood or plasma, but the circulation is not the site of action for nerve agents or MedCM. Cholinergic synapses in central and peripheral tissues are the target sites at which nerve agents act and therefore where the PK and PD of nerve agents and MedCM should be determined. The concentration of MedCM at these target sites may lag behind that in the plasma, if the drug does not readily distribute from the systemic circulation into the tissues. Thus, effective tissue concentrations may not be achieved as suggested by plasma PK, as has been reported for the antibiotic clarithromycin in soft tissues [143].

Microdialysis is an established sampling technique, which enables the measurement of analytes in the extracellular space of tissues [144]. Microdialysis probes have semi-permeable membranes that, when perfused with physiological buffer, enable analytes to pass from the tissue into the buffer (Figure 1.10). The flow of buffer maintains a concentration gradient, across which the analyte diffuses. Fractions of the buffer are collected and the concentration of the analytes of interest determined. Microdialysis probes are available with different membranes, allowing different analytes to be sampled, ranging from small molecule drugs [144] to large molecule proteins [145].

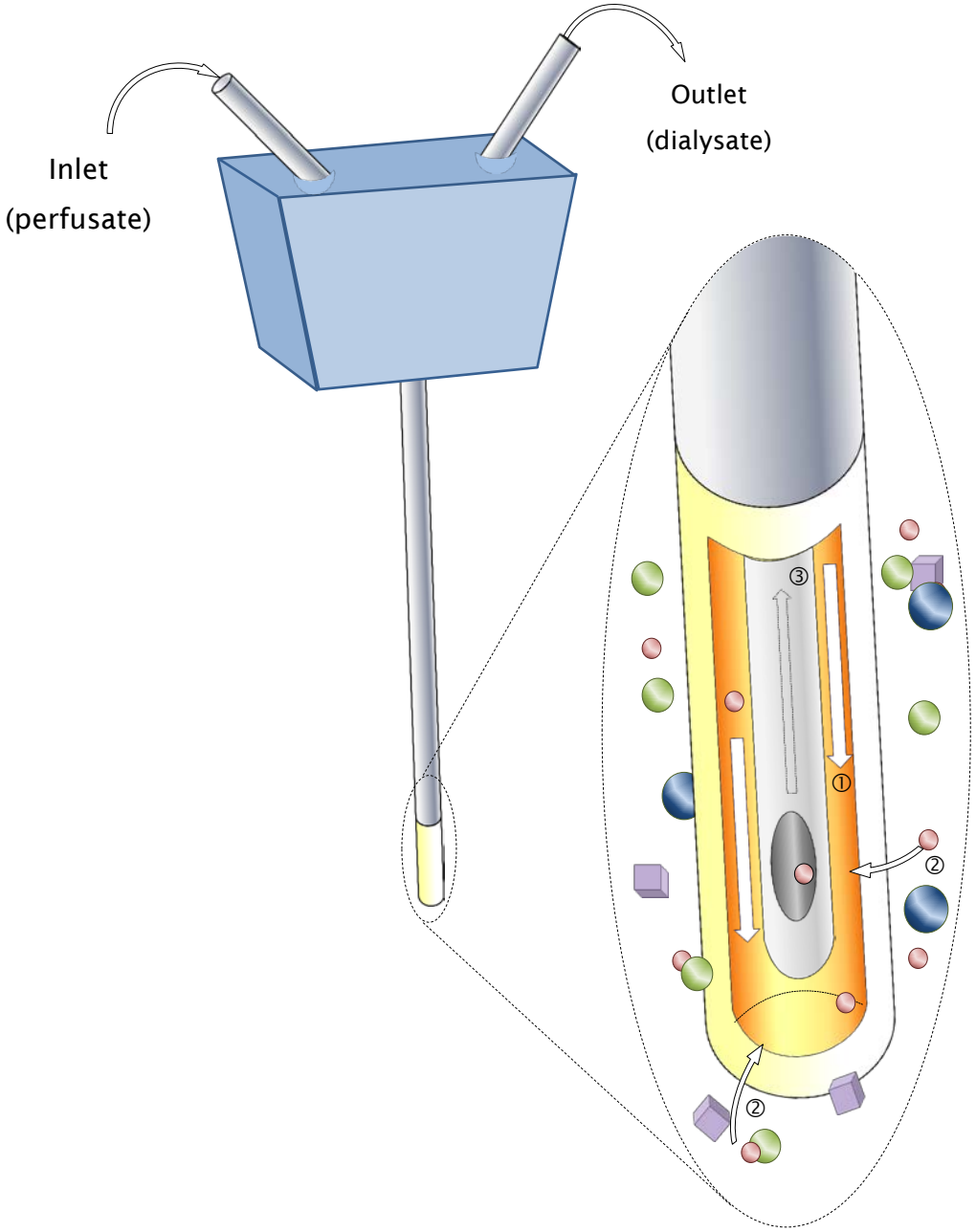

Figure 1.10. Schematic diagram illustrating the flow of physiological buffer within the probe enabling analyte to pass through the semi-permeable membrane for analysis.

Physiological buffer (perfusate) flows from the inlet to the microdialysis probe semi-permeable membrane ①. Some perfusate diffuses out of the probe into the interstitial space. Analyte (red sphere) passes down a concentration-gradient through the semi-permeable membrane into the probe ②. The perfusate (now dialysate) flows into the outlet from the probe, fractions of this dialysate are collected and assayed ③.

The alternative methods of open-flow microsampling [146], cerebro-spinal fluid sampling [135] and post-mortem tissue sampling (with subsequent homogenisation) [17] could be used in place of microdialysis. Open-flow microsampling is similar to microdialysis but without the membrane. It is typically used for high molecular mass analytes. As the MedCM are of low molecular mass open-flow microsampling was not considered necessary or appropriate. Cerebro-spinal fluid sampling is able to provide a good estimation of concentration in the CNS but only relatively few samples can be collected from individual animals. These samples could not be collected without analgesia or anaesthesia and are therefore usually collected post-mortem, due to the volumes required [135]. Microdialysis provides the distinct advantage over post-mortem sampling that multiple samples can be collected from individual animals, thus reducing the total number of animals required.

Death following exposure to nerve agents is usually by respiratory arrest, caused either by failure of the central respiratory centre or directly by paralysis at the diaphragm neuromuscular junction [16;17]. Using microdialysis in the brain and skeletal muscle has the potential to improve the understanding of toxic concentrations of nerve agent and therapeutic concentrations of MedCM in these target tissues. To date, there has been no systematic study of nerve agent or MedCM PK using microdialysis in any species, although microdialysis has been used to investigate the PK of HI-6 in rat brain [134], as well as the effect of nerve agent and subsequent MedCM treatment on neurotransmitter concentrations [26;31;95;147-151]. The use of microdialysis in the brain is an established technique, whereas fewer studies have used microdialysis in skeletal muscle of anaesthetised animals [152-155]. One such study reported the effect of pyridostigmine bromide on the release of ACh from the skeletal muscle [155]. The studies by Newman *et al* [154] and Close *et al* [153;156] in which microdialysis probes were used in contracting skeletal muscle of anaesthetised animals, indicate that it is possible to use microdialysis in the skeletal muscle of conscious ambulatory animals to determine the PK of MedCM.

1.9 Aims and hypotheses

The aim of the studies described in this thesis was to determine the PK and PD of nerve agents and MedCM against nerve agents, in the blood and tissues of guinea pigs, to enable a better understanding of nerve agent MedCM efficacy. In order to determine these PK and PD data a new methodology was developed. This novel methodology included vascular cannulation (both venous and arterial) and implantation of microdialysis probes in brain and muscle. The combination of discrete blood samples and integrated microdialysis sampling enabled parallel sampling in three different compartments of individual animals (Figure 1.11).

The efficacy of nerve agent MedCM in guinea pigs has been established in many studies, yet there have been very few studies of the PK and PD of these MedCM in this species. Furthermore, the PK of MedCM has not been integrated with the PK and/or PD of nerve agents. To address this knowledge gap the studies reported here will test three linked hypotheses:

1. The efficacy of MedCM against nerve agents in guinea pigs can be better understood, rationalised and explained through determination of the PK and/or PD of MedCM and nerve agents in the blood and target tissues.

2. Co-administration of MedCM or administration of combined MedCM following nerve agent exposure may impact on efficacy through disrupted physiology and therefore, alteration of their PK. Assessment of the PK in these different administration scenarios can be used to understand the interactions and their impact on protection.

3. Simulation and modelling of MedCM and nerve agent concentration-time or concentration-effect profiles can be used to design animal efficacy studies and optimise MedCM administration regimens, to achieve maximal efficacy.

Chapter specific aims in support of these over-arching and broad aims and hypotheses can be found in Sections 3.2, 4.2 and 5.2 on pages 88, 147 and 184, respectively.

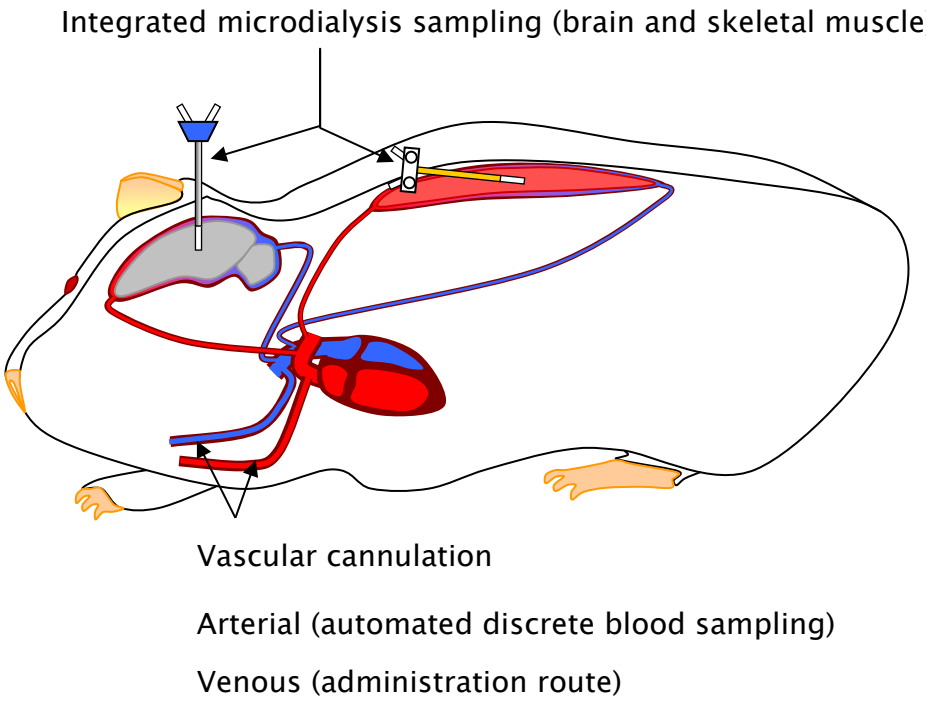

Figure 1.11. Schematic diagram illustrating concept for new methodology required to complete PK and PD studies of MedCM and nerve agents, in conscious ambulatory guinea pigs.

2. MATERIALS AND METHODS

2.1 Animals

All procedures using guinea pigs were carried out under a Home Office Animals (Scientific Procedures) Act 1986 Procedure Project Licence.

Male Dunkin Hartley guinea-pigs (Harlan Interfauna, UK) 387 ± 39 g (mean ± standard deviation (SD), n=125, range = 299 – 538 g) were used in the studies reported here. Animals were implanted on arrival with subcutaneous temperature/identity transponders (IPTT300, Plexx B.V., Netherlands) under local anaesthetic (Xylocaine 2%). Following arrival the guinea pigs acclimatised to their home cages in the laboratory for a minimum of four days. Body mass was recorded daily until surgery and connection to the blood sampling equipment. Temperatures were recorded prior to and immediately following surgery, to ensure the animals had emerged from anaesthesia and had returned to normal body temperature. Animals were kept in UK Home Office defined, standardised conditions throughout the study (room temperature 21 °C, humidity 50 %). The laboratory lights were on from 06:00 to 18:00 with 30 minutes graduated dawn and dusk periods.

2.1.1 Animal supply and background

Part way through the studies described in this thesis the supplier (Harlan Interfauna, UK) changed the colony from which the guinea pigs were supplied. This change was from a colony with a Porcellus background to a colony with a David Hall background and was made for animal welfare purposes. The strain remained Dunkin-Hartley throughout the studies described in this thesis. A bridging study carried out to determine whether this change in colony background had an effect on the PK of nerve agent MedCM, showed little difference between these two sources of guinea pigs. The results from the bridging study are detailed in Appendix A.

2.1.2 Animal training

Animals were trained to be accustomed to wearing a harness attached to a tether (Covance Harness, Instech Solomon, USA) and liquid swivel (2 channel and 5 channel swivel, Instech Solomon, USA). This equipment (Figure 2.1) was needed to enable blood sampling from conscious ambulatory animals. The training commenced following the initial acclimatisation of the guinea pigs to their home cages. Animals wore a harness attached to a tether and a 1 channel liquid swivel (Instech Solomon, USA) for a period of 10 – 15 minutes on the first occasion. Subsequent training sessions with increasing duration each time, were carried out to the point where the animal was harnessed and tethered for a period greater than 2 hours and did not show adverse behaviour. Animals that displayed adverse behaviour, such as biting and vocalisation during training, were trained on fewer occasions. All animals were suitably accustomed to the harness and tether prior to surgery taking place.

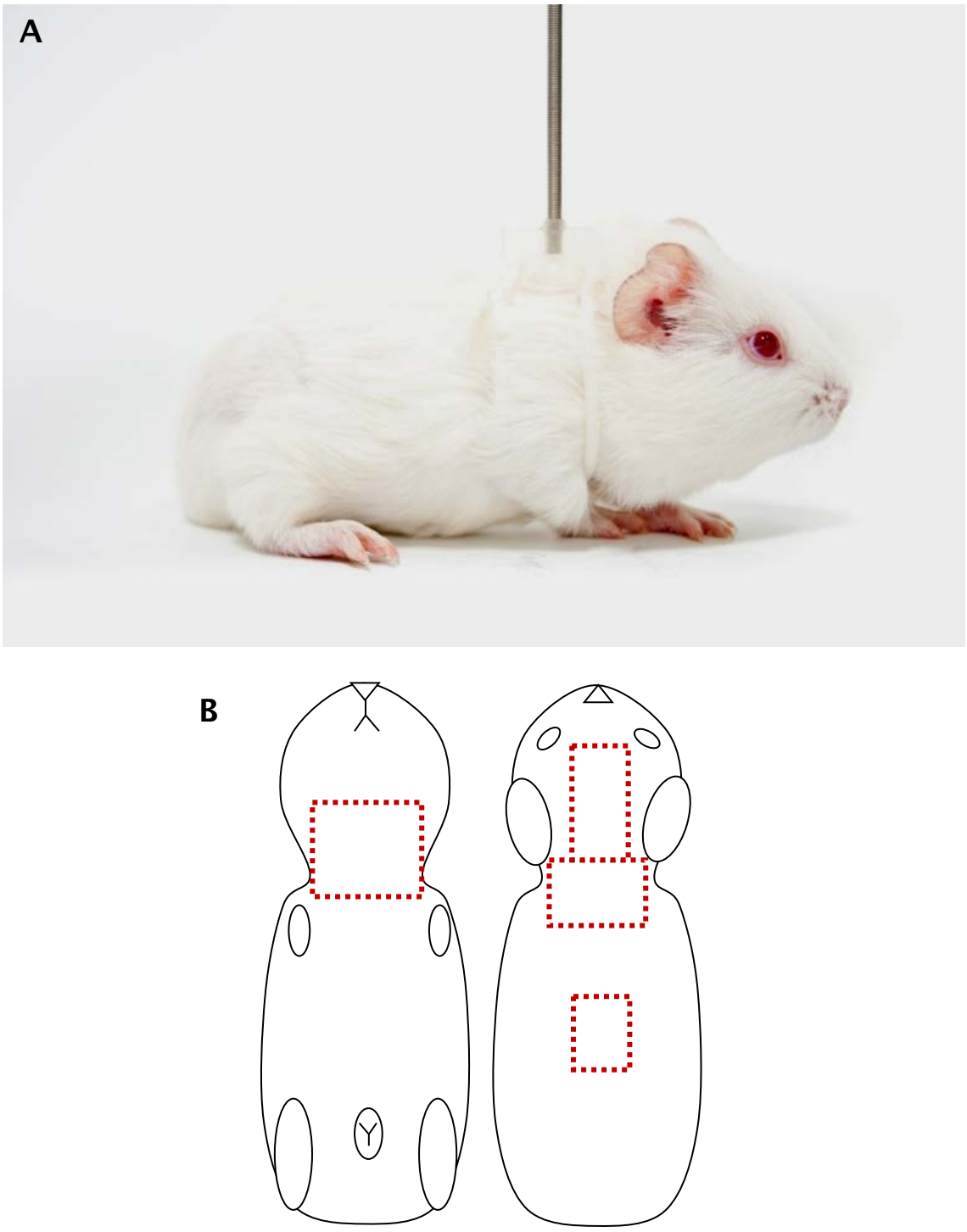

Figure 2.1. (A) Photograph of a guinea pig wearing a harness connected to a tether and swivel (latter not shown). (B) Schematic diagram showing areas close clipped prior to surgical procedures.

2.1.3 Pre-surgical preparation

To ensure that the cannulae and microdialysis probe (inlet/outlet) tubing were exteriorised at the correct site the areas of fur at the surgical incision sites were close clipped approximately 18 hours prior to anaesthesia as illustrated in Figure 2.1.

A multimodal analgesic regime and a broad-spectrum antibiotic were administered by the subcutaneous route to all animals. This consisted of the antibiotic duphatrim (30mg/kg), the non-steroidal anti-inflammatory carprofen (3.3–3.5 mg/kg) and the μ-opioid receptor agonist tramadol (10 mg/kg).

Tramadol with subsequent anaesthesia can have an additive effect on the respiratory centre in the brain [157], making adjustment of the anaesthetic dose required to achieve the appropriate depth of anaesthesia difficult. For this reason tramadol was removed from the pre-medication regime, following review of the anaesthetic and analgesic regimen, in response to the death of one animal during surgery. The Veterinary Surgeon recommended that buprenorphine was introduced to the regimen, as a substitute [158].

2.2 Surgical procedures

All surgical procedures were agreed with the Veterinary Surgeon prior to commencement of the studies, to ensure current best practice was followed and stress on the animals minimised. Implantation of cannulae and microdialysis probes were carried out at the same time, in order to reduce the number of separate surgical procedures each animal was subjected to.

The *in vivo* studies detailed in this thesis were carried out over a 32 month period. To ensure that the animals were treated with the appropriate anaesthesia and analgesia pursuant with the Home Office Personal Licence

standard conditions, several changes were made to the surgical protocol. Each of these changes to the protocol was recommended by the Veterinary Surgeon and was introduced in response to adverse events or changes in best practice. The changes made are detailed in the appropriate sections of this chapter. All changes made to the peri-operative anaesthetic / analgesia protocol are not expected to have affected the results of the PK studies. For all substances administered as part of the protocol, the recovery period between surgery and commencement of the PK studies (2 or 7 days) was adequate to provide suitable washout.

Local anaesthetic (Xylocaine) was applied to wound margins at the time of incision. Initially the xylocaine (2 %) solution contained adrenaline (the adrenalin is contained in the formulation for its vasoconstrictive action to increase the speed of onset and duration of action). Following review of the anaesthetic/analgesic regimen, the Veterinary Surgeon recommended that the total amount of xylocaine used during surgery should be reduced below 4 mg/kg, used without adrenaline and the volume used recorded. The initial doses of xylocaine used were in the toxic range (12 mg/kg); approximately 0.3 mL of 2% solution ($\approx$ 6 mg/kg). Adrenaline was excluded from the analgesic regimen because it is a natural product that is not stable and was not supplied at a known concentration.

Local anaesthetic gel (Lignocaine 2%, Biorex Laboratories, UK) was introduced to the ear canals of animals undergoing brain microdialysis guide cannulae implantation. This was completed immediately after induction of anaesthesia.

2.2.1 Anaesthesia

Anaesthesia was induced with halothane (5% with 4 L/min O_2 for 5 min) and maintained using isoflurane (1.5-2% with O_2 0.8 L/min and N_2O 0.8 L/min). The level of isoflurane and the proportions of the gases were adjusted during the procedure as required, according to the depth of anaesthesia and the rate and depth of respiration for each individual animal. N_2O was turned off at least 5

minutes before the end of anaesthesia, to prevent hypoxia during recovery. Supplementary heat was used throughout anaesthesia and for a minimum of 30 minutes following emergence from anaesthesia.

The N_2O was removed from the anaesthetic/analgesic regime following the death of one animal during surgery (the same review in which Tramadol was removed from the analgesic regimens) and review by the Veterinary Surgeon. The benefit of N_2O in small animal species is not as marked as in humans [160]. Transfer of N_2O to gaseous spaces (e.g. gastrointestinal tract and alveoli) due to its greater blood solubility [160], may worsen hypoxia should an animal stop breathing whilst under anaesthesia. For these reasons the use of N_2O during surgery was stopped.

2.2.2 Implantation of venous and arterial cannulae

All guinea pigs had a cannula implanted in their carotid artery. Animals in which MedCM were administered by the intravenous route also had a cannula implanted in their jugular vein. The procedure for cannulation was as follows: the anaesthetised guinea pig was placed in a supine position and an incision was made on the ventral side of the neck. The jugular vein was isolated by blunt dissection and was tightly ligated at the rostral end of the isolated vessel, stopping flow. A loose ligature was tied at the caudal end of the isolated section. An incision was made in the vein and a 25 cm round tip polyurethane 3 French gauge cannula (Instech Solomon, USA) filled with heparin solution (5 or 100 IU/mL) was inserted approximately 3 cm into the vessel. The loose ligature was tightened around the cannula and vessel (patency of the cannula was checked prior to the cannula being secured with two ligatures). The carotid artery was isolated by blunt dissection and was ligated as described above for the jugular vein. A small vessel clamp (Fine Science Tools, Canada) was applied to the caudal end of the exposed section below the loose ligature to occlude flow. An incision was made in the artery using small sprung iris scissors (Fine Science Tools, Canada) and a 25cm round tip polyurethane 2 French gauge cannula (Instech Solomon, USA) filled with heparin solution (5 or 100 IU/mL) was inserted approximately 3cm into the vessel. The loose ligature was

tightened around the cannula near the incision; patency of the cannula was checked prior to the cannula being secured with the two ligatures. The guinea pig was then placed in the prone position and a small incision made in the animals back, between the scapulae. The cannula(e) was/were tunnelled and exteriorised through the incision on the animals back using a trochar (Data Sciences International, USA). The guinea pig was returned to the supine position and the wound on the animal's neck was closed with sutures.

2.2.3 Muscle microdialysis probe implantation

The anaesthetised guinea pig was moved to a prone position and an incision was made to the right of the midline on the animal's back, to expose the surface of the sacrospinalis muscle. The inlet/outlet tubing for the microdialysis probe (CMA20, 20 kDa cut-off, 4 mm PAES membrane, CMA microdialysis, Sweden. Figure 2.2) was tunnelled to the same exteriorisation site as the vascular cannulae using a trochar. A needle and split introducer were used to implant the microdialysis probe in the sacrospinalis muscle [152 :153 :161]. The microdialysis probe was then secured in position using silk sutures prior to the split introducer being removed. The incision over the muscle was closed with sutures. The exteriorisation site was then closed with cyanoacrylate glue, to secure both the microdialysis tubing and cannula(e).

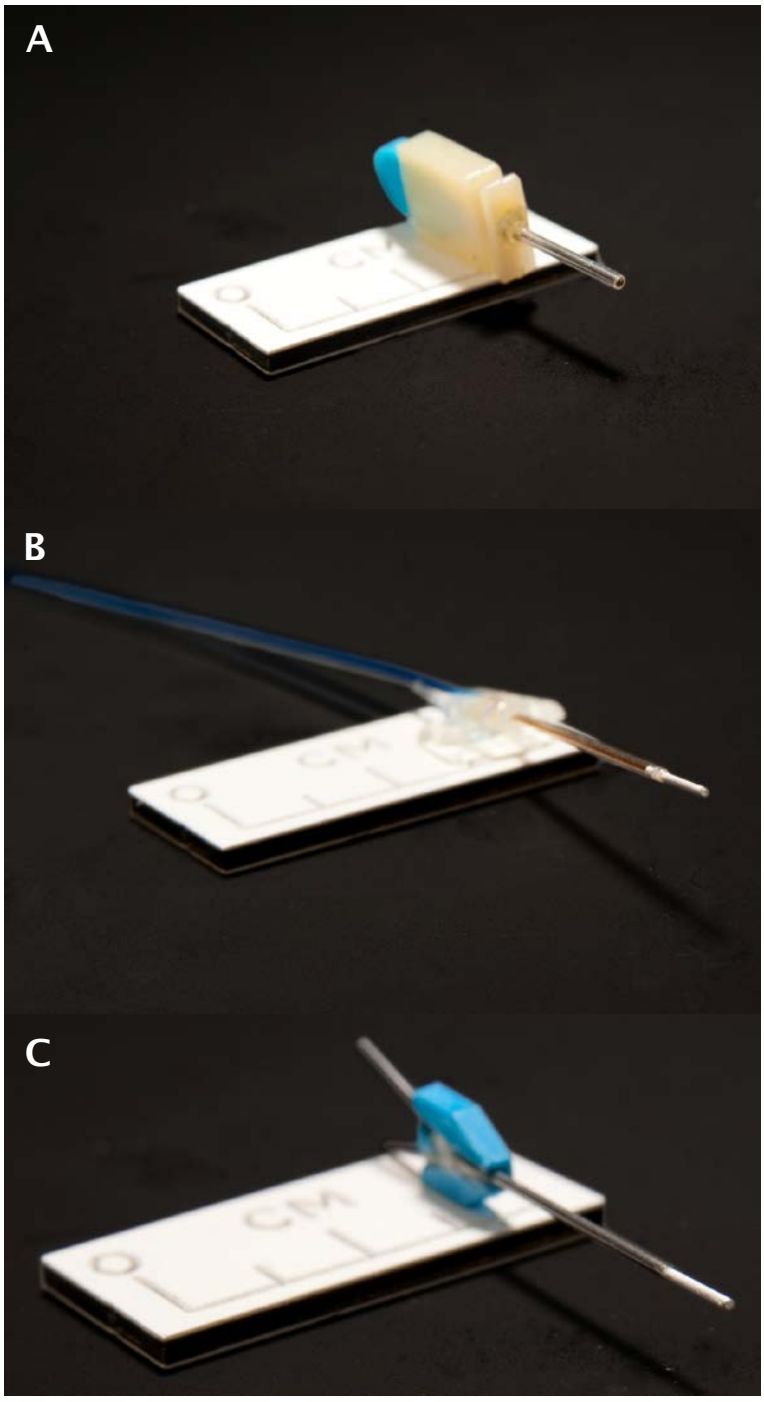

Figure 2.2. Photographs of CMA guide cannula and probes surgically implanted in guinea pigs.

(A) CMA12 guide cannula. (B) CMA20 microdialysis probe with a 4 mm PAES membrane. (C) CMA12 microdialysis probe with a 4 mm PAES membrane.

2.2.4 Brain microdialysis probe implantation

Anaesthetised guinea pigs were positioned centrally (median plane), straight and horizontal in a stereotaxic frame using atraumatic ear bars (David Kopf Instruments, USA). An incision was made along the midline of the scalp approximately 15mm in length, the skull was exposed and using a trephine drill bit (CMA microdialysis, Sweden) a hole was drilled in the skull at co-ordinates from bregma: Rostral +1.3, Lateral +2.8 (Figure 2.3). A guide cannula (CMA microdialysis, Sweden. Figure 2.2) was inserted over the caudate nucleus as detailed by Bourne and Fosbraey [162] and secured in place using two bone screws (Figure 2.3) and dental cement (Glass Ionomer Cement, Fujichem). The wound was closed with sutures.

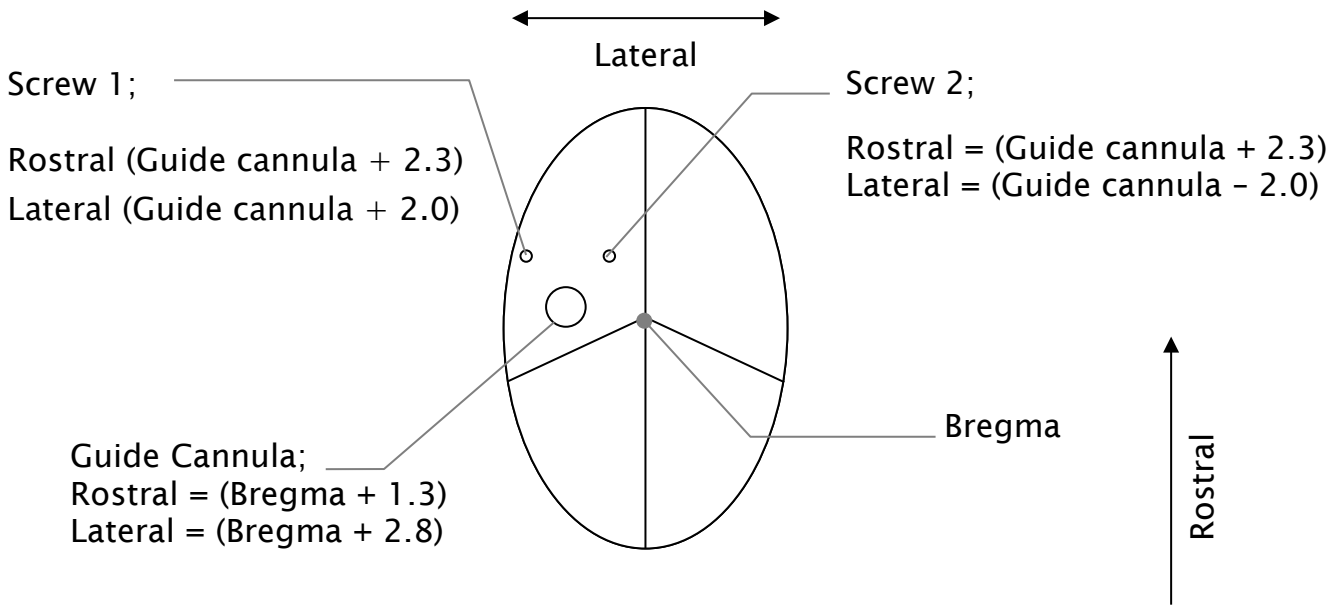

Figure 2.3. Schematic representation of a guinea pig skull during microdialysis guide cannula implantation surgery.

The vertical line and horizontal lines represent the sutures with Bregma labelled. The circles represent the approximate locations of the guide cannula and anchor screws, with co-ordinates for their positioning.

2.2.5 Post-surgical recovery procedures

Following the final surgical procedure, fluid replacement (Duphalyte 5ml *intraperitoneal*) was administered to animals, prior to their being placed in a warming cabinet (MH1200, Peco Services, UK) to assist with restoration of body temperature during emergence from anaesthesia. Following a recovery period of not less than 1 hour and on resumption of normal posture/mobility the guinea pigs were returned to their home cages.

On return of the guinea pigs to the home cage, the cannula(e) were immediately connected via the harness and tether to a syringe (1.0 mL volume 60 mm stroke, BD, UK) containing heparinised saline (5 IU/mL heparin). Cannula patency was checked and a flow of heparinised saline established, to maintain patency (0.5 µL/min, CMA402 syringe pump, CMA microdialysis, Sweden). Syringes were changed daily using fresh heparinised saline. Following a review of procedures by the Veterinary Surgeon, the use of bionectors (Vygon, UK) with heparin saline syringes was introduced, to follow best practice and reduce the risk of infection in the animals.

Muscle microdialysis probes were connected to a syringe (5.0 mL volume, 45 mm stroke, BD, UK) in the syringe pump and were perfused (~0.1 µL/min, T1 perfusate, *NaCl 147 mM, KCl 4 mM, $CaCl_2$ 2.3 mM,* CMA microdialysis, Sweden).

Guinea pigs were administered the multimodal antibiotic and analgesic regimen once daily, for two days following surgical procedures. If animals appeared not to be recovering and thriving post-surgery (e.g. piloerection, hunched posture, response to handling or lack of faecal production) the regime was continued, once daily, as required.

2.3 Study protocol

All studies were carried out after a recovery period of 2 – 7 days if animals were cannulated and 7 days if guinea pigs were cannulated and had microdialysis probes/guide cannulae implanted.

2.3.1 Administration of test compounds

All drugs administered to animals were dissolved or diluted in sterile saline (0.9 % w/v, *NaCl*), unless otherwise stated.

2.3.1.1 Intravenous administration of medical countermeasures

An intravenous bolus dose of the individual MedCM drugs (atropine sulphate [5.8 mg/kg], avizafone hydrochloride [1.05 mg/kg] or HI-6 dimethanesulphonate [9.3 mg/kg]), were administered via indwelling venous (jugular vein) cannulae at a constant dose volume of 333 µL/kg, in sterile saline.

2.3.1.2 Intramuscular administration of medical countermeasures

A single intramuscular dose of the MedCM either individually or as a combination (atropine sulphate [17.4 mg/kg], avizafone hydrochloride [3.14 mg/kg] and HI-6 dimethanesulphonate [27.9 mg/kg]) was administered at a constant dose volume (333 µL/kg), in sterile saline, into the *biceps femoris* muscle of the hind leg. This enabled the PK profile of these drugs by the proposed route of human administration to be determined in the guinea pig. The doses studied were the same as those used in previous efficacy studies [32].

2.3.1.3 Administration of human butyrylcholinesterase

The bioscavenger, huBChE (20.9 mg/mL) was purified from outdated human plasma by Baxter (Baxter International Inc., USA) and supplied for these studies by the United States Army Medical Institute of Chemical Defense, under an

Equipment and Materials Transfer Memorandum of Understanding. The huBChE was administered by the intravenous or intramuscular routes, at a volume of 163 µL/kg (3.4 mg/kg ≡ 10 nmol/kg, formula weig

2.3.1.4 Subcutaneous administration of sarin

Sarin was supplied by Detection Department, Dstl, Porton Down, at a concentration of approximately 5.0 mg/mL (98 % pure by ^{31}P nuclear magnetic resonance), in isopropyl alcohol. Sarin (43.7 µg/kg ≡ 1 × LD_{50}) was administered by the subcutaneous route to guinea pigs at a constant dose volume (1.0 mL/kg).

2.3.1.5 Application of percutaneous VX

VX was supplied by Detection Department, Dstl, Porton Down, at a concentration of approximately 10 mg/mL (>95 % pure by ^{31}P nuclear magnetic resonance) in isopropyl alcohol. The site of VX application on the dorsal side of the animal over the rump, was close clipped approximately 18 hours prior to dosing. Administration of VX by the percutaneous route was at a constant volume of 33 µL/kg, in isopropyl alcohol, at a dose of 267.4 µg/kg ≡ 1 µmol/kg.

2.3.2 Automated blood sampling

To enable multiple samples of blood to be collected from individual animals, an automated blood sampling system (ABS: Instech Solomon, USA) was used. This enabled full PK profiles to be determined from individual animals. The ABS was calibrated and animals connected to the unit by the harness and tether . The keep vessel open (KVO) function was enabled to give a 5 µL pulse of heparinised saline (5 U/mL) every minute, ensuring cannula patency was maintained. The trim volume (interface between blood and saline, Figure 2.4) was set to 80 µL and the wash volume was set to 120 µL. The ABS unit was used in low-loss mode to ensure that all but ≈ 4 µL of surplus blood removed from the animal was returned to the circulating volume of the animal. Blood

samples, when collected, were withdrawn from animals at a rate of 250 µL/min. Figure 2.5illustrates the different steps the ABS completes to collect a sample.

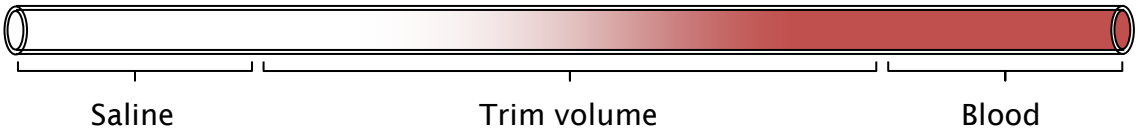

Figure 2.4. Schematic representation of blood sample in the tubing of an ABS.

The interface of saline and blood is referred to as the trim volume. Setting the trim volume on an automated blood sampler protocol ensures that only pure blood is collected in the sample vial.

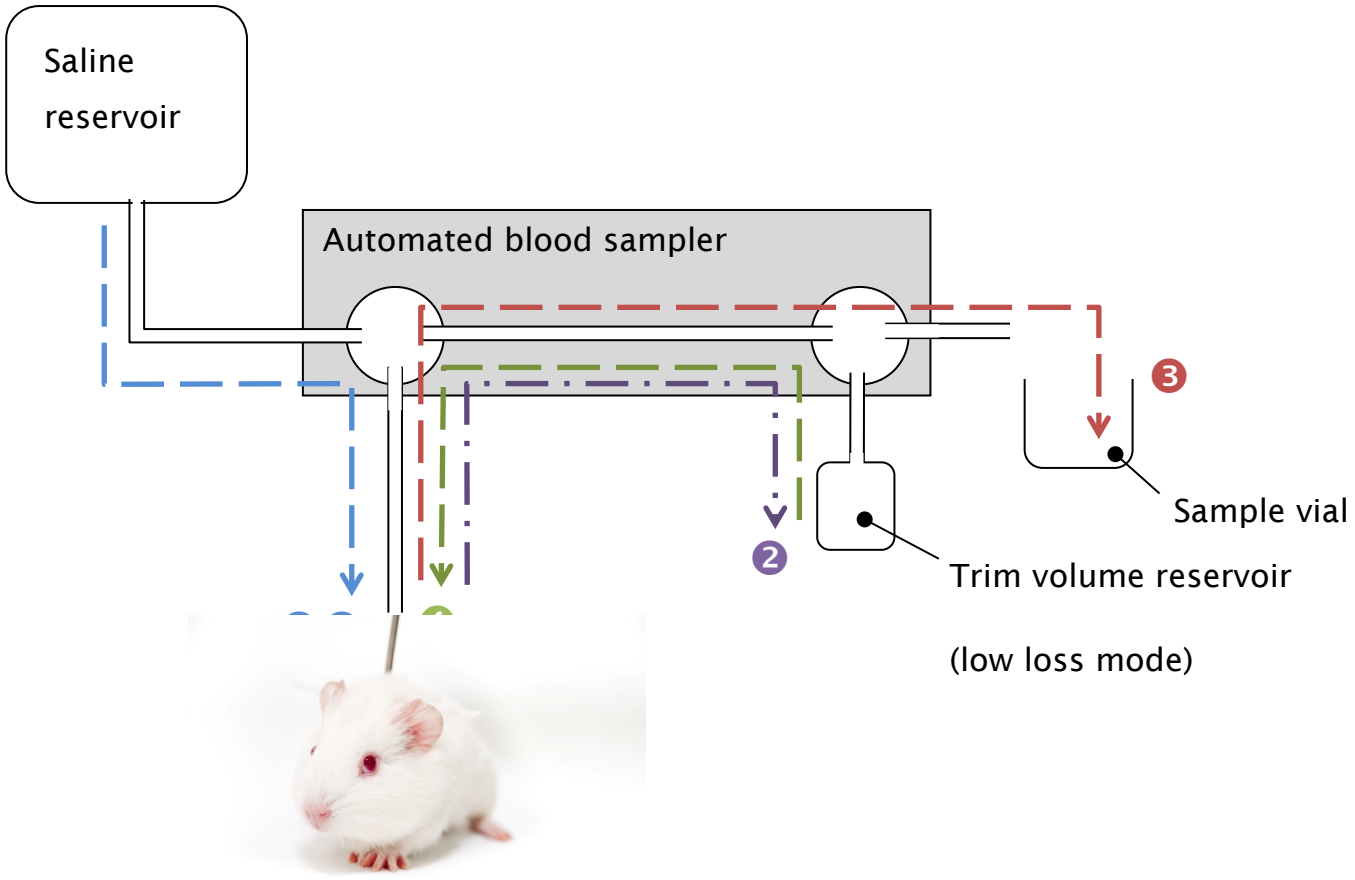

Figure 2.5. Schematic representation of procedures carried out by automated blood samplers.

❶ KVO ensures patency of cannulae is maintained; heparinised saline is pumped from reservoir to animal. ❷ Blood flows from guinea pig, trim volume stored in reservoir. ❸ Blood sample collected from guinea pig into vial for further processing. ❹ Trim volume returns

from reservoir to guinea pig. ❺ Saline, of the same volume as the blood sample, is administered to maintain fluid volume in the guinea pig.

2.3.2.1 Sampling volumes

In order to comply with the Home Office project licence, the volumes of blood collected were restricted to <10 % of total blood volume for a single sample and ≤15 % of total blood volume for repeated samples over a 28 day period. The total blood volume of a guinea pig is 67 – 92 mL/kg [164], therefore, a 350 g guinea pig was assumed to have 23.5 – 32.2 mL of blood. As the sampling from the animal was repeated a total 15 % of blood volume or 3.5 – 4.8 mL could be collected. Using the ABS unit enabled a total of 15 pre-programmed samples to be collected automatically, so a volume of 230 - 320 µL per sample was possible. The sample volume collected was set to 150 - 250 µL on the ABS. These volumes of blood provided approximately 75 - 125 µL of plasma, sufficient for quantitation of the MedCM and determination of cholinesterase activity.

2.3.3 Blood sampling protocols

The fifteen pre-programmed blood samples were collected by ABS at different time-points. These were altered depending on the MedCM or nerve agent being studied and the route of administration. The time-points for each protocol are listed in Table 2.1 and schematic figures of each protocol are also presented in the relevant chapter of this thesis.

Time of sample acquisition (hours)					
MedCM		Nerve Agent		huBChE	
i.v.	i.m.	s.c.	p.c.	i.v.	i.m.
0.02	0.02	0.02	0.5	0.02	6.0
0.08	0.08	0.08	1.0	0.25	12.0
0.17	0.17	0.17	1.5	0.5	18.0
0.25	0.33	0.33	2.0	1.0	20.0
0.33	0.5	0.5	2.5	1.5	22.0
0.50	0.67	0.67	3.0	2.0	24.0
0.75	0.83	0.83	3.5	4.0	26.0
1.0	1.0	1.0	4.0	6.0	28.0
1.5	1.25	1.25	4.5	8.0	30.0
2.0	1.5	1.5	5.0	12.0	36.0
3.0	2.0	2.0	5.5	24.0	42.0
6.0	2.5	2.5	6.0	36.0	48.0
8.0	3.0	3.0	7.0	48.0	60.0
12.0	3.5	3.5	8.0	60.0	72.0
24.0	4.0	4.0	12.0	72.0	84.0
No 0 hours time-point	Manual 0 hours time-point		Manual samples at 0, 18, 24, 30 and 48	Manual samples at 0, 96, 120 and 144.	

Table 2.1. Blood sampling protocols used with the automated blood sampling system.

Each of these protocols aimed to achieve greatest temporal resolution at the expected T_{max} [130:136] or the fastest rate of change in concentration of the MedCM or nerve agent being studied. All time-points are listed in hours and notes indicate times that blood samples were collected manually via the cannulae.

2.3.4 Microdialysis sampling

Prior to the administration of nerve agent or MedCM, the stop in the surgically implanted guide cannula was removed and a microdialysis probe (CMA12, 20 kDa cut-off, 4 mm PAES membrane, CMA microdialysis, Sweden) inserted into the brain, via the guide cannula. These brain microdialysis probes were perfused with **CNS** perfusate (*NaCl 147 mM, KCl 2.7 mM, $CaCl_2$ 1.2 mM, $MgCl_2$ 0.85 mM*, CMA, Sweden). The rate of perfusion of the surgically implanted muscle microdialysis probe was also increased from 0.1 µL/min (rate used to maintain patency) to the rate to be used in the pharmacokinetic study (2.0 or 1.0 µL/min for conventional MedCM studies or percutaneous VX and bioscavenger studies, respectively). Both microdialysis probes were perfused for a 60 minutes period, to enable equilibration of the probes, prior to the administration of the test compound, as detailed for previous studies [134 :151 :152 :165]. Microdialysate fractions were collected at regular intervals and these were altered depending on the MedCM or nerve agent being studied and the route of administration. The time-points for each protocol are listed in Table 2.2. Schematic figures of each protocol are also presented in the relevant chapter of this thesis.

Time of fraction collection (hours)		
MedCM	Nerve agent	
i.m.	s.c.	p.c.
2.0 µL/min	2.0 µL/min	1.0 µL/min
0 – 0.25	0 – 0.25	0 – 1
0.25 – 0.5	0.25 – 0.5	1 – 2
0.5 – 0.75	0.5 – 0.75	2 – 3
0.75 – 1.0	0.75 – 1.0	3 – 4
1.0 – 1.25	1.0 – 1.25	4 – 5
1.25 – 1.5	1.25 – 1.5	5 – 6
1.5 – 2.0	1.5 – 2.0	6 – 7
2.0 – 2.5	2.0 – 2.5	7 – 8
2. 5 – 3.0	2. 5 – 3.0	8 – 10
3.0 – 3.5	3.0 – 3.5	10 – 12
3.5 – 4.0	3.5 – 4.0	12 – 14
		14 – 16
		16 – 18
		18 – 20
		20 – 22
		22 – 24
		24 – 28
		28 – 32
		32 – 36
		36 – 40
		40 – 44
		44 - 48

Table 2.2. Microdialysis fraction collection protocols.

Each of these protocols aimed to achieve greatest temporal resolution at the expected time of the fastest rate of change in concentration of the MedCM or nerve agent being studied. All time-points are listed in hours.

2.3.5 Sample preparation

Following collection, blood samples were removed from the refrigerated ABS carousel and centrifuged for 1 minute (13,300 revolutions per minute ≡ 17,000 × gravity, Heraeus Pico 17 centrifuge, Thermo Scientific, UK). The plasma was decanted from the erythrocyte pellet into a separate vial. The erythrocytes were re-suspended in saline (0.9 % w/v, *NaCl*) to the original volume. Aliquots (5 µL) of plasma or re-suspended erythrocytes from animals exposed to VX were diluted in 1 mL of 0.1 M phosphate buffer (pH 8.0), for cholinesterase analysis. The plasma and erythrocyte samples were immediately frozen (-20 ˚C) and stored at -80 ˚C until analysis.

Microdialysate samples were removed from the refrigerated fraction collector carousel, sealed and immediately frozen (-20 ˚C) and subsequently stored at -80 ˚C until analysis.

2.4 Assay of cholinesterase activity

Both plasma butyrylcholinesterase and erythrocyte acetylcholinesterase activity were determined spectrophotometrically using a modified version of the method described by Ellman et al [166]. Briefly; the reagents 5-5'-Dithiobis(2-nitrobenzoic acid) (Sigma-Aldrich, UK), acetylthiocholine or butyrylthiocholine (Sigma-Aldrich, UK) were prepared in distilled water to achieve final cuvette concentrations of 330 µM, 1 mM or 10 mM, respectively. The plasma or erythrocyte samples were diluted 1:200 in 0.1 M phosphate buffer (pH 8.0) and subsequently 1:3 in the cuvettes. The samples, reagents and assay were incubated at 30 ˚C. The reaction was started by addition of the sample and the change in absorbance was measured at 412 nm on a spectrophotometer (UV 1800, Shimadzu, UK) over six minutes for plasma samples and over ten minutes for erythrocyte samples. If the reaction rate was not linear over this period the samples were diluted to achieve linearity (this occurred primarily with samples containing human butyrylcholinesterase, for which a dilution of 1:1000 was routinely required). The rate of change in absorbance and

subsequent activities were calculated (Equation 2.1) from raw absorbance data using Prism (version 5.01, GraphPad Software, Inc. USA).

$$R = \left(\frac{\Delta A}{\varepsilon}\right) \times L \times \left(\frac{V}{v}\right) \times D$$

Equation 2.1. Method of calculating AChE or BChE activity using spectrophotometric data.

Where, R = rate (μmol/min/mL); ΔA = change in absorbance (mAbs/min); ε = molar extinction coefficient of 5-5'-Dithiobis (2-nitrobenzoic acid) = 13,600 (L/mol/cm); L = cuvette path length (cm); V = cuvette volume (mL), v = sample volume (mL) and D = dilution factor of sample.

2.5 Quantitation of analytes

2.5.1 Quantitation of VX

Quantitation of VX in microdialysates, plasma and erythrocytes was carried out by the Dstl Analytical Chemistry team, Detection Department, using liquid chromatography tandem mass spectrometry with electrospray ionisation (LC-MS-MS-ESI). The methods were similar to those described by Wetherell *et al* [141] but with some modifications.

The methods detailed here were written by Robert Read, the analytical chemist who developed the methodology for quantitation of VX in the samples.

Microdialysates in both muscle and brain buffer were analysed as received, with no dilution necessary. VX was quantitated against calibration standards prepared in the appropriate buffer over the range 0.002 to 1 ng/mL. Following addition of Russian VX (*o*-isobutyl S-(N,N-diethylaminoethyl)methyl phosphonothioate, RVX) internal standard (final concentration = 0.05 ng/mL) and basification with sodium hydroxide (1 M), plasma and erythrocytes were

extracted with methanol / hexane and the solvent exchanged to water as previously described [141]. Plasma (50 µL) was extracted without dilution; entire samples of erythrocytes were diluted to the original blood volume (250 µL) prior to extraction. VX was quantitated against calibration standards prepared in plasma and erythrocytes over the range 0.01 to 1 ng/mL (plasma) or 0.002 to 0.5 ng/mL (erythrocytes). Linear calibrations with R^2 >0.99 were obtained.

LC-MS-MS of microdialysates and plasma extracts was performed using an Accela 1250 pump and autosampler (Thermo Scientific, UK), and TSQ Quantum Ultra triple quadrupole mass spectrometer (Thermo Scientific, UK). The mass spectrometer was equipped with a heated electrospray ionisation (HESI) source. Liquid chromatography was performed on Gemini-NX C18, 3 µm particle size, columns (Phenomenex, UK). A 150 x 2.1 mm column with isocratic elution was used for microdialysates and a 50 x 2.1 mm column with gradient elution, for plasma and red cell extracts. The mobile phase consisted of A: 0.05 % trifluoroacetic acid in water and B: 0.05% trifluoroacetic acid in acetonitrile. The isocratic elution for microdialysates used a composition of 80 % A: 20 % B at a flow rate of 0.2 mL/min. The gradient for plasma and red cell extracts was 5 % B for 1 min, increasing to 90 % B at 9 min, and held at 90 % B for 1 min, at a flow rate of 0.2 mL/min. In both cases, the column was held at 25 °C and column eluent was diverted to waste for the first 2 min. Autosampler tray temperature was 10 °C and injection volume 10 µL.

The mass spectrometer was operated in positive ion selected reaction monitoring mode. Transitions monitored were *m/z* 268 → 128 at 17 eV collision energy for VX and *m/z* 268 → 100 at 17 eV collision energy for RVX. Collision gas was argon at 1 mTorr pressure. Source conditions were: HESI vaporiser 350 °C, spray voltage 4.5 kV, sheath gas (nitrogen) 40 (arbitrary units), auxiliary gas (nitrogen) 15 (arbitrary units) and ion transfer tube temperature 300 °C. Skimmer offset was set at 5 V.

Red cell extracts were analysed using a Surveyor MS pump, autosampler, and TSQ Quantum mass spectrometer with electrospray ionisation (Thermo

Scientific, UK) as previously reported [141]. The LC column and conditions were as above, and mass spectrometer settings as previously reported, with the addition of the transition for RVX internal standard.

2.5.2 Quantitation of pharmacological medical countermeasures

Quantitation of atropine, diazepam, hyoscine, HI-6 and physostigmine in guinea pig plasma was carried out by Dstl Analytical Chemistry team, Detection Department, Porton Down, UK. Quantitation was performed using LC-MS-MS-ESI.

The methods detailed here were written by Sarah Stubbs, the analytical chemist who developed the methodology for quantitation of the MedCM in the samples.

Calibration curves were prepared in guinea pig plasma (50 µL) across the range 0.1 – 100 ng/mL for atropine and diazepam, 0.1 – 50 ng/mL for hyoscine and 0.1 – 20 ng/mL for physostigmine. Calibration curves were prepared in guinea pig plasma (20 µL) across the range 100 – 50,000 ng/mL for HI-6.

HI-6-d_4 chloride was used as an internal standard for HI-6 quantitation. Where deuterated internal standards were not available alternative compounds were used. Atropine was used as an internal standard for quantitation of hyoscine and *vice versa*, prazepam was used as an internal standard for diazepam and phenserine was used as an internal standard for quantitation of physostigmine.

Where necessary, samples were diluted with guinea pig plasma prior to extraction to enable quantitation within the calibration range.

For quantitation of atropine, diazepam, hyoscine and physostigmine, guinea pig plasma (50 µL) was spiked with corresponding internal standard at a

concentration of 10 ng/mL. Guinea pig plasma (50 µL) was precipitated with acetonitrile (150 µL), vortexed (30 s) and centrifuged (12,000 × g, 10 min). Supernatant (150 µL) was removed and taken to dryness using a centrifugal evaporator (40 ˚C, 80 min). Extract was re-dissolved in water (50 µL) and analysed by LC-MS-MS-ESI.

Samples were quantitated using calibration curves, by comparison of peak area ratios between compound and corresponding internal standard. All calibration curves were linear with $R^2 > 0.99$.

LC-MS-MS of plasma extracts for atropine, diazepam, hyoscine and physostigmine quantitation, was performed using a Surveyor MS pump and autosampler (Thermo Scientific, UK), and TSQ Quantum triple quadrupole mass spectrometer with electrospray ionisation (Thermo Scientific, UK). Liquid chromatography was performed on Gemini-NX C18, 3 µm particle size, 150 x 2 mm I.D. columns (Phenomenex, UK), fitted with Gemini-NX C18 security guard cartridges (Phenomenex, UK). Mobile phase consisted of A: 0.05% formic acid in water and B: 0.05% formic acid in acetonitrile. The gradient was 2% B for 2 min, increasing to 90% B at 5 min, held at 90% B for 2 min, decreasing to 2% B at 10 min and held for 2 min. Mobile phase flow rate was 0.2 mL/min. Column oven temperature was 30 ˚C. Autosampler tray temperature was 10 ˚C, needle wash solvent was acetonitrile: water (50:50) and injection volume was 10 µL.

The mass spectrometer was operated in positive ion selected reaction monitoring mode. Ion transitions and collision energies for target compounds and internal standards are detailed in Table 2.3.

Collision gas was argon at 1.5 mTorr pressure. Source conditions were: spray voltage 3.0 kV, sheath gas (nitrogen) 45 (arbitrary units), auxiliary gas (nitrogen) 20 (arbitrary units) and ion transfer tube temperature 275 ˚C. Skimmer offset was set at 15 V.

For quantitation of HI-6, guinea pig plasma (20 µL) was precipitated with 0.1% formic acid in water: methanol, 1:1, v/v, (250 µL) containing internal standard (200 ng/mL HI-6-d_4 chloride). Extracts were vortexed (30 s) and centrifuged (13,800 × g, 10 min). Supernatant (200 µL) was removed and analysed by LC-MS-MS-ESI.

Samples were quantitated using calibration curves, by comparison of peak area ratios between compound and corresponding internal standard. All calibration curves were linear with $R^2 > 0.99$.

LC-MS-MS of plasma extracts for HI-6 quantitation, was performed using a Surveyor MS pump, autosampler and TSQ Quantum triple quadrupole mass spectrometer with electrospray ionisation (Thermo Scientific, UK). Liquid chromatography was performed on ZIC HILIC, 3.5 µm particle size, 50 x 2.1 mm I.D. columns (Phenomenex, UK). Mobile phase consisted of A: 40 mM ammonium formate in water (adjusted to pH 3 with formic acid) and B: methanol. Isocratic separation was performed using a mobile phase composition of 50% A and 50 % B with a flow rate of 0.2 mL/min, the run time was 5 min. Column oven temperature was ambient and autosampler tray temperature was 10 ˚C. Needle wash solvents were A: 0.1% formic acid in acetonitrile: propan-2-ol: water (4:3:3, v/v) and B: methanol. Injection volume was 5 µL.

The mass spectrometer was operated in positive ion selected reaction monitoring mode. Ion transitions monitored were *m/z* 287.1 → 165.1 at 12 eV collision energy for HI-6 and *m/z* 291.2 → 165.1 at 1
HI-6-d_4 chloride.

Collision gas was argon at 1.0 mTorr pressure. Source conditions were: spray voltage 3.0 kV, sheath gas (nitrogen) 45 (arbitrary units), auxiliary gas

(nitrogen) 20 (arbitrary units) and ion transfer tube temperature 275 ˚C. Skimmer offset was set at 12 V.

Compound	Selected reaction monitoring ion transition (*m/z*)		Collision energy (eV)
Atropine	290.0	→ 124.0	30
Diazepam	285.0	→ 257.0	20
Hyoscine	304.0	→ 138.0	20
Physostigmine	276.3	→ 162.2	20
Prazepam	325.4	→ 271.2	25
Phenserine	338.4	→ 281.2	15

Table 2.3. Selected reaction monitoring ion transitions and collision energies for target compounds and internal standards.

2.5.3 Quantitation of butyrylcholinesterase

The concentrations of human butyrylcholinesterase in plasma samples from guinea pigs administered human butyrylcholinesterase were determined from a standard curve. The standard curve was constructed from serial dilutions of the stock solution supplied from Baxter and the concentrations used were 209.9 – 0.1 µg/mL. The cholinesterase activity of each of these concentrations was assayed in triplicate by the Ellman method. GraphPad Prism (version 5.01, GraphPad Software, Inc. USA) was used to determine the unknown concentrations from the standard curve.

2.6 *In vitro* calibration of microdialysis probes

Brain and muscle microdialysis probes were calibrated *ex vivo* to determine the efficiency with which they were able to equilibrate with the MedCM or VX concentration in the interstitial fluid in which they were sited.

2.6.1 Medical countermeasure calibration

Atropine sulphate, diazepam or HI-6 dimethanesulphonate were used to calibrate the probes. *Ex vivo* microdialysis probes (n=4) were placed in chambers (1.5 mL volume) containing 5 ng/mL of the atropine or diazepam or 5 µg/mL of HI-6. The chambers were maintained at 37 ˚C. The probes were perfused as per the *in vivo* studies (2.0 µL/min with T1 or CNS perfusion fluid for muscle and brain probes respectively). Microdialysate fractions were collected at 60-minute intervals. The equilibration of the probes with the analyte solution was carried out over four hours (the same duration as the *in vivo* studies. Microdialysate fractions were immediately frozen, stored at -80 ˚C prior to transfer to the analytical chemistry laboratory for analysis by LC-MS-MS-ESI.

2.6.2 VX calibration

Radiolabelled (^{14}C) VX (radiochemical purity > 98% measured by ^{1}H and ^{31}P NMR, specific activity = 1.33 GBq/mmol) was used to determine the efficiency of the probes. Microdialysis probes, both new and *ex vivo* probes (n=4), were placed in chambers containing 250 ng/mL of VX (5.32 kBq/µg VX) which were maintained at 37 °C. The probes were perfused as per the *in vivo* studies (1.0 µL/min, with T1 or CNS perfusion fluid for muscle and brain probes respectively). Microdialysate fractions were collected at hourly intervals. After six hours of equilibration and fraction collection, the VX solution chambers were replaced with chambers containing saline (0.9 % w/v, *NaCl*) and sampling continued for further 18 hours.

Scintillation fluid (20 mL, Ultima Gold cocktail, Perkin-Elmer, UK) was added to the dialysate fractions (60 µL) and radioactivity was counted for five minutes on a liquid scintillation counter (Tri-Carb 2910 TR, Perkin-Elmer, UK), using the ^{14}C-quench curve library supplied by the manufacturer. Single-photon (non-radioactive) events were excluded. Radioactivity counts in both microdialysates and the original chamber solutions were converted to VX amounts and concentrations using specific activity of the VX and the respective volumes. Efficiency of the microdialysis probes was calculated using these concentrations.

2.7 Pharmacokinetic analyses

All pharmacokinetic and pharmacodynamic analysis was carried out using Phoenix WinNonlin (version 6.1, Pharsight, USA).

2.7.1 Noncompartmental analysis

Noncompartmental analysis was initially carried out on mean concentration-time data, to provide area under the concentration-time curve, terminal rate constants (λ_z) and a semi-logarithmic XY plot of the concentration-time data.

To calculate λ_z (slope of the terminal decrease in concentration, Figure 2.6) the software completes regression using the natural logarithm of the last three data points (non-zero), then the last four, the last five and so on until C_{max}. An R^2 value is calculated for each regression and the λ_z for the regression with the largest R^2 is reported.

2.7.2 Compartmental analysis

The concentration-time data were examined on the semi-logarithmic XY plot to determine whether the concentration declined in an exponential, bi-exponential or tri-exponential manner. A compartmental model with corresponding number of compartments was then fitted to the pooled concentration data and PK parameters were generated (Table 2.4, Figure 2.6 and Figure 2.7). In addition, the choice of model was also based on which compartmental model or weighting had the lowest Akaike Information Criterion (AIC), as detailed in Abbara *et al* [167]. The AIC provides a measure of goodness of fit of a compartmental model.

Initial estimates of parameters for the compartmental models were taken from noncompartmental analysis of the same data. However, if compartmental analysis had already been carried out on data for the same MedCM, by a different route or under different experimental conditions (e.g. individual intramuscular administration), the PK parameters generated from these analyses were used as initial estimates.

Parameter	Definition	Equation
Maximum concentration (C_{max})	Highest concentration of the drug following extravascular administration.	see Figure 2.6
Time of maximum concentration (T_{max})	Time at which C_{max} was achieved.	see Figure 2.6
Exposure (AUC)	Area under the concentration–time curve.	Calculated using trapezoidal rule (see Figure 2.6) or $AUC = \frac{Dose}{CL}$
Volume of distribution (V_d)	Apparent volume of distribution of the drug.	$V = \frac{Dose}{C_0}$ or $V = \frac{CL}{k}$
Rate of clearance (Cl)	Total clearance of the drug from plasma.	$Cl = \frac{Dose}{AUC}$ or $Cl = k \cdot V$
Rate constant (k, k_a or k_{10} *etcetera*)	Rate of absorption or elimination (k_a or k).	$k = \frac{CL}{V}$ (also see Figure 2.6)
Half-life (T½)	Amount of time taken for the concentration to increase or decrease by a factor of 2	$T½ = \frac{ln(2)}{k} = \frac{0.693}{k}$

Table 2.4. PK parameters and the equations for calculating them.

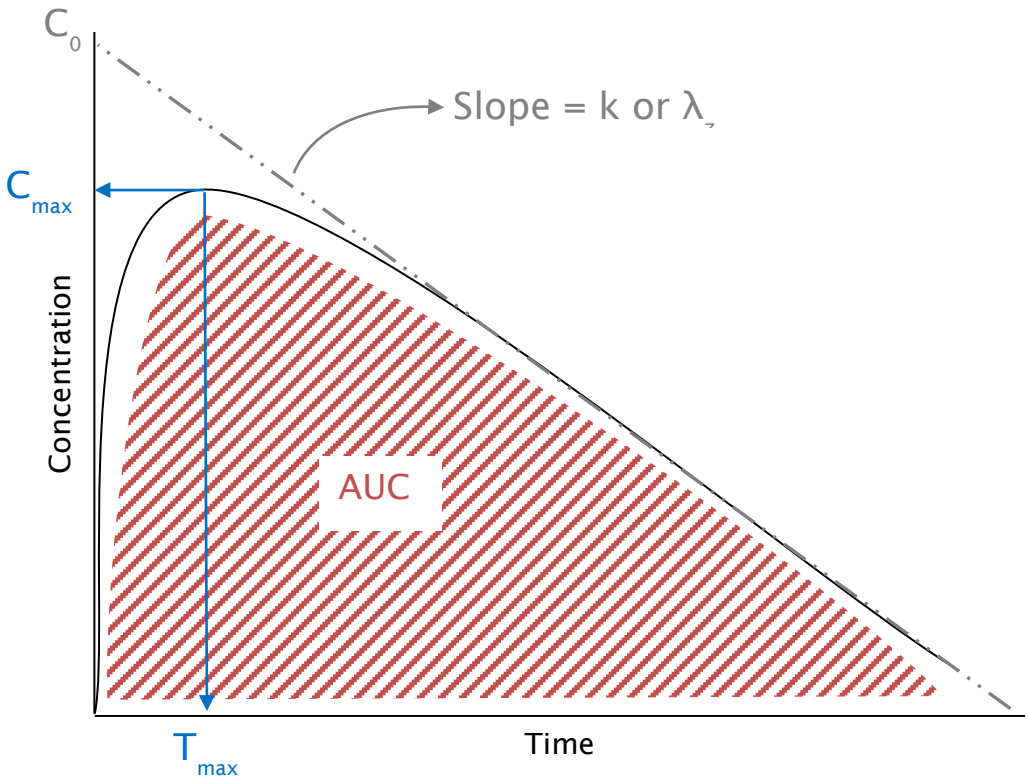

Figure 2.6. Schematic concentration-time profile showing PK parameters calculated or measured.

AUC can be calculated as detailed in Table 2.4 or by summing the trapezoid areas (mean concentration × time) of the measured concentrations at each time interval.

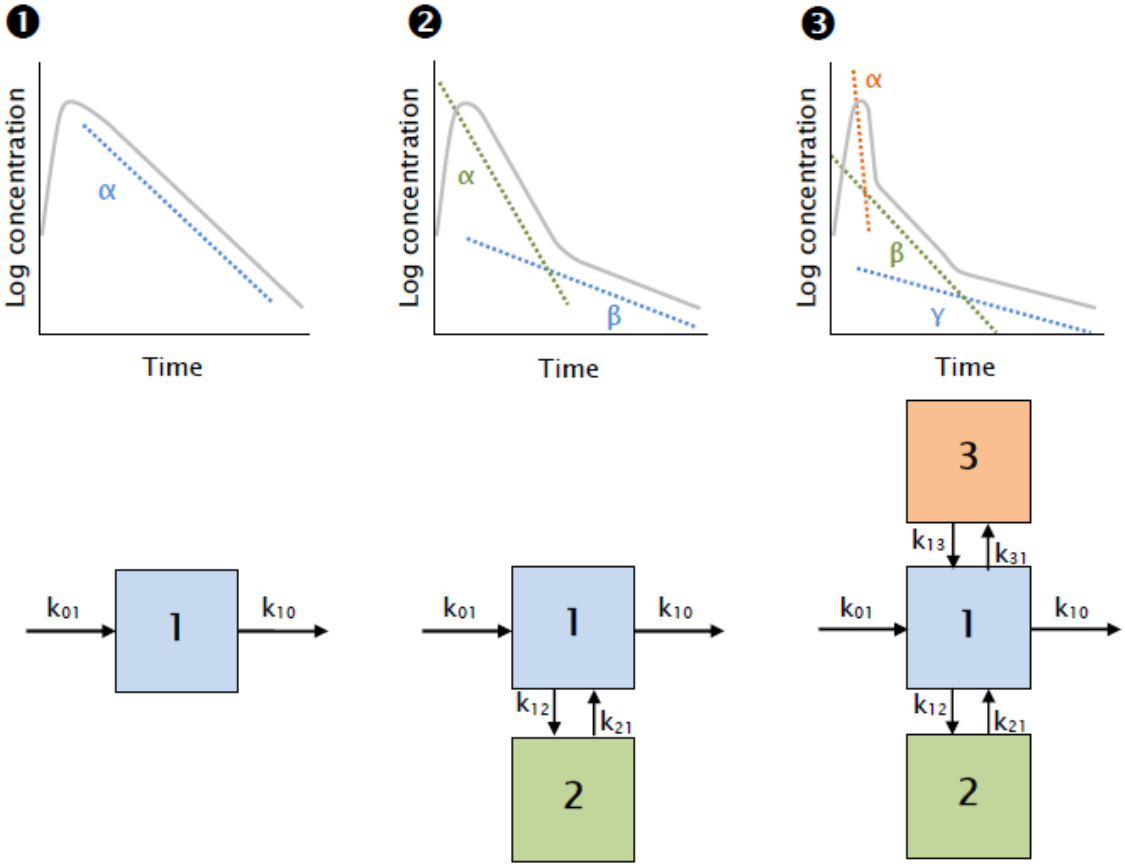

Figure 2.7. Schematic representation of one, two and three compartment PK models. ❶ Shows a typical concentration time plot with a single exponential decrease (α = slope) and below is the theoretical one compartment model. ❷ Shows a typical concentration time plot with a double exponential decrease (α and β = slopes) and below is the theoretical two-compartment model, with compartment 2 accounting for distribution into a reservoir. ❸ Shows a typical concentration time plot with a triple exponential decrease (α,β and γ = slopes) and below is the theoretical three-compartment model, with compartments 2 and 3 accounting for distribution into two different reservoirs at different rates (e.g. low and high perfusion rates respectively).

2.8 Pharmacodynamic analysis

All pharmacodynamic analysis was carried out using Phoenix WinNonlin (version 6.1, Pharsight, USA).

2.8.1 Noncompartmental analysis

Noncompartmental analysis was carried out on mean AChE or BChE activity data, where no concentration data was available. The analysis provided baseline effect (E_0), maximum inhibition of activity (I_{max}), minimum activity (R_{min}) as a percentage of baseline and the time of R_{min} or I_{max} (T_{min}). The analysis also calculated two slopes; the rate of inhibition and the rate of recovery of activity.

To calculate these slopes the software completed regression analysis as for λ_z (see section 2.7.1), once at the beginning and once at the end of the activity-time curves.

2.8.2 Pharmacodynamic model

Concentration data were plotted against cholinesterase activity on a semi-logarithmic scale. Inhibitory PD models were fit to the pooled concentration-effect data. The choice of model used to fit the data was based on the AIC, as detailed in Section 2.7.2. If PD analysis had already been carried out on concentration-effect data for the same MedCM drug, the PD parameters generated from these analyses were used as initial estimates. In cases where this information was not available, no initial estimates were provided.

The PD parameters calculated by the inhibitory models and the equations used to calculate these are detailed in Table 2.5 and Figure 2.8.

Parameter	Definition	Equation
Baseline effect (E_0)	Baseline effect measurement.	see Figure 2.8
Maximum inhibition (I_{max})	Maximum inhibition caused by drug.	see Figure 2.8
Concentration at 50% inhibition. (IC_{50})	Concentration at which half the maximum inhibition was achieved.	see Figure 2.8
Observed maximum inhibition (R_{max})	Maximum inhibition from baseline	$R_{max} = E_0 - I_{max}$
Change from baseline effect (FI_{max})	Fractional change in effect from baseline	$FI_{max} = \frac{I_{max}}{E_0}$
Gamma (γ)	Hill slope (shape parameter)	see Figure 2.8

Table 2.5. Pharmacodynamic parameters calculated by inhibitory pharmacodynamic models.

The equations used to calculate these parameters are included.

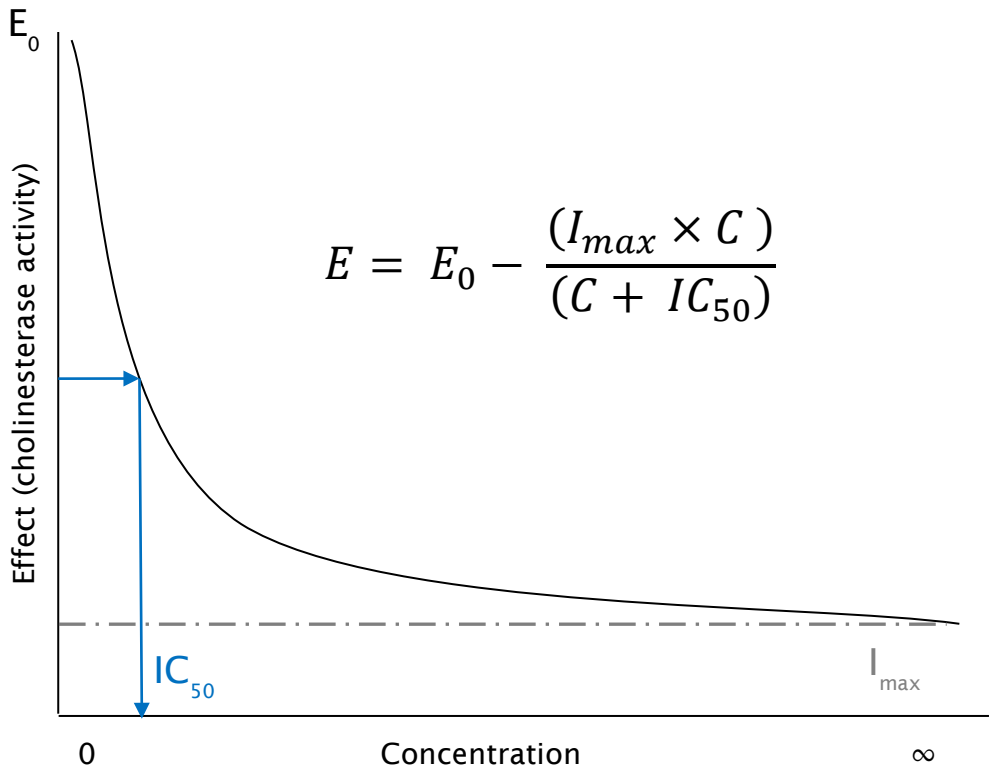

Figure 2.8. Schematic concentration-effect profile showing PD parameters calculated or measured.

The effect (E) at any given concentration can be calculated using the equation shown. If a sigmoidal model was used the shape parameter ɣ was added to the equation, as an exponent f or all concentration terms.

2.9 Linked pharmacokinetic and pharmacodynamic analysis

PK and PD data were linked in a model which combined the PK and PD models found to best fit the data. This enabled the characterisation of inhibition of cholinesterase with time and concentration. The same PK and PD parameters as defined in Sections 2.7.2 and 2.8.2 were calculated in addition to the exit rate constant from the effect compartment (k_{e0}). The k_{e0} parameter linked the hypothetical effect compartment to the PK model [168] (Figure 2.9), by providing an estimate for the lag between the plasma concentration-time curve and the effect compartment concentration-time curve. The k_{e0} enabled the concentration in the effect compartment to be calculated. The choice of model and weighting used to fit the data was based on the AIC, as detailed in Section 2.7.2. The PK and PD parameters generated from previous analyses were used as initial estimates for the model.

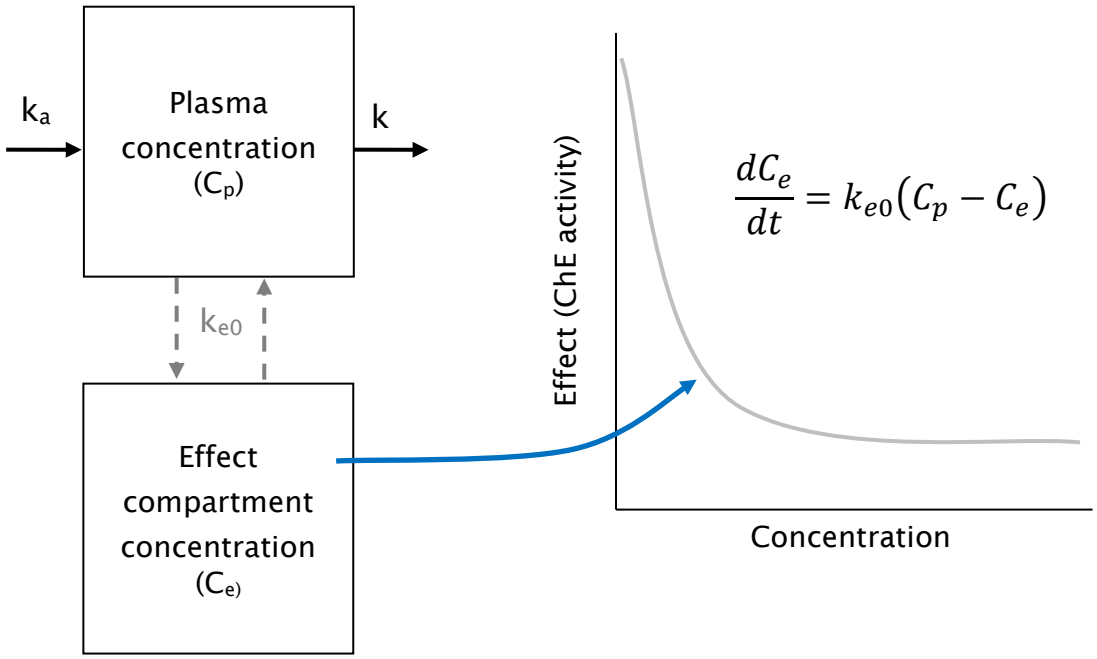

Figure 2.9. Schematic representation of the linked PKPD model showing the effect compartment exit constant, k_{e0}.

2.10 Bioavailability

Bioavailability (the fraction of the dose administered entering the systemic circulation) following intramuscular administration of a MedCM, was calculated using Equation 2.2. Mean AUCs were used to calculate bioavailability and therefore, the error on the bioavailability was calculated by compounding the errors associated with the two mean AUCs using Equation 2.3. The mean AUCs used to calculate bioavailability were determined by non-compartmental analysis.

$$Bioavailability\ (F) = \left(\frac{AUC_{im}}{AUC_{iv}}\right) \cdot \left(\frac{Dose_{iv}}{Dose_{im}}\right)$$

Equation 2.2. Equation used to calculate bioavailability.

AUC_{im} and AUC_{iv} are the area under the concentration curves following intramuscular and intravenous administration respectively. $Dose_{im}$ and $Dose_{iv}$ are the doses administered by these respective routes.

$$Bioavailability\ error = \left(\sqrt{\left(\frac{AUC_{im}error}{AUC_{im}}\right)^2 + \left(\frac{AUC_{iv}error}{AUC_{iv}}\right)^2}\right) \cdot F$$

Equation 2.3. Equation used to compound the errors associated with AUCs into an error associated with the bioavailability.

The equation was adapted from Taylor [169].

The relative bioavailability of a MedCM (in which the reference was not intravenous administration, as for bioavailability) was calculated using Equation 2.4. For example, the relative bioavailability of MedCM in poisoned animals compared to naïve animals.

$$Relative\ bioavailability\ (F_{Rel}) = \left(\frac{AUC_a}{AUC_b}\right) \cdot \left(\frac{Dose_b}{Dose_a}\right)$$

Equation 2.4. Equation used to calculate the relative bioavailability.

The different experimental conditions are represented by *a* and *b* (e.g. *a* = naïve animals, *b* = nerve agent exposed animals). The equation is adapted from Rowland and Tozer [170].

2.11 Statistical analysis

The raw concentration-time data were tested for normality using the Anderson-Darling test at the 5% significance level using Minitab (v16, Minitab Ltd., UK).

Statistical analysis was carried out using Prism (version 5.01, GraphPad, USA). PK or PD parameters were compared by two tailed unpaired t test at the 5 % significance level. Multiple comparisons were made using one way analysis of variance (ANOVA) and a *post hoc* test, with the confidence intervals set to 95 %.

2.12 Histopathological analysis

Brains and sacrospinalis muscles were collected from guinea pigs *post mortem* and were immediately immersion fixed, using neutral buffered formalin (NBF: 10% v/v), for a minimum of 48 hours. The tissue samples were resected into segments approximately 5 mm in width. These segments were further fixed in NBF for 24 hours, prior to vacuum infiltration with paraffin wax on a vacuum infiltration processor (Tissue-Tek E300, Sakura Finetek, UK). Tissues were embedded in wax blocks, cut into nominally 5 µm sections using a rotary

microtome (Leica; RM2035) and mounted on glass slides. Sections were stained with hematoxylin and eosin, using a Linear Stainer (DRS2000, Sakura Finetek, UK), before automated coverslipping with glass coverslips and DPX mountant (Sigma Aldrich, UK). Skin sections were examined using a microscope (Axioskop, Zeiss, UK) fitted with a camera (Axiocam; MRc5 CCD). Digital photomicrographs were captured using Axiovision 4.3 software (Zeiss Ltd). Low magnification micrographs were captured using the camera (Axiocam; MRc5 CCD) attached to a binocular dissection microscope (Olympus).

2.13 Electron microscopy

At the end of the *in vivo* studies microdialysis probes were removed from guinea pigs *post mortem* and immediately fixed by immersion in NBF, for a minimum of 24 hours. Probes were subsequently dehydrated, using an alcohol series (70 – 100 %), air dried and sputter coated with gold (approximately 20 nm; Automatic Sputter Coater, Agar Scientific, UK), prior to examination in a scanning electron microscope, which operated at 15kV (SU3500, Hitachi, UK).

3. PHARMACOLOGICAL MEDICAL COUNTERMEASURES AGAINST NERVE AGENTS

3.1 Chapter specific introduction

As discussed in Chapter 1 of this thesis, post-poisoning MedCM currently fielded by the UK Armed Forces comprises atropine sulphate, avizafone hydrochloride and pralidoxime methane sulphonate [30]. These MedCM supported by pretreatment with pyridostigmine bromide, have proven effective at preventing lethality following acute exposure to nerve agent [32-34]. However, this combination does not provide protection against some of the incapacitating effects of nerve agent. In part this is because the pralidoxime has limited ability to reactivate AChE inhibited by several nerve agents and does not readily penetrate the BBB, which would enable it to protect central AChE. The replacement of pralidoxime with HI-6 dimethanesulphonate in the autoinjectors has been proposed, because HI-6 provides better protection against soman, cyclosarin and VX than does pralidoxime [76 :171 :172].

The efficacy of MedCM administered post-poisoning is dependent on their rapid administration following exposure to nerve agent, with protection being significantly reduced if delayed for 8 minutes or more [173]. Understanding this efficacy in terms of the absorption and distribution of MedCM to target tissues can be achieved through determination of their PK, in plasma and the target tissues. The PK of some of the individual MedCM have previously been determined, in anaesthetised or poisoned guinea pigs [129 :135], however, there has been no systematic study of all the MedCM in conscious guinea pigs, either as individual drugs or in combination. Therefore, the first part of this study was carried out to investigate the PK of atropine, diazepam and HI-6 in conscious ambulatory guinea pigs following individual intravenous bolus administration of these MedCM.

The intramuscular route is the proposed route of administration for MedCM against nerve agents in humans, so understanding the PK of these drugs by this route in the animal species used for efficacy testing is important. As the MedCM are physiologically active it is conceivable that when administered in combination their absorption, distribution or elimination may be altered, compared to when the MedCM are administered alone, this change in PK may have knock on effect on

efficacy. Thus the second part of this study was to determine the plasma concentrations of atropine, diazepam and HI-6 in conscious ambulatory guinea pigs following their individual, and subsequently their combined, intramuscular administration. PK parameters were determined for the MedCM and were compared to the intravenous bolus PK parameters, enabling the bioavailability of the MedCM to be calculated. These data also enabled any changes in PK to be identified following administration by the intramuscular route. The PK parameters determined for individual and combined MedCM (by the intramuscular route) were compared to identify PK interactions between the drugs. These PK data are discussed in light of the potential effects on efficacy against nerve agent.

The MedCM PK data obtained in unpoisoned guinea pigs can be used for extrapolation of doses and administration regimens to humans. However, as nerve agents disrupt normal physiology it is hypothesised that the ADME of the MedCM in poisoned guinea pigs may differ from that in unpoisoned guinea pigs, so the PK of the MedCM may change. In addition direct drug-drug interactions (i.e. reactivation of nerve agent inhibited AChE by HI-6) may take place. The PK interactions between MedCM and nerve agents have, to date, not been systematically investigated. However, two published studies have indicated that nerve agent may alter the PK of MedCM. Cassel *et al* investigated the PK of HI-6 in naïve and nerve agent poisoned rats. From their study it can be inferred that the BBB may change, as brain concentrations of HI-6 were greater in poisoned animals [134]. Separately, Capacio *et al* showed that the C_{max} of diazepam was significantly reduced in guinea pigs in which soman induced seizure was not terminated compared to guinea pigs in which soman induced seizure was terminated [135]. Unfortunately, in these latter studies the PK of diazepam in unpoisoned guinea pigs was not determined. Therefore, to identify the PK interactions between MedCM and nerve agents, the plasma concentrations of atropine, diazepam and HI-6 were determined, following combined administration of atropine sulphate, avizafone hydrochloride and HI-6 dimethanesulphonate to sarin-exposed guinea pigs. The PK parameters calculated for the atropine, diazepam and HI-6 were compared to their PK parameters in unpoisoned guinea pigs. These data are discussed in light of efficacy and the appropriate extrapolation of data from guinea pigs to humans, to provide the best estimate of an efficacious dose in humans.

3.2 Chapter specific aims

To determine the pharmacokinetics of the MedCM, atropine, diazepam and HI-6. Thus providing data to aid the understanding of MedCM efficacy against acute exposure to nerve agent.

a. To determine the PK of atropine, diazepam and HI-6 after intravenous bolus and intramuscular administration of individual atropine, avizafone and HI-6 in guinea pigs.

b. To calculate the intramuscular bioavailability of these MedCM, using the intravenous bolus and intramuscular data.

c. To determine the PK interaction between atropine, diazepam and HI-6 when the MedCM are administered in combination.

d. To determine the PK interaction of combined atropine, diazepam and HI-6 with sarin, when administered in association with one another.

e. To determine the cholinesterase inhibition-time profile of the nerve agent sarin, by the subcutaneous route of exposure and the effect of administration of combined atropine, avizafone and HI-6 on this profile.

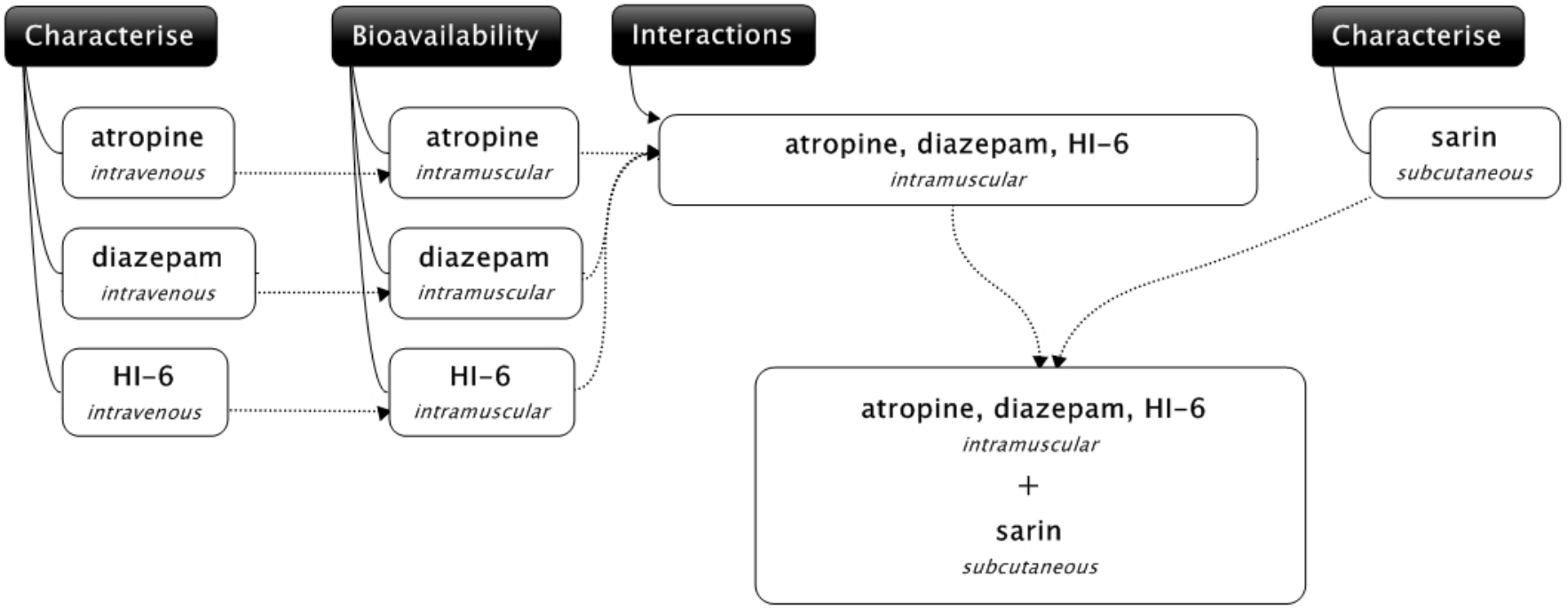

Figure 3.1. Concept for guinea pig studies investigating the PK of conventional pharmacological MedCM.

3.3 Materials and methods specific to the study of pharmacological medical countermeasure pharmacokinetics

To determine the PK of atropine, diazepam and HI-6 after intravenous bolus administration, twelve male Dunkin-Hartley guinea pigs (0.387 ± 0.043 kg, mean ± SD) were implanted with arterial and venous cannulae, as detailed in Chapter 2. Atropine sulphate (5.8 mg/kg), avizafone hydrochloride (1.05 mg/kg) or HI-6 dimethanesulphonate (9.3 mg/kg) were administered as an intravenous bolus to the animals (n=4 for each MedCM drug). Blood samples were collected at set time points post administration, as shown in Figure 3.2. The sample collection time points were set to provide the greatest resolution around the expected distribution phase of these MedCM [170]. Blood samples were processed, stored, assayed and analysed as described in Chapter 2.

To determine the PK of atropine, diazepam and HI-6 after intramuscular administration of individual and subsequently combined atropine, avizafone and HI-6, fifty male Dunkin-Hartley guinea pigs (0.368 ± 0.020 kg, mean ± SD) were implanted with arterial cannulae and brain and muscle microdialysis probes, as detailed in Chapter 2. The brain and muscle microdialysis probes were perfused at 2.0 µL/min with CNS and T1, respectively. All probes were perfused for a 1 hour equilibration period prior to administration of MedCM or sarin. Atropine sulphate (17.4 mg/kg), avizafone hydrochloride (3.14 mg/kg) and HI-6 dimethanesulphonate (27.9 mg/kg) were administered individually (n=8 for each MedCM drug), or in combination (n=8), by the intramuscular route. Sarin (43 µg/kg) was administered to animals by the subcutaneous route one minute prior to treatment with either saline (n=5) or combined intramuscular atropine sulphate, avizafone hydrochloride or HI-6 dimethanesulphonate (n=7, at the doses detailed above). Blood samples and microdialysis fractions were collected at set time points following administration of MedCM or exposure to sarin, as shown in Figure 3.3. These time points were chosen to give the greatest resolution around the likely C_{max} [170]. The samples were processed, stored assayed and analysed as detailed in Chapter 2.

Each of the different MedCM administration conditions (i.e. intravenous, individual intramuscular, combined intramuscular and combined intramuscular following sarin exposure) were statistically compared using one way ANOVA. The results of the Bonferroni *post hoc* multiple comparisons test were reported for specific comparisons between two administration conditions.

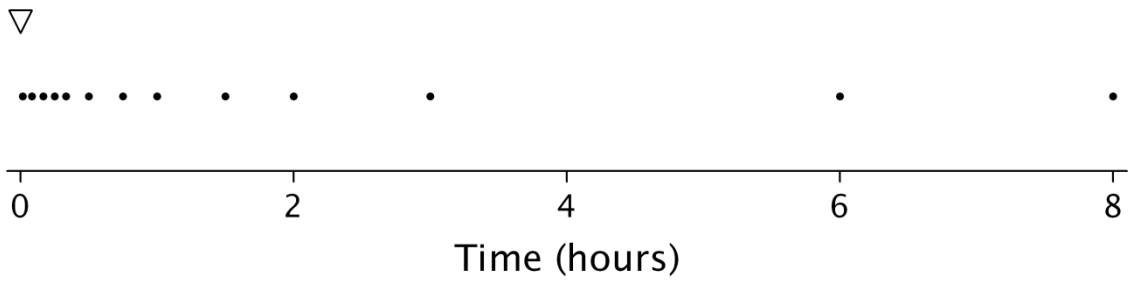

Figure 3.2. Schematic representation of the blood samples (●) collected following individual intravenous bolus administration (▽) of atropine sulphate, avizafone hydrochloride or HI-6 dimethanesulphonate in guinea pigs.

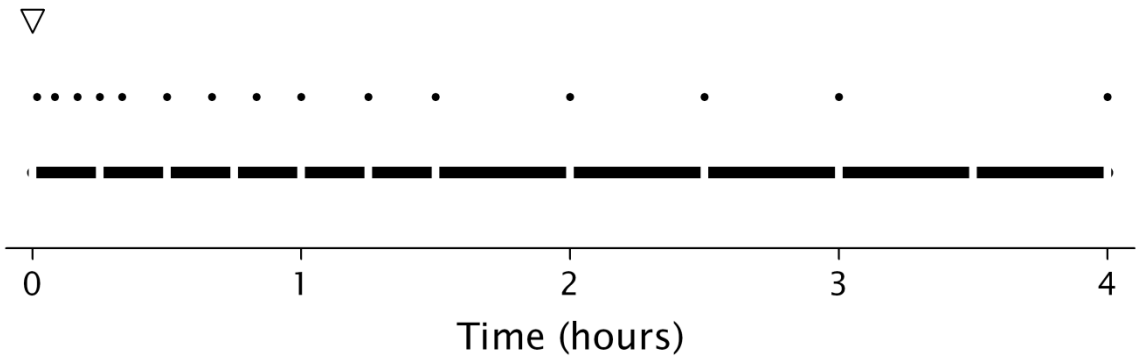

Figure 3.3. Schematic representation of the PK discrete blood samples (●) and integrated microdialysate fraction samples (▬) collected following intramuscular administration of MedCM to conscious guinea pigs.

3.4 Results

3.4.1 General results

A total of 62 guinea pigs (372 ± 27 g, mean ± SD) were anaesthetised and underwent surgical procedures. Of these, 54 recovered from surgery (a surgical success rate of 87 %) and were administered MedCM in one of the studies. One vascular cannula did not remain patent, whereas 79 % of the muscle microdialysis probes remained patent during the surgical procedure, recovery and the study protocols. All brain microdialysis probes remained patent. A summary of the surgical procedure success and cannula/microdialysis probe patency is shown in Table 3.1.

3.4.2 Characterisation of microdialysis probes

3.4.2.1 Histopathological assessment

Histopathological assessment of brain and muscle tissue collected post mortem at the end of the PK studies confirmed consistent placement of the microdialysis probes, at the base of the caudate putamen and centre of the sacrospinalis muscle, respectively (Figure 3.4 and Figure 3.5). These assessments also showed some haemorrhage and oedema, localised to the probes in the brain, as well as necrosis, most likely associated with the implantation of the guide cannula (Figure 3.4). The histopathological assessment of the muscle probes showed no oedema and where present inflammatory cell infiltration was mild (

Figure 3.5). When observed using scanning electron microscopy, microdialysis probes removed from guinea pigs post mortem had a biofilm on their surface (Figure 3.6 and Figure 3.7). This was not observed on unused sterile probes (Figure 3.6 and Figure 3.7). The probes implanted in muscle for 7 days showed more biofouling than the probes that had been implanted in the brain for 5 hours (Figure 3.6 and Figure 3.7).

3.4.2.2 *In vitro* microdialysis probe efficiency

The brain microdialysis probes recovered 23.2 ± 0.7 %, 21.7 ± 1.0 % and 19.4 ± 0.5 % of the atropine, diazepam and HI-6, respectively. The muscle microdialysis probes recovered 15.6 ± 1.2 %, 13.6 ± 0.7 and 20.0 ± 0.9 % of the atropine, diazepam and HI-6, respectively.

	Dose (mg/kg)	**Body mass** (kg)	**Number of animals**		**Cannula patency**	**Microdialysis patency**		**Notes**
			Undergoing surgery	**Entering study**		**Brain**	**Muscle**	
Atropine (i.v.)	5.8	0.350 ± 0.051	4	4	4/4 (arterial) 4/4 (venous)	n/a	n/a	
Avizafone (i.v.)	1.05	0.398 ± 0.016	4	4	4/4 (arterial) 4/4 (venous)	n/a	n/a	
HI-6 (i.v.)	9.3	0.414 ± 0.031	4	4	4/4 (arterial) 4/4 (venous)	n/a	n/a	
Atropine (i.m.)	17.4	0.379 ± 0.027	8	8	8/8	8/8	6/8	
Avizafone (i.m.)	3.14	0.378 ± 0.017	8	7	7/7	7/7	6/7	• Muscle probe flow not optimal (n=1) • Animal culled (n=1) due to poor condition, the day after surgery.
HI-6 (i.m.)	27.9	0.380 ± 0.014	8	7	6/7	7/7	6/7	• Animal culled (n=1) due to poor condition, the day following surgery. • Muscle probe flow not optimal (n=1)
Atropine, Avizafone HI-6 (i.m.)	17.4 3.14 27.9	0.357 ± 0.020	10	8	8/8	8/8	5/8	• Animal died (n=1) due to complications, within 24 h following surgery .
Sarin (s.c.)	0.043	0.360 ± 0.014	6	5	5/5	5/5	3/5	• Animal culled (n=1) due to poor condition, three days after surgery.

Sarin (s.c.) + Atropine, Avizafone HI-6 (i.m.)	0.043 17.4 3.14 27.9	0.356° ± 0.013	10	7	7/7	7/7	7/7	• Animals culled (n=2) due to poor condition, the day after surgery. • Animal died (n=1) during surgical procedures. • Cannula not patent (n=1).

Table 3.1. Summary information on the surgical procedure success and cannula/microdialysis probe patency for the different study groups of guinea pigs used in the PK studies of conventional MedCM.

Body mass data presented as mean ± SD.

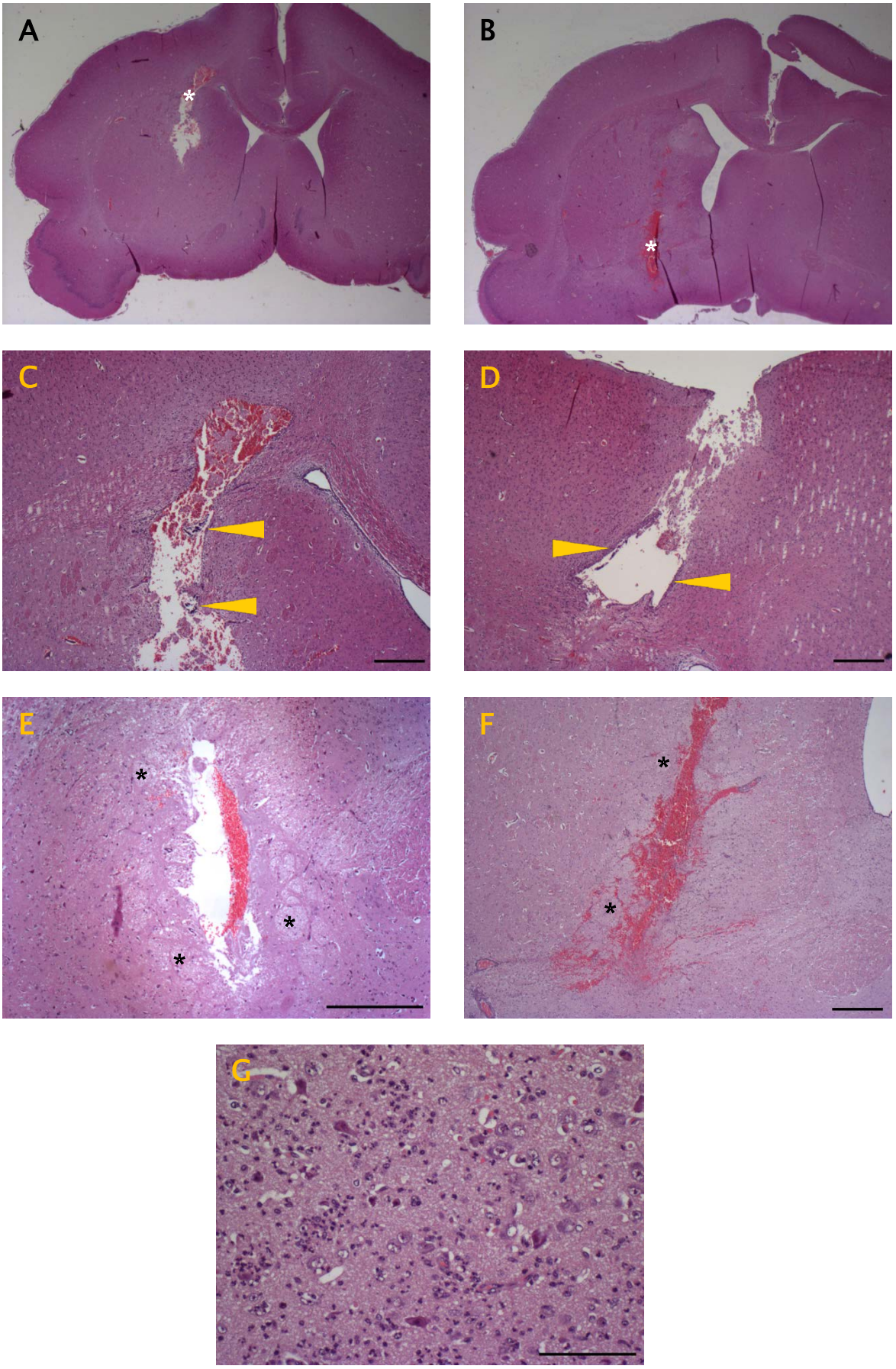
A
B
C
D
E
F
G

Figure 3.4. Representative micrographs of hematoxylin and eosin-stained sections of guinea pig brain, in which microdialysis probes were surgically implanted.

(A) and (B) are low magnification micrographs, showing the location of the probe in the brain. The areas of haemorrhage (*) were likely to have occurred immediately *post mortem,* as they were confined to the removal track of the probe (removal of the probe was *post mortem*). (C) Micrograph (scale bar = 200 μm) of the same section as (A), arrows indicate necrotic tissue likely to have resulted following the implantation of the guide cannula. (D) Micrograph (scale bar = 200 μm) showing tissue disruption toward the top of the implantation site, which was likely to have been due to probe removal *post mortem*. Arrows indicate a well-defined demarked edge with a thin area of necrotic tissue. (E) Micrograph (scale bar = 200 μm) showing an area of tissue with oedema around the probe implantation site (*). (F) Micrograph (scale bar = 200 μm) showing tissue oedema (*). (G) Micrograph (scale bar = 50 μm) of a section from the same animal as (F), the dark purple cells are neutrophils that have infiltrated the tissue.

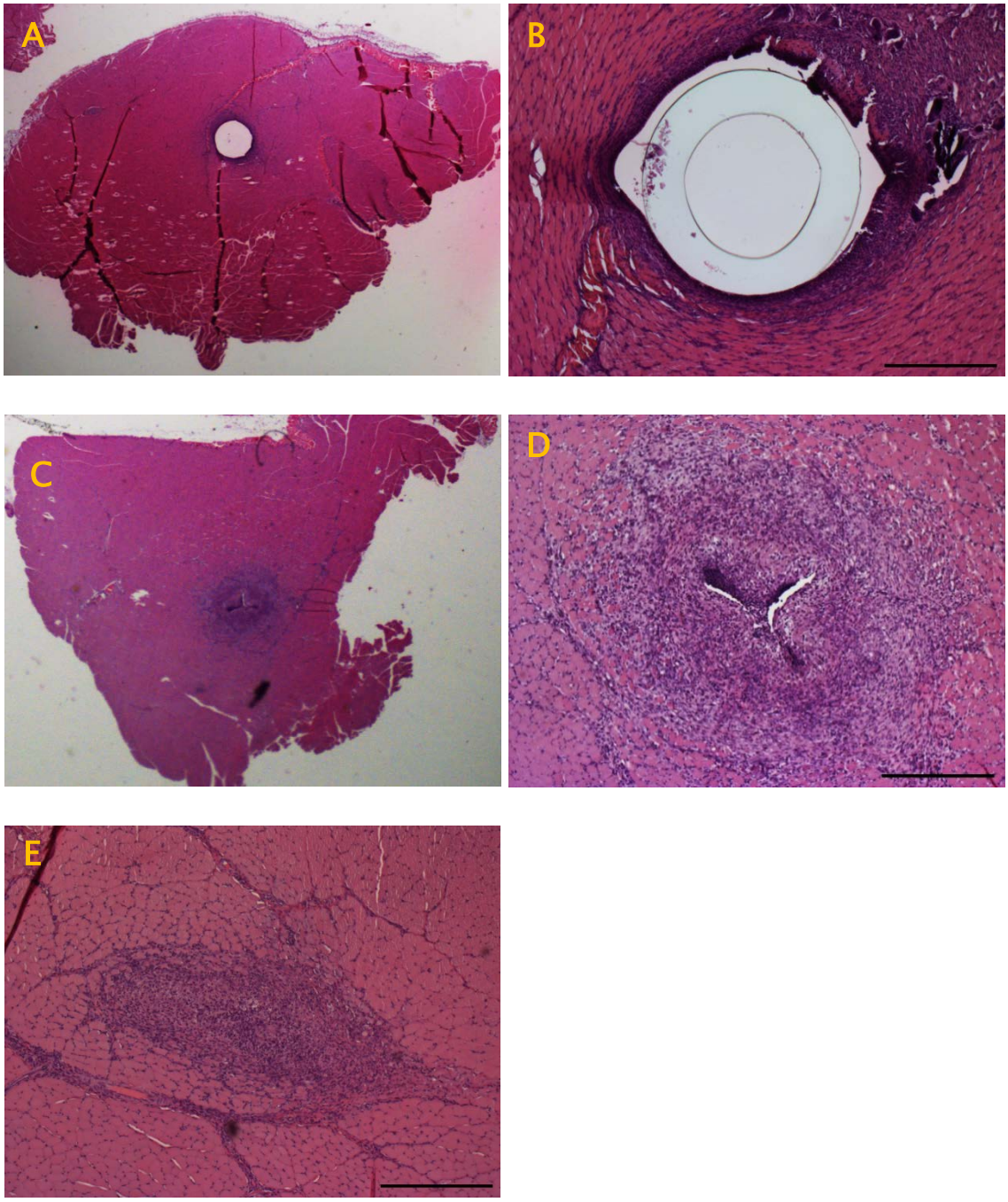
A
B
C
D
E

Figure 3.5. Representative micrographs of hematoxylin and eosin-stained sections of guinea pig sacrospinalis muscle, in which microdialysis probes were surgically implanted.

(A) and (C) are low magnification micrographs, showing the location of the probe in the muscle. In (A) the probe membrane remained *in situ* following removal of the probe *post mortem*. (B) Photomicrograph (scale bar = 200 μm) of the same section as (A), showing small areas of tissue necrosis proximal to the probe circumference. The PAES membrane from the microdialysis probe can clearly be seen in the image. (D) Photomicrograph (scale bar = 200 μm) of the same section as (C), showing tissue necrosis and fibrotic tissue in the location of the probe, which was likely to have been similar to (B), when the probe was *in situ*. (E) Photomicrograph (scale bar = 200 μm) showing tissue necrosis, fibrotic tissue is evident in the location of the probe.

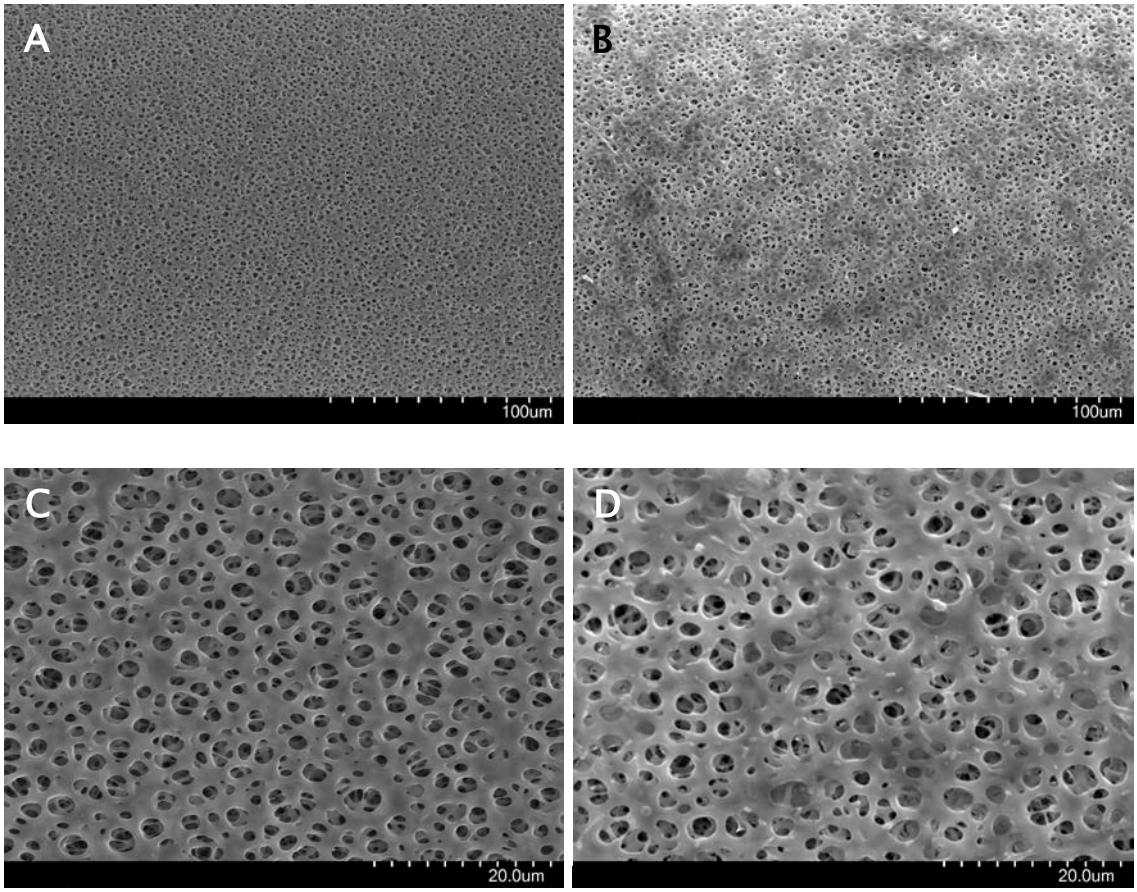

Figure 3.6. Electron micrographs of microdialysis probes (CMA12).

The pores on a sterile PAES membrane (20 kDa cut-off; images (A) and (C)) can clearly be seen. Biofouling of the surface of the microdialysis probe that had been implanted in a guinea pig brain (images (B) and (D)).

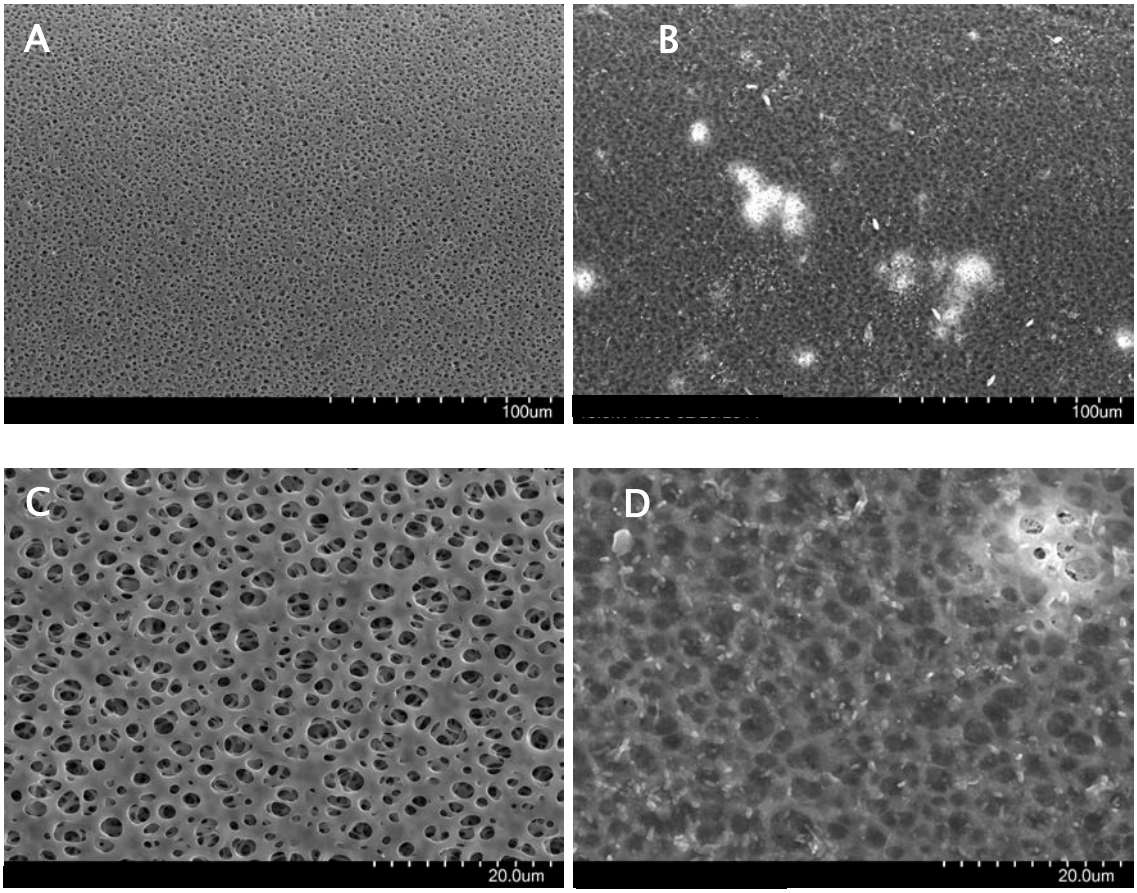

Figure 3.7. Electron micrographs of microdialysis probes (CMA20).

The pores on a sterile PAES membrane (20 kDa cut-off; images (A) and (C)) can clearly be seen. Biofouling of the surface of the microdialysis probe that had been implanted in skeletal muscle of a guinea pig is evident (images (B) and (D)) and to a greater extent than that on the microdialysis probe implanted in guinea pig brain (Figure 3.6, image (D)).

3.4.3 Medical countermeasure pharmacokinetics administered by the intravenous route

The plasma concentration-time profiles of atropine, diazepam and HI-6 following individual intravenous bolus administration of atropine sulphate (5.8 mg/kg, n=4), avizafone hydrochloride (1.05 mg/kg, n=4) and HI-6 dimethanesulphonate (9.3 mg/kg, n=4) were determined in conscious ambulatory guinea pigs. These pharmacological MedCM drugs were rapidly distributed from the blood and subsequently rapidly eliminated from the body (Figure 3.8). When plotted on semi-logarithmic graphs the concentration-time data for atropine and HI-6 decreased in a biexponential manner and two-compartment PK models were fitted to the data to calculate the PK parameters. The diazepam concentration decreased in a tri-exponential manner when plotted on a semi-logarithmic graph and a three-compartment PK model was used to fit the data, to calculate the PK parameters. These models were those that best fitted the data, as determined by the AIC values associated with the fits. The PK parameters from these models are presented in Table 3.2.

All concentration-time data were normally distributed. Data are presented as mean ± standard error of the mean (SEM), unless stated otherwise.

Atropine had the largest V_d of the three MedCM, at approximately 5.9 L. Atropine also had the fastest Cl, being approximately 230 mL/min (Table 3.2). In contrast HI-6 had the lowest V_d and Cl, these being approximately 75 mL and 6 mL/min, respectively. Diazepam distributed into a V_d of approximately 300 mL; this distribution occurred in two phases (Figure 3.8). The elimination T½ for diazepam was determined as the shortest at less than one minute. However, the terminal T½ was much greater at approximately 13 hours, due to the redistribution from the third PK compartment. The terminal T½ of atropine and HI-6 were 16 and 116 minutes, respectively.

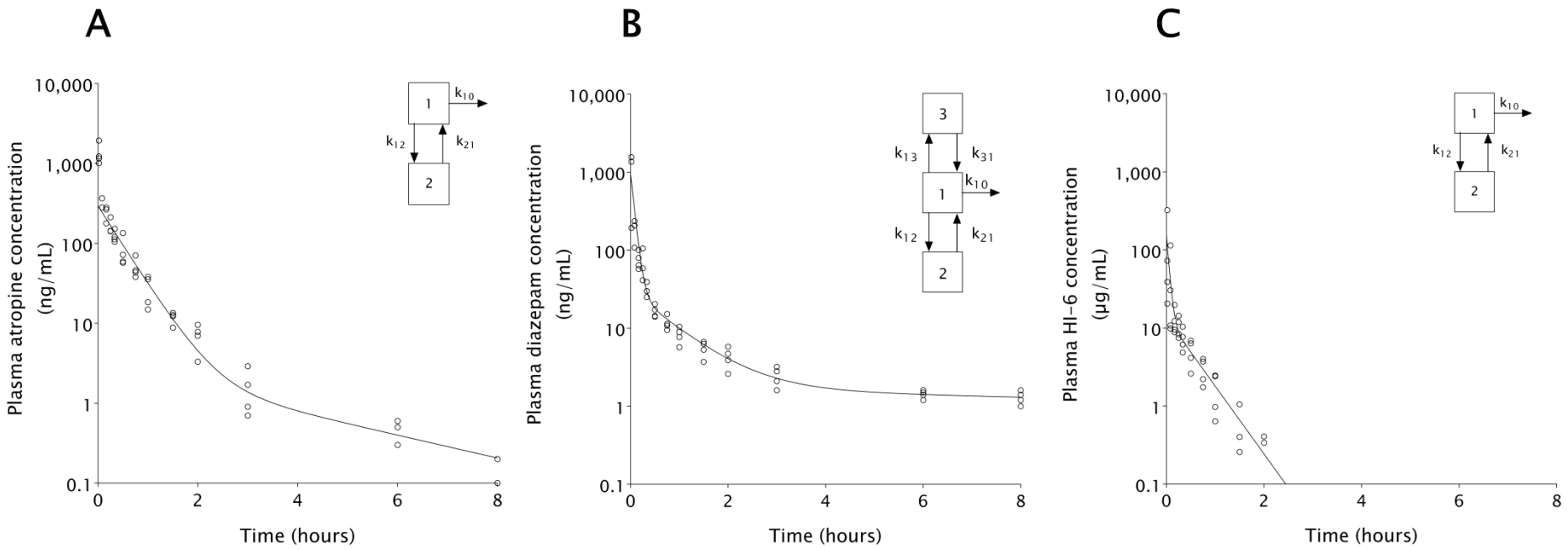

Figure 3.8. Concentration-time profiles of MedCM, quantified in plasma from individual guinea pigs following intravenous administration.

(A) Guinea pig plasma atropine concentration following administration of an intravenous bolus dose of atropine sulphate (5.8 mg/kg). (B) Guinea pig plasma diazepam concentration following administration of an intravenous bolus dose of avizafone hydrochloride (1.05 mg/kg). (C) Guinea pig plasma HI-6 concentrations following administration of an intravenous bolus dose of HI-6 dimethanesulphonate (9.3 mg/kg). Open circles plot concentrations from individual animals (n=4 for each MedCM). Mean concentrations predicted by the PK model (solid lines) were calculated from the pooled data. Insets show the schematic compartmental PK model fitted to the data.

	Atropine	diazepam	HI-6
Dose (mg)	1.70 ± 0.12	0.28 ± 0.01	2.32 ± 0.09
Elimination T½ (min)	17.4 ± 1.5	6.5 ± 1.2	8.6 ± 3.5
AUC (min□μg/mL)	7.3 ± 0.7	8.8 ± 1.2	380 ± 39
Cl (mL/min)	233.6 ± 21.0	31.4 ± 4.3	6.1 ± 0.6
V_d (L)	5.86 ± 0.91	0.30 ± 0.06	0.076 ± 0.034
k_{10} ($1/min$)	0.040 ± 0.004	0.107 ± 0.020	0.080 ± 0.033
k_{12} ($1/min$)	0.002 ± 0.001	0.048 ± 0.009	0.097 ± 0.129
k_{21} ($1/min$)	0.006 ± 0.001	0.025 ± 0.005	0.129 ± 0.087
k_{13} ($1/min$)	n/a	0.068 ± 0.013	n/a
k_{31} ($1/min$)	n/a	0.0009 ± 0.0003	n/a

Table 3.2. Compartmental PK parameters for atropine, diazepam or HI-6 following their individual intravenous bolus administration.

Atropine and HI-6 were best fit by a two-compartment PK model. Diazepam was best fit by a three-compartment model. Data are shown as the estimate of the parameter for the pooled concentration-time profile ± standard error of the estimate.

3.4.4 Plasma bioavailability of medical countermeasures following intramuscular administration

The plasma concentration-time profiles of atropine, diazepam and HI-6 following individual intramuscular administration of atropine sulphate (17.4 mg/kg, n=4), avizafone hydrochloride (3.14 mg/kg, n=4) and HI-6 dimethanesulphonate (27.9 mg/kg, n=4), were determined in conscious ambulatory guinea pigs. All drugs were rapidly absorbed, achieving C_{max} within 10 minutes. Atropine and diazepam were more readily absorbed than HI-6 and the intramuscular bioavailabilities were 0.95 ± 0.20, 0.95 ± 0.24 and 0.43 ± 0.19, respectively. The MedCM were also distributed and subsequently eliminated rapidly from the plasma (Figure 3.8). The concentrations of HI-6 in the plasma decreased mono-exponentially, with the absorption of HI-6 into the plasma masking the rapid distribution phase, which was evident following intravenous bolus administration (Figure 3.9). A one-compartment PK model was fit to the HI-6 data to calculate the PK parameters. Two-compartment models were fit to the atropine and diazepam data to calculate the PK parameters. These models best fit the data as determined by the AIC values associated with the fits. The PK parameters from these models are presented in Table 3.3.

Of the three drugs atropine was again determined to have the greatest V_d and Cl following intramuscular administration and these were not significantly different ($p > 0.05$ and $p > 0.05$, respectively) from the corresponding values determined following intravenous bolus administration (Table 3.2). The PK model fit to the intramuscular diazepam data did not accurately define the rate constants for the second compartment, as shown by the large errors associated with these parameters (Table 3.3). The two-compartment model was chosen and best fit the data, as defined by the AIC value associated with the fit. The V_d of diazepam was significantly reduced compared to the V_d following intravenous bolus administration ($p < 0.01$). The Cl of HI-6 was significantly increased compared to intravenous bolus administration ($p<0.01$; Table 3.2), although this had no effect on the elimination T½ ($p > 0.05$).

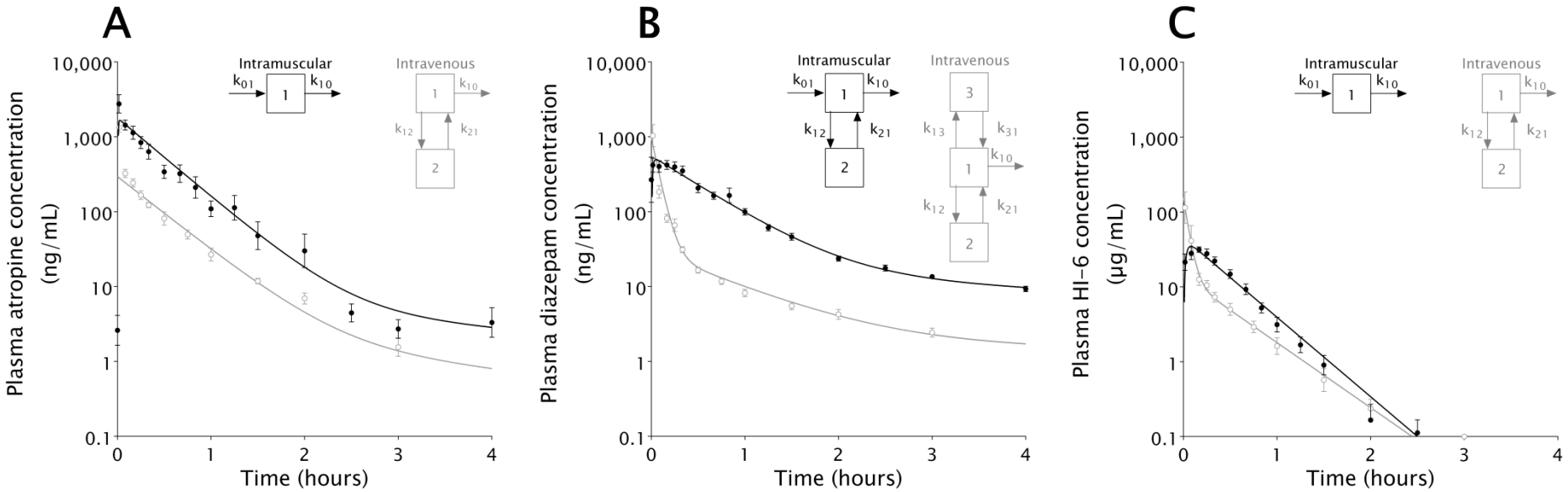

Figure 3.9. Plasma concentration-time profiles of MedCM quantified in plasma from individual conscious ambulatory guinea pigs following individual intramuscular administration.

(A) Atropine plasma concentrations determined following intramuscular administration of atropine sulphate (n=8,17.4 mg/kg). (B) Diazepam plasma concentrations determined following intramuscular administration of avizafone hydrochloride (n=6, 3.14 mg/kg). (C) HI-6 plasma concentrations determined following administration of HI-6 dimethanesulphonate (n=6, 27.9 mg/kg). Plasma concentrations of atropine, diazepam and HI-6 following intravenous administration (Figure 3.8) are included for comparison. Data shown as mean ± SEM. Mean concentrations predicted by the PK model (solid lines) were calculated from the pooled data. Insets show the schematic compartmental PK model fitted to the data.

	atropine	diazepam	HI-6
Dose (mg)	5.50 ± 0.14	0.78 ± 0.1	6.38 ± 0.08
C_{max} (ng/mL)	1,457 ± 274	569 ± 42	23 ± 3 (µg/mL)
T_{max} (min)	2.3 ± 1.9	3.2 ± 0.7	9.9 ± 1.5
Elimination T½ (min)	19.35 ± 3.08	0.75 ± 0.23	10.51 ± 1.28
AUC (min · µg/mL)	44.4 ± 5.6	26.1 ± 4.4	666.6 ± 66.0
CL (mL/min)	123.9 ± 15.7	30.0 ± 5.0	9.6 ± 1.0
Vd (L)	3.46 ± 0.74	0.03 ± 0.01	0.15 ± 0.02
k_{01} (1/min)	1.667 ± 1.834	0.031 ± 0.003	0.147 ± 0.050
k_{10} (1/min)	0.036 ± 0.006	0.929 ± 0.287	0.066 ± 0.008
k_{12} (1/min)	0.002 ± 0.001	0.251 ± 0.148	n/a
k_{21} (1/min)	0.006 ± 0.014	0.004 ± 0.005	n/a

Table 3.3. Compartmental PK parameters for atropine, diazepam or HI-6 following their individual intramuscular administration.

Atropine and diazepam were best fit by a two-compartment PK model. HI-6 was best fit by a one-compartment PK model. Data are shown as the estimate of the parameter for the pooled concentration-time profile ± standard error of the estimate.

3.4.5 Muscle and brain pharmacokinetics of medical countermeasures following intramuscular administration

Concentration-time profiles of free atropine, free diazepam and free HI-6 were determined in muscle and brain by microdialysate, from the same guinea pigs that contributed the plasma data. Data are presented in Figure 3.10. The concentrations of all MedCM drugs in these tissues decreased mono-exponentially and one-compartment PK models were fitted to the data, to calculate PK parameters. The diazepam and HI-6 concentrations in brain and muscle showed a delay before they were quantified in the microdialysate. These data were best fit with PK models that incorporated a lag time following administration.

Atropine concentration was determined in muscle and brain microdialysate fractions, with the AUC being significantly greater ($p < 0.0001$, unpaired t-test) in the former compared to the latter tissue. The concentrations of diazepam in brain and muscle were similar and remained below the plasma concentrations. HI-6 was quantified in muscle, with the exception of two animals, in which the concentration was below the limit of quantitation. HI-6 was not measured in the brain, with the exception of one guinea pig (see Figure 3.10 (C)). Correction of the concentrations determined in the microdialysate fractions for probe efficiency showed them to be the same as plasma concentrations (see section below). Diazepam and HI-6 had a lag time in the brain and muscle compared to plasma, whereas atropine did not. The time to achieve peak concentrations of the MedCM in the brain and muscle were delayed compared to the plasma. The λ_z (calculated by non-compartmental analysis) of all the MedCM in the tissues was the same as that in the plasma ($p > 0.05$).

		atropine	Diazepam	HI-6
C_{max} (ng/mL)	Brain	19.8 ± 2.7	17.8 ± 1.3	n/a
	Muscle	1,343 ± 305	6.1 ± 0.7	12,348 ± 2,372
T_{max} (min)	Brain	42 ± 9	53 ± 6	n/a
	Muscle	35.6 ± 6.9	98 ± 13	27 ± 4
T_{lag} (min)	Brain	n/a	28 ± 1	26 ± 10
	Muscle	n/a	38 ± 8	15 ± 0
Elimination T½ (min)	Brain	29 ± 811	72 ± 8	n/a
	Muscle	26 ± 73	67 ± 55	18 ± 2
AUC (min · µg/mL)	Brain	2.2 ± 0.3	2.4 ± 0.1	n/a
	Muscle	129.9 ± 21.0	1.1 ± 0.2	514.7 ± 50.5
λ_z (1/min)	Brain	0.020 ± 0.002	0.010 ± 0.001	n/a
	Muscle	0.023 ± 0.002	0.010 ± 0.001	0.039 ± 0.007
	Plasma	0.029 ± 0.006	0.010 ± 0.001	0.042 ± 0.006

Table 3.4. Tissue compartmental PK parameters for atropine, diazepam or HI-6 following their individual intramuscular administration.

Each of the drugs was best fit by a one-compartment PK model. Data are shown as the estimate of the parameter for the pooled concentration-time profile ± standard error of the estimate. The terminal rate of decrease in concentration λ_z; calculated by non-compartmental analysis of the mean data are included for comparison between the tissue data and the plasma data. These tissues were considered to be individual PK compartments, so no volume or clearance values are presented.

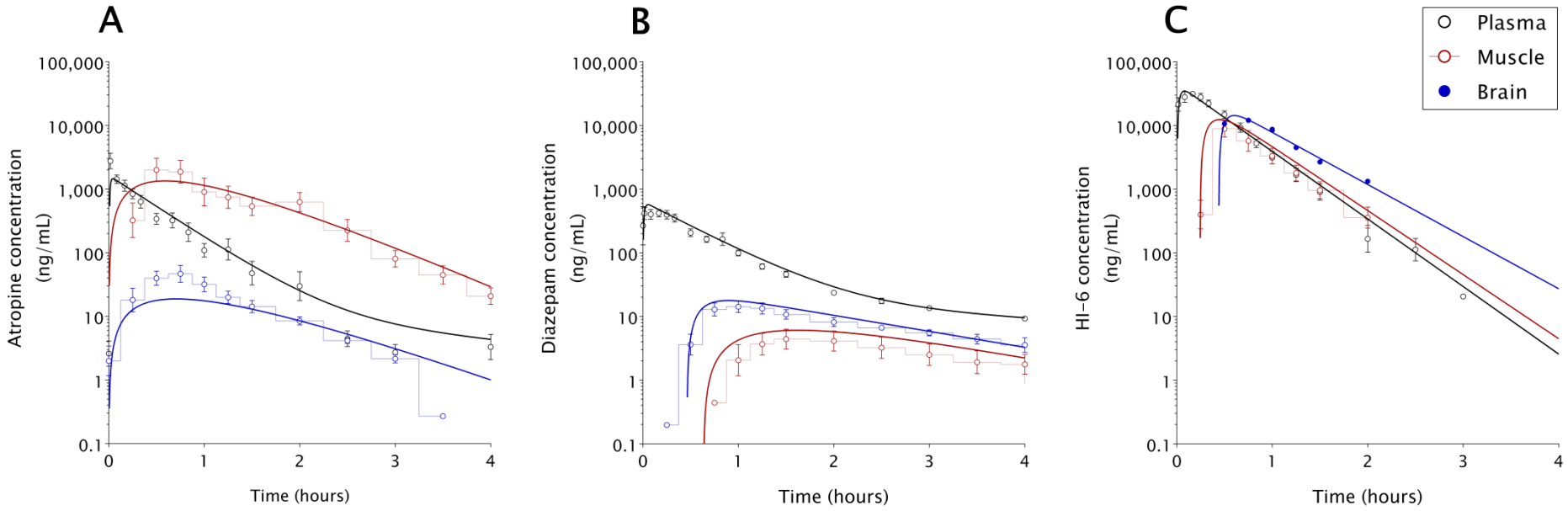

Figure 3.10. Plasma, muscle and brain concentration-time profiles of MedCM quantified in plasma and microdialysates, from individual conscious ambulatory guinea pigs, following individual intramuscular administration.

(A) Atropine plasma (n=8), muscle (n=6) and brain microdialysate (n=8) concentrations determined following intramuscular administration of atropine sulphate (17.4 mg/kg). (B) Diazepam plasma (n=6), muscle (n=6) and brain microdialysate (n=7) concentrations determined following intramuscular administration of avizafone hydrochloride (3.14 mg/kg). (C) HI-6 plasma (n=6), muscle (n=6) and brain microdialysate (n=1, HI-6 was only quantified in the brain of one animal) concentrations determined following administration of HI-6 dimethanesulphonate (27.9 mg/kg). Microdialysis concentrations shown, were corrected for microdialysis probe efficiency and shown as mean ± SEM. The number of samples is indicated in parentheses. The plasma data was shown in Figure 3.9.

3.4.6 Medical countermeasure pharmacokinetics following combined administration by the intramuscular route

The plasma, muscle and brain concentration-time profiles of atropine, diazepam and HI-6 following the combined intramuscular administration of atropine sulphate (17.4 mg/kg), avizafone hydrochloride (3.14 mg/kg) and HI-6 dimethanesulphonate (27.9 mg/kg) were determined in conscious ambulatory guinea pigs (Figure 3.11, Figure 3.12 and Figure 3.13). The PK parameters are presented in Table 3.5.

The plasma PK parameters determined for atropine or diazepam were not significantly different from their PK parameters determined following their individual intramuscular administration ($p > 0.05$). Compared to the PK parameters determined following individual intramuscular administration of HI-6, Cl was significantly reduced ($p < 0.0001$), whereas C_{max}, elimination T½, and AUC were significantly increased ($p < 0.05$, $p < 0.01$ and $p < 0.001$, respectively). Furthermore, HI-6 was quantified in brain microdialysate fractions, whereas measurable concentrations were only observed in one of six animals following intramuscular administration of HI-6 alone (Figure 3.10 (C)). The concentration of HI-6 in both brain and muscle showed a lag compared to plasma concentrations, prior to being measureable. The lag for diazepam reduced in brain and was not evident in muscle, compared to the diazepam concentration-time profiles in these tissues following individual administration of avizafone. Conversely, atropine concentration showed a lag in the brain, whereas, there was no lag evident in the brain following administration of the atropine alone. Non-compartmental analysis calculated λ_z (the rate of terminal decrease in concentration, akin to k_{10}, Figure 2.6), which was the same in brain, muscle and plasma for the three MedCM drugs.

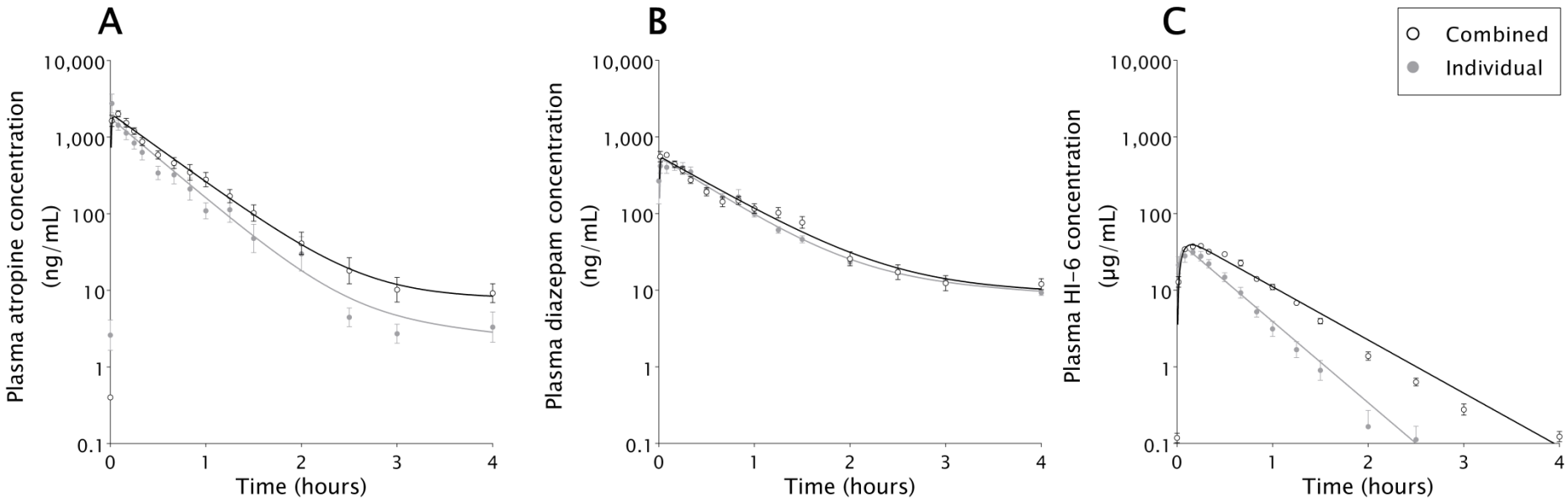

Figure 3.11. Plasma concentration-time profiles of MedCM quantified in plasma (n=6) following their combined intramuscular administration to conscious ambulatory guinea pigs.

(A) Atropine (B) diazepam and (C) HI-6 plasma concentrations determined following their combined intramuscular administration (atropine sulphate 17.4 mg/kg, avizafone hydrochloride 3.14 mg/kg HI-6 dimethanesulphonate 27.9 mg/kg). Plasma concentration-time profiles of atropine, diazepam and HI-6 following individual intramuscular administration (Figure 3.9) are included for comparison. Data shown as mean ± SEM. Mean concentrations predicted by the PK models (lines) were calculated from the pooled data.

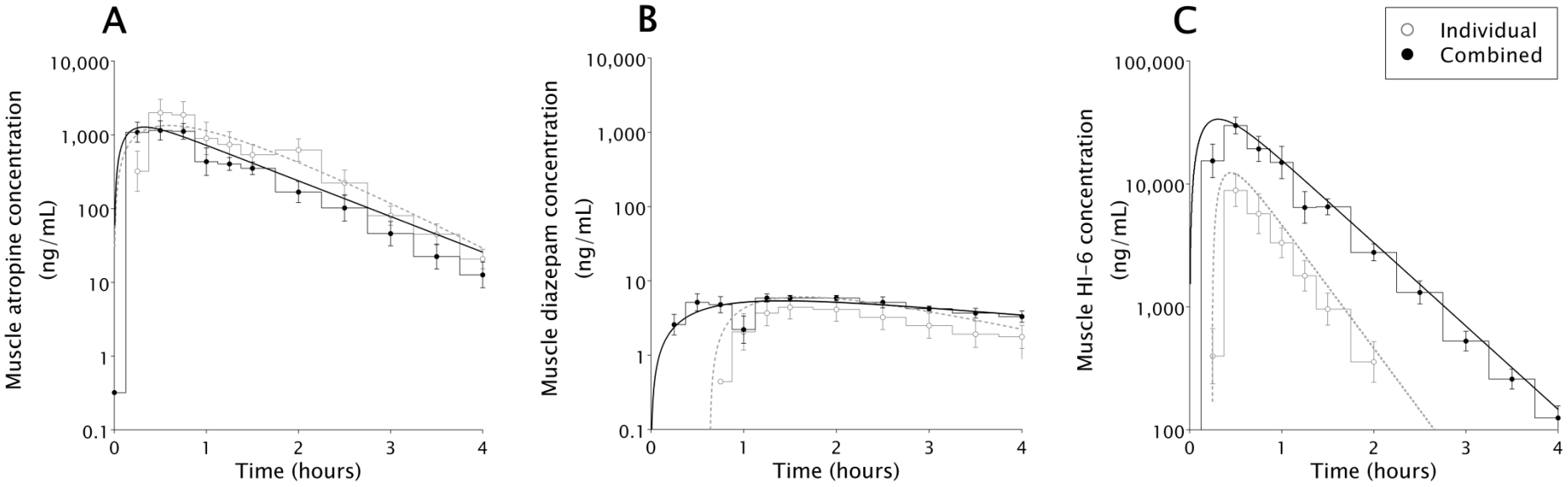

Figure 3.12. Muscle concentration-time profiles of MedCM quantified in microdialysates (n=4) following their combined intramuscular administration to conscious ambulatory guinea pigs.

(A) Atropine (B) diazepam and (C) HI-6 muscle microdialysate concentrations determined following their combined intramuscular administration (atropine sulphate 17.4 mg/kg, avizafone hydrochloride 3.14 mg/kg HI-6 dimethanesulphonate 27.9 mg/kg). Muscle microdialysate concentration-time profiles of atropine, diazepam and HI-6 following their individual intramuscular administration (Figure 3.10) are included for comparison. Concentrations shown were corrected for microdialysis probe efficiency and shown as mean ± SEM. Mean concentrations predicted by the PK models (lines) were calculated from the pooled data.

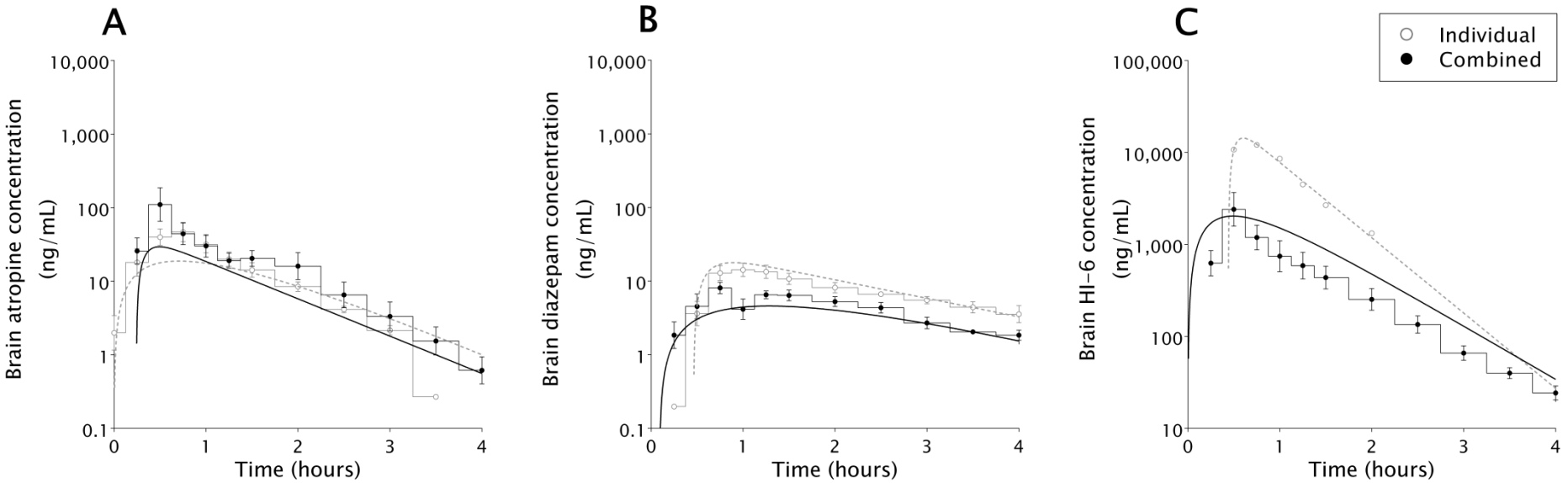

Figure 3.13. Brain concentration-time profiles of conventional MedCM quantified in microdialysates (n=7) following their combined intramuscular administration to conscious ambulatory guinea pigs.

(A) Atropine (B) diazepam and (C) HI-6 brain microdialysate concentrations determined following their combined intramuscular administration (atropine sulphate 17.4 mg/kg, avizafone hydrochloride 3.14 mg/kg HI-6 dimethanesulphonate 27.9 mg/kg). Brain microdialysate concentration-time profiles of atropine, diazepam and HI-6 following their individual intramuscular administration (Figure 3.10) are included for comparison. Concentrations shown were corrected for microdialysis probe efficiency and shown as mean ± SEM. Mean concentrations predicted by the PK models (lines) were calculated from the pooled data.

	atropine	diazepam	HI-6
Dose (mg)	5.23 ± 0.12	0.75 ± 0.02	6.06 ± 0.14
C_{max} (ng/mL)	1,680 ± 198	594 ± 49	39 ± 2 (µg/mL)
T_{max} (min)	2.3 ± 1.3	2.4 ± 1.0	11.4 ± 1.0
Elimination T½ (min)	22.12 ± 3.28	0.48 ± 0.29	21.41 ± 0.57
AUC (min · µg/mL)	57.9 ± 6.0	29.6 ± 14.2	1730.0 ± 77.8
CL (mL/min)	90.3 ± 9.4	25.3 ± 12.1	3.7 ± 0.2
V_d (L)	2.88 ± 0.39	17.6 ± 9.6	0.11 ± 0.01
k_{01} (1/min)	1.743 ± 1.274	0.027 ± 0.004	0.186 ± 0.027
k_{10} (1/min)	0.031 ± 0.005	1.436 ± 0.856	0.032 ± 0.001
k_{12} (1/min)	0.002 ± 0.002	0.391 ± 0.677	n/a
k_{21} (1/min)	0.004 ± 0.011	0.003 ± 0.008	n/a

Table 3.5. Compartmental plasma PK parameters for atropine, diazepam or HI-6 following their combined intramuscular administration to conscious ambulatory guinea pigs (n=6).

Atropine and diazepam were best fit by a two-compartment PK model. HI-6 was best fit by a one-compartment PK model. Data are shown as the estimate of the parameters for the pooled concentration-time data ± standard error of the estimate.

		atropine	diazepam	HI-6
C_{max}	**Brain**	29.4 ± 8.9	4.6 ± 0.4	2,031 ± 455
(ng/mL)	**Muscle**	1,277 ± 275	5.4 ± 0.4	33,606 ± 5,643
T_{max}	**Brain**	30 ± 13	77 ± 11	30 ± 7
(min)	**Muscle**	20 ± 8	86 ± 15	19 ± 4
T_{lag}	**Brain**	15 ± 1	5 ± 8	n/a
(min)	**Muscle**	n/a	n/a	n/a
Elimination T½	**Brain**	35 ± 10	50 ± 4,070	31 ± 5
(min)	**Muscle**	37 ± 3	180 ± 114	27 ± 1
AUC	**Brain**	2.0 ± 0.3	0.9 ± 0.1	175.9 ± 26.7
(min · μg/mL)	**Muscle**	98.8 ± 11.4	1.9 ± 0.7	2,104 ± 204
λ_z	**Brain**	0.022 ± 0.002	0.011 ± 0.002	0.020 ± 0.003
(1/min)	**Muscle**	0.023 ± 0.002	0.006 ± 0.001	0.026 ± 0.001
	Plasma	0.026 ± 0.004	0.013 ± 0.002	0.026 ± 0.003

Table 3.6. Tissue compartmental PK parameters for atropine, diazepam or HI-6 following their combined intramuscular administration.

Each of the drugs was best fit by a one-compartment PK model. Data shown as the estimate of the parameter for the pooled concentration-time profile ± standard error of the estimate. The terminal rate of decrease in concentration λ_z; calculated by non-compartmental analysis of the mean data is included for comparison between the tissues data and the plasma data.

3.4.7 Medical countermeasures pharmacokinetics in sarin-exposed guinea pigs

Due to the operational requirement for LC-MS-MS analysis of samples from different projects [174], there was a long delay between sample collection and LC-MS-MS analysis for atropine, diazepam and HI-6. Atropine and diazepam were not stable in the samples over the duration of storage [175]. Therefore, the concentration-time data for atropine and diazepam was not reliable and was not included in this section. These data are available in Appendix B for reference. HI-6 was stable in plasma and microdialysate fractions over the duration of the delay prior to analysis.

The plasma, muscle and brain concentration-time profiles of HI-6 following combined administration of atropine sulphate, avizafone hydrochloride and HI-6 dimethanesulphonate (17.4 mg/kg, 3.14 mg/kg and 27.9 mg/kg, respectively) to guinea pigs previously exposed to sarin (43 µg/kg) were determined in conscious ambulatory guinea pigs (Figure 3.14). Microdialysate fractions were collected from seven animals but the fraction volume was too low following assay of atropine and diazepam to complete the analysis of HI-6 in samples collected from four animals.

The concentrations of HI-6 in the plasma decreased mono-exponentially, a one-compartment PK model was the best fit for the data. The PK parameters from this model are presented in Table 3.7. Compared to the same plasma PK parameters determined in unpoisoned guinea pigs the HI-6 C_{max} was significantly increased ($p < 0.05$, one-way ANOVA). The HI-6 elimination T½ was significantly reduced ($p < 0.01$, one-way ANOVA), to a duration not significantly different from that following intramuscular administration of HI-6 alone ($p > 0.05$, one-way ANOVA).

The concentrations of HI-6 in muscle and brain decreased mono-exponentially, however compartmental models were not good fits for the

data, with large errors associated with the parameter estimates. Non-compartmental analysis was completed on the concentration-time profile data. There was no significant difference in λ_z between plasma, brain and muscle. There was no significant difference in λ_z in brain or muscle compared to HI-6 administered as part of the combination in unexposed guinea pigs. The AUC of HI-6 in muscle was significantly increased ($p < 0.001$) compared to the AUC following administration of combined HI-6, atropine and avizafone to unexposed guinea pigs.

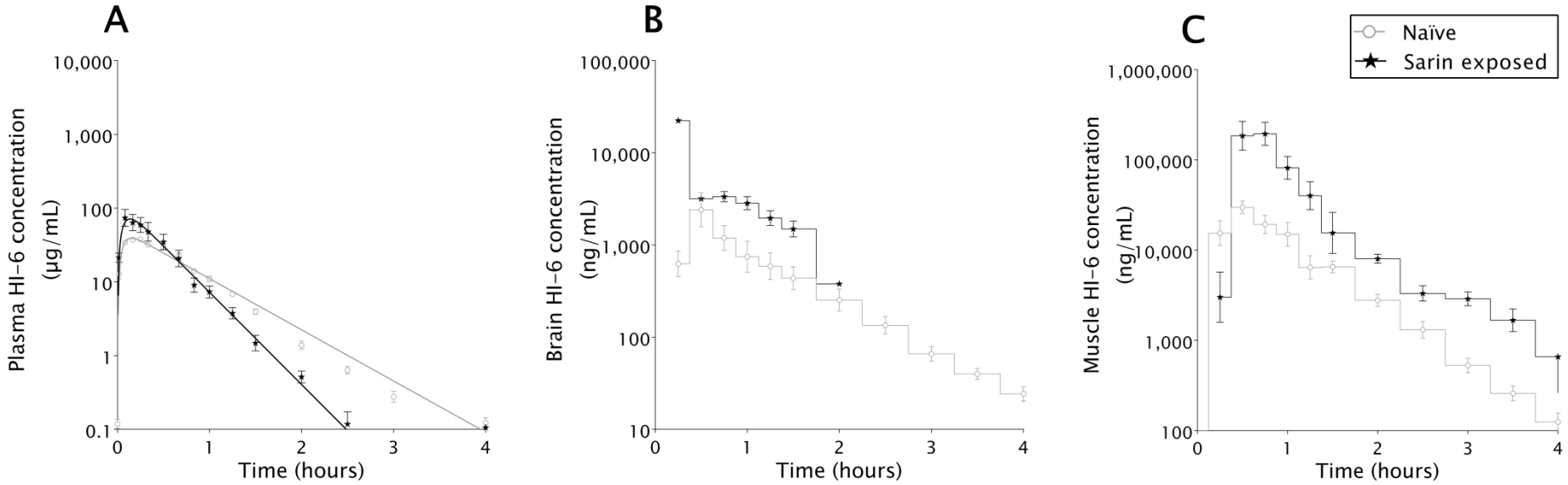

Figure 3.14. Guinea pig plasma, brain and muscle HI-6 concentration-time profiles determined following combined intramuscular administration of conventional MedCM, to sarin exposed guinea pigs.

(A) Plasma (n=6), (B) brain (n=3) and (C) muscle concentrations (n=3) following combined intramuscular administration of atropine sulphate (17.4 mg/kg), avizafone hydrochloride (3.14 mg/kg) and HI-6 dimethanesulphonate (27.9 mg/kg). HI-6 plasma, brain and muscle concentration-time profiles following combined administration of the MedCM, to naïve guinea pigs (Figure 3.12 and Figure 3.13), are included for comparison. Concentrations shown were corrected for microdialysis probe efficiency and shown as mean ± SEM. Mean concentrations predicted by the PK models (lines) were calculated from the pooled data.

	HI-6
Dose (mg)	6.06 ± 0.08
C_{max} (μg/mL)	54 ± 5
T_{max} (min)	7.7 ± 1.3
T½ (min)	12.02 ± 1.84
AUC (min · μg/mL)	1443.8 ± 120.6
CL (mL/min)	4.2 ± 0.4
V_d (L)	0.07 ± 0.01
k_{01} (1/min)	0.248 ± 0.081
k_{10} (1/min)	0.058 ± 0.009

Table 3.7. Compartmental plasma PK parameters for HI-6 following combined intramuscular administration of combined MedCM, to conscious ambulatory sarin exposed guinea pigs (n=6).

HI-6 was best fit by a one-compartment model. Data shown as the estimate of the parameters for the pooled concentration-time data ± standard error of the estimate.

		HI-6
C_{max} (μg/mL)	Brain	4.8 ± 4.1
	Muscle	44.3 ± 11.9
T_{max} (min)	Brain	30 ± 9
	Muscle	35 ± 5
T_{lag} (min)	Brain	10 ± 5
	Muscle	5 ± 5
Elimination T½ (min)	Brain	32 ± 2
	Muscle	31 ± 4
AUC (min·μg/mL)	Brain	114 ± 62
	Muscle	1,662 ± 460
λ_z (1/min)	Brain	0.022 ± 0.001
	Muscle	0.023 ± 0.003
	Plasma	0.035 ± 0.006

Table 3.8. Tissue compartmental PK parameters for HI-6 following intramuscular administration of combined MedCM in sarin exposed guinea pigs.

The HI-6 did not fit any compartmental PK models, therefore mean non-compartmental parameter estimates are shown ± standard error of the mean. The terminal rate of decrease in plasma concentration (λ_z) was also calculated by non-compartmental analysis from the mean data and is included for comparison.

3.4.8 HI-6 pharmacodynamics in sarin-exposed guinea pigs

The erythrocyte AChE and plasma BChE activities were measured in blood samples from sarin-exposed guinea pigs receiving combined MedCM or saline. Sarin inhibited 94.9 ± 2.3 % erythrocyte AChE activity and 94.5 ± 1.5 % plasma BChE activity, within 15 minutes of exposure, in saline treated guinea pigs (Figure 3.15). Three of the five animals died between 15 and 30 minutes after exposure. The AChE and BChE inhibition increased to approximately 98 % and 95 %, respectively in the two surviving animals. In guinea pigs treated with atropine, avizafone and HI-6, the inhibition was only 67.2 ± 6.8 % and 71.4 ± 14.5 % for erythrocyte AChE and plasma BChE activities, respectively. The AChE and BChE activity showed a slow and partial recovery from maximal inhibition over the following hour.

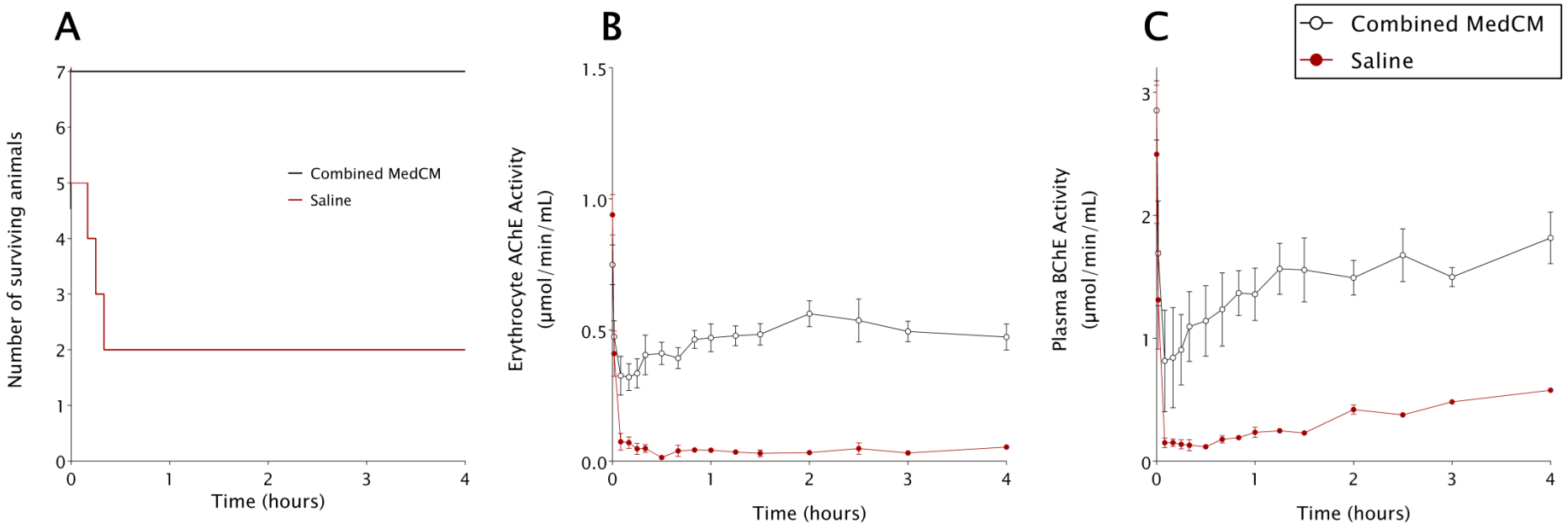

Figure 3.15. Effect of treatment with combined conventional MedCM by the intramuscular route on sarin lethality, inhibition of erythrocyte AChE activity and plasma BChE activity.

Treatment with intramuscular combined atropine, avizafone and HI-6: (A) prevented sarin lethality (group sizes of n=7 for MedCM and n=5 for saline treated guinea pigs); (B) reduced the inhibition of erythrocyte AChE activity compared to saline treated animals; (C) reduced the inhibition of plasma BChE activity. Cholinesterase data are shown as mean ± SEM.

3.5 Discussion

The aim of the studies reported here was to characterise the MedCM PK, in order to understand and interpret the efficacy of these as post-exposure therapeutic MedCM against acute nerve agent (e.g. sarin) exposure. To achieve this, these studies used a novel methodology, involving guinea pigs with implanted vascular cannulae and microdialysis probes in brain and skeletal muscle. Multiple blood, muscle and brain samples were collected from individual conscious animals and, LC-MS-MS analysis of these samples enabled the determination of MedCM PK. The results of these studies have provided fundamental PK parameters for intravenous and intramuscular administration of the MedCM. Atropine, diazepam and HI-6 demonstrated rapid absorption, distribution and clearance following both intravenous and intramuscular administration. When the MedCM were administered in combination, the PK of atropine and diazepam was not affected but the clearance of HI-6 was significantly reduced. Furthermore, HI-6 was centrally available only following its combined administration with atropine and avizafone. The PK data for the drugs in the muscle and brain suggest that they are in equilibrium with the plasma, as the λ_z for the drugs in the tissues was the same as the plasma.

The studies reported here are the first to use microdialysis sampling from skeletal muscle of conscious ambulatory animals and the first to combine muscle microdialysis, brain microdialysis and blood sampling, in individual animals. Understanding the concentrations of MedCM at these sites is important, as these tissues are the target sites for nerve agent and where the MedCM must exert their pharmacological action, to protect against the nerve agent.

The methodology developed here used conscious animals to provide information about the pharmacokinetics of the MedCMs. These PK data could have been obtained using anaesthetised animals but the effects of anaesthesia on the autonomic nervous system would have been likely to alter physiology

and ADME processes. This altered physiology may also change the PD. Changes in the concentration-time or effect-time profiles may also have increased the variability of the PKPD parameters determined, necessitating an increase in the number of animals required [176]. The mechanisms by which anaesthesia alters PKPD can involve reduced organ blood flow (absorption and elimination) [177], reduced renal function (elimination) [178], altered protein binding (distribution) [177] or even reduced metabolism [179]. Furthermore, the duration of anaesthesia can increase the magnitude of the changes in PK [179]. Evidence of differences in MedCM PK is provided by the differences in clearance and half-life reported for HI-6 by Bohnert *et al* [129] when compared to that described in this chapter (see Section 3.5.1.3). Whilst determination of the PK of MedCM in anaesthetised animals would provide data this would be difficult to interpret compared to those generated in conscious ambulatory animals, as reported here. Similarly determining efficacy of MedCM in anaesthetised animals, as may be preferable from an animal welfare viewpoint, may underestimate MedCM efficacy as anaesthetics have demonstrated a protective effect against the nerve agent sarin [180].

3.5.1 Medical countermeasure pharmacokinetics administered by the intravenous route

3.5.1.1 Atropine

The concentration-time profile of atropine determined in guinea pigs is the first PK data in this species to be reported for this drug. The large V_d, being greater than the plasma volume and body mass for guinea pigs, suggesting atropine readily penetrates and is sequestered in tissues, so it is widely distributed. Similar V_d is seen in humans [181 :182] and these data are consistent with the tissue site of action of atropine at muscarinic receptors. .

The rate of clearance of atropine of approximately 250 mL/min, is greater than both liver and kidney blood flow at approximately 30.5 mL/min* in total, implying that extra-hepatic metabolism of atropine occurs in the guinea pig. The reported rate of clearance of atropine in humans [181 :182] was less than total liver blood flow (1.35 L/min/70 kg [184]), with the hepatic extraction being considered intermediate. This species difference will need to be considered if rate of clearance is to be used in extrapolation of efficacious atropine doses, from guinea pigs to humans. These clearance data for atropine in guinea pigs provide a PK rationale for the use of large doses of atropine in efficacy studies. The hypothesis that atropinesterase metabolises the atropine has previously been proposed to justify these large atropine doses in efficacy studies [46]. However, Harrison *et al* reported guinea pig plasma did not contain atropinesterase based on *in vitro* assays in which the concentration of atropine was determined by high performance liquid chromatography [133]. The rapid clearance of atropine observed could be effected by carboxylesterase (CaE) which is known to be present in the blood, liver and lungs of guinea pigs [120 :185-187]. It is possible that CaE binds and metabolises atropine. For example, Bencharet *et al* used homatropine, a closely related analogue of atropine and cocaine (Table 3.9), to determine the crystal structure of the enzyme-drug complex and provide evidence for the metabolism of cocaine by CaE [188]. To confirm the metabolism of atropine by CaE, a series of *in vivo* studies could be completed, in which a specific inhibitor of CaE such as a bisbenzene sulphonamide [189] could be administered to guinea pigs, prior to the concentration-time profile of atropine being determined.

* Guinea pig cardiac output is 17.64 L/h/kg, liver and kidney perfusion rates are 18 % and 11.4 % of cardiac output, respectively[183]. The calculations below provide values for the guinea pigs in which the concentrations of atropine were determined.

$$Renal blood\ flow = (17.6\ L/h/kg\ \times 0.35\ kg) \times 11.4\ \% = 0.7\ L/h\ \equiv 11.7\ mL/min$$

$$Liver\ blood\ flow = (17.64\ L/h/kg\ \times 0.35\ kg)\ \times 18\ \% = 1.11\ L/h\ \equiv 18.5\ mL/min$$

Homatropine	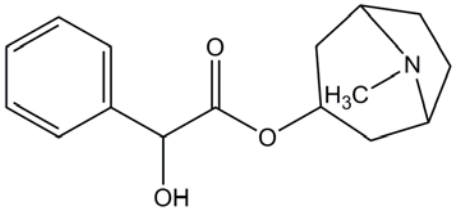 $C_{16}H_{21}NO_3$	275.35
Atropine	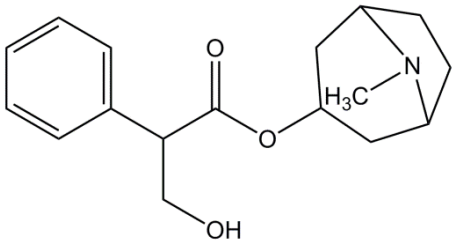 $C_{17}H_{23}NO_3$	289.38
Cocaine	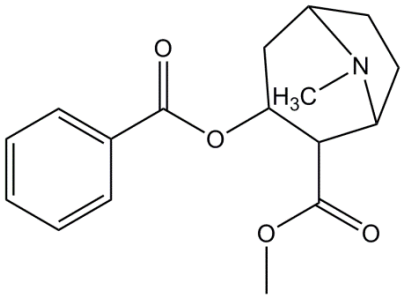 $C_{17}H_{21}NO_4$	303.36

Table 3.9. Chemical structure and formula mass of homatropine and cocaine.

The structure, formula and mass of atropine are provided for reference. Homatropine was used in studies of crystal structure as a cocaine analogue to elucidate the metabolism of cocaine by carboxylesterase[188].

3.5.1.2 Diazepam

Diazepam following administration of avizafone, was rapidly distributed but with slow elimination, following distribution into two different compartments (rapid and slowly equilibrating). The diazepam was rapidly detected following administration of avizafone. Avizafone is rapidly converted to diazepam by a plasma aminopeptidase, with a conversion half-life of approximately 25 seconds in the guinea pig [56]. There may have been some *ex vivo* conversion of the avizafone into diazepam, as no stabilising compound was added. However, the avizafone was circulating in the blood of the animal following administration and on conversion to diazepam, would exert its effect [56:57]. The Cl and the AUC reported in this chapter for diazepam following the administration of avizafone were similar to those previously reported by Maidment and Upshall [57]. However, the V_d was approximately half of that previously determined [57], with the distribution T½ and the elimination T½ being longer in the data reported here. The V_d was equivalent to total body water, indicating that diazepam was likely to have partitioned into lipid rich tissues, thus having lower plasma concentrations than a less lipophilic drug for a given dose. While there are no comparable data for the distribution of diazepam following intravenous administration of avizafone in humans, there are data following intramuscular administration of avizafone [190]. Therefore, these intramuscular data will be discussed in the next section, with the guinea pig intramuscular data.

3.5.1.3 HI-6

HI-6 was less well distributed than either atropine or diazepam, having a V_d smaller than that of these two drugs. This V_d was approximately twice the blood volume of a guinea pig, indicating HI-6 is likely to distribute within the extracellular fluid. The slower Cl gave rise to an elimination T½ (Equation 3.1) that was comparable to both atropine and diazepam. The PK of HI-6 in anaesthetised guinea pigs have previously been reported [129]. In that study the Cl was more rapid than reported here and consequently the T½ was shorter. HI-6 appeared to have different V_d in conscious and anaesthetised guinea pigs but the difference was not significant ($p > 0.05$, unpaired two-tailed t test). The likely reason for the differences in these PK parameters is the anaesthesia and

the resultant changes in heart rate and blood flow. Previously, approximately 50 % of HI-6 has been shown to be excreted in the urine unchanged [191 :192]. However, without collecting the urine from the guinea pigs it was not possible to estimate the rate of renal excretion in this species. It should be noted that the Cl of HI-6 was within the range of renal blood flow of guinea pigs [183]. The PK of HI-6 has been investigated in humans but only by the intramuscular route of administration [192], so these data will be discussed in the next section.

$$k\uparrow = \frac{Cl\leftrightarrow}{V\downarrow} \qquad \Rightarrow \qquad T\frac{1}{2}\downarrow = \frac{\ln 2}{k\uparrow}$$

Equation 3.1. Relationship of volume of distribution and rate of clearance to the elimination rate constant and therefore half-life.

In summary the PK parameters determined for the three MedCM drugs following intravenous administration provide fundamental data. These data were generated from a small number of animals (n=4), but a low n has been used in other recent intravenous PK studies [193-197]. The intravenous route is less variable than other routes, due to absorption of the drug from the site of administration being negated. These PK data for the MedCM have now been characterised and can be used for reference when the MedCM are administered by other routes or under different experimental conditions. Future studies investigating the PK of atropine, diazepam and HI-6 should collect urine for determination of the concentration-time profile in urine. This will enable the renal excretion of these drugs to be better understood. The rapid distribution of the drugs highlighted by these studies can be interpreted as advantageous for the protection against acute nerve agent poisoning, as the MedCM are likely to penetrate target tissues and exert their pharmacological effect quickly after administration.

3.5.2 Plasma bioavailability of medical countermeasures following their intramuscular administration

3.5.2.1 Atropine

Following intramuscular administration atropine was more rapidly absorbed than diazepam (following administration of avizafone) and HI-6, with the concentration at peak in the first sample collected within 1 minute after administration. The absorption of atropine did not mask its distribution phase, so the PK parameters for atropine following intramuscular administration were similar to those determined following intravenous administration (Table 3.2 and Table 3.3). Atropine can be considered bioequivalent by the intravenous and intramuscular routes of administration, with the fraction of the dose absorbed by the latter route being approximately 1.0. The PK of atropine was very similar for the two routes of administration, as shown in Figure 3.9, with the concentration-time profiles being parallel.

The AUC of atropine achieved after intramuscular administration was approximately 10 times greater than the reported human AUC following 4.0 mg (approximately 60 μg/kg for a nominal 70 kg human) by the intramuscular route [198], these being approximately 45 and 3.7 min□μg/mL[‡], respectively. The C_{max} in guinea pigs was approximately 100 times greater than that in humans following the 4.0 mg dose [198], these being approximately 1500 and 14 ng/mL, respectively. These differences in exposure to atropine suggest that the dose used in guinea pig efficacy studies is high compared to human doses, especially as the dose contained in an autoinjector is only 2.0 mg of atropine sulphate [30]. However, studies have shown the importance of higher doses of atropine in combination with other MedCM drugs for the protection against a range of nerve agents [58 :199]. One of those studies did suggest that atropine masks the protective action of the other MedCM [199]. Atropinisation of nerve

[‡] From Ellinwood *et al* [198] Cl = 64.38 L/h ≡ 1,073 mL/min. Substituting this value and the dose into the following equation (previously presented in Table 2.4). $AUC = \frac{Dose}{Cl} = \frac{4.0\ mg}{1{,}073\ ml/min} = 3.7\ min \cdot \mu g/mL$

agent poisoned humans has long been the standard MedCM approach, with administration based on control of the muscarinic signs of cholinergic poisoning [27]. In a clinical study the requirement for atropine was correlated with the degree of AChE inhibition and worsening muscarinic symptoms [200]. The requirement for atropine may differ between the First Aid, buddy-administered, scenario and the continued Medical Management of a poisoned patient, as with the clinical trial data. The Medical Management of nerve agent casualties is discussed in more detail in Chapter 6.

3.5.2.2 Diazepam

The absorption of avizafone and its subsequent conversion to diazepam, following administration of avizafone by the intramuscular route, was fast with T_{max} being achieved within 5 minutes following administration. The absorption phase of diazepam masked the fast distribution phase previously determined following intravenous administration, reducing the number of compartments in the PK model used to fit the data. Diazepam had a high bioavailability, with the fraction of the dose absorbed by the intramuscular route being 0.95. This is the first study to calculate intramuscular bioavailability of diazepam following avizafone administration, as to date, published studies have used diazepam administration as the reference AUC [57,59]. Administration of avizafone by the intramuscular route in guinea pigs can be considered as bioequivalent to intravenous administration of avizafone. This bioequivalence is in agreement with the bioavailability of avizafone calculated using data presented by Maidment and Upshall[57], which was approximately 1.0[‡].

The reduced V_d of diazepam following intramuscular administration compared to intravenous administration was likely to have been due to absorption from the administration site being slower than the rapid distribution phase following

[‡] $F = \left(\frac{AUC_{im}}{AUC_{iv}}\right) \cdot \left(\frac{Dose_{iv}}{Dose_{im}}\right) = \left(\frac{90.6 \pm 11.0}{111.9 \pm 19.2}\right) \cdot \left(\frac{3.5\ \mu M/kg}{2.8\ \mu M/kg}\right) = 1.01 \pm 0.21$

Bioavailability calculated using AUCs and doses from Maidment and Upshall[57].

intravenous administration. This slow absorption possibly prevented distribution of a large amount of the drug into the compartments. The diazepam elimination T½ was significantly shorter following intramuscular administration of avizafone, compared to intravenous administration. The change in T½ may have been related to the reduced V_d. That is, the elimination rate constant is inversely proportional to V_d, so a reduction in V_d leads to an increase in the elimination rate constant and subsequently a reduction in half-life. The diazepam elimination rate constant appeared to increase when avizafone was administered by the intramuscular route but the difference was not statistically significant. The other PK parameters for diazepam were the same as those determined following intravenous administration of avizafone.

The AUC of diazepam following intramuscular administration of avizafone was more than 250 fold greater than the AUC in humans following a dose of 20 mg of avizafone hydrochloride [190]. However, the C_{max} in that human study was approximately half of that reported here, whereas the Cl was very similar, these being approximately 30 mL/min and 34 mL/min in guinea pigs and humans, respectively. A proposed C_{max} of > 1 µg/mL required to stop soman induced seizures, achieved following an intramuscular dose of 10 mg/kg diazepam [135], was approximately twice the C_{max} reported here. Preventing seizures is critical for survival following nerve agent poisoning [201]. It should be noted that the diazepam median effective dose (ED_{50}) for stopping nerve agent associated seizures (tabun = 2.57 mg/kg, sarin = 0.47 mg/kg, soman 2.33 mg/kg, cyclosarin 1.24 mg/kg and VX 0.74 mg/kg) when administered with a low dose of atropine and pralidoxime was less than the dose studied here [131]. These data suggest that the dose of avizafone used in efficacy studies is appropriate compared to the human dose.

3.5.2.3 HI-6

HI-6 by the intramuscular route was quickly absorbed, with T_{max} being achieved within 10 minutes following administration. The absorption phase of HI-6 masked the distribution phase previously determined following intravenous administration, reducing the number of compartments in the model used to fit

the data. HI-6 was shown to have the lowest bioavailability of the three MedCM following intramuscular administration, with the fraction of the dose absorbed being approximately 0.5. Concentrations of HI-6 were equivalent to those achieved following intravenous administration of one third of the dose. This reduced systemic availability was not expected, as HI-6 had previously been determined to be bioequivalent by the intramuscular route in rats [202]. This change in bioavailability may have been related to the significant increase in Cl, reducing the plasma concentrations of HI-6, thereby reducing the AUC and subsequently bioavailability. The change in Cl did not change the elimination T½ of HI-6. The duration over which HI-6 remains at effective concentrations will be reduced, not because of increased clearance but due to the lower concentrations achieved.

The HI-6 AUC in guinea pigs following intramuscular administration was lower than that achieved in humans (1037 min□μg/mL) following an intramuscular dose of 250 mg [192]. Conversely, the C_{max} in guinea pig was greater than the human C_{max} achieved following a 500 mg intramuscular dose. The data reported here can be used in PK guided scaling [126] or basic *in silico* simulation [203], to ensure the dose of HI-6 used in efficacy studies is equivalent to a specific human dose (such as one that could be contained within an autoinjection device ≈ 600 mg). Scaling of MedCM doses is discussed in more detail in Chapter 6. The use of equivalent doses must be completed with caution, as no single therapeutic concentration akin to that suggested by Sundwall [204] (2×10^{-5} M; the minimum therapeutic concentration of oximes; cited many times erroneously as 4 μg/mL) can be used in two species due to differences in the nerve agent-AChE complex [69 :205].

3.5.3 Muscle and brain pharmacokinetics following intramuscular administration

This study is the first to determine the concentration-time profile of MedCM against nerve agent in tissues as well as plasma, using microdialysis probes in conscious ambulatory animals. The data obtained demonstrate that with the exception of HI-6 in the brain, these MedCM are available in the target tissues

to exert their pharmacological actions against nerve agents. Atropine, diazepam and HI-6 rates of elimination in the tissues mirrored those in the plasma, the tissue concentrations decreasing in a single exponential pattern, indicating the drugs re-distributed back into the plasma, subsequently being cleared.

HI-6 was not measured in brain microdialysate samples from guinea pigs except in one animal. The corresponding muscle microdialysate fractions collected from this animal did not contain HI-6. It is probable that microdialysate fractions from this animal were mislabelled at some point in the processing and LC-MS-MS assay. Notwithstanding this single animal, the microdialysis data provides evidence that HI-6 is not able to cross the blood brain barrier (BBB) and penetrate into the brain (at the dose tested). The brain is a critical site of action of nerve agents and optimising the ability of oximes to penetrate into the brain has been shown to improve efficacy, through reactivation of central AChE [206]. There was an apparent lag in the appearance of HI-6 in the muscle compared to plasma, which may have been due to slower penetration of HI-6 into the interstitial space of the muscle than was indicated by the plasma PK. Alternatively, this lag time could be an artefact of the integrated microdialysis sampling, which was unable to sample at sufficient temporal resolution to determine rapid changes in concentration. It is conceivable, that the lag could be a combination of both of these explanations.

There are no PK data for atropine in brain or muscle with which to compare the data reported here, so therapeutic concentrations of atropine in these tissues are not known. Studies using microdialysis could be carried out to determine therapeutic concentrations of atropine with the possibility of linking these to plasma PK and subsequently, to efficacious doses (this is discussed in more detail in Chapter 6).

The brain concentrations of diazepam reported here were much lower than those reported by Capacio *et al*, in guinea pig brain tissue collected *post mortem*, following administration of diazepam to soman exposed guinea pigs

(0.3 – 1.0 μg/mL) [135]. These differences were most likely due to the differing sample collection methods, i.e. microdialysis samples unbound drug, whereas tissue homogenate provides total drug concentrations. Another reason for the difference may be that the samples were from naïve animals, in the present study, whereas the data collected by Capacio *et al* was from poisoned animals. Microdialysis presents the opportunity to link the brain concentrations to plasma concentrations. Therefore, a study in which plasma and brain concentrations are correlated with electroencelaphograpy, similar to those carried out by Bourne and Fosbraey [162], may identify the therapeutic concentrations required to prevent seizure. The brain concentration of diazepam appeared to lag behind the plasma concentrations. This may have been due to the lipophilicity of this drug causing it to preferentially distribute to the lipids in the brain and muscle, prior to being available in the aqueous interstitial space, from which the microdialysis probe collects samples. However, as stated previously, these lags may be artefacts of the integrated sampling.

The muscle and brain PK data reported here can be referenced as baseline data for muscle and brain PK data following combined intramuscular administration of MedCM, in naïve or sarin poisoned animals.

3.5.4 Effect of combined administration of medical countermeasures on the pharmacokinetics of the component drugs

The absorption, distribution and elimination of atropine and diazepam did not change in plasma after combined administration of atropine, avizafone and HI-6, compared to individual intramuscular administration of these MedCM drugs. However, atropine concentration in the brain appeared to lag behind both plasma and muscle. Conversely, the lag was reduced and eliminated for diazepam in the brain and muscle, respectively.

In contrast to atropine and diazepam the plasma PK of HI-6 did change following combined administration with atropine and avizafone. These changes

in PK were unlikely to be direct drug-drug interactions between atropine or diazepam and HI-6. It is more likely that the pharmacological action of atropine caused physiological changes, such as increased heart rate or vasoconstriction, leading to the reduced Cl and increased C_{max}, T½ and AUC. The exact mechanisms by which the PK has changed cannot be determined from the data presented here; further investigation is required to understand the physiological interaction between HI-6 and atropine. These increases in concentration and elimination T½ should be viewed as positive changes for HI-6, in that the duration HI-6 was at therapeutic concentrations was increased.

The most marked difference on HI-6 PK following combined administration with the other MedCM was the change in ability to penetrate the BBB. Previous studies have implicated P-glycoprotein, an efflux transporter, in the ability of HI-6 to cross the BBB [206]. Studies investigating the membrane permeability of HI-6 *in vitro* may identify the transporter(s) that prevent this drug from penetrating the brain when administered alone and may identify additional opportunities to increase the penetration of HI-6 into this tissue to exert its protective effect. This finding possibly renders current research designing, evaluating and developing centrally active oximes [207-212] unnecessary. The data reported here suggest that administration of HI-6 with atropine and avizafone alters the BBB, beneficially enabling HI-6 to penetrate and reactivate central AChE. In addition, the lag in HI-6 muscle concentrations following individual administration of HI-6 was not evident when HI-6 was administered in combination with atropine and avizafone. This can again be viewed as beneficial, with the HI-6 being available in target tissues a short time after administration.

3.5.5 Effect of acute exposure to sarin on the pharmacokinetics of medical countermeasures

Administration of atropine, avizafone and HI-6 following exposure to sarin changed the PK of HI-6. The increase in C_{max}, caused by a more rapid absorption than in naïve animals, was likely to have been due to physiological changes elicited by the over-stimulation of the cholinergic system. The

reduction in HI-6 Cl back to the rate determined following intramuscular administration of HI-6 alone can be rationalised through the mutually antagonistic effects of atropine and sarin. If muscarinic receptor effects are involved in clearance, it can be expected that the changes in HI-6 PK discussed in the previous section of this chapter were reversed in the presence of sarin. As noted in the previous section, the mechanism of these changes cannot be determined from the data presented here and further studies will need to be carried out to elucidate them.

The PD cholinesterase data determined following exposure of guinea pigs to sarin, illustrate the rapid nature of the effects following acute exposure to nerve agents. Even when MedCM were administered one minute post exposure the cholinesterase activity in plasma and erythrocytes quickly decreased. This decrease was to a lesser extent and was followed by a recovery of activity not observed in the saline animals. Integrating the PK with the PD provides a rationale for the recovery of cholinesterase in activity in MedCM treated animals to approximately 1 hour but not beyond this time (Figure 3.16). Coincidentally, the concentration of HI-6 prior to 1 hour was above 5.77 µg/mL, equivalent to the concentration of 2×10^{-5} M, proposed by Sundwall *et al* as the minimum therapeutic concentration required for an oxime [204] (discussed in Section 3.5.2.3). In a human PK study of intramuscular HI-6, the time above this arbitrary threshold concentration was approximately 90 and 150 minutes, following doses of 250 and 500 mg, respectively. That study indicated the doses used in guinea pigs may need to be increased to achieve this duration at the target concentration and to model the human scenario.

The significant increase in HI-6 AUC determined in the muscle and brain after sarin exposure when compared to the AUC in naïve animals, should be viewed as beneficial. As discussed in the previous section, the recent research into oxime with improved penetration through the BBB seems unnecessary. The data reported here indicate that sarin alters the BBB, enabling HI-6 to penetrate into this tissue and reactivate the nerve agent inhibited AChE.

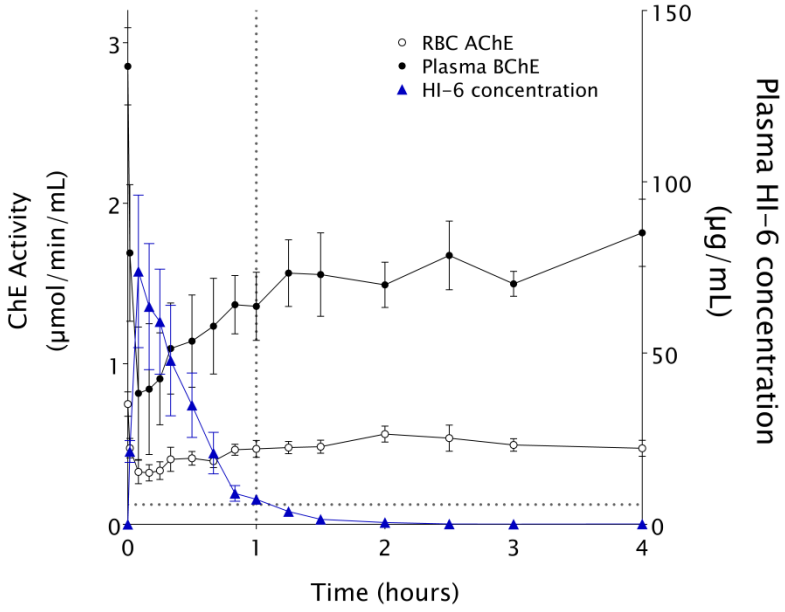

Figure 3.16. Erythrocyte and plasma cholinesterase activity inhibited by sarin recovers up to approximately 1 hour post administration of HI-6, after which the HI-6 concentration decreases below 5.77 μg/mL.

Composite figure uses data previously presented in Figure 3.11 and Figure 3.15. The dotted lines on the x and y axes indicate the 1 hour post administration time point and the threshold concentration of 5.77 μg/mL (2×10^{-5} M).

3.5.6 Summary

The studies reported in this chapter are the first using a new methodology combining vascular cannulae, brain and muscle microdialysis in individual conscious ambulatory guinea pigs. Indeed, these studies were the first to sample drug concentrations in skeletal muscle of conscious animals using microdialysis. This methodology was used to determine the PK of atropine, diazepam and HI-6 by various routes, individually, in combination with one another and in sarin poisoned animals.

Atropine, diazepam and HI-6 were quickly distributed and eliminated from the plasma. Following intramuscular administration atropine and diazepam were bioequivalent to intravenous administration, with approximately 95 % of the administered dose being systemically available. Conversely, approximately 50 % of the administered dose of HI-6 was available following intramuscular administration. Tissue concentrations of atropine, diazepam and HI-6 were generally in equilibrium with the plasma, with the decrease in concentration seemingly governed by plasma clearance. The one exception was HI-6, which was not able to penetrate the BBB.

Combined administration of the MedCM by the intramuscular route altered the PK of HI-6 but not atropine or diazepam. The major change was the ability of HI-6 to penetrate the BBB in the presence of atropine and diazepam, enabling this drug to act centrally. This finding has implications for the efforts of several research groups to design central acting oximes, i.e. there may not be an applied requirement for these oximes. The microdialysis PK data provide evidence that the combined MedCM are able to penetrate target tissues and exert their pharmacological action to protect against nerve agent poisoning. However, the PK models fitted to these microdialysis data may not accurately describe the concentration-time profiles, due to the integrated sampling and lack of temporal resolution, as shown by the various lag times. The fitting of non-compartmental PK models to microdialysis data may be a better approach, particularly as the tissues in which the microdialysis probes are implanted can be considered as individual PK compartments. Combining such microdialysis

PK data with PD data in the same tissues (e.g. ACh concentrations or electroencephalographic data), as has already been reported by Bourne *et al* [150:162], Joosen *et al* [26] and O'Donnell *et al* [147:148], will enable the determination of the concentrations required to counter the effects of nerve agent in these target tissues.

Following administration of combined MedCM, HI-6 reached greater concentrations in sarin poisoned animals compared to naïve animals, although it was more rapidly cleared from the plasma (meaning there was no change in plasma AUC). These data are further evidence that the HI-6 is able to penetrate the target tissues of poisoned animals to reactivate the inhibited AChE and protect against nerve agent lethality, notwithstanding the survival of the sarin poisoned animals treated with combined MedCM that includes HI-6.

The PK data presented in this chapter can now be used to extrapolate the doses used in guinea pig efficacy studies to human equivalent doses, be that through allometric scaling or through a PK guided approach as suggested by Baggot [127] and Sharma and McNeill [126], respectively. Extrapolation of doses is discussed in Chapter 6.

4. BIOSCAVENGER MEDICAL COUNTERMEASURES AGAINST PERCUTANEOUS NERVE AGENT

4.1 Chapter specific introduction

Bioscavengers such as human butyrylcholinesterase (huBChE) have proven efficacious as pretreatments to acute nerve agent exposure [130] and plasma-derived huBChE is in advanced development in the United States of America. Their development, specifically as pretreatments, is in response to the requirement for inactivation of nerve agents, prior to their binding to endogenous cholinesterases and inhibiting normal cholinergic function [102] (Figure 4.1). Stoichiometric bioscavengers, of which huBChE is one example, inactivate nerve agents by irreversibly binding to them in a 1:1 ratio, in the same way as endogenous AChE or BChE.

Ensuring sufficient bioscavenger is present in the systemic circulation and over a long enough period of time is critical to ensure a pretreatment regimen is effective and practicable. The PK of huBChE has previously been determined in several species [130 :213-215], with the aim of assessing the longevity of huBChE in the systemic circulation. More recently huBChE has demonstrated efficacy as a post exposure therapeutic MedCM against percutaneous nerve agent exposure [109]. In this scenario the speed of absorption may be more important than the longevity of huBChE in the systemic circulation. The PK of huBChE has previously been determined in guinea pigs [130] but the PK interaction between the bioscavenger and the nerve agent when huBChE is administered to nerve agent poisoned animals has not. Quantifying the amount of bioscavenger consumed in neutralising nerve agent will improve the understanding of efficacy of bioscavengers. Knowing the threshold amount of bioscavenger required to neutralise the nerve agent will enable efficacious doses that are known to maintain this amount in the circulation for a prolonged duration, to be calculated for humans. Of equal importance for the effectiveness of bioscavenger approaches is knowledge of the amount of the nerve agent absorbed into the circulation following percutaneous exposure, ensuring the amount of bioscavenger in the blood is appropriate to the amount of said nerve agent.

Determination of the PK or toxicokinetics (TK; PK of a toxic dose) of a nerve agent following percutaneous exposure can complement the huBChE PK, to show the fraction of the exposure dose that penetrates the systemic circulation, which therefore must be neutralised by the bioscavenger. Such PK data may be supplemented with target tissue PK data, which can be used to demonstrate the ability of bioscavenger to prevent the nerve agent from reaching its sites of action (as shown in Figure 4.1). The PK/TK of nerve agents following percutaneous exposure has previously been investigated [136:141], these studies were of short duration (6 – 8 hours) and were carried out in anaesthetised and atropinised animals. Percutaneous poisoning occurs over a protracted time-course compared to inhalation/acute nerve agent poisoning. For example, signs of poisoning that triggered administration of MedCM in guinea pig efficacy studies did not occur until ≈ 6 hours after percutaneous exposure [110]. Long duration PK/PD studies of percutaneous nerve agent (≥ 48 hours) have to date, not been carried out. This is probably due to the doses of nerve agent studied having been supralethal (> 1 × LD_{50}) and animals are not likely to survive a longer duration study, thus limiting observations to a shorter period. The PK of percutaneous nerve agent in target tissues has not been studied. Thus, the studies reported in this chapter were completed to determine the plasma PK of huBChE following intravenous and intramuscular administration, as well as the PK of percutaneous VX. Studies reported here were also completed to determine the PK interaction between huBChE and percutaneous VX. The data from these studies are discussed with respect to efficacy of huBChE as a post exposure therapeutic MedCM against percutaneous nerve agent.

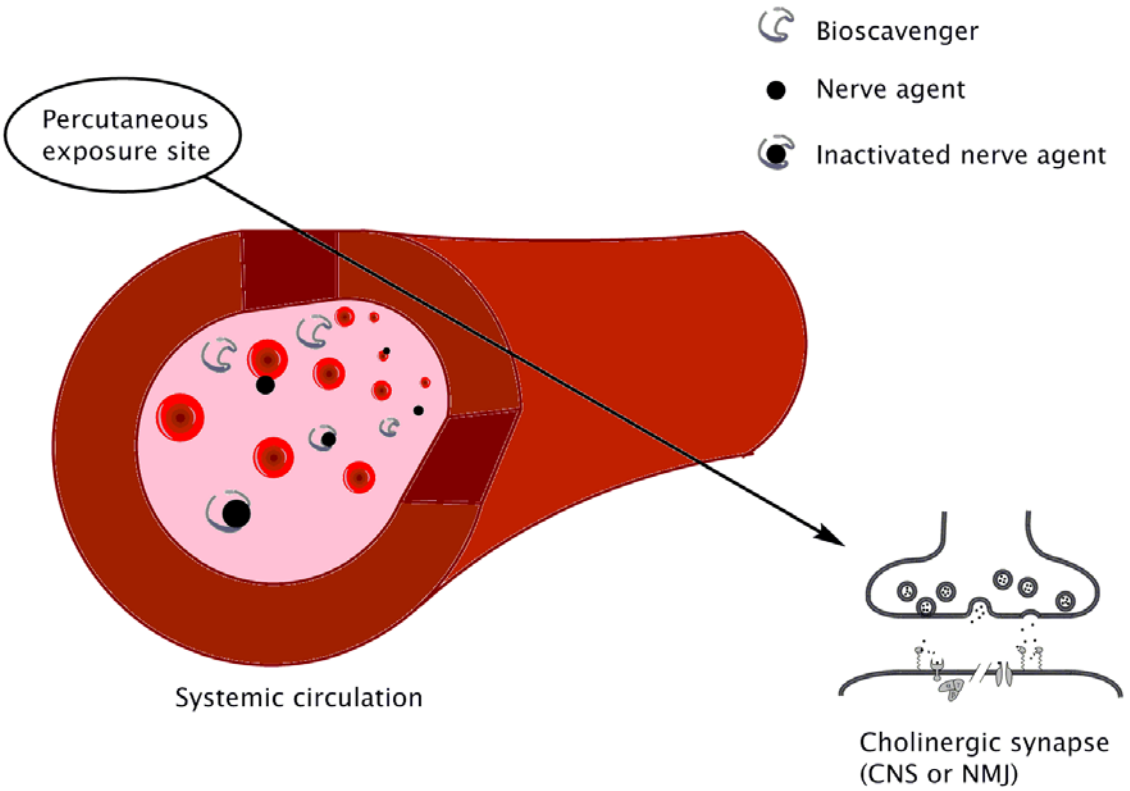

Figure 4.1. Schematic diagram showing percutaneous route of entry of nerve agent into the body, through the vascular system, to its sites of action.

Nerve agent moves from the skin, through the extracellular space, to the blood (arrow) and once here the nerve agent is transported around the body. From the blood the nerve agent moves into the extracellular space of the tissues and to the target sites (CNS; central nervous system, NMJ; neuromuscular junction), where it inhibits acetylcholinesterase. Pretreatment with bioscavenger increases the irreversible binding sites for nerve agent, effectively forming a sink, preventing onward movement to the target sites.

4.2 Chapter specific aims

To determine the pharmacokinetics of human butyrylcholinesterase and the toxicokinetics of VX following exposure by the percutaneous route and thus provide data to aid the understanding of huBChE efficacy against percutaneous nerve agent exposure, including limitations of bioscavenger therapy.

a. To determine the PK of huBChE bioscavenger after intravenous and intramuscular administration in guinea pigs.

b. To calculate the intramuscular bioavailability of huBChE using the intravenous and intramuscular data.

c. To determine the TK and TD profile of the nerve agent VX by the percutaneous route of exposure.

d. To determine the PK interactions between VX and huBChE when this bioscavenger is administered to poisoned guinea pigs.

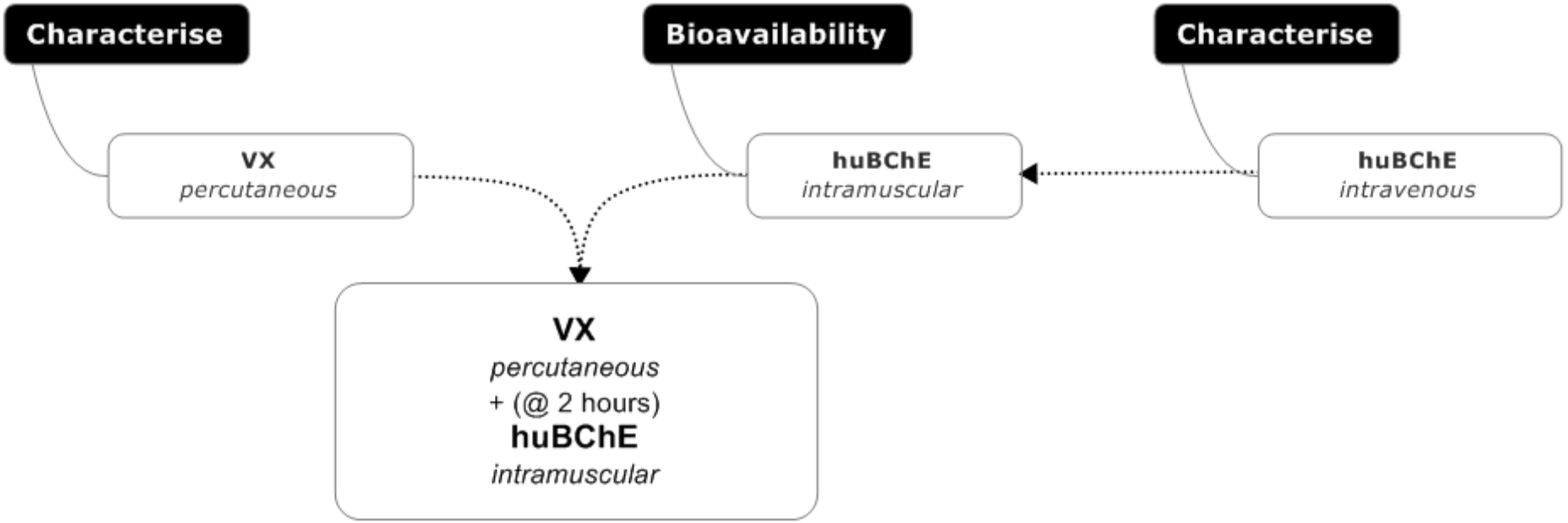

Figure 4.2. Diagram showing concept/aims and design of the *in vivo* guinea pig studies described in this chapter.

Determining the concentration-time profile of huBChE following intravenous administration will characterise the PK. Determining the concentration-time profile of huBChE following intramuscular administration will enable calculation of huBChE bioavailability by this route. Determining the concentration-time and effect-time profile of percutaneous VX will characterise the TK and TD of this nerve agent. Each of these can be used to provide fundamental data to improve the understanding of huBChE bioscavenger efficacy against percutaneous nerve agent poisoning. The determination of the PK interaction of huBChE and VX in the final part of the study will further improve the understanding of efficacy.

4.3 Materials and methods specific to the study of bioscavenger medical countermeasure and percutaneous nerve agent pharmacokinetics

To determine the PK of huBChE after intravenous bolus and separate intramuscular administration, eleven male Dunkin-Hartley guinea pigs (470 ± 45 g, mean ± SD) were implanted with arterial and venous cannulae (intravenous bolus) or just arterial cannulae (intramuscular), as detailed in Chapter 2. HuBChE (3.4 mg/kg) was administered as an intravenous bolus (n=4) or as an intramuscular dose (n=7). Blood samples were collected at set time points following administration of huBChE, as shown in Figure 4.3. These sample collection time points were chosen based on previously published studies [130] and aimed to focus on determining the T_{max}. Blood samples were collected for up to 7 days (168 hours). Blood samples were processed, stored, assayed and analysed for cholinesterase activity, as described in Chapter 2.

To determine the TK and TD of VX after percutaneous exposure and separately the effect of huBChE on the PK of VX (and *vice versa*), 20 male Dunkin-Hartley guinea pigs (374 ± 22 g, mean ± SD) were implanted with arterial cannulae and brain and muscle microdialysis probes, as detailed in Chapter 2. The brain and muscle microdialysis probes were perfused at 1.0 µL/min with CNS and T1 perfusion fluids (CMA microdialysis, Sweden), respectively. All probes were perfused for a 1 hour equilibration period, prior to exposure to VX. Animals (n=8) were exposed to VX (267.4 µg/kg) by application of VX onto the skin (percutaneous route). HuBChE (3.4 mg/kg) was administered to animals two hours after percutaneous exposure to VX (n=8). Blood samples and microdialysis fractions were collected at set time points for 48 hours after exposure to VX, as shown in Figure 4.4. These blood sample time points were chosen to enable the greatest temporal resolution around the VX T_{max}, which was reported by van der Schans *et al* [136]. The blood samples were processed, stored, assayed and analysed for VX concentration and cholinesterase activity, as detailed in Chapter 2. Microdialysis samples were immediately frozen at -20 ˚C and subsequently stored at – 80 ˚C before being assayed for VX concentration, as detailed in Chapter 2.

To determine the effect of bioscavenger on the blood PK of VX after percutaneous exposure to VX, 10 male Dunkin-Hartley guinea pigs (382 ± 14, mean ± SD) were anaesthetised and implanted with cannulae in the jugular vein and microdialysis probes (6 kDa cut-off PAES membrane, Microbiotech AB, Sweden) in the carotid artery. These guinea pigs remained anaesthetised throughout the study, which was of eight hours duration. Microdialysis probes were perfused at 1.0 µL/min with physiological Ringer's solution (Vetivex® 9, *NaCl 147 mM, KCl 4 mM, $CaCl_2$ 3 mM,* Dechra, UK). Animals were exposed to VX (740 µg/kg) by the percutaneous route and 30 minutes later were treated with either recombinant human butyrylcholinesterase (rBChE; 71.96 mg/kg, PharmAthene Inc., USA) or albumin (73.62 mg/kg, Sigma Aldrich, UK). Microdialysis fractions were collected at 30-minute intervals. Microdialysis samples were immediately frozen at -20 ˚C and subsequently stored at – 80 ºC before being assayed for VX concentration, as detailed in Chapter 2.

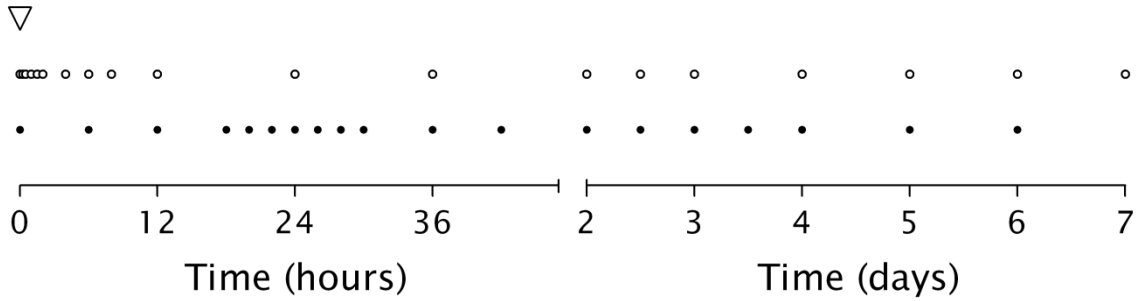

Figure 4.3. Schematic representation of the pharmacokinetic study sampling protocol for huBChE.

The bioscavenger was administered at time zero (▽) by the intravenous or intramuscular routes, samples were collected at set time-points following administration (○ intravenous protocol or ● intramuscular protocol). The majority of samples were collected around the expected T_{max}.

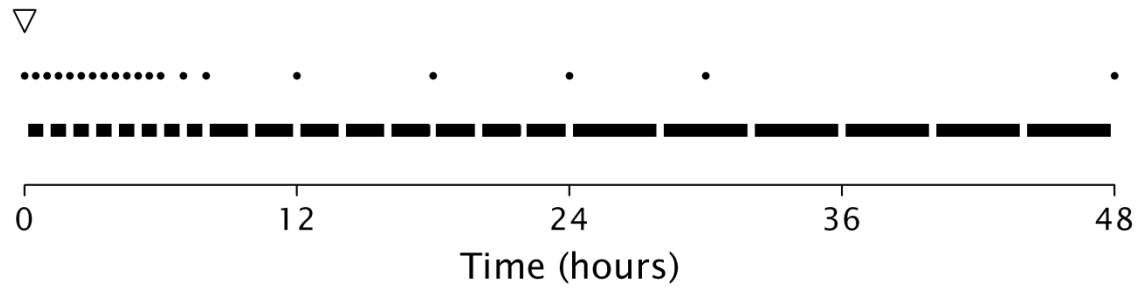

Figure 4.4. Schematic representation of the pharmacokinetic study sampling protocol for percutaneous VX.

The majority of blood samples (●) and microdialysate fractions (▬) were collected to give greater temporal resolution around the expected absorption and distribution of VX. Each bar represents a microdialysate fraction, the duration of which became longer throughout the protocol.

4.4 Results

Of the 30 guinea pigs that underwent surgery 27 successfully recovered from surgery and entered the study. The majority of cannulae and microdialysis probes remained patent. Details for each experimental group are listed in Table 4.1. The 10 guinea pigs that were terminally anaesthetised, cannulated and had microdialysis probes implanted in the carotid arteries survived the surgical procedures. All of these animals were used in, and survived, the subsequent eight-hour study.

	Dose (mg/kg)	**Body mass** (g)	**Animals undergoing surgical procedures** (n)	**Animals used in study** (n)	**Cannula patency**	**Microdialysis patency**	**Notes**
huBChE (iv)	3.4	0.439 ± 0.019	4	4	4/4 (arterial) 4/4 (venous)	n/a	
huBChE (i.m.)	3.4	0.487 ± 0.047	7	7	7/7	n/a	• Animals had greater body mass due to postponement of surgical procedures.
VX (pc)	0.267	0.370 ± 0.015	9	8	8/8	6/8 (brain) 7/8 (muscle)	• One animal died during surgical procedures.
VX + huBChE (pc) (i.m.)	0.267 +3.4	0.377 ± 0.028	10	8	7/8	8/8 (brain) 6/8 (muscle)	• One animal died during surgical procedures. • One animal found dead the morning after surgical procedures.

Table 4.1. Summary information on the surgical procedure success and cannula/microdialysis probe patency, for the different study groups.

4.4.1 Human butyrylcholinesterase bioscavenger pharmacokinetics and intramuscular bioavailability

The plasma concentration-time profile of huBChE following intravenous administration was determined in conscious guinea pigs (Figure 4.5). PK parameters were calculated from these data and are presented in Table 4.2. The V_d following intravenous administration was approximately 60 mL/kg, similar to the reported plasma volume of guinea pigs (67 – 93 mL/kg) [164]. The Cl of huBChE was approximately 1 mL/h/kg. The huBChE remained in the plasma at measurable concentrations for the seven day duration of the study. Based on the AIC value, the two-compartment model fit to the data to describe the distribution and subsequent elimination was not as good a fit as the one-compartment model.

The plasma concentration of huBChE following intramuscular administration increased for approximately 24 hours (Figure 4.6 and Table 4.2). The concentrations of huBChE after intramuscular T_{max} were not significantly different to those achieved following intravenous administration. The huBChE Cl after intramuscular administration was significantly lower from the Cl following intravenous administration ($P < 0.05$, unpaired two-tailed t test), however, the V_d was not different following intramuscular administration. The terminal half-life of huBChE appeared to be longer following intramuscular than intravenous administration but this difference was not statistically significant ($p > 0.05$, unpaired two-tailed t test). The absorption of huBChE following intramuscular administration was extensive, with the fraction of the dose absorbed being 0.83 ± 0.15 (mean ± SEM). The 0 – 24 hour bioavailability of butyrylcholinesterase was 0.38 ± 0.03.

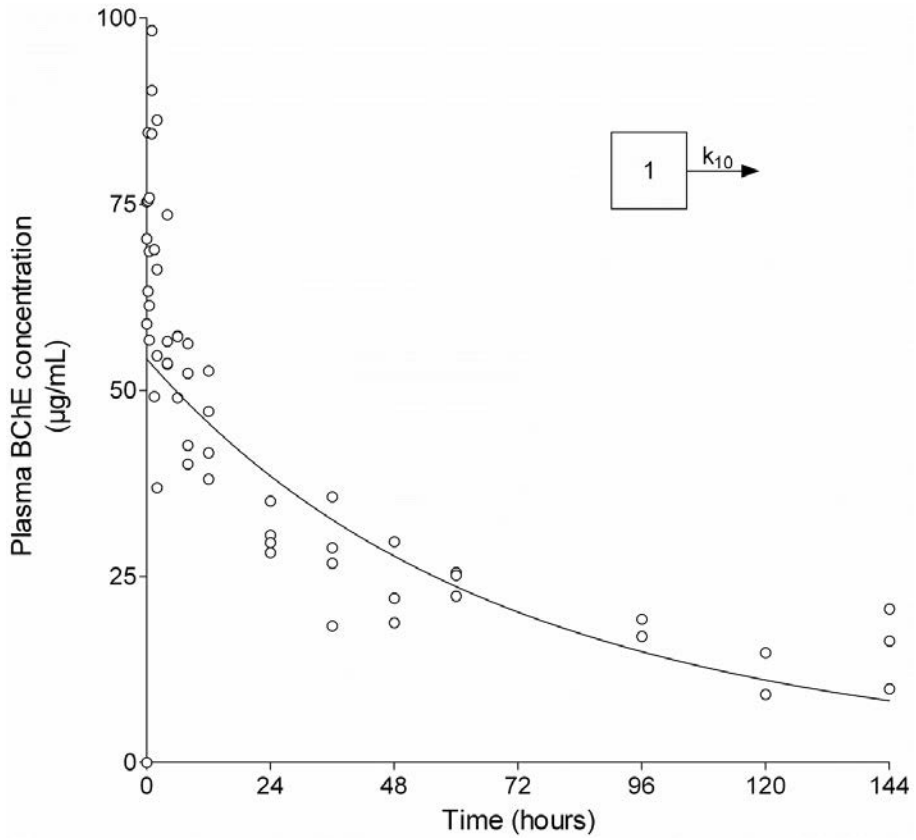

Figure 4.5. Concentration-time profile of huBChE bioscavenger quantified in plasma from individual conscious ambulatory guinea pigs following intravenous administration.

Concentrations from individual animals (n=4, ○) are shown with the mean concentration predicted by the PK model (solid line), which was calculated from the pooled data. The dose of huBChE administered was 3.4 mg/kg. Inset shows the schematic compartmental PK model fitted to the data.

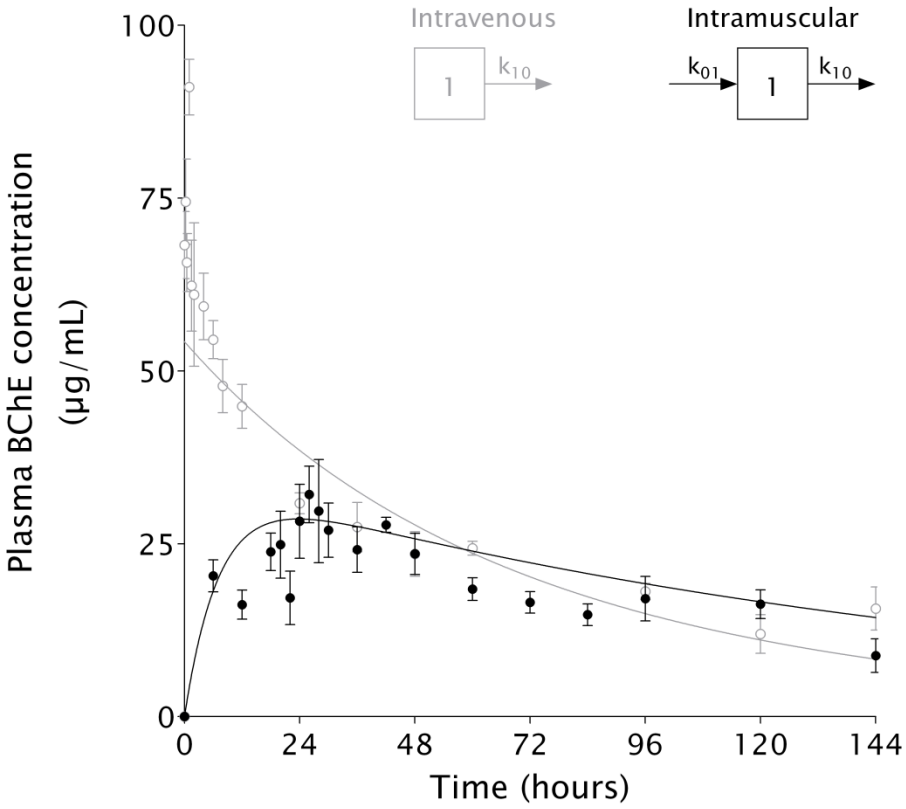

Figure 4.6. Concentration time profile of huBChE bioscavenger quantified in plasma from individual conscious ambulatory guinea pigs following intramuscular administration.

Data shown as mean ± SEM (n=7), plasma concentrations following intravenous administration (Figure 4.5) are included for comparison. Mean concentrations predicted by the PK model (solid line) were calculated from the pooled data. The dose administered was 3.4 mg/kg. Inset shows the schematic compartmental PK model fitted to the data.

	Intravenous	**Intramuscular**
Dose (mg)	1.49 ± 0.03	1.66 ± 0.06
$\mathbf{C_{max}}$ (ng/mL)	n/a	24.2 ± 1.3
$\mathbf{T_{max}}$ (h)	n/a	22.3 ± 4.8
Elimination T½ (h)	67.8 ± 9.6	113.3 ± 28.4
AUC (h□µg/mL)	4878 ± 562	4527 ± 820
$\mathbf{V_d}$ (mL)	68.2 ± 4.9	61.4 ± 5.6
Cl (mL/h)	0.70 ± 0.08	0.38 ± 0.07*
$\mathbf{k_{01}}$ (1/h)	n/a	0.15 ± 0.05
$\mathbf{k_{10}}$ (1/h)	0.0102 ± 0.0015	0.0061 ± 0.0015

Table 4.2. Compartmental PK parameters huBChE following intravenous and intramuscular administration in conscious ambulatory guinea pigs.

HuBChE PK profiles were best fit by a one-compartment PK model. Data shown as the estimate of the parameter for the pooled concentration-time profile ± standard error of the estimate.

* =$p<0.05$, unpaired two-tailed t test.

4.4.2 Percutaneous VX pharmacokinetics and pharmacodynamics

Following percutaneous exposure to VX (267.4 µg/kg) plasma VX concentrations were below the limit of quantitation in all the plasma samples collected. Therefore, the concentration-time profile and TK parameters could not be determined in plasma.

The inhibition-time profiles of guinea pig erythrocyte AChE and endogenous plasma BChE activities were determined (Figure 4.7) following percutaneous exposure to VX (267.4 µg/kg). Maximal inhibition of cholinesterase activity by VX was 67.4 ± 5.2 % and 79.2 ± 3.7 % in plasma and erythrocytes, respectively (Table 4.3). The rate of inhibition of erythrocyte AChE activity (20.5 ± 6.3 %/h) was significantly faster than inhibition of plasma BChE activity (11.5 ± 2.1 %/h) ($p < 0.05$, unpaired two-tailed t test). Erythrocyte AChE activity did not recover from the maximal inhibition, whereas plasma BChE activity recovered at a significantly increased rate ($p < 0.01$, unpaired two-tailed t-test).

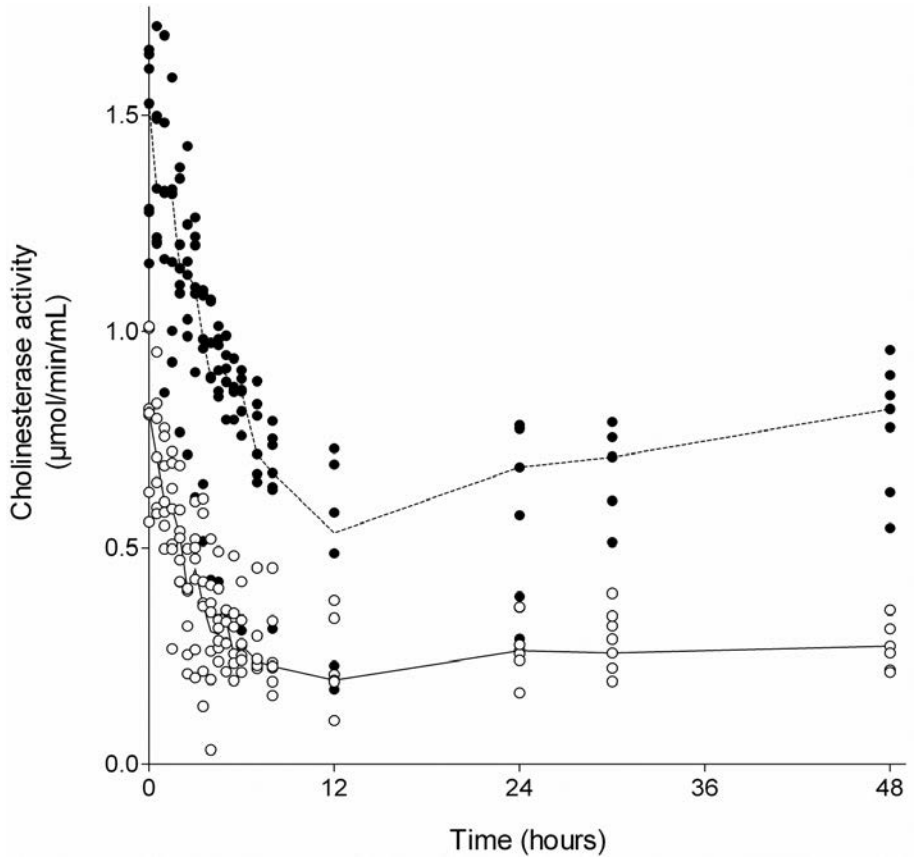

Figure 4.7. Effect-time profile of VX on guinea pig erythrocyte acetylcholinesterase (○, n=7) and plasma butyrylcholinesterase (●, n=7) following VX exposure by the percutaneous route (267.4 µg/kg). Data shown as individual replicate cholinesterase activities with median values (solid and dotted lines, erythrocytes and plasma, respectively).

	Erythrocyte AChE	Plasma BChE
E_0 (µmol/min/mL)	0.807 ± 0.065	1.449 ± 0.077
I_{max} (µmol/min/mL)	0.229 ± 0.036	0.482 ± 0.096
Rate of inhibition (%/h)	-20.5 ± 6.3*	-11.5 ± 2.1
R_{min} (%)	20.8 ± 3.7	32.6 ± 5.2
T_{min} (h)	18.5 ± 6.2	15.6 ± 3.1
Rate of recovery (%/h)	0.4 ± 0.3	0.5 ± 0.1**

Table 4.3. Noncompartmental TD parameters determined for normalised guinea pig plasma BChE and erythrocyte AChE activity following percutaneous exposure to VX.

E_0 and I_{max} were calculated from the raw data. Data shown are mean ± SEM or standard error of the estimate.

* $p<0.05$, **$p<0.01$: Paired two-tailed t-test.

4.4.3 Muscle and brain toxicokinetics of percutaneous VX

The efficiency of the microdialysis probes was determined to be 31 ± 7 % and 45 ± 3 % for *ex vivo* brain and muscle probes, respectively, using radiolabelled VX. The VX did not persist in microdialysate fractions after removal of the probe from the stock VX solution and being placed in saline. The data presented have been corrected for the efficiency of the probes.

The concentration-time profile of VX in target tissues (brain and muscle) was determined by quantitation of VX in microdialysates (Figure 4.8) following exposure to VX by the percutaneous route. After an initial small increase to ≈ 0.03 ng/mL, concentrations of VX plateaued until the time of maximal inhibition of blood cholinesterases (approximately 12 hours). Thereafter, tissue VX concentrations increased to peak at 42 and 38 hours after percutaneous exposure in muscle and brain, respectively. The mean C_{max} values were 64 ± 11 pg/mL (239 ± 41 pM) in muscle and 203 ± 61 pg/mL (759 ± 228 pM) in brain microdialysates. Mean total exposure to VX (AUC) was greater in the brain than the muscle being 1,698 ± 322 h□pg/mL (6.4 ± 1.2 h□nM) and 5,071 ± 1,690 h□pg/mL (19.0 ± 6.3 h□nM), respectively.

The brain microdialysate concentration in one animal was greater than in all the other animals (more than 10 SD from the mean): these data for this animal were excluded from the mean profile (Figure 4.8, inset).

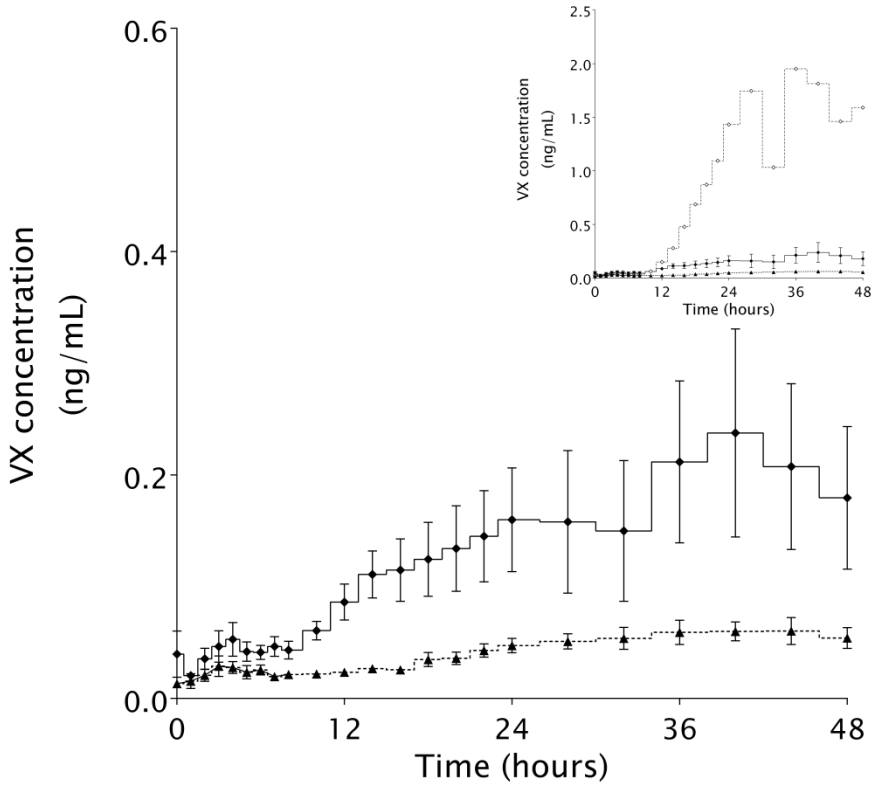

Figure 4.8. Concentration-time profile of free VX in brain and muscle microdialysate fractions following percutaneous exposure of conscious ambulatory guinea pigs.

Concentration-time profile in brain (◆, n=6) and muscle (▲, n=7) following a percutaneous VX dose of 267.4 µg/kg. Data shown are mean ± SEM.

Inset: Individual animal with AUC >10 SD from the mean of the other animals in the group (◇, n=1).

4.4.4 Blood toxicokinetics of percutaneous VX in anaesthetised guinea pigs

The concentration-time profile of free VX was determined in the blood of anaesthetised guinea pigs for eight hours following exposure to percutaneous VX (297 μg/kg = 1 × LD_{50}, Figure 4.9). The concentration was generally consistent within subjects but there were large increases in concentration in some microdialysate fractions. TK analysis of these data was not possible as the models would not fit the data. The concentrations of VX quantified in the blood of anaesthetised guinea pigs were similar to the VX concentrations quantified in the muscle and brains of conscious ambulatory guinea pigs. The AUC of the blood concentration-time curve was 800 ± 222 h□pg/mL (2.99 ± 0.83 h□nM), this was significantly greater than the eight hours AUC for muscle or brain, these being 144 ± 37 h□pg/mL ($p < 0.01$, one-way ANOVA) and 311 ± 62 h□pg/mL ($p < 0.05$, one-way ANOVA), respectively.

The efficiency of the blood microdialysis probes was determined at 38 ± 10 % by *in vitro* VX and 31 ± 3 % by *in vivo* retrodialysis using VR. The data presented were corrected for the efficiency of the probes, using the *in vivo* retrodialysis efficiency.

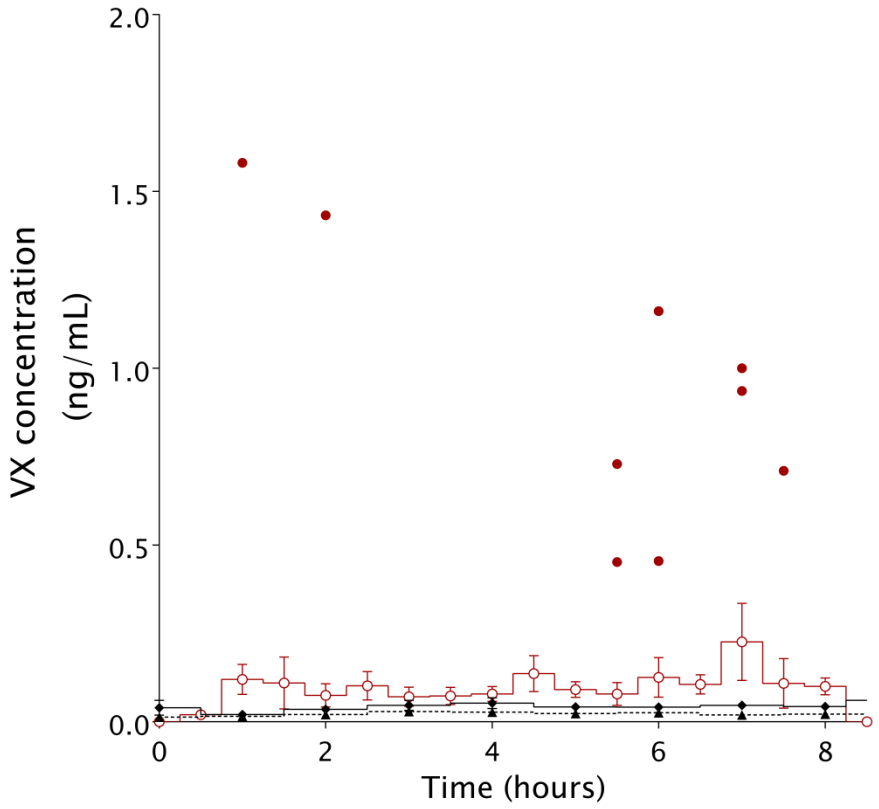

Figure 4.9. Concentration-time profile of free VX determined in blood microdialysate fractions following exposure of anaesthetised guinea pigs to percutaneous VX.

Data shown are mean ± SEM (○, n=5), outliers (●) are shown as separate and were more than 2 SD from the mean concentrations and were not from one individual animal. Muscle (▲) and brain (◆) microdialysate VX concentrations from conscious ambulatory animals exposed to percutaneous VX are included for reference.

4.4.5 Toxicokinetics of percutaneous VX followed by treatment with intramuscular human butyrylcholinesterase

In these studies, percutaneous VX exposure (267.4 µg/kg) occurred at 0 h with bioscavenger being administered two hours later (huBChE 3.4 mg/kg). Blood samples and microdialysate fractions were collected over 48 hours. VX concentrations in the plasma could not be measured, as it was below the limit of quantitation in all of the plasma samples collected. The effect of intramuscular huBChE on the concentration-time profile of VX could not be determined in conscious ambulatory guinea pigs. However, VX was measured in microdialysate fractions from a microdialysis probes implanted in the carotid artery of anaesthetised guinea pigs that were exposed to VX by the percutaneous route (297 µg/kg). In these studies, intravenous rBChE (72.0 mg/kg) significantly reduced the AUC for free VX ($p = 0.05$, one-tailed unpaired t test, Figure 4.10).

The muscle and brain TK of percutaneous VX (267.4 µg/kg) was determined in conscious guinea pigs treated at two hours after exposure with intramuscular huBChE (3.4 mg/kg) (Figure 4.11). The free VX AUC in muscle and brain microdialysates were 3,738 ± 1,076 h□pg/mL (14.0 ± 4.0 h□nM) and 3,061 ± 939 h□pg/mL (11.5 ± 3.5 h□nM), respectively. These AUC were not significantly different from the AUC in untreated animals ($p > 0.05$, one-tailed unpaired t test). The concentration remained constant throughout the 48 hours in the brain microdialysate fractions at 107.7 ± 51.6 pg/mL, the C_{max} and T_{max} were 232.3 ± 77.4 pg/mL (869 ± 290 pM) and 6.6 ± 5.6 h, respectively. The free VX concentration in muscle appeared to peak at one hour, although the variability was very high (267 ± 140 pg/mL), thereafter concentrations remained constant at 78.0 ± 23.3 pg/mL.

The TD profile (inhibition of AChE and endogenous BChE activity) of VX following treatment with huBChE could not be determined, due to the inability of the colourimetric Ellman assay to differentiate between endogenous cholinesterases and exogenous huBChE.

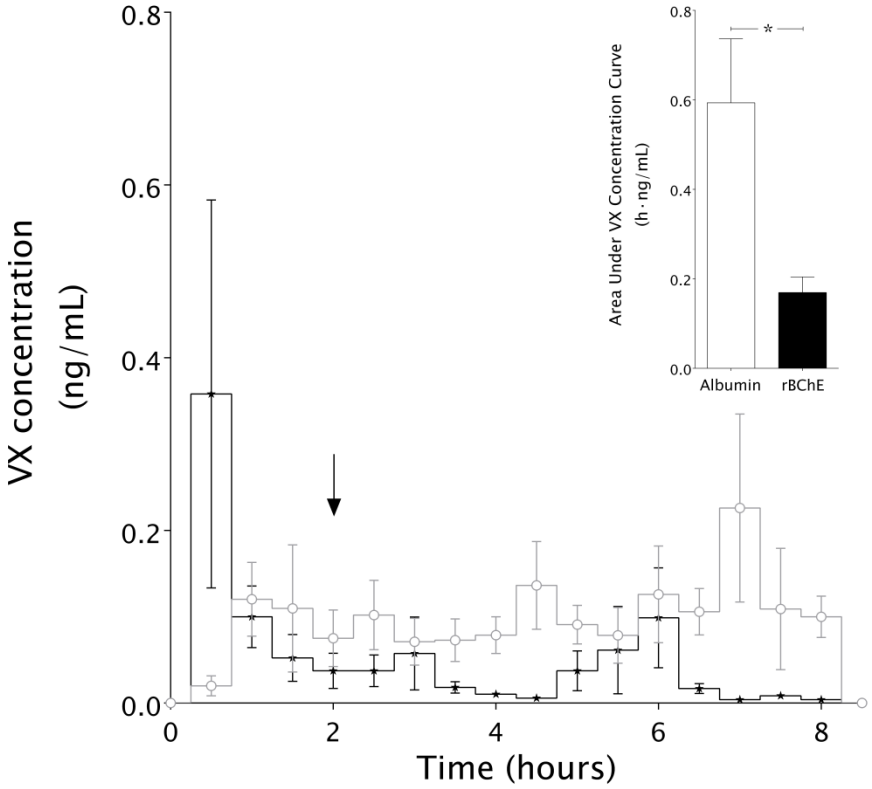

Figure 4.10. Concentration-time profile of free VX determined in blood microdialysate fractions following exposure of anaesthetised guinea pigs to percutaneous VX and treatment at two hours with rBChE.

Data shown are mean ± SEM (⋆, n=5). Concentration-time profile of free VX determined in blood microdialysate fractions of anaesthetised guinea pigs treated with albumin (○, n=5, Figure 4.9) are included for reference.

Inset: The AUC of free VX following treatment at 2 hours post percutaneous VX exposure with rBChE was significantly reduced compared to the treatment with albumin (* $p < 0.05$, one-tailed unpaired t test).

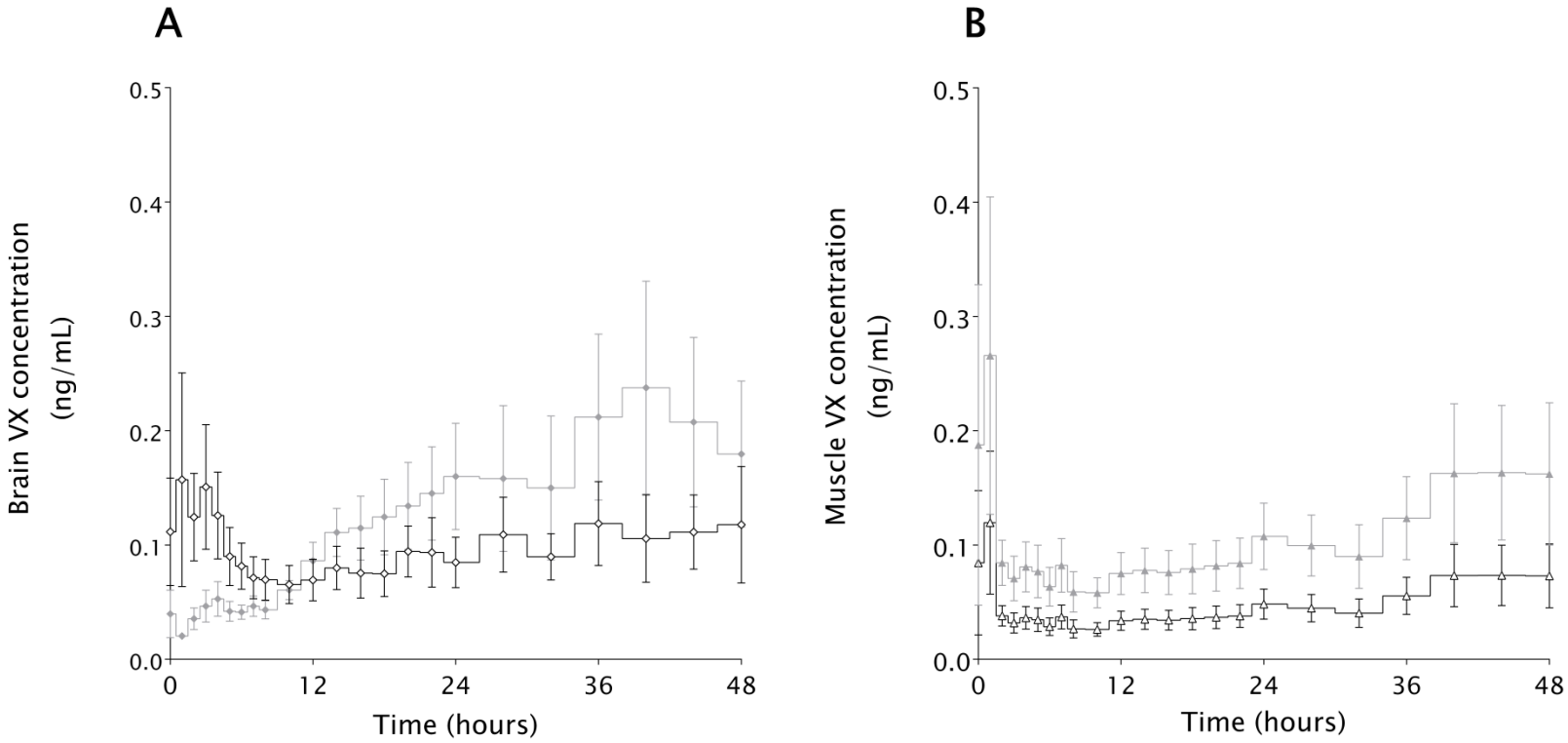

Figure 4.11. Concentration-time profile of free VX in microdialysate fractions collected from brain and muscle of conscious ambulatory guinea pigs following percutaneous exposure to VX and treatment at two hours with huBChE.

(A) Brain microdialysate (◇, n=8) and (B) muscle microdialysate (△, n=6) VX concentrations following percutaneous exposure to VX (267.4 µg/kg) and treatment with huBChE (3.4 mg/kg). Data shown as mean ± SEM. VX concentrations in (A) brain (◆) and (B) muscle (▲) of untreated animals (Figure 4.8) are shown for reference.

4.4.6 Pharmacokinetics of human butyrylcholinesterase in percutaneous VX exposed guinea pigs

The PK of intramuscular huBChE was determined over 48 hours duration in guinea pigs exposed to VX by the percutaneous route (Figure 4.12). The AUC was 40 ± 11 % lower than the AUC of intramuscular huBChE determined in naïve guinea pigs, a significantly reduction ($p < 0.01$, one-tailed unpaired t test).

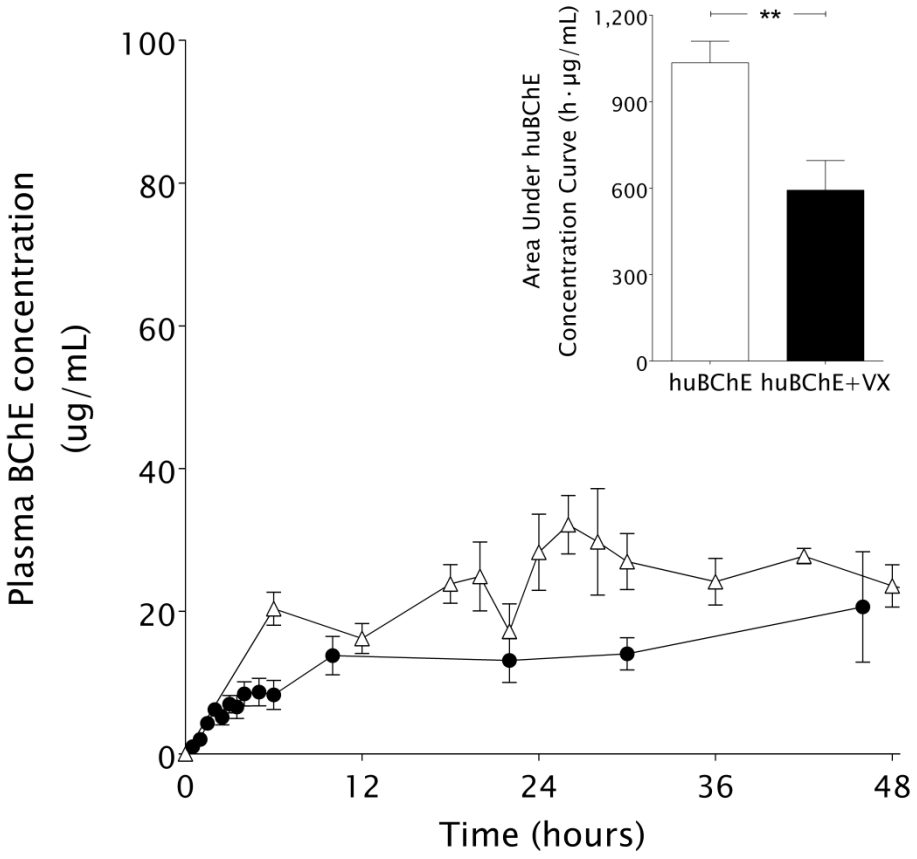

Figure 4.12. Concentration-time profile of intramuscular huBChE determined in percutaneous VX exposed conscious ambulatory guinea pigs.

Data shown are mean ± SEM (●, n=8). Concentration-time profile of intramuscular huBChE in naïve conscious ambulatory guinea pigs (△, n=7, Figure 4.6) is included for reference. The doses of huBChE and VX were 3.4 mg/kg and 267.4 µg/kg, respectively.

Inset: AUC of huBChE calculated from the concentration-time profile data. Data shown as mean ± SEM. ** $p < 0.01$, one-tailed unpaired t test.

4.5 Discussion

The efficacy of huBChE bioscavenger against nerve agent poisoning is dependent on delivery of sufficient scavenging capacity at the appropriate time to prevent inhibition of endogenous AChE. The aim of the studies reported here was to provide data to aid the understanding of the efficacy of huBChE against percutaneous VX. To achieve this aim the plasma concentration-time course of huBChE following intravenous and intramuscular administration was determined in conscious guinea pigs over 7 days. The concentration-time courses of free VX in the brain and muscle were also determined. Plasma concentrations of VX could not be determined in these animals. The concentration-time course of free VX was however quantified in microdialysate fractions from microdialysis blood probes implanted in arteries of anaesthetised guinea pigs. The PK interaction between huBChE and percutaneous VX was quantified in subsequent studies. Each of these studies is discussed in more detail.

4.5.1 Human butyrylcholinesterase bioscavenger

The huBChE PK profile characterised following intravenous and intramuscular administration exhibited a similar PK profile to that previously published by Lenz *et al* [130], although these studies administered a lower dose (3.4 mg/kg compared to 19.9 and 32.5 mg/kg [130]). The huBChE remained in the plasma for the full seven days duration of the study, so would be available to bind percutaneous nerve agent in the event of exposure.

The V_d of huBChE following intravenous administration was low compared to the conventional MedCM (atropine, diazepam and HI-6), approximating to total blood volume (63 – 92 mL/kg [164]), as might be expected for a large protein molecule. These data indicate that the huBChE remains in the vasculature and is unable to cross vascular epithelium [216]. HuBChE is therefore not widely distributed into the tissues (Figure 4.13). Whilst it may be possible that small amounts of huBChE were able to cross the vascular endothelium into the

interstitial space, these small amounts are likely to be returned to the blood by lymphatic drainage, maintaining the low V_d observed [216].

The absorption of huBChE into the systemic circulation following intramuscular administration was slow compared to conventional MedCM. The T_{max} of 26 hours suggests that the primary route of distribution from the injection site was via the lymphatic system, rather than as a result of direct uptake into the blood stream, causing the low bioavailability in the first 24 hours. Again this is probably due to the limited ability of the large huBChE molecule to cross the vascular epithelium [216]. This low bioavailability of huBChE in the first 24 hours following intramuscular administration explains the better reported efficacy of intravenous administration [109], when used as a post exposure therapeutic MedCM. The rate of clearance was also slow compared to the conventional MedCM, leading to the long elimination half-lives observed. The elimination of large protein molecules such as huBChE is through breakdown by proteolytic enzymes, non-specific endocytosis and formation of immune-complexes [217]. For large native molecules these are typically slower processes than the elimination processes for small molecule drugs, such as the conventional MedCM, which are eliminated by renal excretion or hepatic metabolism.

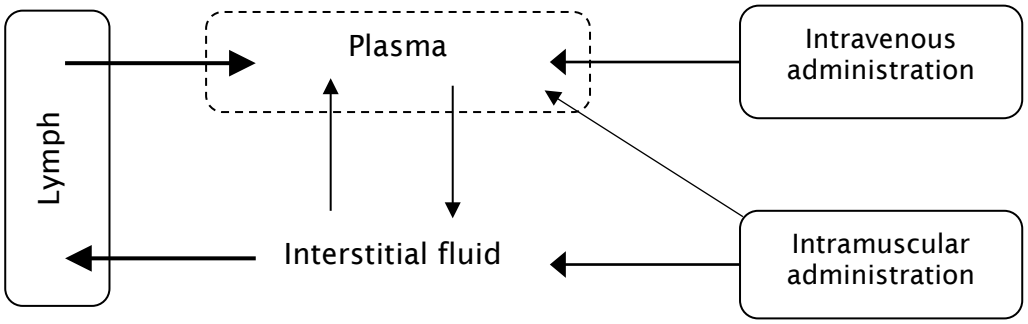

Figure 4.13. Low vascular epithelium permeability of huBChE most likely governs its plasma PK following intravenous and intramuscular administration. The low V_d is probably maintained by the flow of lymph in which the huBChE is transported, this is also likely to cause the late T_{max}. Adapted from Rowland and Tozer [216].

4.5.2 Plasma pharmacokinetics and pharmacodynamics of percutaneous VX

The combination of discrete blood sampling and continuous microdialysis sampling enabled the PK and PD of percutaneous VX to be determined over a long duration compared to previously published TK studies. These techniques have previously only been used individually [26;151], or if combined, using less refined blood sampling methods (e.g. toe nail clip [147]). Therefore, the methodology used here represents a refinement that enabled more data to be obtained from individual animals, in keeping with the responsibility of *in vivo* scientists to refine the techniques used in animal studies and reduce or replace the animals used in research.

The lack of measurable concentrations of VX in plasma samples was not expected, especially as VX has been measured in blood previously by van der Schans *et al* [136] and Joosen *et al* [31]. However, these two previous studies used anaesthetised, atropinised and artificially ventilated hairless guinea pigs at twice the dose of VX (500 µg/kg) compared to the studies reported here. The dose of VX used in the studies reported here was chosen as a dose with minimal toxicity, to avoid agitation of the animals and damage to the harness, tether and sampling equipment, yet sufficient to enable quantitation and sample collection for the full 48 hours study protocol. The measurement of free VX by microdialysis of blood in anaesthetised guinea pigs at concentrations approximating those quantified in the tissues indicate VX was likely to be in the systemic circulation of the conscious ambulatory animals. These data suggest that the storage, handling or processing of the blood samples from the conscious guinea pigs were not optimal, especially as the limit of quantitation for VX reported here (10 pg/mL) was similar to that reported by van der Schans *et al* (25 pg/mL) [136]. The submaximal inhibition of AChE and BChE may have led to *ex vivo* binding of VX to these enzymes, preventing the VX from being quantified. Further evidence for the sub-optimal methodology leading to the lack of PK data in the blood was the VX quantified in the brain and muscle microdialysates collected from the same animals. These tissue data also suggest that VX was present in the systemic circulation. The systemic circulation is the most likely route of transport for VX to have

reached these tissues and only unbound drug (VX) is able to pass between the blood and tissues [218]. Knowledge of how much of a percutaneous dose penetrates into the plasma and therefore the tissues is currently lacking.

The studies reported here provide some data that can be used to estimate the amount of VX absorbed through the skin and therefore yield an approximate bioavailability for this nerve agent. For example, the amount of VX in the brain at C_{max} was approximately 200 pg/mL in a 370 g guinea pig. Making the assumption that VX distributes uniformly throughout the body, the total amount of VX in the body calculated from the C_{max} would be 74 ng, which is approximately 0.00075 of the exposure dose (99 µg). The stoichiometric dose of bioscavenger required to neutralise this amount of VX would be 9.4 µg (277 pmol), a much lower dose than was administered to the guinea pigs in this study. These PK data indicate that much lower doses of bioscavenger are required compared to the dose applied to the skin of the animal (the stoichiometric dose of bioscavenger calculated from the VX exposure dose would be 12.5 mg). The fate of the VX that was applied to the skin is unknown but it may have been located in the stratum corneum, it may have penetrated the skin and partitioned into lipid rich tissues, non-specific binding may have occurred or the agent could even have been metabolised and/or eliminated from the body [136].

To maximise the likelihood of quantifying VX in plasma samples, it is recommended that future PK/TK studies of percutaneous VX should use a larger exposure dose of VX than was used in the studies reported here. However, this increased exposure dose may require the use of atropine to prevent lethality, enabling the full TK profile of VX to be determined. Stabilising compounds should also be used to prevent any *ex vivo* protein binding/AChE and BChE inhibition, as has previously been reported in PK/TK studies [137-139]. Alternatively, future studies could administer VX by intravenous infusion. This method potentially enables VX to be administered directly into the systemic circulation in a controlled manner. In this situation, measurement of cholinesterase inhibition or discrete physiological or behavioural responses

can be linked to VX amount, as opposed to VX concentration (overcoming the difficulty in measuring VX concentration). This method of administration would also enable the rate of infusion to be increased or decreased, to elucidate what effect this has on the signs of poisoning. Studies have previously shown that different signs of poisoning manifest when agent enters the body by different routes and therefore different rates [3].

A prolonged absorption of VX at the dose studied can be inferred from the blood and plasma PD profile (VX inhibition of AChE and BChE), determined following percutaneous exposure of conscious ambulatory guinea pigs. Maximum inhibitions of AChE and BChE activities were not achieved until twelve hours after exposure, although, this is dose dependent, as maximum inhibition has been achieved more rapidly following larger doses of VX [31]. Erythrocyte AChE was inhibited to a greater extent than was plasma BChE; a similar result has previously been reported in guinea pigs[31] and humans [3], probably due to a greater affinity of AChE for VX [219]. Once this maximum inhibition had been achieved, it persisted throughout the 48 hours study with no recovery of erythrocyte activity. Plasma BChE activity recovered by approximately 20 %. Similar differential recovery of cholinesterases has been observed in humans [220]. This differential recovery was most likely to have been due to the different mechanisms for replacement of the different cholinesterases, with the recovery of erythrocyte AChE activity being by erythropoiesis [27] and plasma BChE recovery by *de novo* synthesis in the liver [220]. Erythrocyte AChE is often used as a surrogate marker for tissue AChE because of its convenient accessibility but the slow recovery of this enzyme (80 day life span for erythrocyte [221]) does not reflect the recovery of normal cholinergic function in the tissues, which has been shown in some brain areas to occur within 7 days of exposure to nerve agent [222].

4.5.3 Brain and muscle pharmacokinetics of percutaneous VX

The absorption of VX into target tissues, brain and skeletal muscle was slow compared to the absorption of the MedCM described in Chapter 3 of this thesis but in line with the inhibition of blood cholinesterases. The increase from

initial plateau concentrations of VX in these tissues was concurrent with the maximal inhibition of blood cholinesterases achieved. These data suggest that the blood and more specifically AChE and BChE acted as endogenous scavengers for VX and once the inhibition reached a plateau the VX then distributed to the tissues to a greater extent. . The tissue concentrations of VX reported here (*circa* 1 nM) were below the concentration of AChE in the diaphragm (2.6 nM) [136] and brain (120 nM) [223] and thus might be considered to be below those of toxicological relevance. Importantly however, VX will continue to distribute to the tissues following its continued percutaneous absorption, so it will continue to irreversibly inhibit the tissue cholinesterase. Despite this continued absorption, the sub-lethal exposure dose, the incomplete blood cholinesterase inhibition and the lack of signs of poisoning indicate that insufficient inhibition of tissue AChE had occurred to disrupt normal cholinergic function (greater than 95 % inhibition of AChE is required to affect function). These results may be explained by a slowing of the inhibition of blood cholinesterases, as the amount of VX entering the blood slowed, which was likely to have been caused by the diminished amount of VX in the skin available for distribution into the blood, leading to subsequent distribution of the free VX from the blood to the tissues. Without determination of the plasma VX concentrations this cannot be proven but the concentrations of VX in the blood reported by van der Schans *et al* [136] were similar to those reported here in the tissues. Future studies can improve the understanding of toxicologically relevant concentrations of VX and the PKPD or TKTD of VX following percutaneous exposure. These future studies will need to use higher toxic doses, which should inhibit all of the blood cholinesterase, subsequently inhibiting the tissue cholinesterase, causing toxicity and even lethality in the guinea pigs.

4.5.4 Pharmacokinetic interactions between percutaneous VX and human butyrylcholinesterase

Evidence for the binding capacity of huBChE has previously been shown *in vivo* in studies that titrated the amount of nerve agent (soman and VX) administered to an animal, against the concentration of huBChE [213 :224]. The significant

reduction in the 48 hours AUC of huBChE in VX poisoned guinea pigs compared to naïve guinea pigs, provides additional evidence for the *in vivo* binding of nerve agent and huBChE. These data support the hypothesis that huBChE prevents VX from reaching the target tissues by binding and inactivating the VX in the blood (as shown in Figure 4.1). The huBChE may also change the distribution and elimination of VX. Indeed, binding to the bioscavenger can be considered a route of elimination. It is possible that the change in huBChE AUC determined in VX poisoned guinea pigs was due to changes in absorption of huBChE through altered physiology associated with VX exposure (e.g. decreased cardiac output). VX has been shown to cause prolonged bradycardia at doses similar to that used in the studies reported here [25]. However, large changes in physiology and absorption of huBChE are unlikely, as there was incomplete inhibition of the AChE and the concentrations of VX in the tissues were not toxicologically relevant (see section 4.5.3 above).

The free VX AUC in the muscle and brain of conscious guinea pigs following treatment with huBChE, was not significantly different from untreated animals. This result was unexpected and was in contrast to the reduction in plasma huBChE AUC determined following percutaneous VX exposure. The concentrations of VX in the tissues showed high variability at the early time points and would suggest that VX is distributing to these tissues relatively quickly (within 3 hours). These data are not in agreement with the concept that percutaneous exposure is a slow route of entry into the body. The reason for this variability is unclear. Unfortunately, as the concentration of VX in the blood of these animals could not be measured, it was not possible to determine the effect of huBChE on the plasma PK of VX. The VX in the untreated animals did not fully inhibit the blood cholinesterases and these endogenous cholinesterases remained in excess of the VX. The measurement of VX in plasma following administration of bioscavenger was even less likely, due to the increase in available binding sites for the nerve agent. Subsequent study of free VX concentrations in blood by microdialysis using anaesthetised animals and larger doses of both VX and rBChE showed a significant reduction in VX AUC following treatment with rBChE. These are the first *in vivo* data showing a reduction in the concentration of VX following treatment with a bioscavenger. There was large variability in the blood microdialysis data,

similar to the muscle and brain microdialysis data, following administration of rBChE. There was also large variability measured in individual blood microdialysate fractions collected from control animals. This variability may have been due to intermittent occlusion of the probe against the blood vessel wall or from stagnant flow in the blood vessel, caused by the probe itself. The technique of using microdialysis in blood vessels is increasing in popularity, with the most recently published studies reporting PK of various drugs, with no apparent issues with variability [225-227]. However, the drug concentrations reported in those studies were much greater than the limits of quantitation compared to VX (being 1:100 – 1:1000 higher than the lower limit of quantitation compared to 1:25 – 1:50 higher than the lower limit of quantitation).Also the published PK studies followed a standard administration via the intravenous or intramuscular routes, whereas percutaneous penetration is less well understood. Future studies in which blood samples and microdialysate fractions are collected following percutaneous exposure to a larger dose of VX, will enable the blood microdialysis methodology to be validated.

When observed together, the plasma concentration-time profile of huBChE and the tissue concentration-time profile of percutaneous VX illustrate that the bioscavenger was available in the plasma over an appropriate time period for treatment of percutaneous VX poisoning (Figure 4.14). Other treatment strategies for percutaneous VX poisoning are discussed in Chapter 6 of this thesis.

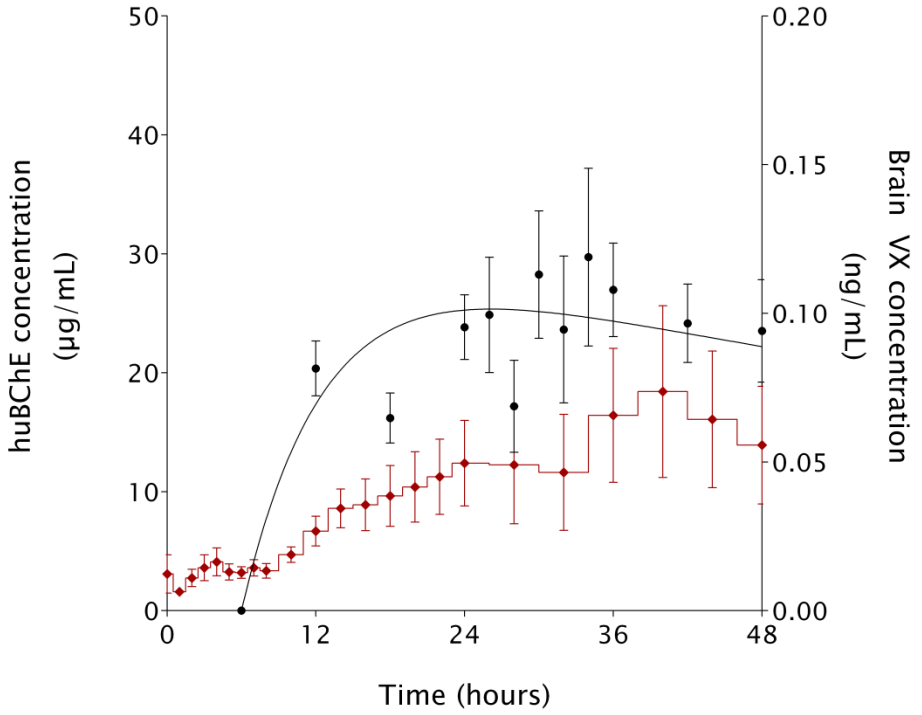

Figure 4.14. Composite figure showing huBChE bioscavenger was available in the systemic circulation, over an appropriate duration to provide protection against percutaneous exposure to VX.

Plasma huBChE data previously shown in Figure 4.6, mean ± SEM (n=7, ●) and the predicted concentrations from the PK model fit of the data (line). VX concentration in brain previously shown in Figure 4.8, mean ± SEM (◆, n=6)

4.5.5 Summary

The studies in this chapter aimed to determine the PK of huBChE and the TK of percutaneous VX to improve the understanding of bioscavenger efficacy.

The PK of huBChE reported here was similar to that previously reported in guinea pigs [130]. The lower bioavailability of huBChE in the first 24 hours following intramuscular administration may explain the better reported efficacy achieved by the intravenous administration route [109].

The plasma TK of VX could not be determined, as no VX was measured in blood samples collected from guinea pigs. However, concentrations of VX were determined in brain and muscle using microdialysis, the first time that VX has been measured in these tissues. These data have enabled an estimate of the amount of VX that penetrates the body following percutaneous exposure. Further studies are required to better understand the absorption of VX by the percutaneous route and thus inform the doses of bioscavenger required to protect against lethality.

PK and TK data, such as those determined for both huBChE and percutaneous VX, can be used in the design of altered administration regimens of conventional MedCM, aimed at achieving greater efficacy and shown experimentally by Joosen *et al* [31]. This is discussed in greater detail in Chapter 6 of this thesis.

5. *IN SILICO* SIMULATION AND MODELLING OF MEDICAL COUNTERMEASURES AGAINST NERVE AGENTS

5.1 Introduction to *in silico* pharmacokinetic modelling and simulation

The majority of PK studies investigating nerve agents and their MedCM have focussed on developing and validating physiologically based pharmacokinetic (PBPK) models, specifically aimed at understanding nerve agent exposure [22 :183 :223 :228]. PBPK modelling is a "bottom up" strategy, which uses physicochemical data, partition coefficients and other parameters determined *in vitro* for the drug being investigated. Integrating the drug data with physiological data for the animal species of interest (e.g. cardiac output and liver blood flow) enables improved understanding of the processes governing the PK of the drug. PBPK models can be used to simulate the concentration-time profiles of the drugs but require appropriate parameters such as: tissue blood flow, tissue partition coefficients or metabolic enzyme profiles, for the species of interest. These data are not always available, so other approaches are also used.

It is possible to simulate concentration-time, concentration-effect profiles and effect-time profiles of drugs using basic PK and PD data [229], such as that presented in earlier chapters of this thesis. This approach is an accepted method of simulation to aid the design of studies [230-232] and has been used before to predict HI-6 concentrations [233]. Simulations using the basic PK parameters may not be as sophisticated as the PBPK approach but they require fewer parameters, less onerous validation and do not require an understanding of all the ADME processes involved. The lack of PK data for MedCM has meant that modelling and simulation of concentration-time profiles have not traditionally been considered as methods available for the development or optimisation of MedCM. This chapter aims to test the hypothesis that simulation and modelling the concentration-time profiles of MedCM and nerve agents can be used to improve the understanding of efficacy and aid the design of experiments. The studies described here determined PK and PD data for physostigmine and hyoscine following intravenous bolus administration, subsequently using the data to predict the concentration-time profiles of these drugs following three intravenous infusions. A third phase to the studies described here determined, *in vivo,* the concentration-time profile of the two

drugs administered by intravenous infusion to provide validation of the predictions.

As discussed in Chapter 1, the combination of physostigmine and hyoscine is in advanced development for licensure as a pretreatment MedCM against nerve agent poisoning. Physostigmine and hyoscine have been formulated in a transdermal patch, which sustains the delivery of the drugs, enabling once daily administration (the current pretreatment pyridostigmine bromide is a tablet, taken three times a day). The transdermal patch is not suitable for guinea pigs, so in efficacy studies the dosing paradigm is to deliver the two drugs by subcutaneous osmotic pump [84]. It is necessary therefore to be able to understand and manipulate the administration of physostigmine and hyoscine to achieve relevant plasma concentrations in animals, in order to design appropriate efficacy studies to support the advanced development of this MedCM. Given that the mechanism of action of physostigmine involves the reversible protection of a portion of the acetylcholinesterase activity, determining the relationship between the concentration of physostigmine and its effect is also important for understanding efficacy.

The studies reported here were completed for the physostigmine and hyoscine pretreatment development programme.

5.2 Chapter specific aims

The aim of this study was to validate PKPD simulation methodology using physostigmine and hyoscine.

- To determine the PK and PD of physostigmine and hyoscine following intravenous bolus administration in guinea pigs, providing parameters that can be used for simulation of intravenous infusion.
- To simulate the intravenous infusion concentration-time profile for physostigmine and hyoscine as well as the AChE inhibition-time profile for physostigmine.
- To determine these concentration-time and inhibition-time profiles *in vivo*, comparing these with the *in silico* predicted profiles.

The order of this series of experiments is shown in Figure 5.1.

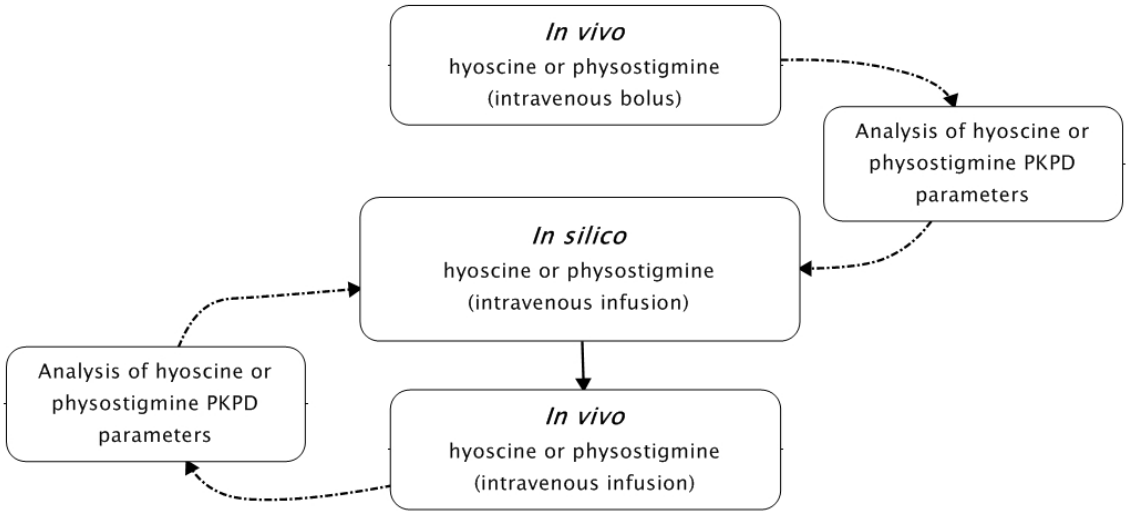

Figure 5.1. Flow diagram illustrating the order in which the studies were carried out to investigate the PKPD of physostigmine and hyoscine, i.e. *in vivo*, *in silico*, with a final *in vivo* validation.

5.3 Materials and methods specific to the study of *in vivo* and *in silico* physostigmine and hyoscine pharmacokinetics

5.3.1 *In vivo* intravenous bolus administration

Male Dunkin Hartley guinea pigs (412 ± 26 g (mean ± SD), Harlan Interfauna, UK: n=8; n=4 physostigmine, n=4 hyoscine), were implanted with temperature/identity transponders (IPTT300, Plexx B.V., Netherlands) and vascular cannulae (as detailed in Chapter 2). Microdialysis probes were not used in any of the studies investigating hyoscine or physostigmine. Physostigmine salicylate (0.2 mg/kg) or hyoscine hydrobromide (4.0 mg/kg) were administered to guinea pigs by intravenous bolus administration (constant dose volume of 333 µL/kg in sterile saline, 0.9 % w/v) via the implanted jugular cannula.

Blood samples (250 µL) were collected by automated blood sampling units following intravenous bolus administration of physostigmine or hyoscine, as detailed previously in Section 2.3.2. Plasma was prepared from these samples as detailed in Section 2.3.5. Aliquots (25 µL) of erythrocytes and plasma from animals treated with physostigmine, were diluted in 5 mL of 0.1 M phosphate buffer (pH 8.0), for determination of cholinesterase activity by the Ellman method (Section 2.4). Diluted samples were stored frozen (- 20 ˚C) until assay. Neostigmine bromide (50 µg/mL) was added to the remaining plasma to prevent *in vitro* hydrolysis of physostigmine [128], ensuring the full amount of physostigmine was available for quantitation. The process of preparing the erythrocytes for measurement of cholinesterase activity diluted the physostigmine, causing it to dissociate from the enzyme. No inhibition was therefore measured in the erythrocytes, so these data are not presented.

The concentrations of physostigmine or hyoscine in the plasma samples were determined by liquid chromatography tandem mass spectrometry (see Section

2.5.2). The lower limit of quantitation for both physostigmine and hyoscine in plasma was 0.1 ng/mL.

5.3.2 *In silico* intravenous infusion simulation

Steady state plasma concentrations of 10, 100 and 1000 ng/mL or 0.1, 1.0 and 10 ng/mL for physostigmine and hyoscine, respectively, were targeted in this study. Infusion rates required to achieve these concentrations were calculated using Equation 5.1. The clearance rates used in this equation are presented in the results section of this chapter. The assumption that the PK of physostigmine and hyoscine following intravenous infusion are dose proportionate across the three different infusion rates was made when using the PK data from the intravenous bolus administration study.

$$R_{inf} = C_{ss} \times Cl$$

Equation 5.1. Equation used to calculate the rate of infusion of a drug required to achieve a target steady state concentration.

Where R_{inf} = Rate of infusion, C_{ss} = Concentration at steady state and Cl = Rate of clearance. The rate of clearance must have previously been determined for the drug being studied.

The elimination T½ calculated from the *in vivo* intravenous bolus administration study for physostigmine and hyoscine was used to ensure the intravenous infusion was of sufficient duration to enable steady state concentrations to be achieved. Steady state is considered to be achieved after 3.3 half-lives, when the concentration is approximately 90 % of the plateau (i.e. 1 × T½ = 50%, 2 × T½ = 75 %, 3 × T½ = 87.5 %, 4 × T½ = 93.75 %, *etc.*) [234].

Physostigmine and hyoscine concentration-time profiles were predicted by *in silico* simulation, using the same compartmental PK models as best fit the

intravenous bolus data. The PK parameters determined following the intravenous bolus study were used in the simulation model. The infusion rates calculated using Equation 5.1, were used in the simulation PK models. The PK models calculated the plasma concentrations using Equation 5.2.

$$C = \frac{R_{inf}}{Cl}\left(f_1(1 - e^{-\alpha t}) + f_2\left(1 - e^{\beta t}\right)\right)$$

Equation 5.2. Equation to calculate plasma concentration following intravenous infusion in a compartmental PK model.

Where α and β are the concentration-time curve phases and f_1 and f_2 are the fractions of the elimination associated with α and β phases, respectively; as shown in Equation 5.3.

$$f_2 = \frac{C_2/\beta}{AUC}$$

Equation 5.3. Equation to calculate the fraction of elimination associated with the β phase of the concentration-time curve. The fraction of elimination associated with the α phase of the concentration-time curve was calculated as $f_1 = 1 - f_2$.

The physostigmine concentration-effect profile was predicted by *in silico* simulation with an inhibitory effect I_{max} PD model, using the PD parameters derived from the *in vivo* intravenous bolus study of physostigmine. Similarly, the physostigmine effect-time profile was predicted by *in silico* simulation by linking the *in silico* PK and PD models.

5.3.3 Validation of the *in silico* simulation by *in vivo* study of intravenous infusion pharmacokinetics.

Male Dunkin Hartley guinea pigs (402 ± 16 g (mean ± SD), Harlan Interfauna, UK: n=14; n=8 physostigmine, n=6 hyoscine) were implanted with temperature/identity transponders and vascular cannulae as detailed previously. Physostigmine base or hyoscine base were administered by intravenous infusion at the rates of infusion calculated using Equation 5.1. The infusions were administered at a dose volume of 1.0 mL/kg/h, in sterile solution (comprising; 70 % 1:2000 (v/v) glacial acetic acid, 20 % propylene glycol, 10 % ethanol), via the implanted jugular cannula using a syringe pump (CMA402, CMA microdialysis, Sweden).

Blood samples (250 µL) were collected by ABS during and following intravenous infusion of physostigmine or hyoscine. Samples were collected at 1, 1.5 and 2 hours following the start of each infusion and at 5, 10, 20, 40 minutes 1 and 2 hours following the end of the third infusion (1, 1.5, 2, 3, 3.5, 4, 5, 5.5, 6, 6.1, 6.2, 6.3, 6.7, 7 and 8 hours from commencement of the study (Figure 5.2). These time-points were calculated using the *in silico* simulations. Samples were prepared, stored and analysed as described previously.

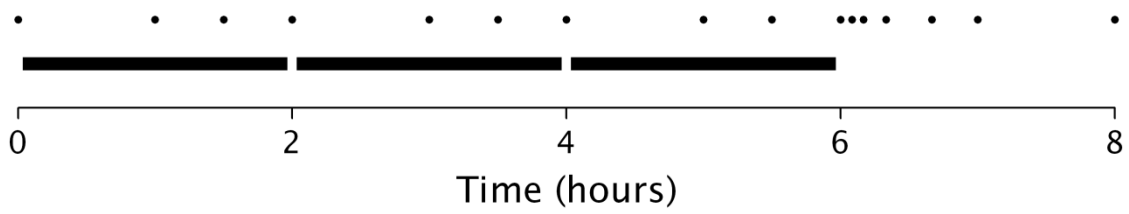

Figure 5.2. Schematic representation of the intravenous infusion experimental protocol.

Physostigmine or hyoscine were administered at three intravenous infusion rates, each of 2 hours duration (▬). Blood samples (●) were collected during each infusion. The first of the three samples was collected prior to achievement of steady state concentration and the latter two samples were collected to confirm steady state concentrations had been achieved. Six more blood samples were collected to determine elimination PK after the third infusion rate had stopped.

5.4 Results

5.4.1 *In vivo* intravenous bolus administration

All animals successfully recovered from surgery and entered the study. All cannulae (both venous and arterial) remained patent, although the carotid artery cannula of one animal became temporarily blocked during blood sample collection. Both drugs were quickly distributed and eliminated from the body (Figure 5.3 and Figure 5.4), with elimination half-lives of 10.3 ± 1.6 and 14.4 ± 2.6 minutes for physostigmine and hyoscine, respectively. The concentrations decreased biexponentially, so two-compartment PK models were fitted to the data. These models best fit the data as determined by the AIC values associated with the fits. The PK parameters from this model are presented in Table 5.1.

Physostigmine caused a concentration-dependent inhibition of cholinesterase activity in plasma (Figure 5.4). The inhibition was greatest immediately following administration and decreased with time (Figure 5.4). An inhibitory effect PD model best described these cholinesterase data (Table 5.2). Linking the PK and PD models calculated an effect compartment rate constant (K_{e0}) of 4.3 ± 82.4 1/min.

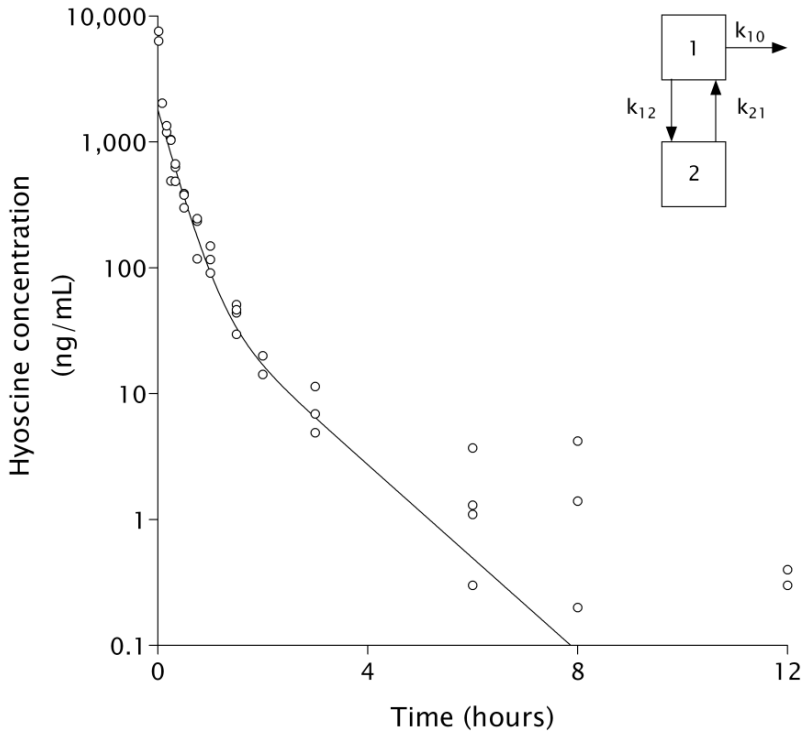

Figure 5.3. Concentration-time profile of plasma hyoscine following intravenous bolus administration of hyoscine.

Hyoscine concentration following administration of hyoscine hydrobromide (4.0 mg/kg). Open circles plot concentrations from individual animals (n=4). Mean concentrations predicted by the PK model (solid line) were calculated from the pooled data. Inset shows the schematic compartmental PK model fitted to the data.

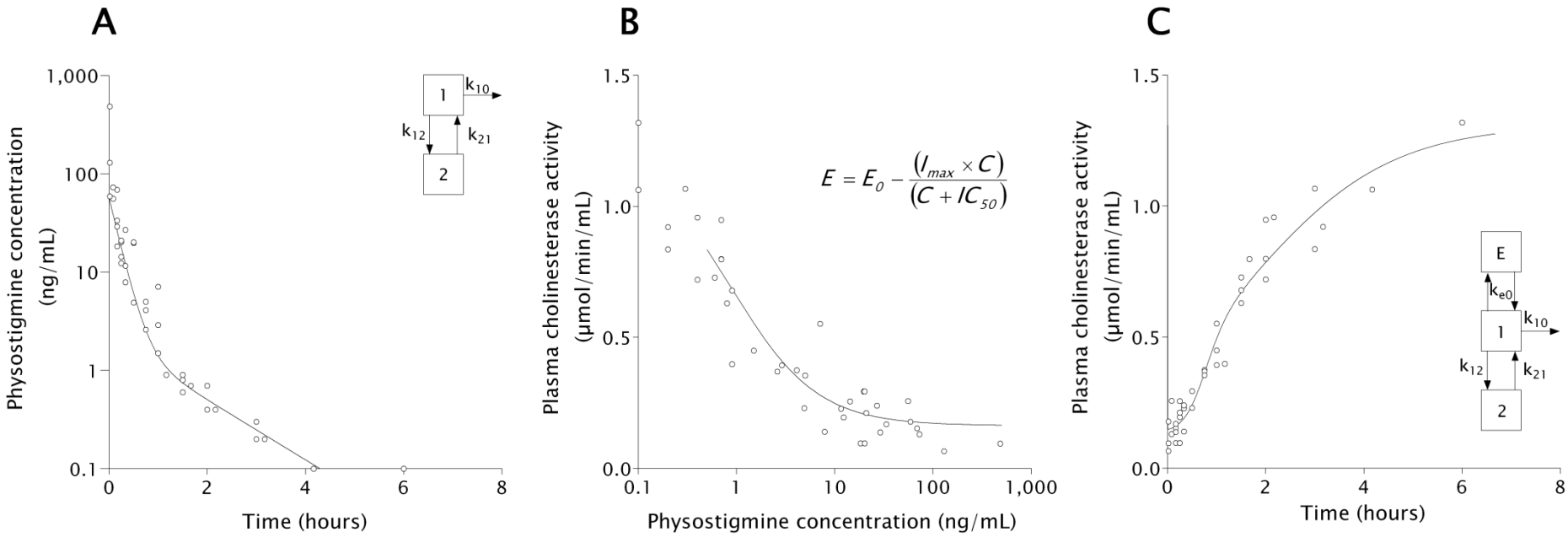

Figure 5.4. Physostigmine plasma concentration and cholinesterase activity determined following intravenous bolus administration of physostigmine.

(A) Physostigmine concentration; (B) physostigmine concentration-plasma cholinesterase activity; (C) plasma cholinesterase activity-time plots following administration of physostigmine salicylate (200 μg/kg). Open circles plot data from individual animals (n=4). Mean concentrations or cholinesterase activities predicted by the PK or PD models (solid line) were calculated from the pooled data. Insets show the schematic compartmental PK model, PD equation or PKPD linked model fitted to the data.

	Hyoscine	Physostigmine
Dose (mg)	1.65 ± 0.06	0.082 ± 0.002
Elimination T½ (min)	14.4 ± 2.6	10.3 ± 1.6
AUC (min□μg/mL)	35.5 ± 5.8	0.9 ± 0.1
V_d (L)	0.92 ± 0.28	1.4 ± 0.3
Cl (mL/min)	47 ± 8	98 ± 10
k_{10} (1/min)	0.048 ± 0.009	0.068 ± 0.011
k_{12} (1/min)	0.004 ± 0.003	0.012 ± 0.003
k_{21} (1/min)	0.015 ± 0.003	0.014 ± 0.003
α (1/min)	0.054 ± 0.011	0.082 ± 0.014
β (1/min)	0.013 ± 0.002	0.012 ± 0.002

Table 5.1. Compartmental PK parameters for physostigmine and hyoscine following their individual intravenous bolus administration.

Physostigmine and hyoscine PK were best fit by two-compartment models. Data shown as the estimate of the parameter for the pooled concentration-time profile ± standard error of the estimate (n=4).

	Physostigmine
Dose (mg)	0.082 ± 0.002
$\mathbf{E_0}$ (μmol/min/mL)	1.214 ± 0.096
$\mathbf{I_{max}}$ (μmol/min/mL)	1.087 ± 0.091
$\mathbf{IC_{50}}$ (ng/mL)	0.756 ± 0.204
$\mathbf{R_{max}}$ (μmol/min/mL)	0.158 ± 0.029
$\mathbf{FI_{max}}$	0.873 ± 0.022

Table 5.2. PD parameters for physostigmine following its intravenous bolus administration.

Physostigmine concentration-cholinesterase activity data were best fit by an inhibitory effect I_{max} PD model.

The data shown as the estimate of the parameter for the pooled concentration-effect data ± standard error of the estimate (n=4).

5.4.2 *In silico* simulation of intravenous infusions

The infusion rates required to achieve the target steady state concentrations for physostigmine and hyoscine were calculated (Table 5.3). The elimination half-lives of physostigmine and hyoscine were calculated at approximately 10 and 14 minutes, respectively. Therefore, 90 % (3.3 half-lives) of steady state was predicted to be achieved at approximately 33 and 46 minutes for physostigmine and hyoscine, respectively. The infusion durations were set to two hours for the simulation to ensure the steady state concentrations could be determined during the validation.

In silico simulation predicted that steady state concentrations of physostigmine and hyoscine would be achieved following each two-hour infusion (Figure 5.5). A concentration dependent inhibition of plasma cholinesterase was predicted by the PD *in silico* simulation and when linked to the PK simulation the inhibition-time profile was predicted (Figure 5.5).

	Hyoscine	**Physostigmine**
Body mass (kg)	0.402 ± 0.012	0.403 ± 0.020
Rate of Clearance (L/h/kg)	8.2 ± 1.6	11.1 ± 1.5
Target concentrations (ng/mL)	10, 100, 1000	0.1, 1.0, 10
Infusion rates (µg/h/kg)	80, 800, 8000	1.1, 11, 110

Table 5.3. PK parameters used to calculate the rate of infusion required to achieve target plasma concentrations of physostigmine or hyoscine.

Body mass is presented as mean ± SD, whereas the rate of clearance data are presented as mean ± standard error of parameters calculated for each individual animal (n=4) following intravenous bolus administration of physostigmine salicylate (0.2 mg/kg) or hyoscine hydrobromide (4.0 mg/kg).

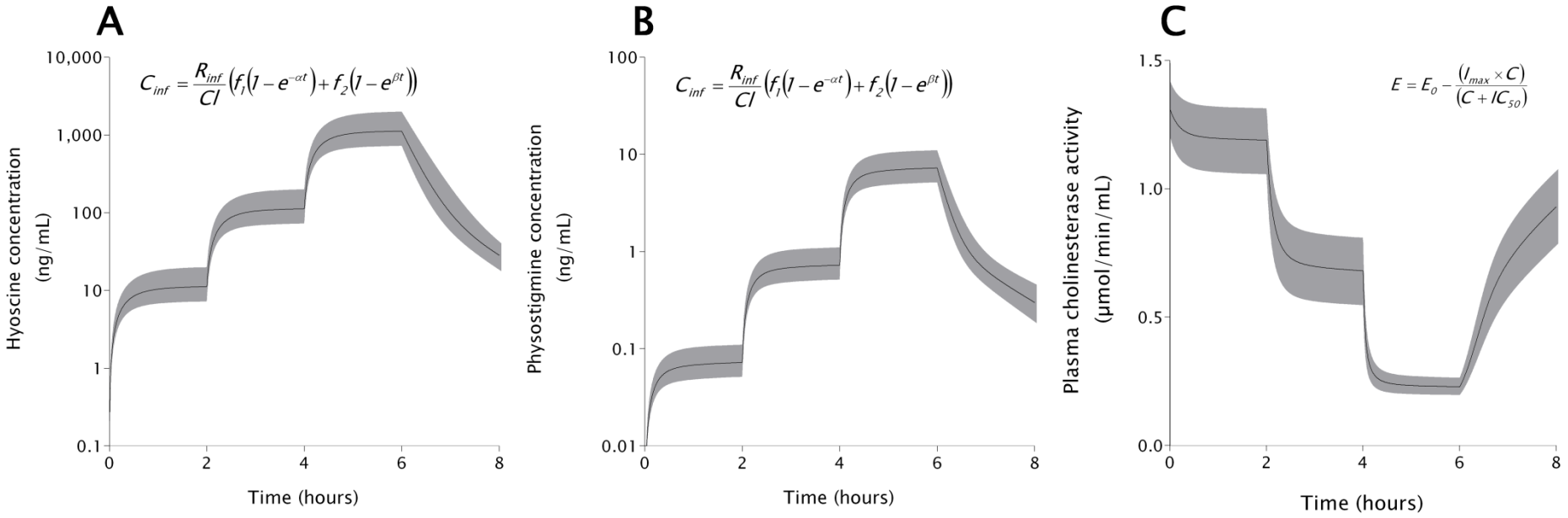

Figure 5.5. *In silico* simulation predicted concentration-time profiles of physostigmine and hyoscine and the inhibition of plasma cholinesterase activity following intravenous infusion administration at three rates.

(A) Predicted hyoscine plasma concentration following intravenous infusion of hyoscine base (80, 800 and 8000 µg/h/kg between 0 – 2, 2 – 4 and 4- 6 hours, respectively); (B) predicted physostigmine concentration and (C) predicted plasma ChE activity following intravenous infusion of physostigmine base (1.1, 11 and 110 µg/h/k between 0 – 2, 2 – 4 and 4 – 6 hours, respectively). The simulations used PK parameters presented in Table 4.2 and PD parameters presented in Table 4.3. The output is shown as the mean predicted concentration (solid line) ± standard error of the prediction (grey area fill). Insets show the equations used to calculate the predicted data.

5.4.3 Validation of the *in silico* simulation by *in vivo* study of intravenous infusion pharmacokinetics.

All animals successfully recovered from surgery and entered the study, with all cannulae (arterial and venous) remaining patent throughout the study. The surgery for the physostigmine and hyoscine *in vivo* studies had a success rate of 100 %. B

Both physostigmine and separately hyoscine achieved the target steady state concentrations following intravenous infusion (Figure 5.6). Following cessation of the infusions, the physostigmine and hyoscine decreased in a biexponential manner and two-compartment PK models were fitted to the data to calculate the PK parameters (Table 5.4). These models best fit the data as determined by the AIC values associated with the fits. The majority of PK parameters from the intravenous infusion data were not significantly different compared to the intravenous bolus data ($p > 0.05$, unpaired two-tailed t test), however the rate of clearance of hyoscine was significantly increased ($p < 0.05$) following infusion compared to bolus administration.

A concentration dependent inhibition of plasma cholinesterase activity was observed following infusion of physostigmine (Figure 5.6). An inhibitory effect I_{max} PD model was fitted to the cholinesterase activity-physostigmine concentration data (Figure 5.7), this model best fit the data as determined by the AIC values associated with the fit. The PD parameters from this model are presented in Table 5.5. There were no significant differences in the PD parameters calculated from the intravenous infusion data compared to the intravenous bolus data ($p > 0.05$, unpaired two-tailed t test).

A PKPD linked model was also fitted to the cholinesterase activity and physostigmine concentration data. The effect compartment parameter (k_{e0}) was 0.020 ± 0.002 (1/min) (Figure 5.8). This appeared to be different from the inhibition of plasma cholinesterase following intravenous bolus administration, however, due to the large variability in the k_{e0} value following bolus

administration statistical difference could not be determined ($p > 0.05$, unpaired two-tailed t test).

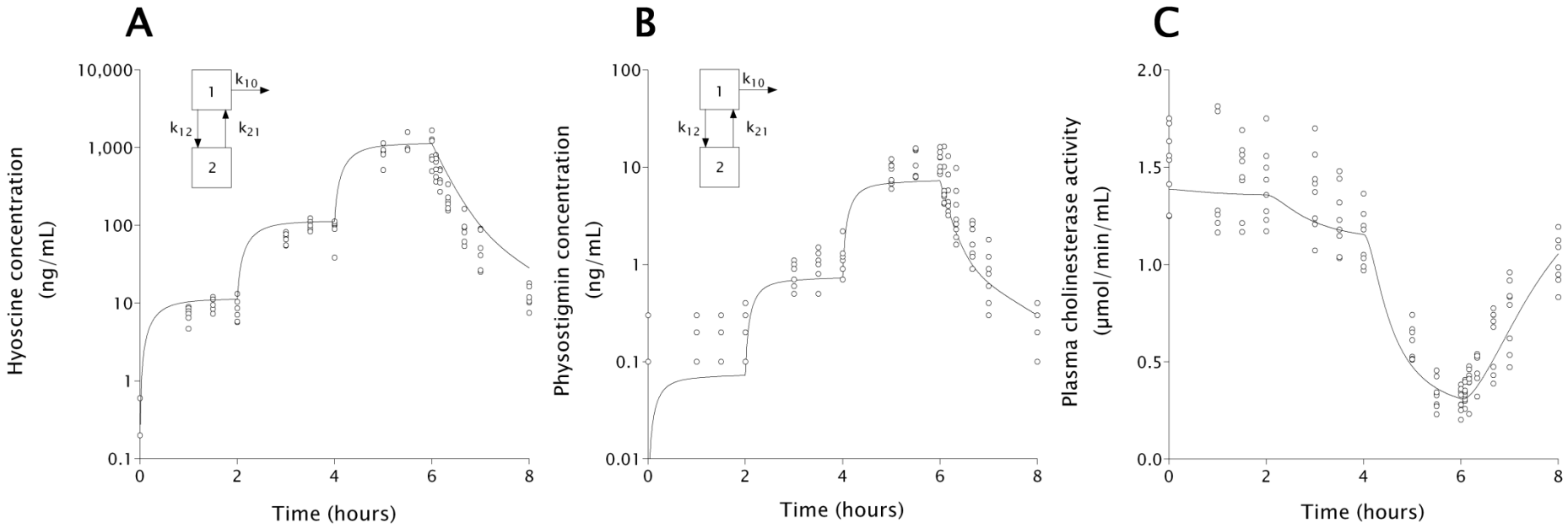

Figure 5.6. Concentration-time profile of physostigmine and hyoscine and inhibition of the plasma cholinesterase activity, following intravenous infusion administration at three rates.

(A) Hyoscine concentrations following infusion of hyoscine base (80, 800 and 8000 µg/kg/h between 0 – 2, 2 – 4 and 4 – 6 hours, respectively; n=6); (B) physostigmine concentrations and (C) plasma ChE activity following intravenous infusion of physostigmine base (1.1, 11 and 110 µg/kg/h between 0 – 2, 2 – 4 and 4 – 6 hours, respectively; n=80. Open circles plot concentrations from individual animals. Mean concentrations or ChE activities predicted by the PK or linked PKPD models (solid line) were calculated from the pooled data.

Insets show the schematic compartmental PK model fitted to the data.

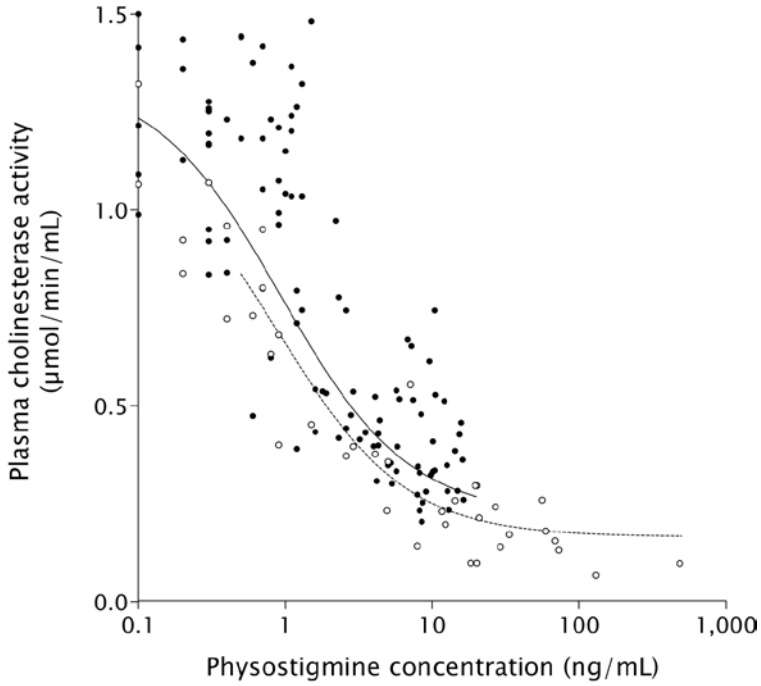

Figure 5.7. Physostigmine concentration-plasma ChE activity following intravenous bolus administration and intravenous infusion.

Intravenous bolus data (○) following administration of physostigmine salicylate (0.2 mg/kg, n=4). Intravenous infusion data (●) following three rates of infusion of physostigmine base (1.1, 11, and 110 μg/h/kg, n=8).

Mean concentration-ChE activity data (lines) were predicted by the PD model fitted to the pooled data.

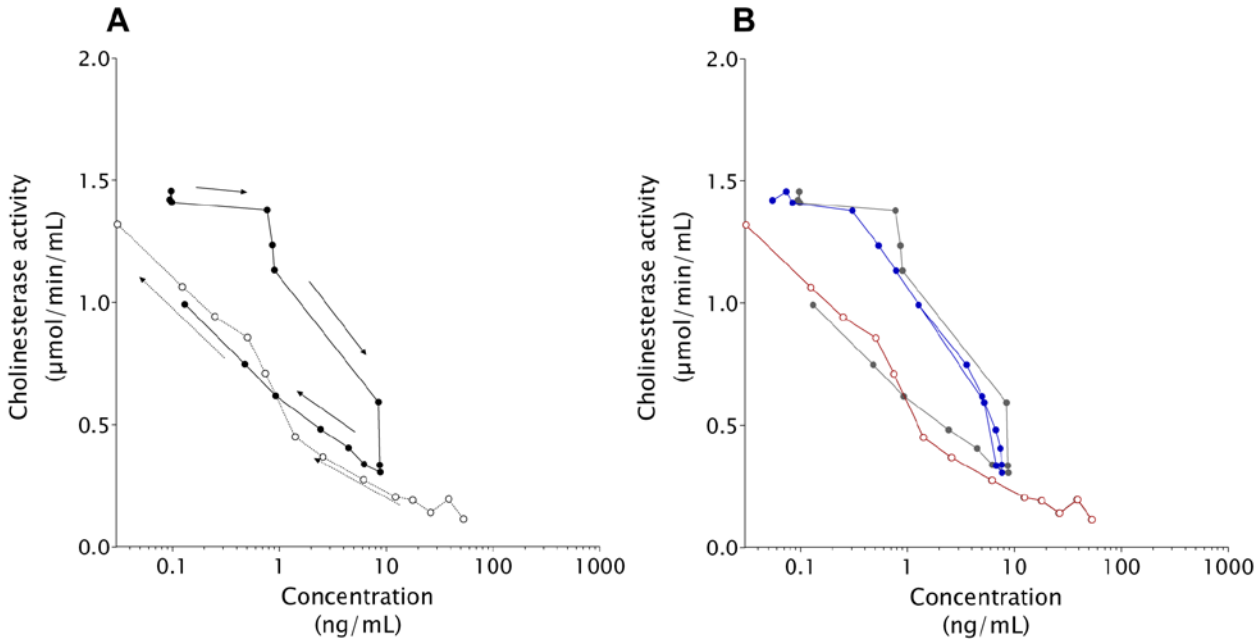

Figure 5.8. Mean plasma concentrations and cholinesterase activities following intravenous bolus and intravenous infusion administration of physostigmine.

(A) Mean plasma physostigmine concentration-cholinesterase activity plot following either intravenous bolus administration (○) or intravenous infusion (●), arrows show the clockwise hysteresis. (B) Mean effect-site physostigmine concentration-cholinesterase activity plot following either intravenous bolus (○) or intravenous infusion (●), the hysteresis has been removed by the PKPD parameter k_{e0} [168]. Note the intravenous bolus effect site data superimposes over the mean plasma data.

	Hyoscine	physostigmine
Dose administered (μg)	69.8 ± 1.1 660.1 ± 10.2 6598.7 ± 110.2	1.0 ± 0.03 9.1 ± 0.2 89.2 ± 2.3
Infusion times (min)	0 – 120 120 – 240 240 – 360	0 – 120 120 – 240 240 – 360
AUC (min□μg/mL)	0.956 ± 0.46	0.120 ± 0.006
V_d (L)	1.0 ± 0.2	1.2 ± 0.2
Cl (mL/min)	73 ± 4	83 ± 5
k_{10} (1/min)	0.072 ± 0.010	0.070 ± 0.011
k_{12} (1/min)	0.006 ± 0.004	0.007 ± 0.005
k_{21} (1/min)	0.019 ± 0.007	0.022 ± 0.009
α (1/min)	0.080 ± 0.014	0.079 ± 0.017
β (1/min)	0.018 ± 0.006	0.019 ± 0.006

Table 5.4. Compartmental PK parameters determined from the concentration-time data determined in conscious guinea pigs following intravenous infusion at three rates for physostigmine or hyoscine.

The PK parameters were estimated by fitting two-compartment models to the pooled concentration-time profile. PK data are shown ± the standard error of the estimate (hyoscine n=6, physostigmine n=8).

	physostigmine (n=8)
Dose administered (µg)	1.0 ± 0.03 9.1 ± 0.2 89.2 ± 2.3
$\mathbf{E_0}$ (µmol/min/mL)	1.34 ± 0.082
$\mathbf{I_{max}}$ (µmol/min/mL)	1.127 ± 0.077
$\mathbf{IC_{50}}$ (ng/mL)	0.928 ± 0.217
$\mathbf{R_{max}}$ (µmol/min/mL)	0.216 ± 0.031
$\mathbf{FI_{max}}$	0.839 ± 0.021

Table 5.5. PD parameters determined in individual animals following intravenous infusion of physostigmine at three rates.

The PK parameters were estimated by fitting a PD model to the pooled cholinesterase activity-physostigmine concentration data. PK data are shown ± the standard error of the estimate (n=8).

5.5 Discussion

5.5.1 *In vivo* intravenous bolus administration

The fast distribution and elimination of hyoscine following intravenous administration described here have not been reported previously in guinea pigs. Hyoscine is very similar in chemical structure to atropine (Table 1.2) and its PK may therefore be expected to be similar to that of atropine. However, the hyoscine V_d was significantly smaller and the Cl was significantly slower than these parameters for atropine ($p < 0.05$ and $p < 0.001$, respectively, unpaired two-tailed t tests). The elimination rate constant (k_{10}) and therefore T½ were not significantly different ($p > 0.05$, unpaired two-tailed t tests). The smaller V_d and slower Cl for hyoscine led to a greater AUC ($p < 0.01$, unpaired two-tailed t test). The larger exposure (AUC) for hyoscine than atropine following administration of similar amounts indicates that the protection against nerve agent provided by hyoscine may be for a longer duration than atropine. These PK data for hyoscine in addition to its greater central activity mean that hyoscine could be a better candidate for immediate therapy against nerve agent poisoning than atropine.

Physostigmine was also quickly distributed following intravenous bolus administration but was more rapidly eliminated than hyoscine ($p < 0.01$, unpaired two-tailed t test). The V_d for physostigmine reported here was similar to that reported for guinea pigs in the literature [128]. The rate of clearance in the present study was significantly greater than that reported following intramuscular administration ($p < 0.0001$, unpaired t-test). The quick elimination of physostigmine was one reason that the transdermal patch currently being developed was proposed, as a method to manipulate the administration of this drug, enabling the maintenance of concentrations that inhibit AChE activity at the target level for protection.

Guinea pig plasma cholinesterase activity was rapidly inhibited by physostigmine. Its activity subsequently increased as the concentration of physostigmine decreased, in accordance with its established mechanism of

action [8]. The *in vivo* IC_{50} was approximately 3 nM, whereas the *in vitro* IC_{50} was previously reported as 26 nM for rat AChE [235] and 14 - 127 nM for human AChE [236 :237]. This difference was likely to have been due to the lack of an *in vivo* cholinesterase baseline sample and incomplete inhibition of the cholinesterase, as can be achieved *in vitro*. No baseline measurement of cholinesterase activity was taken, due to an oversight in planning the protocol primarily for PK sampling.

5.5.2 *In silico* prediction of intravenous infusions and its validation *in vivo*

Plasma concentrations following intravenous infusion of hyoscine and physostigmine were predicted by *in silico* simulation, using the PK parameters calculated following intravenous bolus administration of the two drugs (Section 5.4.1). These predictions suggested that the target concentrations calculated by the simple equation (Equation 5.1) would be achieved within the two-hour infusions. The simulated concentration-time profiles indicated that collection of blood samples at 60, 90 and 120 minutes after each infusion in an *in vivo* study would provide confirmation of steady state being achieved. Furthermore, these simulations provided the opportunity to aid the design of the subsequent *in vivo* study, with respect to the time-points of blood sample collection after the cessation of the infusions.

Inhibition of plasma cholinesterase activity following infusion of physostigmine was predicted by *in silico* simulation, using the PD parameters determined following intravenous bolus administration of physostigmine. The simulation suggested that inhibition of cholinesterase would occur in a rapid, stepped manner, mirroring the plasma concentration of physostigmine. The plateaux inhibitions of cholinesterase activity were predicted to occur when steady state plasma physostigmine concentrations were attained at each infusion rate.

The PK of physostigmine and hyoscine and the PD of physostigmine were determined following intravenous infusion administration. Achievement of the

target steady state concentrations of both physostigmine and hyoscine provided evidence that the PK parameters determined following intravenous bolus administration enabled accurate calculation of the infusion rates.

Comparison of the hyoscine PK parameters following infusion (Table 5.4) to those calculated from bolus administration (Table 4.2) showed that Cl calculated from the infusion data was significantly increased ($p < 0.05$). This difference was evident in the concentration-time profile predicted by *in silico* simulation and the profile measured *in vivo* (Figure 5.9). However, despite this difference the terminal slope (β) and therefore the terminal T½ were not significantly different, being 51.6 ± 8.2 and 39.7± 13.1 minutes for infusion and bolus administration respectively ($p>0.05$ unpaired two-tailed t test). Thus the *in silico* simulation accurately predicted the times at which steady state concentration would be achieved. Whilst the clearance rates were statistically different there is likely to be little biological difference in the concentration-time profiles. This lack of biological difference was illustrated by the *in silico* predicted concentration-time profile which was within two-fold of the *in vivo* data, so it can be considered a successful prediction [238]. No other PK parameters were significantly different between the two administration regimens.

There were no significant differences between any of the PK or PD parameters determined for physostigmine by the two administration regimens in the experimental studies ($p > 0.05$, unpaired two-tailed t test). However, the ChE inhibition-time profile predicted by *in silico* simulation was different from that determined by *in vivo* study. The simulation correctly predicted the maximum inhibition of cholinesterase activity and the rate of recovery of activity (Figure 5.9), whereas the rate and extent of inhibition at the two lower infusion rates were not accurate. This difference was most likely to have been due to the *in silico* simulation using the parameters calculated from inhibited cholinesterase after intravenous bolus administration. In this situation, the cholinesterase was rapidly inhibited by the high concentration of physostigmine. That is, the rapid decrease in inhibition (decarbamoylation) from the high level of inhibition,

which has been shown to follow first order kinetics [239], incorrectly predicted a rapid inhibition with increasing physostigmine concentration. The lower concentrations of physostigmine inhibited the cholinesterase more slowly than predicted. The rate of inhibition (carbamoylation) is dependent on the concentration of physostigmine, enzyme and the enzyme-physostigmine complex [240], thus hysteresis was observed. That is, the rates of carbamoylation and decarbamoylation were most likely different [236 :241]. The hysteresis was corrected by calculation of the physostigmine concentration at a hypothetical effect site (C_e) through the use of the constant k_{e0} (Figure 5.8).

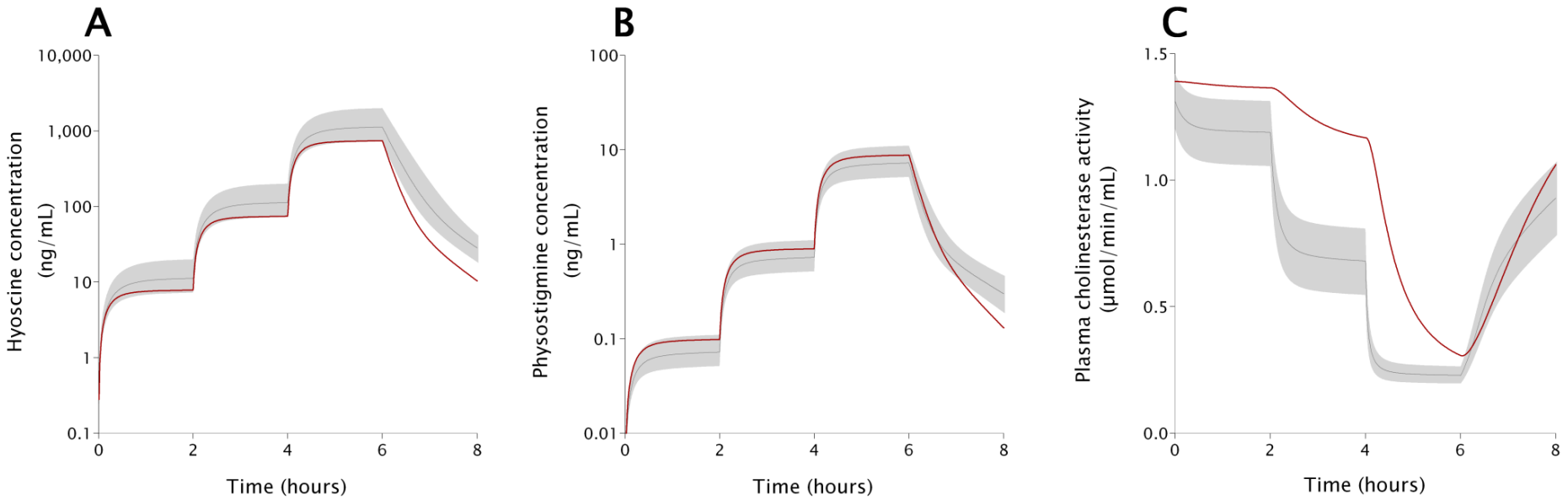

Figure 5.9. *In silico* simulation accurately predicted the plasma concentrations of (A) hyoscine and (B) physostigmine, however the simulation did not accurately predict (C) plasma cholinesterase associated with physostigmine concentration.

Data shown are mean plasma concentrations/plasma cholinesterase activity (red line) and mean predicted plasma concentrations/plasma cholinesterase activity (grey line) ± standard error of the prediction (grey area fill). *In silico* simulations used PK parameters presented in Table 4.2 and PD parameters presented in Table 4.3.

5.5.3 Summary

These data demonstrate that *in silico* simulation, using PK parameters determined in previous studies, can be used to accurately predict *in vivo* results for different doses or administration regimens. Caution must be exercised in using the simulated data (as shown by the PD data for physostigmine), in that the parameters used (e.g. the rate of carbamoylation and decarbamoylation being the same) must be understood and considered when interpreting the output from the model. Validation of the model with *in vivo* data can identify incorrect assumptions prior to further simulation of other *in vivo* studies.

The studies presented in this chapter have validated PKPD simulation methodology. In determining the physostigmine and hyoscine PK and the physostigmine PD following intravenous administration *in silico* simulation of an intravenous infusion was made possible. The PK simulations were demonstrated to be accurate following *in vivo* study of physostigmine and hyoscine, which gave results akin to the simulations. These studies illustrate the usefulness of *in silico* simulation and this approach is discussed in more detail with other examples in the next chapter of this thesis.

6. General discussion

6.1 Introduction

Chapters 3 to 5 of this thesis have each presented and discussed PK data for conventional MedCM, bioscavengers and pretreatments. This chapter consolidates these MedCM PK data, putting them in context with existing animal efficacy studies. This has involved using examples of MedCM treatment regimens from the literature to identify whether the efficacy of MedCM against nerve agents in guinea pigs can be better understood, rationalised and explained by the PK and/or PD of MedCM and nerve agents.

6.2 Conventional medical countermeasures against rapid inhaled nerve agent poisoning

The combination of atropine, avizafone and HI-6 is in advanced development in order to achieve licensure for human use in the UK. The results reported in Chapter 3 provide a PK rationale for the efficacy of this combination of drugs against nerve agent poisoning by the inhalation route of exposure. Atropine, diazepam (following conversion of avizafone) and HI-6 are absorbed quickly, achieving C_{max} within 15 minutes of intramuscular administration, so they are at pharmacodynamic active concentrations in the plasma and tissues providing protection to nerve agent poisoned guinea pigs. Although atropine, diazepam and HI-6 are rapidly cleared, having elimination half-lives under 20 minutes, these drugs are at pharmacodynamic active concentrations for durations sufficiently long to ensure protection against the inhaled nerve agent (Figure 6.1).

Inhalation of sarin, soman or other volatile nerve agents is the most likely route of exposure for these nerve agents, as evidenced by the Tokyo, Matsumoto and Syrian nerve agent attacks [14 :20 :242 :243]. The TK of both sarin and soman has been determined in guinea pigs following inhalation exposure [119 :120 :122]. The authors of those TK studies reported that plasma concentrations of sarin and soman peaked within 3 minutes of the end of the inhalation exposure (8 minute exposures were studied, therefore, C_{max} was achieved

within 11 minutes). Thereafter, the elimination half-lives of sarin and soman were approximately 30 minutes and 10 minutes, respectively (Figure 6.1). This demonstrates the very rapid nature of nerve agent poisoning by the inhalation route, necessitating self or buddy-administered MedCM. However, these data also show that the plasma concentrations of nerve agents quickly decrease, be that through rapid binding to plasma proteins, inhibition of BChE or CaE, spontaneous hydrolysis or enzymatically catalysed hydrolysis [223 :244 :245] (from a kinetic perspective inhibition of AChE is a minor consideration as it only accounts for approximately 1 % of binding in plasma [223]).

The TK of soman following subcutaneous exposure was determined by Due *et al*, who suggested that subcutaneous exposure is a suitable model for short duration inhalation exposure (5 – 7 minutes) [246]. This is of importance because in the laboratory setting, animals are generally exposed to nerve agent by the subcutaneous route, due to the ease and reproducibility of this route, compared to the technically more difficult inhalation exposure. It is against subcutaneous exposure to nerve agents that the efficacy of conventional MedCM comprised of atropine, avizafone and HI-6 has been demonstrated in guinea pigs [33 :70 :76 :163 :247].

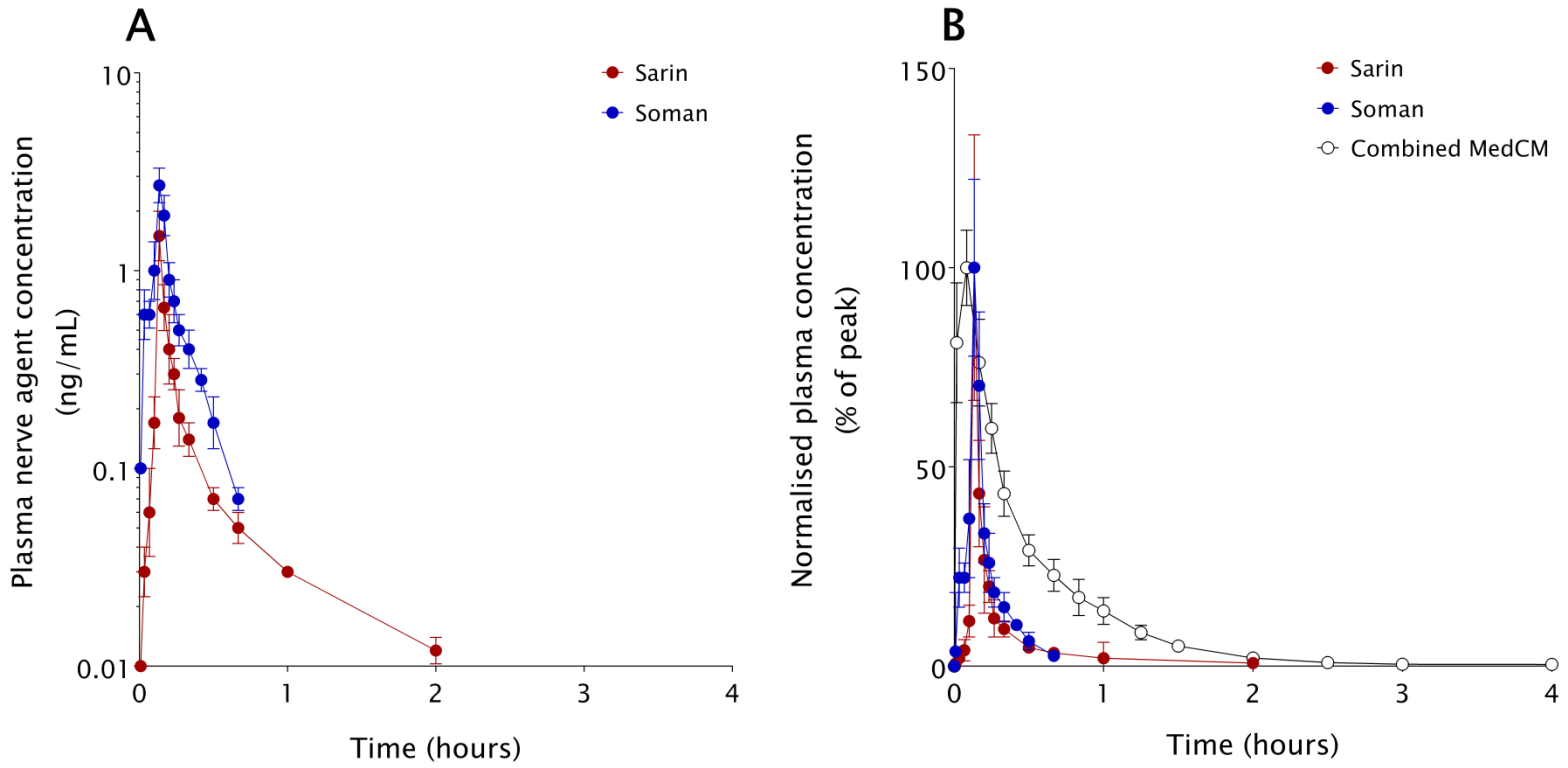

Figure 6.1. Plasma concentration-time profile of inhaled sarin and soman.

(A) Sarin TK data shown is the toxic isomer (-) of sarin determined following 8 minutes exposure of guinea pigs to 0.8 × LCt_{50} racemic sarin [138]. Soman data shown is the most toxic isomer (C(-)P(-)) of soman determined following 8 minutes exposure of guinea pigs to 0.8 × LCt_{50} racemic soman[137]. (B) Composite figure plotting normalised PK and TK data for sarin and soman with data previously presented in Figure 3.11. Atropine data is shown as representative of combined MedCM. Data shown as mean ± standard error of the mean.

6.2.1 Translating efficacy from guinea pigs to humans

Guinea pig efficacy studies show that the MedCM are effective at preventing nerve agent lethality and incapacitation in this species [247]. However, the doses used in guinea pig efficacy studies have not been scaled from the doses contained in the autoinjectors, or what could be contained in an autoinjector for human use. As discussed in Chapters 1 and 3, the atropine concentration is acknowledged as being high in guinea pigs compared to that in man [32 :46]. Therefore, efficacy studies have been completed to investigate the effect of reduced atropine in combined MedCM. Those studies determined that a reduction in the dose of atropine led to a reduction in efficacy of the combined MedCM [199]. However, the reduction in efficacy was dependent on the nerve agent to which the guinea pigs had been exposed and the oxime used [58 :199]. Following those reduced dose atropine studies, Koplovitz *et al* suggested that atropine was able to mask the efficacy of the other component drugs of combined MedCM [199] and that may have been due, in part, to the anticonvulsant effect of atropine [131]. Poole and Rudall recently determined in efficacy studies that 3 mg/kg of atropine, in combination with avizafone and HI-6, provided 100 % protection against 2 × LD_{50} of soman [248]. The 3 mg/kg dose of atropine was subsequently incorporated in studies that investigated the efficacy of HI-6. These studies were able to show improved efficacy with increasing dose of HI-6, which may not have been possible had higher doses of atropine been used [163]. The studies by Koplovitz *et al* and Poole and Rudall provide efficacy data for MedCM at doses that are closer to those in man and may present a more representative indication of efficacy in man.

The dose of atropine contained in an autoinjector is not based on animal efficacy data but on human tolerance and the requirement for minimal impairment of military effectiveness should the drug be administered to unpoisoned individuals [27 :249 :250]. Similar reasoning underpins the dose of avizafone contained in the autoinjector, which was limited because the sedative effects of diazepam could reduce the ability of an individual to perform military tasks [60]. This approach to setting human doses protects unpoisoned individuals from the adverse effects of the MedCM, if administered in the absence of exposure to nerve agent but may provide sub-optimal

protection to nerve agent exposed casualties. The efficacy of human equivalent doses of the MedCM should be determined in guinea pigs and subsequently in other animal species. These data may increase military confidence that the MedCM are effective and provide a capability against nerve agents. An alternative approach to human dose selection is to accept adverse effects that may occur in unpoisoned individuals following administration of increased doses. These increased doses may be based on efficacy data from animal studies. The adverse effects associated with the MedCM are likely to be acknowledged by the patient as more agreeable than the alternative: deleterious effects of nerve agent exposure resulting from sub-optimal protection.

Testing the efficacy of current human doses in animals requires scaling of these doses, for which there are several methods available. These methods can also be used to extrapolate doses with proven efficacy (in animals) to equivalent doses in humans. Dose scaling methods can include the use of reference parameters such as body mass [32] or body surface area [125], allometric scaling [251] or a PK guided approach [126]. Each of these methods can yield very different doses as illustrated by the data presented in Table 6.1 for atropine, avizafone and HI-6.

The scaled doses of HI-6 (Table 6.1) were similar to the guinea pig doses used in existing efficacy studies and the work described in Chapter 3 of this thesis. However, the scaled doses of atropine and avizafone were different to those used in existing efficacy studies. The dose of atropine used in guinea pig efficacy studies is much greater than the doses suggested by all of the scaling methods. The PK guided approach to scaling uses the clearance rate and target total exposure (AUC) for the drug, whereas the other scaling methods are arbitrary. For atropine, PK guided scaling suggested the highest atropine dose of all the scaling methods. This dose of atropine is 10 fold lower than the historic 5.8 mg/kg dose used in efficacy studies. The doses of atropine suggested by body mass, body surface area and allometric scaling are much lower than any dose of atropine reported as being tested, so it is unlikely that these doses would be efficacious. The PK guided approach also suggested a

dose much lower than has been given in efficacy studies, although it is of a similar order to the low dose tested by Koplovitz *et al* [199], which had reduced efficacy compared to higher doses.

The PK guided approach also suggested the highest dose of avizafone, which was similar to the human dose and approximately 22 times greater than the dose used in efficacy studies, taking into account the rapid decrease in plasma diazepam concentration. A similar high dose (30 mg/kg ≈ 10 mg dose) has been suggested, by Capacio *et al* [135], as necessary to stop seizure. The doses of avizafone suggested by the three arbitrary scaling methods were lower than the dose used in efficacy studies but they were of a similar order.

The dose of HI-6 predicted by all methods was of a similar order to that used in efficacy studies and would be expected to be efficacious. Whilst the PK guided scaling method uses drug specific data to match the AUC between species, it is likely that in animals the concentrations will be much higher but for a short period. Differences in concentration between species such as those likely to occur could lead to an over/underestimation of efficacy. *In silico* simulation can enhance the PK guided approach and match the AUC whilst ensuring the differences in the concentration-time profile are minimised. This enhanced scaling approach was demonstrated for levofloxacin in Rhesus monkeys by Kao *et al* [203], who simulated levofloxacin concentrations and validated these *in vivo.* The resulting levofloxacin data showed the C_{max}, AUC and effective concentrations were ≈ 95 %, 70 % and 90 % of the corresponding human parameters, respectively.

Scaling method	Atropine	Diazepam (avizafone)	HI-6
Human dose	2 mg	10 mg	500 mg
Body mass (mg/kg)×kg	10 µg	50 µg	2.5 mg
Body surface area (mg/m²)×m²	57 µg	289 µg	14.5 mg
Allometric ($Y=aW^b$)	38 µg	188 µg	9.4 mg
PK guided (AUC×Cl)	216 µg (2.4 min□µg/mL ×90 mL/min)	8.2 mg (329 min□µg/mL × 25 mL/min)	7.3 mg (1,984 min□µg/mL × 3.7 mL/min)
Current guinea pig dose	2.0 mg	366 µg	3.3 mg

Table 6.1. Guinea pig equivalent doses of the three conventional MedCM calculated by different scaling methods from the human doses contained in an autoinjector.

HI-6 is not currently licensed for human use, so the dose used in the calculations was equal to the dose of pralidoxime methane sulphonate in the autoinjector [30]. Guinea pig and human body masses used in the calculations were 0.35 and 70 kg, respectively. The guinea pig and human body surface areas used in the calculations were 0.05 and 1.73 m³, respectively. PK guided approach used Cl data previously presented in Table 3.5 and AUC values reported for atropine, diazepam and HI-6 by Ellinwood *et al* [198], Abbara *et al* [190] and Kusic *et al* [192], respectively. The nominal guinea pig dose used in the studies reported in this thesis are included for comparison (last row).

Using PD data in conjunction with PK data is another alternative method to scale doses between species and also requires drug specific information; this may be more accurate than the PK guided approach. This approach was validated *in vivo* for caramiphen using dogs and monkeys by Levy *et al* [83]. That study infused the caramiphen at a set rate to achieve a target steady state concentration. The PD measure was protection against sarin. Thus a protective concentration of caramiphen determined in two species was recommended for use in humans. Reproducing a target PD measure in animals and humans in this way, then correlating it to a plasma concentration, enables a dose to be calculated from human PK parameters.

The most sophisticated approach to scaling is physiologically-based pharmacokinetics (PBPK). This method provides a mechanistic approach to scaling doses between species through knowledge of the physiological parameters defining ADME of the drug in animals, which is integrated with PK data. These physiological data are also combined with physico-chemical data for the drug in an *in silico* mathematical PKPD model. Simulations predict the concentration-time course of a drug that must then be validated by *in vivo* study. To scale the PK and dose, animal physiological data are substituted for human data and a simulation is carried out to predict the human concentration-time course. Subsequently, doses may be calculated from these simulated data.

The utility of MedCM PBPK models for scaling between routes of exposure, doses and species has been highlighted by Merrill *et al* [252], who noted a paucity of quantitative PK data required for validation of the PBPK models. The data presented in this thesis addresses that knowledge gap, particularly as the MedCM PK data were determined in combination and provide data on the PK interactions. The PBPK models currently available describe individual MedCM [253-255]. It is unfortunate that atropine and diazepam were not quantified following soman exposure in Chapter 3, as these data may have enabled PBPK model validation that incorporated interactions between MedCM and nerve agent.

The majority of PBPK models in this field of research have been developed to describe the nerve agent exposure rather than the MedCM PK [22 :183 :223 :228]. These nerve agent models were validated against published *in vivo* data and in the case of soman the physiological processes involved in the PK/TK are better understood. The explanation of differences in PK/TK between species, enabled by the PBPK models, can be used to logically scale the poisoning scenario to humans. Two of the most recently published nerve agent PBPK models suggest doses of bioscavenger can be calculated through integration of their PK and biochemical data [183 :228]. The data presented in Chapter 4 of this thesis may be used to validate such models. As discussed in Chapter 4 the plasma concentrations of VX could not be measured. These data could have been used to validate a PBPK model of percutaneous exposure. Until MedCM PBPK models are available, scaling of doses from animals to humans must be done by one of the other methods detailed earlier. If data are available, the PK guided approach or the PKPD approach should be used.

The plasma concentrations achieved following administration of any dose of MedCM are critical for protection. Protection against nerve agent can be used as a PD endpoint and the corresponding plasma concentration can therefore be used as a target or pharmacodynamic active concentration (PAC). A PAC has been suggested for each of the MedCM drugs independently by different research groups but these have been determined under different experimental conditions and in different species (Table 6.2).

MedCM	PAC	PD metric	Notes	Reference
Atropine	11.8 ng/mL (40.8 nM)		Retrospective analysis of human clinical cases of pesticide poisoning in which AChE was completely inhibited (achieved by administration of *circa* 0.06 mg/h/kg). In cases of 10 – 30 % AChE inhibition the suggested PAC was 1.5 ng/mL (5.0 nM) The atropine K_i for mAChR of < 1 nM [256].	Thiermann *et al* [200]
Avizafone/diazepam	1000 ng/mL	Termination of soman induced seizures.	Guinea pig PK/efficacy study.	Capacio *et al* [135]
HI-6	2×10^{-5} M (5.8 µg/mL)		*In vitro* rat hemi-diaphragm preparation and *in vivo* anaesthetised cat PK/efficacy studies. Suggested concentration of pralidoxime. No PAC has been proposed for HI-6.	Sundwall *et al* [204].

Table 6.2. Suggested pharmacodynamic active concentrations for the three MedCM, including brief details of how these were determined.

A systematic determination of PACs should be carried out with multiple nerve agents and by different routes of exposure. Doing so will enable doses of MedCM to be calculated that are efficacious (i.e. achieve PACs) against a range of nerve agents. Alternatively, this will provide information that shows the PAC is nerve agent specific, as is expected for oximes, due to the chemical and steric differences with each nerve agent-enzyme complex. It is likely that the PAC is dependent on the nerve agent exposure dose and it is unrealistic to determine the PAC for this. Therefore, set criteria for protection must be used (e.g. 2 × LD_{50}), which can be set by operational analysis of the likely exposure doses and must take into account the species specific mechanisms of action, potency or even efficacy of the MedCM. This information will ensure that the PAC is relevant to each species and will enable accurate scaling of doses from animals to humans.

6.3 Medical countermeasures against percutaneous poisoning

Conventional MedCM administered in accordance with current military doctrine (i.e. administered at 15 minute intervals commencing immediately on development of signs of poisoning [30]) have reduced efficacy against nerve agent when exposure is by the percutaneous route [31]. Efficacy of conventional MedCM can be improved by modifying the regimen to repeated administration at longer intervals or on reappearance/worsening of signs of poisoning [31 :142]. The PK data presented in Chapter 3, for the conventional MedCM and the PK and PD data presented in Chapter 4 for VX, can be used to explain the reduced efficacy of MedCM observed following percutaneous poisoning. These data showed that rapid absorption of atropine, diazepam and HI-6 leads to the C_{max} of these three drugs occuring within 15 minutes of administration. However, the peak concentrations are not maintained due to the rapid distribution and elimination of the MedCM, with the half-lives of each being less than 20 minutes. Compared to the VX PK profile determined in brain or muscle, MedCM concentrations are unlikely to be at PACs over an appropriate period to provide protection (Figure 6.2). The MedCM PACs are not known for percutaneous nerve agent poisoning. However, the atropine dose administered as part of the

successful treatment of the only human case of percutaneous VX poisoning (atropine infusion of 3 mg/day [28]) was much lower than that recommended by Thiermann *et al* [200] (see section 6.2.1). Future studies should determine the PAC of MedCM for percutaneous exposure, as described in the previous section. These data will help to identify appropriate doses or administration regimens of MedCM to protect against percutaneous poisoning. The modified administration regimen is one example of how MedCM administration can be optimised to protect against percutaneous poisoning. This modified regimen was determined empirically, whereas *in silico* simulation of PK profiles may provide a theoretical method for optimising MedCM administration regimens, based on PACs. As discussed in Chapter 5, the simulations must be validated with *in vivo* data if the administration regimen is to be taken forward into *in vivo* animal efficacy studies.

In silico predicted plasma concentrations of MedCM following the modified administration regimen illustrate that the concentrations fluctuated throughout the duration of administration (Figure 6.2). It is suggested that efficacy of MedCM in this scenario is due to the PACs repeatedly being achieved following each administration. It should be noted that the protection afforded by this modified administration regimen is dependent on continuation of the administration of the MedCM [31]. Therefore, it is expected that continuous administration of MedCM will provide protection against percutaneous nerve agent exposure. The duration of treatment required to achieve full recovery from percutaneous exposure to nerve agents is unknown but it will be dependent on the exposure dose of nerve agent. Future *in vivo* studies should investigate the duration of required treatment, linking this with exposure dose. *In vitro* skin penetration data can be used to predict the likely rate of entry of percutaneous nerve agent into humans [257], subsequently enabling a human time-course of poisoning and likely treatment duration to be recommended. Furthermore, toxicokinetic data from pig studies indicate that VX was in the systemic circulation at toxicologically relevant (nM) concentrations 9 hours after percutaneous exposure at 3 × LD_{50} [258], so human treatment is likely to be required for at least this duration. In the only case of human percutaneous

poisoning by VX, treatment was required for 9 days duration [28] [**], which agrees with the animal experimental data. As treatment of percutaneous nerve agent poisoning is likely to be for a prolonged period compared to acute inhaled nerve agent poisoning, intravenous infusion of MedCM may be a more appropriate route than intermittent intramuscular administration.

[**] A second case of human VX poisoning by the subcutaneous/intramuscular route has been reported [29]. In this case treatment with atropine and oxime was not given and the VX exposure was lethal.

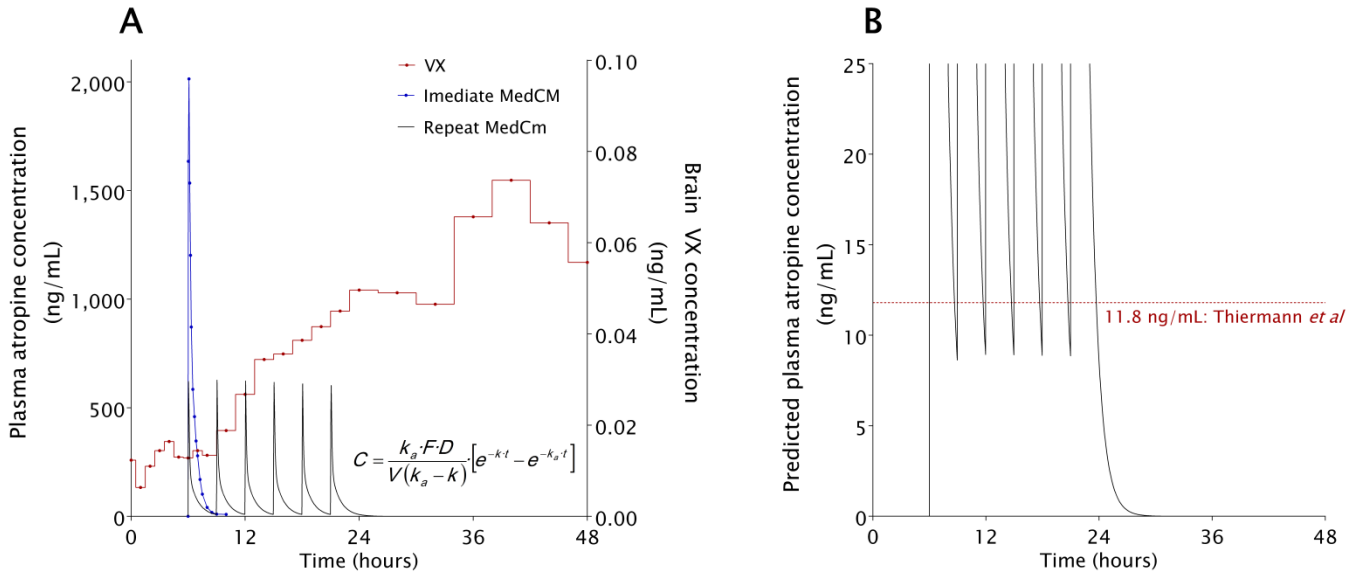

Figure 6.2. Composite plot of VX brain microdialysate concentration following percutaneous exposure to VX and MedCM plasma concentrations following immediate or modified intramuscular administration regimens.

(A) MedCM administration is shown commencing at 6 hours, the mean time of MedCM administration in guinea pig exposure to percutaneous VX [110]. Atropine concentration data is shown alone for clarity. Plasma concentration-time profiles of atropine following modified administration of combined MedCM were predicted by *in silico* simulation with two-compartment models as described in Chapter 5, using PK parameters presented in (Table 3.5). The simulated dosing regimen was based on published efficacy studies [31], at doses of 5.8, 3.14 and 9.3 mg/kg for atropine sulphate, avizafone hydrochloride and HI-6 dimethanesulphonate, respectively. The assumption that the PK was linear at these simulated doses was made with this simulation. (B) Expanded y axis to show the simulated atropine concentration. These data suggest that a trough concentration of approximately 9 ng/mL is achieved prior to the subsequent administration, which was similar to the PAC suggested by Thiermann *et al* [200] (i.e. once this concentration was achieved more MedCM was required).

6.3.1 Medical management of nerve agent casualties

Nerve agent MedCM research typically examines immediate First Aid solutions to nerve agent poisoning. This approach is probably driven by the acute nature of inhalation poisoning. Efficacy of MedCM against subcutaneous exposure is usually determined without supportive treatment beyond the initial administration of MedCM. This is challenging, as the endpoint is often 24 hours survival, because in the military scenario a nerve agent casualty would be expected to reach medical treatment (First Aid) within 1 hour of exposure to nerve agent [259]. Therefore, efficacy of MedCM against acute exposure to nerve agent at 4 hours may be a more appropriate endpoint, as casualty evacuation doctrine states the casualty should be at a field hospital within this time [259]. However, these casualty evacuation times are based on recent operations in Afghanistan. Casualties exposed to nerve agents by the percutaneous route will impose limitations on the evacuation, for example contamination of vehicles or required decontamination prior to additional treatment. Beyond the 4 hour time point, Medical Management of a casualty will continue [260]. Efficacy of MedCM at 4 hours may improve the possibility of identifying effective MedCM but necessitates the requirement for Medical Management to be in place too.

Protection against percutaneous nerve agent to a 24 hours endpoint is an even greater challenge than for acute inhalation exposure (see Figure 6.2; A). Joosen *et al* demonstrated that continued repeat administration of MedCM are required to achieve protection against percutaneous VX [31]. The administration regimen employed by Joosen *et al* changed the treatment scenario from First Aid to Medical Management, thus providing evidence that improvement in efficacy may be gained through Medical Management of a casualty rather than First Aid.

There are approximately 300,000 deaths annually from pesticide self-poisoning [261], so a body of research exists on the treatment of human organophosphate pesticide poisoning [262]. In these cases immediate First Aid treatment does not generally occur, so Medical Management is the only

treatment. Pesticide poisoning may be considered similar to percutaneous nerve agent poisoning, because of the comparable long duration of signs of poisoning following exposure. These long durations of poisoning occur because of two distinct mechanisms: 1 -lipophilic pesticides are slowly distributed from lipid reservoirs to continually inhibit cholinesterases, 2 - metabolic activation of pesticides by cytochrome P450 enzymes is required before inhibition of AChE can occur [263]. Both of these mechanisms produce prolonged exposure to toxic concentrations of pesticide and inhibition of AChE, thus persistent signs of poisoning occur. The reactivation of inhibited AChE by an oxime is dependent on the pesticide [263], the same as for reactivation of nerve agent inhibited AChE [72 :264]. Treatment strategies of human cases of pesticide poisoning available in the literature may be applied to the Medical Management of percutaneous nerve agent poisoning [††]. The recommended treatment for pesticide poisoning is similar to the reported treatment of casualties from the Tokyo sarin attack [243]. In those cases only 21 casualties required more than 2 mg atropine, 106 casualties were treated with pralidoxime (the maximum total dose being 8 g) and eight casualties were administered diazepam (30 - 35 mg) [243]. Very few details are published of the treatment of casualties from the Morimoto sarin attack. Following that attack, 48 - 72 mg atropine was administered to 18 patients and approximately 30 g of pralidoxime was administered to a single person [265]. Diazepam was not reported as being administered to any casualty following the Morimoto attack [265].

[††] The recommended treatment for pesticide poisoning is;

1. Atropinisation: intravenous bolus administration of 1- 3 mg atropine, doubling this dose every 5 minutes until atropinisation is achieved.
    a. A total dose of 6- 65 mg in the first 25 minutes was generally sufficient to achieve atropinisation.
2. Oxime therapy: intravenous bolus administration of pralidoxime or obidoxime at 1 -2 g or 30 mg loading dose, respectively. Followed by corresponding intravenous infusion to maintain the treatment at 1 g/h or 30 mg [262].
3. Treatment of seizures: Generally seizures do not occur in human pesticide poisoning cases. This difference from nerve agents was acknowledged by Eddlestone *et al* [262]

Plasma concentrations of the MedCM drugs have not been reported following the treatment of casualties from either of the Japanese attacks, so the link between PK and PD cannot be made. A systematic program of research to identify and develop Medical Management MedCM, treatment strategies and dosing regimens for both inhaled and percutaneous exposure to nerve agent should be undertaken. The PK data reported in this thesis can inform the recommended programme of work, from identifying a PAC, then using modelling and simulation to suggest doses and administration regimens (e.g. infusion rates) that achieve the required concentrations. The treatment for pesticide poisoning as recommended by Eddlestone *et al* can be used as a starting point for animal efficacy studies and incorporating PK sampling into these studies will enable PACs to be identified and/or confirm that the target concentrations have been achieved. Such studies may improve the survival following nerve agent exposure compared to current treatments. The retrospective analysis of atropine dosage requirements published by Thiermann *et al* for atropine [200] provides the first Medical Management PAC, although this was defined for pesticides.

6.3.2 Intravenous infusion of medical countermeasures against percutaneous nerve agent

Intravenous infusion of MedCM drugs is the administration regimen of choice for Medical Management of pesticide and nerve agent poisoning [28 :200 :243 :262 :265]. The efficacy of an intravenous infusion of combined atropine, avizafone and HI-6 against percutaneous VX was determined in a guinea pig study by Mann. Intravenous infusion (equivalent to 6 intramuscular administrations of MedCM over 24 hours) was able to provide protection against the lethality of percutaneous VX (1.8 mg/kg, Figure 6.3, A) [266]. *In silico* simulations of the MedCM infusions illustrated that the atropine concentration at steady state was predicted to be greater than the PAC suggested by Thiermann *et al* [200] (Figure 6.3, B). The diazepam and HI-6 concentrations were predicted to be below the suggested PACs for each of these drugs [135 :204]. Of most concern is diazepam, due to the 50 fold difference between the predicted concentration and the PAC of 1 μg/mL[135]. The results reported by Capacio *et al* were determined in a guinea pig model optimised to produce seizure. The other MedCM used in that

model were not optimised for protection but to induce and maintain seizure. Therefore, with increased oxime and atropine doses, optimised for protection, it is conceivable that the diazepam PAC may be lower than 1 μg/mL. EEG was not measured in the intravenous infusion efficacy study, so the information on the incidence of seizure and the prevention or termination of seizures that did occur, does not exist. Notwithstanding this lack of EEG data and the low concentrations of diazepam and HI-6, the guinea pigs treated by intravenous infusion of MedCM survived the challenge to 24 hours. Intravenous infusion has, to date, proved to be the most efficacious treatment regimen against percutaneous VX poisoning. Studies should continue to be carried out in this model to determine the optimal MedCM doses, the incidence of seizure and the PACs.

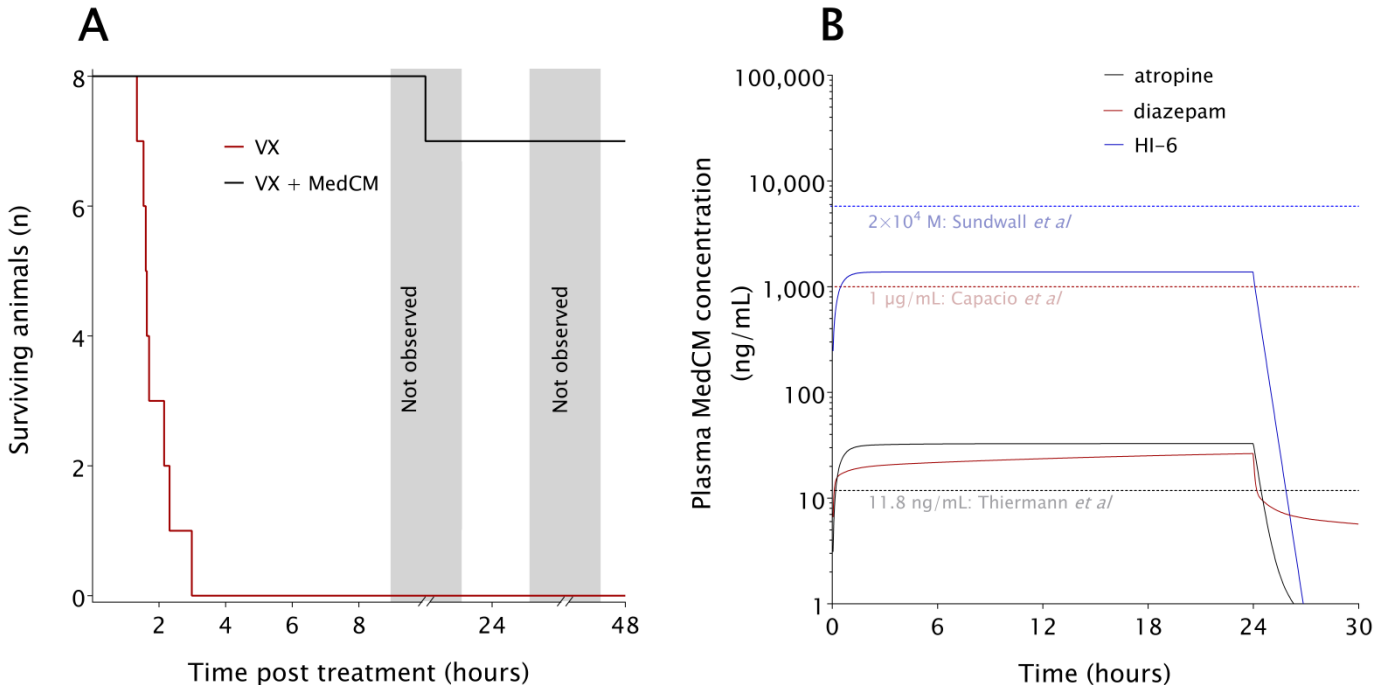

Figure 6.3. Treatment with intravenous infusion of MedCM improved survival following percutaneous exposure to VX in guinea pigs.

(A) In the absence of MedCM percutaneous VX (1.8 mg/kg) was lethal within 4 hours of exposure. Treatment with 24 hours intravenous infusion of atropine sulphate (1.5 mg/h/kg), avizafone hydrochloride (0.3 mg/h/kg) and HI-6 dimethanesulphonate (2.3 mg/h/kg) [266] protected seven out of eight animals to 48 hours post exposure. (B) Predicted plasma concentration-time profiles of the intravenous infusion of the combined MedCM. The total dose used for the simulated infusion was the same as the six repeat intramuscular simulation presented in Figure 6.2. The suggested PACs for the MedCM are included for reference. Only atropine exceeded the suggested PAC during the infusion.

6.3.3 Controlled-release of medical countermeasures for treatment of percutaneous poisoning

Maintenance of plasma PACs for atropine, diazepam and HI-6 through sustained administration of the combined MedCM, appears to be a good strategy to achieve protection against percutaneous nerve agent. The sustained treatment of percutaneous nerve agent poisoning through either repeat intramuscular administration or intravenous infusion should be considered as Medical Management, not First Aid. The ability to control the release of drugs using different matrices have been investigated for many drugs including MedCM against nerve agents (e.g. oxybutynin a muscarinic receptor antagonist) [267], diazepam [268] and pralidoxime [269]. Controlled release of MedCM represents a potential First Aid scenario of sustaining plasma concentrations of the MedCM akin to that achieved in a Medical Management scenario. Indeed, controlled release may even be used in a Medical Management scenario.

A proof-of-concept controlled-release formulation of microspheres containing atropine, diazepam and HI-6, in a cotton seed oil vehicle, was developed as part of a separate project [270,271]. The challenge of that development was to ensure the delivery of the required large doses of MedCM over an appropriate duration for percutaneous poisoning. PK data generated from the studies reported here were used in conjunction with *in vitro* drug release rates of the controlled-release formulation, to predict the MedCM plasma concentrations following simulated administration of the formulation. The controlled-release formulation was intended to be administered by the intramuscular route but the physical properties of the formulation were not suitable, and thus subcutaneous administration was considered more appropriate. Due to the lack of subcutaneous PK data, the assumption that the PK of atropine, diazepam and HI-6 was the same by the subcutaneous and intramuscular routes was made for the simulations. Whilst the absorption of the MedCM by the subcutaneous and intramuscular routes is likely to differ, the absorption of atropine, diazepam and HI-6 will be dependent on the release from the formulation, whereas their distribution and elimination were expected to be the same.

The predicted concentration-time data were compared to the VX data reported in Chapter 4 and to the suggested PACs to give an indication of likely efficacy against percutaneous VX. The predicted concentration-time profiles of the MedCM are presented in Figure 6.4. Subsequent to the *in silico* simulations, *in vivo* guinea pig PK studies determined the concentration-time profiles of the MedCM following subcutaneous administration [266]. These *in vivo* data demonstrate that the *in silico* simulations did not provide accurate predictions of the concentration-time profiles (Figure 6.4), highlighting the importance and indeed necessity of validating simulated data with *in vivo* data. There are several possible reasons for the discrepancy between the *in silico* and *in vivo* data. The *in vitro* release rates of atropine, diazepam and HI-6, were not determined in a physiological solution but in two release media which incorporated a non-ionic surfactant [270]. The *in vitro* release rates were determined in conditions that maintained a consistent concentration gradient between the formulation and the media [270]. Thus, it is highly likely that the *in vitro* and *in vivo* release of atropine, diazepam and HI-6 from the controlled-release formulation were different. Furthermore, the slow release of diazepam from the formulation is likely to have been different from the intramuscular absorption of avizafone and its subsequent conversion to diazepam, particularly as diazepam is lipophilic and will preferentially remain in the cotton seed oil (lipid) vehicle.

The assumption regarding the similarity of subcutaneous and intramuscular PK for parameterizing the model may have been simplistic and will require validation. However, using the PK data that was available (intramuscular) to parameterize the model allowed predictions to be made that were not previously possible. The physiological characteristics of the subcutaneous space and muscle are different, in terms of local adipose tissue and blood flow (based on data presented for rats, dogs and humans by Brown *et al* [272]). The differences between these tissues may have affected the distribution and subsequently the elimination of the MedCMs. In future, predictions of any MedCM formulation PK (immediate and controlled-release) should be carried out using PK data determined by the same route of administration as the novel

formulation. Doing so will reduce the number of assumptions made about the different routes of administration. The controlled-release simulation demonstrates that it is easy to make assumptions and predict a concentration-time profile but these predictions are only tested and proven useful when validated with *in vivo* data. With respect to modelling controlled-release formulations, it is also recommended that a more physiological approach to *in vitro* release rate calculation is undertaken, rather than forcing the release via a maintained concentration-gradient.

The concentrations of atropine and HI-6 were not maintained above the PACs for a period considered appropriate (Figure 6.4), when compared to the percutaneous VX PK presented in Chapter 4. Thus, the novel controlled-release formulation did not progress to *in vivo* efficacy studies [266]. In addition, the physical characteristics of the formulation (the high viscosity of the formulation required administration via a large bore needle (13 G)), which in turn necessitated the use of local anaesthetic. During the PK studies the formulation was not administered in a reproducible manner.

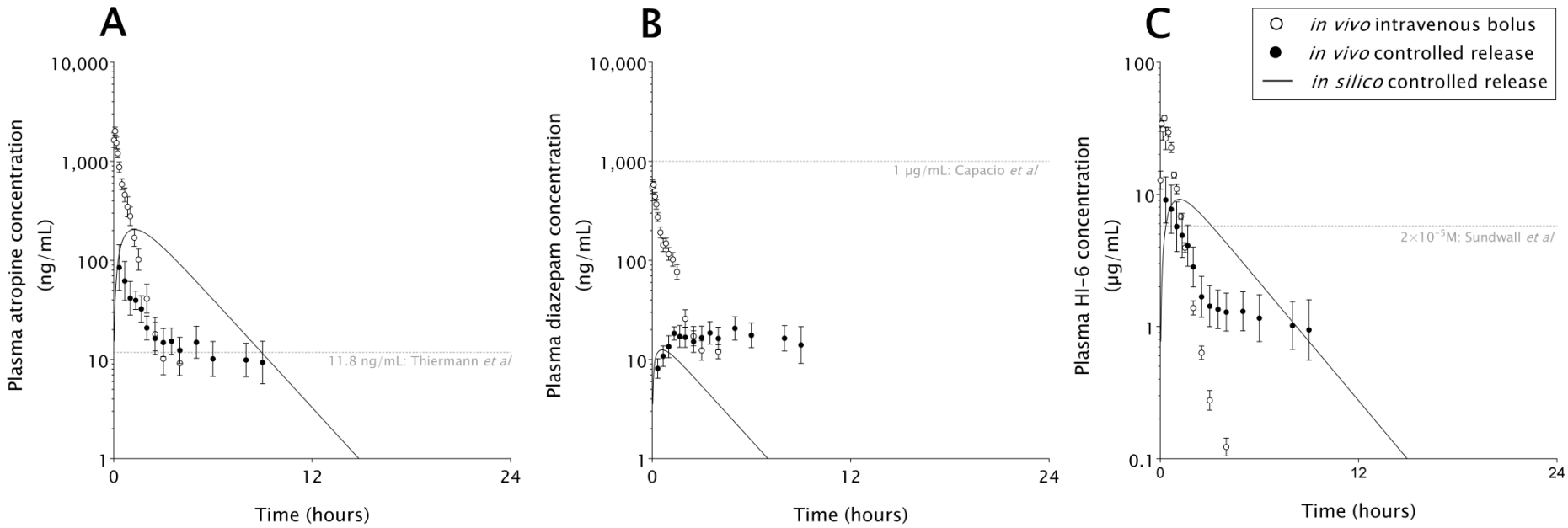

Figure 6.4. *In silico* simulation of controlled-release MedCM formulation did not accurately predict the concentration-time profiles of the MedCM *in vivo.*

Predicted concentration-time profiles (solid lines) following simulated subcutaneous administration of 90 mg/mL of the controlled-release formulation containing (A) atropine, (B) diazepam and (C) HI-6. The one-compartment PK simulations used PK parameters presented in Table 3.2 and *in vitro* release rates from 180 mg/mL of formulation in cotton seed oil (SwRI proprietary *information* [270]). The *in vivo* concentration-time profiles (n=5) demonstrate the predictions were not accurate and illustrate the importance of *in vivo* validation of PK simulations. Concentration-time profiles of non-modified intramuscular MedCM are included to show that the release of the MedCM from the controlled-release formulation was sustained. *In vivo* data shown as mean ± SEM.

6.3.4 Bioscavenger treatment for percutaneous poisoning.

The data presented in Chapter 4 of this thesis demonstrated that huBChE bioscavenger plasma concentration was sustained for at least 7 days following its intravenous or intramuscular administration. This PK data supports the use of huBChE as effective for the prevention and/or treatment of percutaneous nerve agent poisoning, as reported in several efficacy studies [102 :109 :224 :273-276]. In the scenario of human poisoning, post-exposure administration of huBChE is a First Aid treatment. However, in animal studies, efficacy has been shown to be reduced when bioscavengers were administered after the onset of signs of poisoning [109]. The intramuscular huBChE PK data presented in Figure 4.6 and Table 4.2 implies that this bioscavenger is not absorbed rapidly enough to inactivate the nerve agent in sufficient concentrations, thus reducing efficacy. In addition, the low volume of distribution of huBChE indicates that it is unable to penetrate into the tissues to bind the nerve agent. Therefore, on signs of poisoning, nerve agent has distributed to the target tissues and bioscavenger cannot prevent the inhibition of the tissue AChE by this nerve agent [110] (see Figure 4.1).

The reduced efficacy reported in animals following intramuscular administration of bioscavengers [224] is of concern, as this is the most likely route of administration for First Aid in humans (it is quick, reproducible and simple, requiring minimal training; unlike intravenous access). To overcome the slow intramuscular absorption of huBChE, the concept of combined therapy comprised of huBChE and conventional MedCM was considered [110]. This new treatment strategy has demonstrated efficacy *in vivo* (Figure 6.5) [110]. The efficacy can be explained by the PK data previously presented in Chapters 3 and 4 (Figure 6.6). Here the conventional MedCM are quickly absorbed, providing protection against the immediate cholinergic crisis and prolonging the window of opportunity for the bioscavenger to be absorbed, to inactivate the incoming nerve agent.

Further improvement in efficacy may be achieved by further modification of the combination therapy, through intravenous administration of the bioscavenger.

However, a large number of casualties may preclude intravenous administration of bioscavenger, which will be difficult and time consuming [277]. Conventional MedCM administered by the intraosseous route have been shown to be bioequivalent, achieving C_{max} more rapidly than intramuscular administration [278]. Therefore, intraosseous administration of bioscavengers should be considered to potentially increase efficacy compared to intramuscular administration. A set of animal studies to determine the intraosseous PK of huBChE or other bioscavenger should be carried out. These PK studies may show that bioscavenger is rapidly absorbed following intraosseous administration, justifying efficacy studies that use this route of administration.

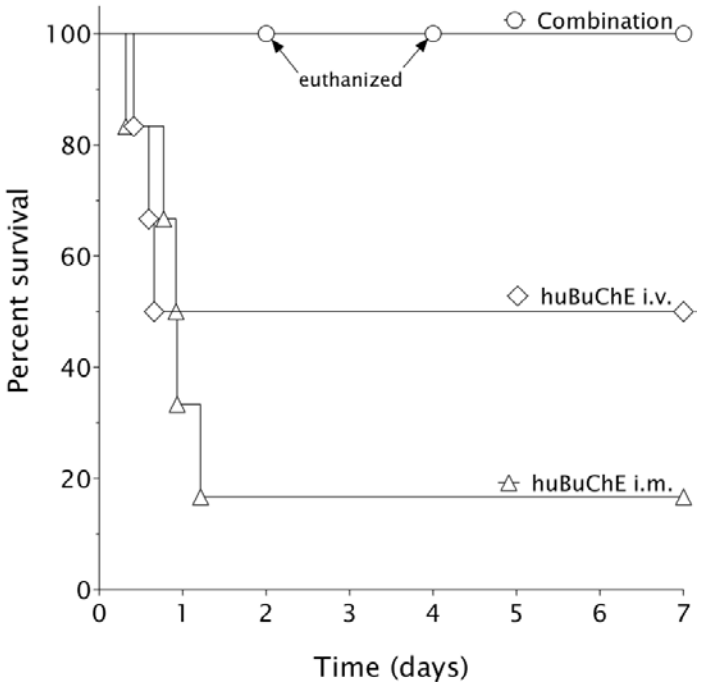

Figure 6.5. Treating guinea pigs on signs of poisoning after percutaneous exposure to VX with combination intramuscular therapy, consisting of conventional MedCM (atropine, avizafone and HI-6) and huBChE bioscavenger, improved survival compared to animals treated with huBChE bioscavenger alone.

In the absence of effective MedCM, VX (0.74 mg/kg) is lethal, with the mean time to death being 13.5 ± 3.7 hours (mean ± SEM). Treatment of animals with conventional MedCM (atropine, avizafone and HI-6) provides similar protection (data not shown) [142] to intramuscular huBChE bioscavenger. Two animals treated with combination therapy were euthanised due to surgical complications that were not related to percutaneous VX exposure. Data kindly provided by Helen Mumford [110].

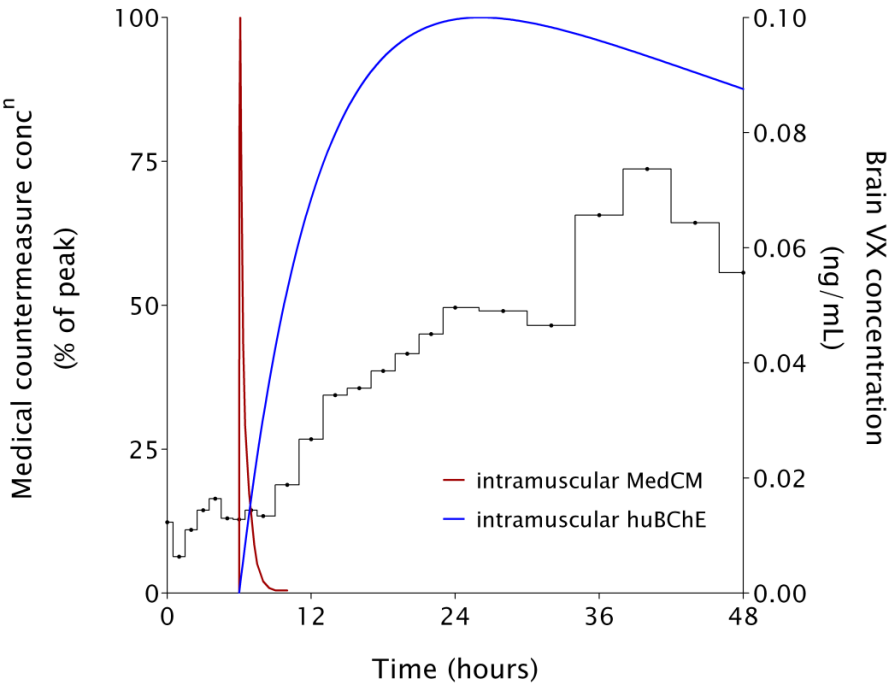

Figure 6.6. Composite plot of normalised (to peak concentration) conventional MedCM and huBChE bioscavenger concentrations following intramuscular administration, against brain microdialysate VX concentrations following percutaneous VX exposure.

MedCM administration is shown commencing at 6 hours; the mean time of MedCM administration in guinea pigs exposure to percutaneous VX [110]. Plasma concentration-time profiles of the conventional MedCM and huBChE were previously presented in Figure 3.11 and Figure 4.6, respectively. Atropine concentration data is shown alone for clarity.

6.4 Conclusions

A new methodology has been developed as part of the programme of work detailed in this thesis. This methodology enabled the collection of multiple blood samples and microdialysate fractions from tissues of conscious ambulatory guinea pigs. This ensured that a full concentration-time profile of MedCM and/or nerve agent was obtained in multiple tissues of individual animals, in order to determine and understand the PK of these MedCM in target tissues. This methodology also reduced the number of animals used.

The studies described in this thesis have determined the PK of MedCM against nerve agents, which have been integrated with PK and PD data for the nerve agents sarin and VX. The data generated from the studies reported here are the first systematic investigations of MedCM and nerve agents in guinea pigs, the small animal species of choice for nerve agent efficacy research. Furthermore, the studies are the first to determine the PK of MedCM and VX in the target tissues, brain and skeletal muscle.

The PK determined for conventional MedCM, atropine, avizafone and HI-6 demonstrate that these drugs are rapidly absorbed, distributed and eliminated. Atropine and diazepam were bioequivalent by the intravenous and intramuscular routes, whereas only one half of the HI-6 administered by the intramuscular route was available in the systemic circulation. The atropine and diazepam had greater volumes of distribution than the HI-6. PK interactions were determined to occur for HI-6, when administered in combination with atropine and avizafone. The most therapeutically significant interaction being the ability of this oxime to penetrate the blood brain barrier (HI-6 did not penetrate the blood brain barrier when administered alone), enabling HI-6 to distribute in the brain and reactivate inhibited AChE. This finding possibly renders current research designing, evaluating and developing centrally active oximes unnecessary. The PK data presented here have enabled a better understanding of the efficacy of conventional MedCM against nerve agents by placing the data in the context of published efficacy studies for both acute and percutaneous exposure.

Using MedCM PK parameters in simulation and modelling has demonstrated utility for the design of animal studies, as evidenced by physostigmine and hyoscine. Simulation and modelling has also further improved the understanding of efficacy and optimisation of MedCM administration regimens by placing the simulated data in the context of published efficacy studies, particularly against percutaneous nerve agent poisoning. However, simulation of concentration-time profiles should be validated with *in vivo* data. Furthermore, predictions should only be made with models that have been parameterized with PK data determined by the same route of administration.

The usefulness of PK as a tool to enable the translation of efficacy from animals to humans, through extrapolation of doses between species has been discussed, with examples provided. The approach of using PK and PD data for the scaling of efficacious doses appears to be the most accurate to date and should be integrated into MedCM development. To aid the scaling of doses using PK and PD data, the pharmacodynamic active concentration (PAC) for each MedCM needs to be defined. Determination of a PAC will enable an efficacious dose to be calculated, which achieves and sustains concentrations above the target concentration for an appropriate duration. The MedCM PK data reported in this thesis may be used to validate MedCM PBPK models, addressing the knowledge gap that currently exists for such models.

The PK data described for the bioscavenger huBChE was similar to previously published data in the guinea pig and has been used to understand the efficacy of this MedCM against percutaneous nerve agent poisoning. Combining bioscavenger PK data with conventional MedCM PK data has enabled the efficacy of this combination of drugs against percutaneous VX to be understood in more detail and has provided evidence to support the hypothesis that guided this combination therapy approach.

Finally, it is recommended that the PKPD of MedCM are determined as a matter of course in future studies. As discussed, these data will be critical for the interpretation of efficacy, ensuring that MedCM are taken forwards into advanced development based on a reliable understanding that their administration was at appropriate times and doses.

Appendices

Appendix A: Guinea pig colony bridging study

A bridging study was completed due to the change in the guinea pig colony background from Porcellus to David Hall, used in the studies described in this thesis. The guinea pig strain remained the same (Dunkin-Hartley).

Six male Dunkin-Hartley (Porcellus background) guinea pigs (375 g ± 17 g, mean ± SD) were cannulated and had microdialysis probes implanted in their skeletal muscle and brain, as described in Chapter 2. Combined atropine sulphate (17.4 mg/kg), avizafone hydrochloride (3.14 mg/kg) and HI-6 dimethanesulphonate (27.9 mg/kg) were administered by the intramuscular route. Blood samples were collected using the ABS at the time-points detailed in Figure 3.3. Analysis of the blood samples was completed using the LCMSMS method detailed in Section 2.5.2.

This bridging study showed little difference in PK of the MedCM between these two guinea pig colony backgrounds.

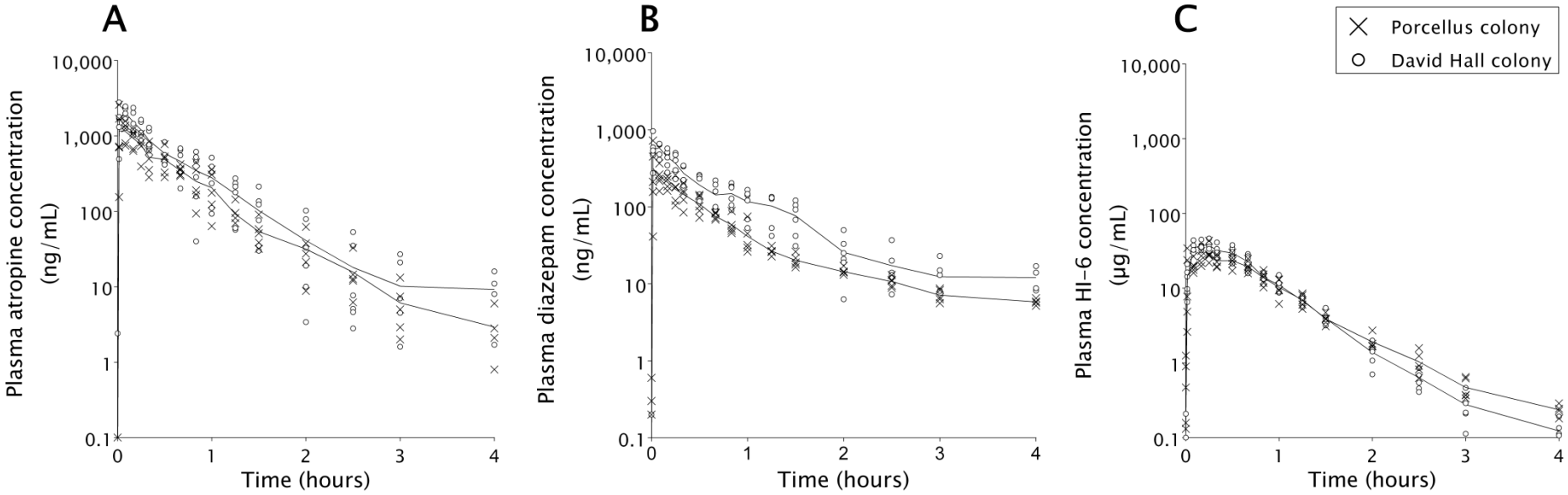

Figure A.1. Concentration-time profile of conventional MedCM quantified in plasma from guinea pigs and David Hall colony guinea pigs, following combined intramuscular administration.

(A) Atropine (B) diazepam and (C) HI-6 plasma concentrations determined following their combined intramuscular administration (atropine sulphate 17.4 mg/kg, avizafone hydrochloride 3.14 mg/kg HI-6 dimethanesulphonate 27.9 mg/kg). Data shown as each replicate with the mean (solid line).

Appendix B: Atropine and diazepam pharmacokinetics in sarin exposed guinea pigs

The data reported here were from the sarin exposed guinea pigs administered combined atropine sulphate (17.4 mg/kg), avizafone hydrochloride (3.14 mg/kg) and HI-6 dimethanesulphonate (27.9 mg/kg) by the intramuscular route (see Section 3.4.7). Due to the operational requirement for LC-MS-MS analysis of samples from different projects [174], there was a long delay between sample collection and LC-MS-MS analysis for atropine, diazepam and HI-6. Atropine and diazepam were not stable in the samples over the duration of storage [175]. Therefore, the concentration-time data for the atropine and diazepam was not reliable and was not included in the thesis.

	Atropine	Diazepam
Dose (mg)	5.22 ± 0.07	0.75 ± 0.01
C_{max} (ng/mL)	299 ± 167	253 ± 38
T_{max} (min)	0.9 ± 9.8	1.6 ± 2.2
T½ (min)	13.80 ± 1.45	0.31 ± 0.53
AUC (min · μg/mL)	6.2 ± 0.9	9.2 ± 1.2
CL (mL/min)	838.7 ± 114.1	81.2 ± 10.4
V_d (L)	16.70 ± 3.06	0.04 ± 0.06
k_{01} (1/min)	5.272 ± 73.230	0.035 ± 0.007
k_{10} (1/min)	0.050 ± 0.005	2.266 ± 3.953
k_{12} (1/min)	0.002 ± 0.001	0.486 ± 0.856
k_{21} (1/min)	0016 ± 0.007	0.006 ± 0.008

Table B.1. Compartmental plasma PK parameters for atropine and diazepam following intramuscular administration of combined MedCM to conscious ambulatory sarin exposed guinea pigs (n=6).

Atropine and diazepam were best fit by two-compartment models. Data shown as the estimate of the parameters for the pooled concentration-time data ± standard error of the estimate.

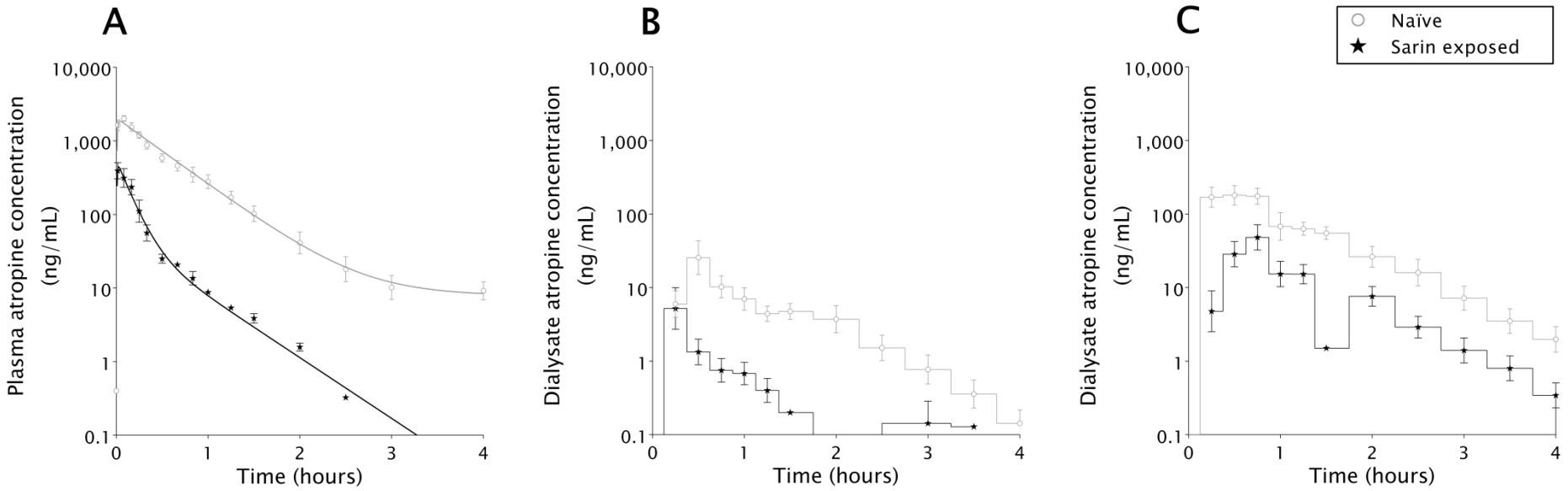

Figure B.1. Guinea pig plasma, brain and muscle atropine concentration-time profiles determined following combined intramuscular administration of conventional MedCM in sarin exposed guinea pigs.

(A) Plasma (n=6), (B) brain (n=7) and (C) muscle concentrations (n=7) following combined intramuscular administration of atropine sulphate (17.4 mg/kg), avizafone hydrochloride (3.14 mg/kg) and HI-6 dimethanesulphonate (27.9 mg/kg). Atropine plasma, brain and muscle concentration-time profiles following combined administration of the MedCM in naïve guinea pigs (Figure 3.12 and Figure 3.13) are included for comparison. Concentrations shown were corrected for microdialysis probe efficiency and shown as mean ± SEM. Mean plasma concentrations predicted by the PK models (lines) were calculated from the pooled data.

There was a long delay between sample collection and quantitation analysis for atropine, which was determined not to be stable in the samples over that duration of storage [175]. The data presented here were therefore not included in the main body of this thesis.

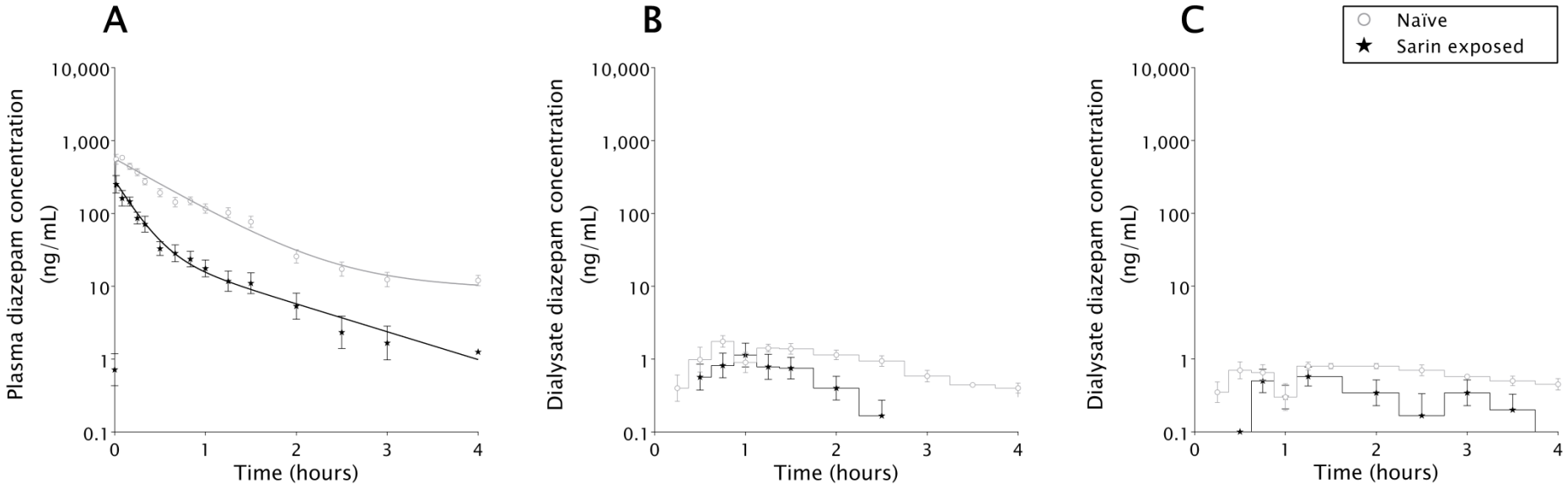

Figure B.2. Guinea pig plasma, brain and muscle HI-6 concentration-time profiles determined following combined intramuscular administration of conventional MedCM in sarin exposed guinea pigs.

(A) Plasma (n=6), (B) brain (n=7) and (C) muscle concentrations (n=7) following combined intramuscular administration of atropine sulphate (17.4 mg/kg), avizafone hydrochloride (3.14 mg/kg) and HI-6 dimethanesulphonate (27.9 mg/kg). Diazepam plasma, brain and muscle concentration-time profiles following combined administration of the MedCM in naïve guinea pigs (Figure 3.12 and Figure 3.13) are included for comparison. Concentrations shown were corrected for microdialysis probe efficiency and shown as mean ± SEM. Mean plasma concentrations predicted by the PK models (lines) were calculated from the pooled data.

There was a long delay between sample collection and quantitation analysis for atropine, which was determined not to be stable in the samples over that duration of storage [175]. The data presented here were therefore not included in the main body of this thesis.

Glossary

α	Initial slope of the pharmacokinetic concentration-time curve (compartmental PK analysis)
ABS	Automated blood sampler/sampling
AChE	Acetylcholinesterase
ADME	Absorption, distribution, metabolism and excretion. The processes involved in the pharmacokinetics of a drug
AIC	Akaike Information Criterion (measure of goodness of fit of a model)
ANOVA	Analysis of variance
AUC	Area under the concentration-time curve
β	Slope of the second phase of the pharmacokinetic concentration-time curve (compartmental PK analysis)
BBB	Blood brain barrier
BChE	Butyrylcholinesterase
C_0	Concentration at time zero
C_e	Concentration in the effect compartment
C_p	Concentration in the plasma
CaE	Carboxylesterase
ChE	Cholinesterase
Cl	Rate of clearance of a drug from the body
C_{max}	Maximum concentration
CNS	Central nervous system
C_{ss}	Concentration at steady state
E	Effect (pharmacodynamic measure)
E_0	Effect at time zero/baseline

ED_{50}	Median effective dose, the dose of a drug or compound which is effective in 50 % of the animals to which it is administered.
EEG	Electroencephalogram
F	Bioavailability
FI	Fractional change in response from E_0/baseline
F_{Rel}	Relative bioavailability
GABA	Gama amino butyric acid
HESI	Heated electrospray ionisation
huBChE	Plasma derived human butyrylcholinesterase
i.m.	intramuscular route of administration
i.p.	intraperitoneal route of administration
i.v.	intravenous route of administration
IC_{50}	Concentration required for 50 % inhibition
I_{max}	Maximum inhibition
IU	International Units
k	Pharmacokinetic rate constant (usually elimination rate constant)
k_{01}	Absorption rate constant into first compartment of a compartmental model
k_{10}	Elimination rate constant from first compartment of a compartmental model
k_{12}, k_{21}	Influx and efflux rate constants for the second compartment in a pharmacokinetic compartmental model
k_{13}, k_{31}	Influx and efflux rate constants for the third compartment in a pharmacokinetic compartmental model
k_a	Absorption rate constant

k_{e0}	Rate constant for the effect compartment in a linked pharmacokinetic and pharmacodynamic model
KVO	Keep vessel open, mode on an automated blood sampler which ensures patency of a cannula is maintained
λ_z	Lambda z, terminal rate constant calculated by non-compartmental pharmacokinetic analysis
LCMSMS	Liquid chromatography tandem mass spectrometry
LD_{50}	Median lethal dose, the dose of a drug or compound which is lethal to 50 % of the animals to which it is administered.
LLoQ	Lowest limit of quantitation
MedCM	Medical Countermeasures against nerve agents
NAPS	Nerve Agent Pretreatment Set: Pyridostigmine bromide tablets
NC3Rs	The National Centre for the Reduction, Refinement and Reduction of Animals in Research
NMDA	N-methyl-D-aspartate
PAC	Pharmacodynamic active concentration
p.c.	Percutaneous route of administration/exposure
PBPK	Physiologically Based Pharmacokinetic
PD	Pharmacodynamic
PK	Pharmacokinetic
rBChE	Recombinant human butyrylcholinesterase
R_{inf}	Rate of infusion
R_{max}	Maximum response
R_{min}	Minimum response

s.c.	subcutaneous route of administration/exposure
SD	Standard deviation
SEM	Standard error of the mean
SwRI	Southwest Research Institute
TK	Toxicokinetic
T_{lag}	Lag time prior to the first measurable concentration in the blood
T½	Elimination or terminal half-life
T_{max}	Time of maximum concentration (C_{max})
T_{min}	Time of minimum response/maximum inhibition
V_d	Apparent volume of distribution

References

1. Organisation for the Prohibition of Chemical Weapons. *Convention on the Prohibition of the Development, Production, Stockpiling and Use of Chemical Weapons and on Their Destruction.* 2005. http://www.opcw.org/index.php?eID=dam_frontend_push&docID=6357 accessed 28th April 2014.
2. HM Government. *A Strong Britain in an Age of Uncertainty: The National Security Strategy.* http://www.direct.gov.uk/prod_consum_dg/groups/dg_digitalassets/@dg/@en/documents/digitalasset/dg_191639.pdf accessed 25th May 2011.
3. Sidell FR, Groff WA. Reactivatibility of Cholinesterase Inhibited by Vx and Sarin in Man. *Toxicology and Applied Pharmacology* 1974; 27(2): 241-52. http://dx.doi.org/10.1016/0041-008X(74)90195-1
4. Schmaltz F. Neurosciences and Research on Chemical Weapons of Mass Destruction in Nazi Germany. *Journal of History of the Neurosciences* 2006; 15(3): 186-209. http://dx.doi.org/10.1080/09647040600658229
5. Rang HP, Dale MM, Ritter JM. Hunter L, Simmons B, Arnott N, et al. (eds). *Pharmacology* 4th ed: Churchill Livingstone; 2002.
6. Moore DH, Clifford CB, Crawford IT, Cole GM, Baggett JM. Review of Nerve Agent Inhibitors and Reactivators of Acetylcholinesterase. In: Quinn DM (ed.) *Enzymes of the Cholinesterase Family*. New York: Plenum Press; 1995. pp 297-304.
7. Eyer P. The Role of Oximes in the Management of Organophosphorus Pesticide Poisoning. *ToxicolRev* 2003; 22(3): 165-90. http://dx.doi.org/10.2165/00139709-200322030-00004

8. Taylor P. Anticholinesterase Agents. In: Hardman JG, Limbird LE, Goodman Gilman A (eds.). *Goodman & Gilman's the Pharmacological Basis of Therapeutics*. 10th International ed: McGraw-Hill; 2001. pp 175-91.

9. Lawler HC. Turnover Time of Acetylcholinesterase. *Journal of Biological Chemistry* 1961; 236(8): 2296-301. http://www.jbc.org/content/236/8/2296.long

10. Lintern M, Taylor C, Wetherell J, Smith ME. Attenuation of the Effects of Physostigmine by Hyoscine in Guinea-Pig Brain Cholinergic Enzymes: Acetylcholinesterase. *Chemico-Biological Interactions* 2005; 157: 327-30. http://dx.doi.org/10.1016/j.cbi.2005.10.098

11. Li B, Sedlacek M, Manoharan I, Boopathy R, Duysen EG, Masson P, Lockridge O. Butyrylcholinesterase, Paraoxonase, and Albumin Esterase, but Not Carboxylesterase, Are Present in Human Plasma. *Biochemical Pharmacology* 2005; 70(11): 1673-84. http://dx.doi.org/10.1016/j.bcp.2005.09.002

12. Koller LD, Gardner DE, Gaylor DW, Green S, Henderson RF, Bakshi KS, Fusco LV, Wagner BM. *Review of Acute Human-Toxicity Estimates for Selected Chemical-Warfare Agents.* National Academy Press, 1997.

13. Szinicz L. History of Chemical and Biological Warfare Agents. *Toxicology* 2005; 214(3): 167-81. http://dx.doi.org/10.1016/j.tox.2005.06.011

14. Sellström Å, Cairns S, Barbeschi M. *Report on the Alleged Use of Chemical Weapons in the Ghouta Area of Damascus on 21 August 2013.* United Nations (OPCW), 2013. http://www.un.org/disarmament/content/slideshow/Secretary_General_Report_of_CW_Investigation.pdf

15. Cannard K. The Acute Treatment of Nerve Agent Exposure. *Journal of the Neurological Sciences* 2006; 249(1): 86-94. http://dx.doi.org/10.1016/j.jns.2006.06.008

16. Watson A, Opresko D, Young R, Hauschild V, King J, Bakshi K. Organophosphate Nerve Agents. In: Gupta RC (ed.) *Handbook of Toxicology of Chemical Warfare Agents*. 1st ed; 2009. pp 43-67.

17. McDonough JH, Shih TM. Neuropharmacological Mechanisms of Nerve Agent-Induced Seizure and Neuropathology. *Neuroscience and Biobehavioral Reviews* 1997; 21(5): 559-79. http://dx.doi.org/10.1016/S0149-7634(96)00050-4

18. Koelle GB. Pharmacology of Organophosphates. *Journal of Applied Toxicology* 1994; 14(2): 105-09. http://dx.doi.org/10.1002/jat.2550140211

19. Jokanovic M, Stojiljkovic MP. Current Understanding of the Application of Pyridinium Oximes as Cholinesterase Reactivators in Treatment of Organophosphate Poisoning. *European Journal of Pharmacology* 2006; 553(1-3): 10-17. http://dx.doi.org/.1016/j.ejphar.2006.09.054

20. Tokuda Y, Kikuchi M, Takahashi O, Stein GH. Prehospital Management of Sarin Nerve Gas Terrorism in Urban Settings: 10 Years of Progress after the Tokyo Subway Sarin Attack. *Resuscitation* 2006; 68(2): 193-202. http://dx.doi.org/10.1016/j.resuscitation.2005.05.023

21. Yanagisawa N, Morita H, Nakajima T. Sarin Experiences in Japan: Acute Toxicity and Long-Term Effects. *Journal of the Neurological Sciences* 2006; 249(1): 76-85. http://dx.doi.org/10.1016/j.jns.2006.06.007

22. Gearhart JM, Robinson PJ, Jakubowski EM. Physiologically Based Pharmacokinetic Modelling of Chemical Warfare Agents. In: Gupta RC (ed.)

Handbook of Toxicology of Chemical Warfare Agents. 1st ed. San Diego: Academic Press; 2009. pp 791-98.

23. Hawrami SA, Ibrahim N. Experiencing Chemical Warfare: Two Physicians Tell Their Story of Halabja in Northern Iraq. *Canadian journal of rural medicine : the official journal of the Society of Rural Physicians of Canada = Journal canadien de la medecine rurale : le journal officiel de la Societe de medecine rurale du Canada* 2004; 9(3): 178-81. http://www.srpc.ca/PDF/cjrm/vol09n3/pg178.pdf
24. Gordon MK, Enzenauer RW, Babin MC. Ocular Toxicity of Sulfur Mustard. In: Gupta RC (ed.) *Handbook of Toxicology of Chemical Warfare Agents*. 1st ed. San Diego: Academic Press; 2009. pp 575-94.
25. Mumford H, Price ME, Wetherell JR. A Novel Approach to Assessing Percutaneous Vx Poisoning in the Conscious Guinea-Pig. *Journal of Applied Toxicology* 2008; 28(5): 694-702. http://dx.doi.org/10.1002/jat.1324
26. Joosen MJA, van der Schans MJ, van Helden HPM. Percutaneous Exposure to Vx: Clinical Signs, Effects on Brain Acetylcholine Levels and Eeg. *Neurochemical Research* 2008; 33(2): 308-17. http://dx.doi.org/10.1007/s11064-007-9508-5
27. Sidell FR. Nerve Agents. In: Zajtchuk R, Bellamy RF (eds.). *Medical Aspects of Chemical and Biological Warfare*. 1st ed: Department of the Army, Office of the Surgeon General, Borden Institute; 1997. pp 129-79.
28. Nozaki H, Aikawa N, Fujishima S, Suzuki M, Shinozawa Y, Hori S, Nogawa S. A Case of Vx Poisoning and the Difference from Sarin. *The Lancet* 1995; 346(8976): 698-99. http://dx.doi.org/10.1016/S0140-6736(95)92306-3

29. Morimoto F, Shimazu T, Yoshioka T. Intoxication of Vx in Humans. *The American Journal of Emergency Medicine* 1999; 17(5): 493–94. http://dx.doi.org/10.1016/S0735-6757(99)90258-9

30. *Package Leaflet – Information for the User Autoject (Combopen®) Nerve Agent Antidote L4a1.* http://www.mhra.gov.uk/home/groups/spcpil/documents/spcpil/con1346646483716.pdf accessed 27th February 2013.

31. Joosen MJA, van der Schans MJ, van Helden HPM. Percutaneous Exposure to the Nerve Agent Vx: Efficacy of Combined Atropine, Obidoxime and Diazepam Treatment. *Chemico-Biological Interactions* 2010; 188(1): 255–63. http://dx.doi.org/10.1016/j.cbi.2010.06.010

32. Wetherell J, Price M, Mumford H, Armstrong S, Scott L. Development of Next Generation Medical Countermeasures to Nerve Agent Poisoning. *Toxicology* 2007; 233(1–3): 120–27. http://dx.doi.org/10.1016/j.tox.2006.07.028

33. Leadbeater L, Inns RH, Rylands JM. Treatment of Poisoning by Soman. *Fundamental and Applied Toxicology* 1985; 5(6): S225–S31. http://dx.doi.org/10.1016/0272-0590(85)90132-0

34. Dawson RM. Review of Oximes Available for Treatment of Nerve Agent Poisoning. *Journal of Applied Toxicology* 1994; 14(5): 317–31. http://dx.doi.org/10.1002/jat.2550140502

35. Wetherell J, Hall T, Passingham S. Physostigmine and Hyoscine Improves Protection against the Lethal and Incapacitating Effects of Nerve Agent Poisoning in the Guinea-Pig. *Neurotoxicology* 2002; 23(3): 341–49. http://dx.doi.org/10.1016/S0161-813X(02)00082-7

36. *Package Leaflet – Information for the User Nerve Agent Pre-Treatment Set L1a1 (Naps*

L1a1). http://www.mhra.gov.uk/home/groups/spcpil/documents/spcpil/con1350277942133.pdf accessed 4th March 2013.

37. *Summary of Product Characteristics: Autoject (Combopen®) Nerve Agent Antidote*
L4a1. http://www.mhra.gov.uk/home/groups/spcpil/documents/spcpil/con1366005014724.pdf accessed 25th October 2013.
38. Newmark J. The Birth of Nerve Agent Warfare - Lessons from Syed Abbas Foroutan. *Neurology* 2004; 62(9): 1590-96. http://dx.doi.org/10.1212/01.WNL.0000124519.85516.50
39. Taysse L, Daulon S, Delamanche S, Bellier B, Breton P. Protection against Soman-Induced Neuropathology and Respiratory Failure: A Comparison of the Efficacy of Diazepam and Avizafone in Guinea Pig. *Toxicology* 2006; 225(1): 25-35. http://dx.doi.org/10.1016/j.tox.2006.04.043
40. Gordon AS, Frye CW. Large Doses of Atropine: Low Toxicity and Effectiveness in Anticholinesterase Intoxication. *The Journal of the American Medical Association* 1955; 159(2): 1181-84. http://dx.doi.org/10.101/jama.1955.02960290007003
41. Brown JH, Taylor P. Muscarinic Receptor Agonists and Antagonists. In: Hardman JG, Limbird LE, Molinoff PB, et al. (eds.). *Goodman & Gilman's the Pharmacological Basis of Therapeutics*. 9th ed. New York: McGraw-Hill; 1996. pp 141-60.
42. Singh S, Batra YK, Singh SM, Wig N, Sharma BK. Is Atropine Alone Sufficient in Acute Severe Organophosphorous Poisoning - Experience of a North-West Indian Hospital. *International Journal of Clinical Pharmacology and Therapeutics* 1995; 33(11): 628-30.
43. Singh S, Chaudhry D, Behera D, Gupta D, Jindal SK. Aggressive Atropinisation and Continuous Pralidoxime (2-Pam) Infusion in Patients

with Severe Organophosphate Poisoning: Experience of a Northwest Indian Hospital. *Human & Experimental Toxicology* 2001; 20(1): 15-18. http://dx.doi.org/10.1191/096032701671437581

44. Spencer KEV. *Substitutes for Atropine in the Treatment of Nerve Gas Poisoning. Part 2, a Comparison between Basic Amides and Atropine in the Treatment of Gb Poisoning in the Rat and Guinea Pig.* Dstl report number: Unpublished - TP 349, 1953.
45. Spencer KEV. *Substitutes for Atropine in the Treatment of Nerve Gas Poisoning. Part 1, the Development of a Screening Test for Examining Atropine Substitutes.* Dstl report number: Unpublished - TP 296, 1952.
46. Askew BM. Oximes and Atropine in Sarin Poisoning. *British Journal of Pharmacology and Chemotherapy* 1957; 12(3): 340-43. http://dx.doi.org/10.1111/j.1476-5381.1957.tb00145.x
47. Berry WK, Davies DR. Use of Carbamates and Atropine in Protection of Animals against Poisoning by 1,2,2-Trimethylpropyl Methylphosphonofluoridate. *Biochemical Pharmacology* 1970; 19(3): 927. http://dx.doi.org/10.1016/0006-2952(70)90256-X
48. Gordon JJ, Leadbeater L, Maidment MP. Protection of Animals against Organophosphate Poisoning by Pretreatment with a Carbamate. *Toxicology and Applied Pharmacology* 1977; 43(1): 207-16. http://dx.doi.org/10.1016/S0041-008X(78)80045-3
49. Dirnhuber P, Green DM. Effectiveness of Pyridostigmine in Reversing Neuromuscular Blockade Produced by Soman. *Journal of Pharmacy and Pharmacology* 1978; 30(7): 419-25. http://dx.doi.org/10.1111/j.2042-7158.1978.tb13278.x
50. Raveh L, Weissman BA, Cohen G, Alkalay D, Rabinovitz I, Sonego H, Brandeis R. Caramiphen and Scopolamine Prevent Soman-Induced Brain

Damage and Cognitive Dysfunction. *Neurotoxicology* 2002; 23(1): 7-17. http://dx.doi.org/10.1016/S0161-813X(02)00005-0

51. Anderson DR, Harris LW, Bowersox SL, Lennox WJ, Anders JC. Efficacy of Injectable Anticholinergic Drugs against Soman-Induced Convulsive/Subconvulsive Activity. *Drug and Chemical Toxicology* 1994; 17(2): 139-48. http://dx.doi.org/10.3109/01480549409014307
52. Capacio BR, Byers CE, Caro ST, McDonough JH. Pharmacokinetics of Intramuscularly Administered Biperiden in Guinea Pigs Challenged with Soman. *Drug and Chemical Toxicology* 2003; 26(1): 1-13. http://dx.doi.org/10.1081/DCT-120017553
53. Shih TM, Koviak TA, Capacio BR. Anticonvulsants for Poisoning by the Organophosphorus Compound Soman - Pharmacological Mechanisms. *Neuroscience and Biobehavioral Reviews* 1991; 15(3): 349-62. http://dx.doi.org/10.1016/S0149-7634(05)80028-4
54. Bhattacharjee AK, Pomponio JW, Evans SA, Pervitsky D, Gordon RK. Discovery of Subtype Selective Muscarinic Receptor Antagonists as Alternatives to Atropine Using in Silico Pharmacophore Modeling and Virtual Screening Methods. *Bioorganic & Medicinal Chemistry* 2013; 21(9): 2651-62. http://dx.doi.org/10.1016/j.bmc.2013.01.072
55. Tattersall J. Seizure Activity Post Organophosphate Exposure. *Frontiers in Bioscience* 2009; 14: 3688-711. http://dx.doi.org/10.2741/4081
56. Upshall DG, Gouldstone SJ, Macey N, Maidment MP, West SJ, Yeadon M. Conversion of a Peptido-Aminobenzophenone Pro-Drug to Diazepam *in Vitro*. Enzyme Isolation and Characterisation. *Journal of Biopharmaceutical Sciences* 1990; 1(2): 111-26.

57. Maidment MP, Upshall DG. Pharmacokinetics of the Conversion of a Peptido-Amino Benzophenon Pro-Drug of Diazepam in Guinea Pig and Rhesus Monkey. *Journal of Biopharmaceutical Sciences* 1990; 1: 19-32.

58. Taysse L, Calvet JH, Buee J, Christin D, Delamanche S, Breton P. Comparative Efficacy of Diazepam and Avizafone against Sarin-Induced Neuropathology and Respiratory Failure in Guinea Pigs: Influence of Atropine Dose. *Toxicology* 2003; 188(2-3): 197-209. http://dx.doi.org/10.1016/S0300-483X(03)00086-6

59. Lallement G, Renault F, Baubichon D, Peoc'h M, Burckhart MF, Galonnier M, Clarencon D, Jourdil N. Compared Efficacy of Diazepam or Avizafone to Prevent Soman Induced Electroencephalographic Disturbances and Neuropathology in Primates: Relationship to Plasmatic Benzodiazepine Pharmacokinetics. *Archives of Toxicology* 2000; 74(8): 480-86. http://dx.doi.org/10.1007/s002040000146

60. Inns RH. *Selection of Avizafone Dose for Nerve Agent Therapy Medical Countermeasures.* Dstl report number: Unpublished - TR 56531, 2011.

61. Capacio BR, Byers CE, Merk KA, Smith JR, McDonough JH. Pharmacokinetic Studies of Intramuscular Midazolam in Guinea Pigs Challenged with Soman. *Drug and Chemical Toxicology* 2004; 27(2): 95-110. http://dx.doi.org/10.1081/DCT-120030727

62. Koplovitz I, Schulz S, Shutz M, Railer R, Macalalag R, Schons M, McDonough J. Combination Anticonvulsant Treatment of Soman-Induced Seizure. *Journal of Applied Toxicology* 2001; 21: S53-S55. http://dx.doi.org/10.1002/jat.811

63. Green MD, Talbot BG, Clark CR. Pharmacokinetics of Pralidoxime Chloride in the Rat. *Life Sciences* 1986; 39(23): 2263-69. http://dx.doi.org/10.1016/0024-3205(86)90405-4

64. Lallement G, Clarencon D, Brochier G, Baubichon D, Galonnier M, Blanchet G, Mestries JC. Efficacy of Atropine/Pralidoxime/Diazepam or Atropine/Hi-6/Prodiazepam in Primates Intoxicated by Soman. *Pharmacology Biochemistry and Behavior* 1997; 56(2): 325-32. http://dx.doi.org/10.1016/S0091-3057(96)00292-4

65. Gunderson CH, Lehmann CR, Sidell FR, Jabbari B. Nerve Agents - a Review. *Neurology* 1992; 42(5): 946-50. http://dx.doi.org/10.1212/WNL.42.5.946

66. Worek F, Aurbek N, Wetherell J, Pearce P, Mann T, Thiermann H. Inhibition, Reactivation and Aging Kinetics of Highly Toxic Organophosphorus Compounds: Pig Versus Minipig Acetylcholinesterase. *Toxicology* 2008; 244(1): 35-41. http://dx.doi.org/10.1016/j.tox.2007.10.021

67. Aurbek N, Thiermann H, Szinicz L, Eyer P, Worek F. Analysis of Inhibition, Reactivation and Aging Kinetics of Highly Toxic Organophosphorus Compounds with Human and Pig Acetylcholinesterase. *Toxicology* 2006; 224(1-2): 91-99. http://dx.doi.org/10.1016/j.tox.2006.04.030

68. Talbot BG, Anderson DR, Harris LW, Yarbrough LW, Lennox WJ. A Comparison of in Vivo and in Vitro Rates of Aging of Soman-Inhibited Erythrocyte Acetylcholinesterase in Different Animal Species. *Drug and Chemical Toxicology* 1988; 11(3): 289-305. http://dx.doi.org/10.3109/01480548809017884

69. Worek F, Reiter G, Eyer P, Szinicz L. Reactivation Kinetics of Acetylcholinesterase from Different Species Inhibited by Highly Toxic Organophosphates. *Archives of Toxicology* 2002; 76(9): 523-29. http://dx.doi.org/10.1007/s00204-002-0375-1

70. Koplovitz I, Menton R, Matthews C, Shutz M, Nalls C, Kelly S. Dose-Response Effects of Atropine and Hi-6 Treatment of Organophosphorus Poisoning in Guinea-Pigs. *Drug and Chemical Toxicology* 1995; 18(2-3): 119-36. http://dx.doi.org/10.3109/01480549509014316

71. Kassa J, Karasova J, Musilek K, Kuca K. An Evaluation of Therapeutic and Reactivating Effects of Newly Developed Oximes (K156, K203) and Commonly Used Oximes (Obidoxime, Trimedoxime, Hi-6) in Tabun-Poisoned Rats and Mice. *Toxicology* 2008; 243(3): 311-16. http://dx.doi.org/10.1016/j.tox.2007.10.015

72. Worek F, Szinicz L, Eyer P, Thiermann H. Evaluation of Oxime Efficacy in Nerve Agent Poisoning: Development of a Kinetic-Based Dynamic Model. *Toxicology and Applied Pharmacology* 2005; 209(3): 193-202. http://dx.doi.org/10.1016/j.taap.2005.04.006

73. van Helden HPM, van der Wiel HJ, de Lange J, Busker RW, Melchers BPC, Wolthuis OL. Therapeutic Efficacy of Hi-6 in Soman-Poisoned Marmoset Monkeys. *Toxicology and Applied Pharmacology* 1992; 115(1): 50-56. http://dx.doi.org/10.1016/0041-008X(92)90366-Z

74. Lundy PM, Hill I, Lecavalier P, Hamilton MG, Vair C, Davidson C, Weatherby KL, Berger BJ. The Pharmacokinetics and Pharmacodynamics of Two Hi-6 Salts in Swine and Efficacy in the Treatment of Gf and Soman Poisoning. *Toxicology* 2005; 208(3): 399-409. http://dx.doi.org/10.1016/j.tox.2004.12.001

75. Lundy PM, Hansen AS, Hand BT, Boulet CA. Comparison of Several Oximes against Poisoning by Soman, Tabun and Gf. *Toxicology* 1992; 72(1): 99-105. http://dx.doi.org/10.1016/0300-483X(92)90089-W

76. Inns RH, Leadbeater L. The Efficacy of Bispyridinium Derivatives in the Treatment of Organophosphonate Poisoning in the Guinea-Pig. *Journal of*

Pharmacy and Pharmacology 1983; 35(7): 427-33. http://dx.doi.org/10.1111/j.2042-7158.1983.tb04316.x

77. Lundy PM, Tremblay KP. Ganglion Blocking Properties of Some Bis-Pyridinium Soman Antagonists. *European Journal of Pharmacology* 1979; 60(1): 47-53. http://dx.doi.org/10.1016/0014-2999(79)90051-7
78. Tattersall JEH. Ion Channel Blockade by Oximes and Recovery of Diaphragm Muscle from Soman Poisoning Invitro. *British Journal of Pharmacology* 1993; 108(4): 1006-15. http://dx.doi.org/10.1111/j.1476-5381.1993.tb13498.x
79. Øydvin OK, Tanso R, Aas P. Pre-Junctional Effects of Oximes on [H-3]-Acetylcholine Release in Rat Hippocampal Slices During Soman Intoxication. *European Journal of Pharmacology* 2005; 516(3): 227-34. http://dx.doi.org/10.1016/j.ejphar.2005.04.041
80. Heilbron E, Tolagen B. Toxogonin in Sarin Soman and Tabun Poisoning. *Biochemical Pharmacology* 1965; 14(1): 73-&. http://dx.doi.org/10.1016/0006-2952(65)90059-6
81. Loomis TA, Salafsky B. Antidotal Action of Pyridinium Oximes in Anticholinesterase Poisoning - Comparative Effects of Soman, Sarin, and Neostigmine on Neuromuscular Function. *Toxicology and Applied Pharmacology* 1963; 5(6): 685-&. http://dx.doi.org/10.1016/0041-008X(63)90062-0
82. Harris LW, Anderson DR, Pastelak AM, Vanderpool B. Acetylcholinesterase Inhibition by (+)Physostigmine and Efficacy against Lethality Induced by Soman. *Drug and Chemical Toxicology* 1990; 13(2-3): 241-48. http://dx.doi.org/10.3109/01480549009018124
83. Levy A, Cohen G, Gilat E, Kapon J, Dachir S, Abraham S, Herskovitz M, Teitelbaum Z, Raveh L. Extrapolating from Animal Studies to the Efficacy

in Humans of a Pretreatment Combination against Organophosphate Poisoning. *Archives of Toxicology* 2007; 81(5): 353-59. http://dx.doi.org/10.1007/s00204-006-0153-6

84. Wetherell JR. Continuous Administration of Low-Dose Rates of Physostigmine and Hyoscine to Guinea-Pigs Prevents the Toxicity and Reduces the Incapacitation Produced by Soman Poisoning. *Journal of Pharmacy and Pharmacology* 1994; 46(12): 1023-28. http://dx.doi.org/10.1111/j.2042-7158.1994.tb03260.x
85. Lallement G, Foquin A, Dorandeu F, Baubichon D, Carpentier P. Subchronic Administration of Various Pretreatments of Nerve Agent Poisoning. 2. Compared Efficacy against Soman Toxicity. *Drug and Chemical Toxicology* 2001; 24(2): 165-80. http://dx.doi.org/10.1081/DCT-100102608
86. Blake P, Gleadle RI, Parkes DC, White RG. *Evaluation of Pyridostigmine Bromide as a Pretreatment for Nerve Agent Poisoning in Man. In-House Studies.* Dstl report number: Unpublished - TP 396, 1985.
87. Masson P. Evolution of and Perspectives on Therapeutic Approaches to Nerve Agent Poisoning. *Toxicology Letters* 2011; 206(1): 5-13. http://dx.doi.org/10.1016/j.toxlet.2011.04.006
88. Pereira EFR, Hilmas C, Santos MD, Alkondon M, Maelicke A, Albuquerque EX. Unconventional Ligands and Modulators of Nicotinic Receptors. *Journal of Neurobiology* 2002; 53(4): 479-500. http://dx.doi.org/10.1002/neu.10146
89. Philippens LHCH, Melchers BPC, Olivier B, Bruijnzeel PLB. Scopolamine Augments the Efficacy of Physostigmine against Soman Poisoning in Guinea Pigs. *Pharmacology Biochemistry and Behavior* 2000; 65(1): 175-82. http://dx.doi.org/10.1016/S0091-3057(99)00171-9

90. Muggleton NG, Bowditch AP, Crofts HS, Scott EAM, Pearce PC. Assessment of a Combination of Physostigmine and Scopolamine as Pretreatment against the Behavioural Effects of Organophosphates in the Common Marmoset (Callithrix Jacchus). *Psychopharmacology* 2003; 166(3): 212–20. http://dx.doi.org/10.1007/s00213-002-1324-7

91. Ketchum JS, Sidell FR, Crowell EB, Aghajani GK, Hayes AH. Atropine, Scopolamine, and Ditran - Comparative Pharmacology and Antagonists in Man. *Psychopharmacologia* 1973; 28(2): 121–45. http://dx.doi.org/10.1007/BF00421398

92. Anderson DR, Harris LW, Lennox WJ, Solana RP. Effects of Subacute Pretreatment with Carbamate Together with Acute Adjunct Pretreatment against Nerve Agent Exposure. *Drug and Chemical Toxicology* 1991; 14(1–2): 1–19. http://dx.doi.org/10.3109/01480549109017866

93. Green DM, Inns RH. *Classified Title.* Dstl report number: Unpublished - TPE 381, 1984.

94. Meshulam Y, Davidovici R, Wengier A, Levy A. Prophylactic Transdermal Treatment with Physostigmine and Scopolamine against Soman Intoxication in Guinea-Pigs. *Journal of Applied Toxicology* 1995; 15(4): 263–66. http://dx.doi.org/10.1002/jat.2550150406

95. Fosbraey P, Wetherell JR, French MC. Effect of Acute Physostigmine-Hyoscine Pretreatment on the Neurochemical Changes Produced by Soman in the Guinea-Pig. *Neurochemistry International* 1991; 18(2): 265–73. http://dx.doi.org/10.1016/0197-0186(91)90194-I

96. Janowsky DS. Central Anticholinergics to Treat Nerve-Agent Poisoning. *Lancet* 2002; 359(9302): 265–66. http://dx.doi.org/10.1016/S0140-6736(02)07434-2

97. Dunn MA, Hackley BE, Sidell FR. Preatreatment for Nerve Agent Exposure. In: Zajtchuk R, Bellamy RF (eds.). *Medical Aspects of Chemical and Biological Warfare*. 1st ed: Department of the Army, Office of the Surgeon General, Borden Institute; 1997. pp 181–96.

98. Lallement G, Baille V, Baubichon D, Carpentier P, Collombet J-M, Filliat P, Foquin A, Four E, Masqueliez C, Testylier G, Tonduli L, Dorandeu F. Review of the Value of Huperzine as Pretreatment of Organophosphate Poisoning. *Neurotoxicology* 2002; 23(1): 1–5. http://dx.doi.org/10.1016/S0161-813X(02)00015-3

99. Aracava Y, Pereira EFR, Akkerman M, Adler M, Albuquerque EX. Effectiveness of Donepezil, Rivastigmine, and (+/−)Huperzine a in Counteracting the Acute Toxicity of Organophosphorus Nerve Agents: Comparison with Galantamine. *Journal of Pharmacology and Experimental Therapeutics* 2009; 331(3): 1014–24. http://dx.doi.org/10.1124/jpet.109.160028

100. Nachon F, Brazzolotto X, Trovaslet M, Masson P. Progress in the Development of Enzyme-Based Nerve Agent Bioscavengers. *Chemico-Biological Interactions* 2013; 206(3): 536–44. http://dx.doi.org/10.1016/j.cbi.2013.06.012

101. Wolfe AD, Rush RS, Doctor BP, Koplovitz I, Jones D. Acetylcholinesterase Prophylaxis against Organophosphate Toxicity. *Fundamental and Applied Toxicology* 1987; 9(2): 266–70. http://dx.doi.org/10.1016/0272-0590(87)90049-0

102. Lenz DE, Yeung D, Smith JR, Sweeney RE, Lumley LA, Cerasoli DM. Stoichiometric and Catalytic Scavengers as Protection against Nerve Agent Toxicity: A Mini Review. *Toxicology* 2007; 233(1–3): 31–39. http://dx.doi.org/10.1016/j.tox.2006.11.066

103. Mumford H. *Human Butyrlcholinesterase (Hubche) Production Capabilities.* Dstl report number: Unpublished - TR 74618, 2014.

104. NIH. *First Time in Human Study of Protexia.* http://www.clinicaltrials.gov.ct2/show/NCT00744146 accessed 13th April 2014.

105. Geyer BC, Kannan L, Garnaud PE, Broomfield CA, Cadieux CL, Cherni I, Hodgins SM, Kasten SA, Kelley K, Kilbourne J, Oliver ZP, Otto TC, Puffenberger I, Reeves TE, Robbins N, Woods RR, Soreq H, Lenz DE, Cerasoli DM, Mor TS. Plant-Derived Human Butyrylcholinesterase, but Not an Organophosphorous-Compound Hydrolyzing Variant Thereof, Protects Rodents against Nerve Agents. *Proceedings of the National Academy of Sciences of the United States of America* 2010; 107(47): 20251-56. http://dx.doi.org/10.1073/pnas.1009021107

106. Ilyushin DG, Smirnov IV, Belogurov AA, Dyachenko IA, Zharmukhamedova TI, Novozhilova TI, Bychikhin EA, Serebryakova MV, Kharybin ON, Murashev AN, Anikienko KA, Nikolaev EN, Ponomarenko NA, Genkin DD, Blackburn GM, Masson P, Gabibov AG. Chemical Polysialylation of Human Recombinant Butyrylcholinesterase Delivers a Long-Acting Bioscavenger for Nerve Agents in Vivo. *Proceedings of the National Academy of Sciences of the United States of America* 2013; 110(4): 1243-48. http://dx.doi.org/10.1073/pnas.1211118110

107. Troyer JK. Vice President, Chemical Defense, Pharmathene, Inc. Personal Communication. 25th October 2012.

108. US Defense Threat Reduction Agency, *Alternate Manufacturing Processes for Recombinant Human Butyrylcholinesterase* HDTRA1-14-CHEM-BIO-BAA. 1st February 2013.

109. Mumford H, Price ME, Lenz DE, Cerasoli DM. Post-Exposure Therapy with Human Butyrylcholinesterase Following Percutaneous Vx Challenge in Guinea Pigs. *Clinical Toxicology* 2011; 49(4): 287-97. http://dx.doi.org/10.1016/j.neuropharm.2011.11.016

110. Mumford H, Docx CJ, Price ME, Green AC, Tattersall JEH, Armstrong SJ. Human Plasma-Derived Buche as a Stoichiometric Bioscavenger for Treatment of Nerve Agent Poisoning. *Chemico-Biological Interactions* 2013; 203(1): 160-66. http://dx.doi.org/10.1016/j.cbi.2012.08.018

111. Masson P, Lockridge O. Butyrylcholinesterase for Protection from Organophosphorus Poisons: Catalytic Complexities and Hysteretic Behavior. *Archives of Biochemistry and Biophysics* 2010; 494(2): 107-20. http://dx.doi.org/10.1016/j.abb.2009.12.005

112. Ashani Y. Prospective of Human Butyrylcholinesterase as a Detoxifying Antidote and Potential Regulator of Controlled-Release Drugs. *Drug Development Research* 2000; 50(3-4): 298-308. http://dx.doi.org/10.1002/1098-2299(200007/08)50:3/4<309::AID-DDR14>3.0CO;2-I

113. Ashani Y, Pistinner S. Estimation of the Upper Limit of Human Butyrylcholinesterase Dose Required for Protection against Organophosphates Toxicity: A Mathematically Based Toxicokinetic Model. *Toxicological Sciences* 2004; 70(2): 358-67. http://dx.doi.org/10.1093/toxsci/kfh012

114. Wales ME, Reeves TE. Organophosphorus Hydrolase as an in Vivo Catalytic Nerve Agent Bioscavenger. *Drug Testing and Analysis* 2012; 4(3-4): 271-81. http://dx.doi.org/10.1002/dta.381

115. Parikh K, Duysen EG, Snow B, Jensen NS, Manne V, Lockridge O, Chilukuri N. Gene-Delivered Butyrylcholinesterase Is Prophylactic against the

Toxicity of Chemical Warfare Nerve Agents and Organophosphorus Compounds. *Journal of Pharmacology and Experimental Therapeutics* 2011; 337(1): 92-101. http://dx.doi.org/10.1124/jpet.110.175646

116. Huang Y-J, Lundy PM, Lazaris A, Huang Y, Baldassarre H, Wang B, Turcotte C, Côte M, Bellemare A, Bilodeau AS, Brouillard S, Touati M, Herskovits P, Begin I, Neveu N, Brochu E, Pierson J, Hockley DK, Cerasoli DM, Lenz DE, Wilgus H, Karatzas CN, Langermann S. Substantially Improved Pharmacokinetics of Recombinant Human Butyrylcholinesterase by Fusion to Human Serum Albumin. *BMC Biotechnology* 2008; 8: 50-61. http://dx.doi.org/10.1186/1472-6750-8-50
117. Somani SM, Dube SN. Physostigmine - an Overview as Pretreatment Drug for Organophosphate Intoxication. *International Journal of Clinical Pharmacology, Therapy and Toxicology* 1989; 27(8): 367-87.
118. Rowland M, Tozer TN. Preface *Clinical Pharmacokinetics and Pharmacodynamics Concepts and Applications*. 4th ed: Lippincott Williams & Wilkins; 2010. pp ix-x.
119. Maxwell DM, Brecht KM. The Role of Carboxylesterase in Species Variation of Oxime Protection against Soman. *Neuroscience and Biobehavioral Reviews* 1991; 15(1): 135-39. http://dx.doi.org/10.1016/S0149-7634(05)80105-8
120. Maxwell DM, Brecht KM, Oneill BL. The Effect of Carboxylesterase Inhibition on Interspecies Differences in Soman Toxicity. *Toxicology Letters* 1987; 39(1): 35-42. http://dx.doi.org/10.1016/0378-4274(87)90254-2
121. Sterri SH, Fonnum F. Carboxylesterase - the Soman Scavenger in Rodents - Heterogeneity and Hormonal Influence. In: Reiner E, Aldridge WN,

Hoskin FCG (eds.). *Enzymes Hydrolising Organophorus Compounds*. Chichester: Ellis Horwood Ltd; 1989. pp 155–64.

122. Duysen EG, Koentgen F, Wiliams GR, Timperley CM, Schopfer LM, Cerasoli DM, Lockridge O. Production of Es1 Plasma Carboxylesterase Knockout Mice for Toxicity Studies. *Chemical Research in Toxicology* 2011; 24(11): 1891–98. http://dx.doi.org/10.1021/tx200237a
123. van der Meer MJ, Hundt HKL, Müller FO. Inhibition of Atropine Metabolism by Organophosphate Pesticides. *Human & Experimental Toxicology* 1983; 2(4): 637–40. http://dx.doi.org/10.1177/096032718300200409
124. Rowland M, Tozer TN. Response Following a Single Dose *Clinical Pharmacokinetics and Pharmacodynamics: Concepts and Applications*. 4th ed: Lippincott Williams and Wilkins; 2010. pp 217–44.
125. FDA. *Guidance for Industry: Estimating the Maximum Safe Starting Dose in Initial Clinical Trials for Therapeutics in Adult Healthy Volunteers.* http://www.fda.gov/downloads/Drugs/Guidances/UCM078932.pdf accessed 18th March 2014.
126. Sharma V, McNeill JH. To Scale or Not to Scale: The Principles of Dose Extrapolation. *British Journal of Pharmacology* 2009; 157: 907–21. http://dx.doi.org/10.1111/j.1476-5381.2009,00267.x
127. Baggot JD. Application of Interspecies Scaling to the Bispyridinium Oxime Hi-6. *American Journal of Veterinary Research* 1994; 55(5): 689–91.
128. Lukey BJ, Parrish JH, Marlow DD, Clark CR, Sidell FR. Pharmacokinetics of Physostigmine Intramuscularly Administered to Guinea-Pigs. *Journal of Pharmaceutical Sciences* 1990; 79(9): 796–98. http://dx.doi.org/10.1002/jps.2600790910
129. Bohnert S, Vair C, Mikler J. Development and Validation of a Sensitive Hplc Method for the Quantification of Hi-6 in Guinea Pig Plasma and Evaluated

in Domestic Swine. *Journal of Chromatography B* 2010; 878(17-18): 1407-13. http://dx.doi.org/10.1016/j.jchromb.2010.03.018

130. Lenz DE, Maxwell DM, Koplovitz I, Clark CR, Capacio BR, Cerasoli DM, Federko JM, Luo CY, Saxena A, Doctor BP, Olson C. Protection against Soman or Vx Poisoning by Human Butyrylcholinesterase in Guinea Pigs and Cynomolgus Monkeys. *Chemico-Biological Interactions* 2005; 157: 205-10. http://dx.doi.org/10.1016/j.cbi.2005.10.025
131. Shih TM, Rowland TC, McDonough JH. Anticonvulsants for Nerve Agent-Induced Seizures: The Influence of the Therapeutic Dose of Atropine. *Journal of Pharmacology and Experimental Therapeutics* 2007; 320(1): 154-61. http://dx.doi.org/10.1124/jpet.106.111252
132. Koplovitz I, Schulz S, Railer R, Sigler M, Kelleher C, Shutz M. The Effect of Atropine Dosage on the Efficacy of Other Pretreatment and Treatment Medical Countermeasures for Nerve Agent Intoxication. *Toxicology* 2007; 233(1-3): 232-33. http://dx.doi.org/10.1016/j.tox.2006.04.020
133. Harrison PK, Tattersall JEH, Gosden E. The Presence of Atropinesterase Activity in Animal Plasma. *Naunyn-Schmiedebergs Archives of Pharmacology* 2006; 373(3): 230-36. http://dx.doi.org/10.1007/s00210-006-0054-5
134. Cassel G, Karlsson L, Waara L, Ang KW, Göransson-Nyberg A. Pharmacokinetics and Effects of Hi 6 in Blood and Brain of Soman-Intoxicated Rats: A Microdialysis Study. *European Journal of Pharmacology* 1997; 332(1): 43-52. http://dx.doi.org/10.1016/S0014-2999(97)01058-3
135. Capacio BR, Whalley CE, Byers CE, McDonough JH. Intramuscular Diazepam Pharmacokinetics in Soman-Exposed Guinea Pigs. *Journal of*

Applied Toxicology 2001; 21: S67-S74. http://dx.doi.org/10.1002/jat.813

136. van der Schans MJ, Lander BJ, van der Wiel H, Langenberg JP, Benschop HP. Toxicokinetics of the Nerve Agent (+/-)-Vx in Anesthetized and Atropinized Hairless Guinea Pigs and Marmosets after Intravenous and Percutaneous Administration. *Toxicology and Applied Pharmacology* 2003; 191(1): 48-62. http://dx.doi.org/10.1016/S0041-008X(03)00216-3
137. Langenberg JP, Spruit HET, van der Wiel HJ, Trap HC, Helmich RB, Bergers WWA, van Helden HPM, Benschop HP. Inhalation Toxicokinetics of Soman Stereoisomers in the Atropinized Guinea Pig with Nose-Only Exposure to Soman Vapor. *Toxicology and Applied Pharmacology* 1998; 151(1): 79-87. http://dx.doi.org/10.1006/taap.1998.8451
138. Spruit HET, Langenberg JP, Trap HC, van der Wiel HJ, Helmich RB, van Helden HPM, Benschop HP. Intravenous and Inhalation Toxicokinetics of Sarin Stereoisomers in Atropinized Guinea Pigs. *Toxicology and Applied Pharmacology* 2000; 169(3): 249-54. http://dx.doi.org/10.1006/taap.2000.9060
139. Benschop HP, Trap HC, Spruit HET, van der Wiel HJ, Langenberg JP, De Jong LPA. Low Level Nose-Only Exposure to the Nerve Agent Soman: Toxicokinetics of Soman Stereoisomers and Cholinesterase Inhibition in Atropinized Guinea Pigs. *Toxicology and Applied Pharmacology* 1998; 153(2): 179-85. http://dx.doi.org/10.1006/taap.1998.8490
140. Whalley CE, McGuire JM, Miller DB, Jakubowski EM, Mioduszewski RJ, Thomson SA, Lumley LA, McDonough JH, Shih TMA. Kinetics of Sarin (Gb) Following a Single Sublethal Inhalation Exposure in the Guinea Pig.

Inhalation Toxicology 2007; 19(8): 667-81. http://dx.doi.org/10.1080/08958370701353296

141. Wetherell JR, Armstrong SJ, Read RW, Clough GF. Vx Penetration Following Percutaneous Poisoning: A Dermal Microdialysis Study in the Guinea Pig. *Toxicology Mechanisms and Methods* 2008; 18(4): 313-21. http://dx.doi.org/10.1080/15376510701884944
142. Mumford H, Price ME, Graham SJ, Wetherell JR. *Percutaneous Poisoning in the Guinea Pig: Iii. Dose-Response Effects on Physiological Indices and Medical Countermeasures.* Dstl report number: Unpublished - TR 15681, 2009.
143. Traunmüller F, Zeitlinger M, Zeleny P, Müller M, Joukhadar C. Pharmacokinetics of Single- and Multiple-Dose Oral Clarithromycin in Soft Tissues Determined by Microdialysis. *Antimicrobial Agents and Chemotherapy* 2007; 51(9): 3185-89. http://dx.doi.org/10.1128/aac.00532-07
144. Westerink BHC, Cremers TIFH (eds). *Handbook of Microdialysis: Methods, Applications and Clinical Aspects* 1st ed: Academic Press; 2007.
145. Clough GF, Stenken JA, Church MK. High Molecular Weight Targets and Treatments Using Microdialysis. In: Müller M (ed.) *Microdialysis in Drug Development*. 1st ed: Springer; 2013. pp 243-68.
146. Bodelenz M, Höfferer C, Magnes C, Shaller-Ammann R, Schaupp L, Feichtner F, Ratzer M, Pickl K, Sinner F, Wutte A, Korsatko S, Köhler G, Legat FJ, Benfeldt EM, Wright AM, Neddermann D, Jung T, Peiber TR. Dermal Pk/Pd of a Lipophilic Topical Drug in Psoriatic Patients by Continuous Intradermal Membrane-Free Sampling. *European Journal of Pharmaceutics and Biopharmaceutics* 2014; 81(3): 635-41. http://dx.doi.org/10.1016/j.ejpb.2012.04.009

147. O'Donnell JC, Acon-Chen C, McDonough JH, Shih TM. Comparison of Extracellular Striatal Acetylcholine and Brain Seizure Activity Following Acute Exposure to the Nerve Agents Cyclosarin and Tabun in Freely Moving Guinea Pigs. *Toxicology Mechanisms and Methods* 2010; 20(9): 600-08. http://dx.doi.org/10.3109/15376516.2010.521208

148. O'Donnell JC, McDonough JH, Shih TM. Changes in Extracellular Striatal Acetylcholine and Brain Seizure Activity Following Acute Exposure to Nerve Agents in Freely Moving Guinea Pigs. *Toxicology Mechanisms and Methods* 2010; 20(3): 143-52. http://dx.doi.org/10.3109/15376511003657439

149. Fosbraey P, Wetherell JR, French MC. Neurotransmitter Changes in Guinea-Pig Brain-Regions Following Soman Intoxication. *Journal of Neurochemistry* 1990; 54(1): 72-79. http://dx.doi.org/10.1111/j.1471-4159.1990.tb13284.x

150. Bourne JA, Fosbraey P, Halliday J. Sch 23390 Affords Protection against Soman-Evoked Seizures in the Freely Moving Guinea-Pig: A Concomitant Neurochemical, Electrophysiological and Behavioural Study. *Neuropharmacology* 2001; 40(2): 279-88. http://dx.doi.org/10.1016/S0028-3908(00)00136-2

151. Cassel GE, Fosbraey P. Measurement of the Oxime Hi-6 after Peripheral Administration in Tandem with Neurotransmitter Levels in Striatal Dialysates: Effects of Soman Intoxication. *Journal of Pharmacological and Toxicological Methods* 1996; 35(3): 159-66. http://dx.doi.org/10.1016/1056-8719(96)00027-5

152. Chang JC, Lee WC, Wu YT, Tsai TH. Distribution of Blood-Muscle for Clenbuterol in Rat Using Microdialysis. *International Journal of*

Pharmaceutics 2009; 372(1-2): 91-96. http://dx.doi.org/10.1016/j.ijpharm.2009.01.015

153. Close GL, Jackson MJ. *The Use of in Vivo Microdialysis Techniques to Detect Extracellular Ros in Resting and Contracting Skeletal Muscle*: Humana Press Inc.; 2008.
154. Newman JMB, Ross RM, Richards SM, Clark MG, Rattigan S. Insulin and Contraction Increase Nutritive Blood Flow in Rat Muscle in Vivo Determined by Microdialysis of L-[C-14]Glucose. *Journal of Physiology-London* 2007; 585(1): 217-29. http://dx.doi.org/10.1113/jphysiol.2007.138818
155. Huang YT, Cheng CJ, Lai TF, Tsai TR, Tsai TH, Chuo WH, Cham TM. An Investigation of Acetylcholine Released in Skeletal Muscle and Protein Unbound Drug Released in Blood Based on the Pyridostigmine Bromide (Pretreatment Drug) Sustained-Release Pellets by Microdialysis Technique in the Rabbit Model. *Neuroscience Letters* 2007; 416(3): 302-06. http://dx.doi.org/10.1016/j.neulet.2007.02.019
156. Close GL, Ashton T, McArdle A, Jackson MJ. Microdialysis Studies of Extracellular Reactive Oxygen Species in Skeletal Muscle: Factors Influencing the Reduction of Cytochrome C and Hydroxylation of Salicylate. *Free Radical Biology & Medicine* 2005; 39(11): 1460-67. http://dx.doi.org/10.1016/j.freeradbiomed.2005.07.009
157. McDonell W. Respiratory System. In: Thurmon JC, Tranquilli WJ, Benson GJ (eds.). *Lumb & Jones' Veterinary Anethesia*. 3rd ed: Lippincott Williams & Wilkins; 1996. pp 115-47.
158. Farnfield B. Personal Communication. 17th September 2012.
159. Dobromylskyj P, Flecknell PA, Lascelles BD, Pascoe PJ, Taylor P, Waterman-Pearson A. Management of Postoperative and Other Acute

Pain. In: Flecknell PA, Waterman-Pearson A (eds.). *Pain Management in Animals*. 1st ed: Harcourt Publishers Limited; 2000. pp 81-145.

160. Steffey EP. Inhalation Anaesthetics. In: Thurmon JC, Tranquilli WJ, Benson GJ (eds.). *Lumb & Jones' Veterinary Anesthesia*. 3rd ed: Lippincott Williams & Wilkins; 1996. pp 297-329.
161. Tasso L, Bettoni CC, Oliveira LK, Costa TD. Evaluation of Gatifloxacin Penetration into Skeletal Muscle and Lung by Microdialysis in Rats. *International Journal of Pharmaceutics* 2008; 358(1-2): 96-101. http://dx.doi.org/10.1016/j.ijpharm.2008.02.023
162. Bourne JA, Fosbraey P. Novel Method of Monitoring Electroencephalography at the Site of Microdialysis During Chemically Evoked Seizures in a Freely Moving Animal. *Journal of Neuroscience Methods* 2000; 99(1-2): 85-90. http://dx.doi.org/10.1016/S0165-0270(00)00217-X
163. Poole SJ, Rudall SR. *Correlates of Protection: Efficacy of Hi-6 Dms in the Guinea Pig Model of Nerve Agent Poisoning.* Dstl report number: Unpublished - TR 59697, 2012.
164. Laboratory Animal Science Association. First Report of the Bva/Frame/Rspca/Ufaw Joint Working Group on Refinement - Removal of Blood from Laboratory Mammals and Birds. *Laboratory Animals* 1993; 27: 1-22. http://dx.doi.org/10.1258/002367793781082412
165. Dahyot C, Marchand S, Bodin M, Debeane B, Mimoz O, Couet W. Application of Basic Pharmacokinetic Concepts to Analysis of Microdialysis Data - Illustration with Imipenem Muscle Distribution. *Clinical Pharmacokinetics* 2008; 47(3): 181-89. http://dx.doi.org/10.2165/00003088-200847030-00004

166. Ellman GL, Courtney KD, Andres V, Featherstone RM. A New and Rapid Colorimetric Determination of Acetylcholinesterase Activity. *Biochemical Pharmacology* 1961; 7(2): 88-95. http://dx.doi.org/10.1016/0006-2952(61)90145-9

167. Abbara C, Rousseau JM, Lelievre B, Turcant A, Lallement G, Ferec S, Bardot I, Diquet B. Pharmacokinetic Analysis of Pralidoxime after Its Intramuscular Injection Alone or in Combination with Atropine-Avizafone in Healthy Volunteers. *British Journal of Pharmacology* 2010; 161(8): 1857-67. http://dx.doi.org/10.1111/j.1476-5381.2010.01007.x

168. Sheiner LB, Stanski DR, Vozeh S, Miller RD, Ham J. Simultaneous Modeling of Pharmacokinetics and Pharmacodynamics - Application to D-Tubocurarine. *Clinical Pharmacology & Therapeutics* 1979; 25(3): 358-71.

169. Taylor JR. *An Introduction to Error Analysis: The Study of Uncertainties in Physical Measurements* 2nd ed: University Science Books; 1997.

170. Rowland M, Tozer TN. Kinetics Following an Extravascular Dose *Clinical Pharmacokinetics and Pharmacodynamics: Concepts and Applications*. 4th ed: Lippincott Williams and Wilkins; 2010. pp 159-215.

171. Boskovic B, Kovacevic V, Jovanovic D. Pam-2 Cl, Hl-6, and Hgg-12 in Soman and Tabun Poisoning. *Fundamental and Applied Toxicology* 1984; 4(2): S106-S15. http://dx.doi.org/10.1016/0272-0590(84)90142-8

172. Passingham SL, Wetherell JR, Hall TL, Irwin M, Pinhorn V. *Treatment of Nerve Agent Poisoning in the Presence of Pyridostigmine Pretreatment: A Comparison of Hi-6 and P2s in the Guinea Pig.* Dstl report number: Unpublished - CR 96, 1997.

173. Inns RH. *Treatment of Nerve Agent Poisoning: Delay of Therapy.* Dstl report number: Unpublished - TR 42266, 2011.

174. Sample I, Borger J. Uk and France Claim Syrian Attack Victims Have Tested Positive for Sarin. *The Guardian* 2013 5th June 2013; http://www.theguardian.com/world/2013/jun/04/syria-nerve-agent-sarin-uk-france (accessed 5th June 2013).

175. Roughley N. *Bioanalytical Method Validation for the Determination of Atropine Sulphate and Diazepam in Guinea Pig Plasma.* Dstl report number: Unpublished - TR 63417, 2012.

176. Flecknell PA. Introduction *Laboratory Animal Anaesthesia*. 3rd ed: Academic Press; 2009.

177. Heavner JE. Drug Interactions. In: Thurmon JC, Tranquilli WJ, Benson GJ (eds.). *Veterinary Anaesthesia*. 3rd ed: Lippincott Williams & Wilkins; 1996.

178. Stypinski D, Wiebe LI, Tam YK, Mercer JR, McEwan AJB. Effects of Methoxyflurane Anesthesia on the Pharmacokinetics of 125i-Iaza in Sprague-Dawley Rats. *Nuclear Medicine and Biology* 1999; 26(8): 959-65. http://dx.doi.org/10.1016/S0969-8051(99)00071-2

179. Tse FLS, Nickerson DF, Aim R. Effect of Isoflurane Anesthesia on Antipyrine Pharmacokinetics in the Rat. *Pharmaceutical Research* 1992; 9(11): 1515-17. http://dx.doi.org/10.1023/A:1015835618709

180. Sawyer TW, Mikler J, Tenn C, Bjarnason S, Frew R. Non-Cholinergic Intervention of Sarin Nerve Agent Poisoning. *Toxicology* 2012; 294(2-3): 85-93. http://dx.doi.org/10.1016/j.tox.2012.02.003

181. Hinderling PH, Gundertremy U, Schmidlin O. Integrated Pharmacokinetics and Pharmacodynamics of Atropine in Healthy Humans .1. Pharmacokinetics. *Journal of Pharmaceutical Sciences* 1985; 74(7): 703-10. http://dx.doi.org/10.1002/jps.2600740702

182. Smallridge RC, Fein HG, Umstott CE, Odonnell VM, Redmond DP, Friedman DS, Pamplin CL. Human Pharmacokinetics of Atropine - Equivalent

Bioavailability (Ba) by Intramuscular and Intravenous Routes. *Clinical Research* 1986; 34(3): A867-A67.

183. Chen K, Seng KY. Calibration and Validation of a Physiologically Based Model for Soman Intoxication in the Rat, Marmoset, Guinea Pig and Pig. *Journal of Applied Toxicology* 2012; 32(9): 673-386. http://dx.doi.org/10.1002/jat.1671

184. Rowland M, Tozer TN. Elimination *Clinical Pharmacokinetics and Pharmacodynamics: Concepts and Applications*. 4th ed: Lippincott Williams and Wilkins; 2010. pp 111-57.

185. Gaustad R, Johnsen H, Fonnum F. Carboxylesterases in Guinea-Pig - a Comparison of the Different Isoenzymes with Regard to Inhibition by Organophosphorus Compounds Invivo and Invitro. *Biochemical Pharmacology* 1991; 42(7): 1335-43. http://dx.doi.org/10.1016/0006-2952(91)90443-9

186. Gaustad R, Løvhaug D. Monoclonal Antibodies Distinguish between Carboxylesterase Isoenzymes in Different Tissues of Rat and Guinea Pig. *Biochemical Pharmacology* 1992; 44(1): 171-74. http://dx.doi.org/10.1016/0006-2952(92)90051-J

187. Hosokawa M. Structure and Catalytic Properties of Carboxylesterase Isozymes Involved in Matabolic Activation of Prodrugs. *Molecules* 2008; 13: 412-31. http://dx.doi.org/10.3390/molecules13020412

188. Bencharit S, Morton CL, Xue Y, Potter PM, Redinbo MR. Structural Basis of Heroin and Cocaine Metabolism by a Promiscuous Human Drug-Processing Enzyme. *Nature Structural and Molecular Biology* 2003; 10: 349-56. http://dx.doi.org/10.1038/nsb919

189. Hatfield MJ, Potter PM. Carboxylesterase Inhibitors. *Expert Opinion on Therapeutic Patents* 2011; 21(8): 1159-71. http://dx.doi.org/10.1517/13543776.2011.586339

190. Abbara C, Rousseau JM, Turcant A, Lallement G, Comets E, Bardot I, Clair P, Diquet B. Bioavailability of Diazepam after Intramuscular Injection of Its Water-Soluble Prodrug Alone or with Atropine-Pralidoxime in Healthy Volunteers. *British Journal of Pharmacology* 2009; 157(8): 1390-97. http://dx.doi.org/10.1111/j.1476-5381.2009.00330.x

191. Clement JG, Bailey DG, Madill HD, Tran LT, Spence JD. The Acetylcholinesterase Oxime Reactivator Hi-6 in Man - Pharmacokinetics and Tolerability in Combination with Atropine. *Biopharmaceutics & Drug Disposition* 1995; 16(5): 415-25. http://dx.doi.org/10.1002/bdd.2510160506

192. Kusic R, Boskovic B, Vojvodic V, Jovanovic D. Hi-6 in Man - Blood-Levels, Urinary-Excretion, and Tolerance after Intramuscular Administration of the Oxime to Healthy-Volunteers. *Fundamental and Applied Toxicology* 1985; 5(6): S89-S97. http://dx.doi.org/10.1016/0272-0590(85)90118-6

193. Myers TM, Sun W, Naik RS, Clark MG, Doctor BP, Saxena A. Characterization of Human Serum Butyrylcholinesterase in Rhesus Monkeys: Behavioral and Physiological Effects. *Neurotoxicology and Teratology* 2012; 34(3): 323-28. http://dx.doi.org/10.1016/j.ntt.2012.02.002

194. Zhao H, Xie YH, Yang Q, Cao Y, Tu HH, Cao W, Wang SW. Pharmacokinetic Study of Cinnamaldehyde in Rats by Gc-Ms after Oral and Intravenous Administration. *Journal of Pharmaceutical and Biomedical Analysis* 2014; 89: 150-57. http://dx.doi.org/10.1016/j.jpba.2013.10.044

195. Su TW, Wu WH, Yan T, Zhang CY, Zhu QG, Bao B. Pharmacokinetics and Tissue Distribution of a Novel Marine Fibrinolytic Compound in Wistar Rat Following Intravenous Administrations. *Journal of Chromatography B-Analytical Technologies in the Biomedical and Life Sciences* 2013; 942: 77-82. http://dx.doi.org/10.1016/j.jchromb.2013.10.031

196. Sim SM, Saremi K, Tan NH, Fung SY. Pharmacokinetics of Cryptelytrops Purpureomaculatus (Mangrove Pit Viper) Venom Following Intravenous and Intramuscular Injections in Rabbits. *International Immunopharmacology* 2013; 17(4): 997-1001. http://dx.doi.org/10.1016/j.intimp.2013.10.007

197. Lee HK, Lebkowska-Wieruszewska B, Kim TW, Kowaski CJ, Giorgi M. Pharmacokinetics of the Novel Atypical Opioid Tapentadol after Intravenous, Intramuscular and Subcutaneous Administration in Cats. *Veterinary Journal* 2013; 198(3): 620-24. http://dx.doi.org/10.1016/j.tvjl.2013.09.011

198. Ellinwood EH, Nikaido AM, Gupta SK, Heatherly DG, Nishita JK. Comparison of Central-Nervous-System and Peripheral Pharmacodynamics to Atropine Pharmacokinetics. *Journal of Pharmacology and Experimental Therapeutics* 1990; 255(3): 1133-39. http://jpet.aspetjournals.org/content/255/3/1133.long

199. Koplovitz I, Shulz SM, Railer RF, Sigler M, Lee RB. Effect of Atropine and Diazepam on the Efficacy of Oxime Treatment of Nerve Agent Intoxication. *Journal of Medical Chemical, Biological and Radiological Defense* 2007; 5. http://www.jmedcbr.org/issue_0501/Koplovitz/Koplovitz_05_07.html

200. Thiermann H, Steinritz D, Worek F, Radtke M, Eyer P, Eyer F, Felgenhauer N, Zilker T. Atropine Maintenance Dosage in Patients with Severe

Organophosphate Pesticide Poisoning. *Toxicology Letters* 2011; 206(1): 77-83. http://dx.doi.org/10.1016/j.toxlet.2011.07.006

201. Shih TM, Duniho SM, McDonough JH. Control of Nerve Agent-Induced Seizures Is Critical for Neuroprotection and Survival. *Toxicology and Applied Pharmacology* 2003; 188(2): 69-80. http://dx.doi.org/10.1016/S0041-008X(03)00019-X
202. Simons KJ, Briggs CJ. Disposition of Hi-6 Oxime in Rats after Intravenous and Intramuscular Administration. *Journal of Pharmacy and Pharmacology* 1985; 37(5): 367-69. http://dx.doi.org/10.1111/j.2042-7158.1985.tb05088.x
203. Kao LM, Bush K, Barnewall R, Estep J, Thalacker FW, Olson PH, Drusano GL, Minton N, Chien S, Hemeryck A, Kelley MF. Pharmacokinetic Considerations and Efficacy of Levofloxacin in an Inhalational Antrhax (Post-Exposure) Rhesus Monkey Model. *Antimicrobial Agents and Chemotherapy* 2006; 50(11): 3535-42. http://dx.doi.org/10.1128/AAC.00090-06
204. Sundwall A. Minimum Concentrations of N-Methylpyridinium-2-Aldoxime Methane Sulphonate (P2s) Which Reverse Neuromuscular Block. *Biochemical Pharmacology* 1961; 8(4): 413-&. http://dx.doi.org/10.1016/0006-2952(61)90059-4
205. Worek F, Thiermann H, Szinicz L, Eyer P. Kinetic Analysis of Interactions between Human Acetylcholinesterase, Structurally Different Organophosphorus Compounds and Oximes. *Biochemical Pharmacology* 2004; 68(11): 2237-48. http://dx.doi.org/10.1016/j.bcp.2004.07.038
206. Joosen MJA, van der Schans MJ, van Dijk CGM, Kuijpers WC, Wortelboer HM, van Helden HPM. Increasing Oxime Efficacy by Blood-Brain Barrier

Modulation. *Toxicology Letters* 2011; 206(1): 67-71. http://dx.doi.org/10.1016/j.toxlet.2011.05.231

207. Kovarik Z, Macek N, Sit RK, Radic Z, Fokin VV, Sharpless KB, Taylor P. Centrally Acting Oximes in Reactivation of Tabun-Phosphoramidated Ache. *Chemico-Biological Interactions* 2013; 203(1): 77-80. http://dx.doi.org/10.1016/j.cbi.2012.08.019
208. Sit RK, Radiç Z, Gerardi V, Zhang L, Garcia E, Katalini-ç M, Amitai G, Kovarik Z, Fokin VV, Sharpless KB, Taylor P. New Structural Scaffolds for Centrally Acting Oxime Reactivators of Phosphylated Cholinesterases. *Journal of Biological Chemistry* 2011; 286(22): 19422-30. http://dx.doi.org/10.1074/jbc.M111.230656
209. DeMar JC, Clarkson ED, Ratcliffe RH, Campbell AJ, Thangavelu SG, Herdman CA, Leader H, Schulz SM, Marek E, Medynets MA, Ku TC, Evans SA, Khan FA, Owens RR, Nambiar MP, Gordon RK. Pro-2-Pam Therapy for Central and Peripheral Cholinesterases. *Chemico-Biological Interactions* 2010; 187(1-3): 191-98. http://dx.doi.org/10.1016/j.cbi.2010.02.015
210. Okolotowicz KJ, Dwyer M, Smith E, Cashman JR. Preclinical Studies of Noncharged Oxime Reactivators for Organophosphate Exposure. *Journal of Biochemical and Molecular Toxicology* 2014; 28(1): 23-31. http://dx.doi.org/10.1002/jbt.21519
211. Chambers JE, Chambers HW, Meek EC, Pringle RB. Testing of Novel Brain-Penetrating Oxime Reactivators of Acetylcholinesterase Inhibited by Nerve Agent Surrogates. *Chemico-Biological Interactions* 2013; 203(1): 135-38. http://dx.doi.org/10.1016/j.cbi.2012.10.017
212. Shih TM, Guarisco JA, Myers TM, Kan RK, McDonough JH. The Oxime Pro-2-Pam Provides Minimal Protection against the Cns Effects of the Nerve Agents Sarin, Cyclosarin, and Vx in Guinea Pigs. *Toxicology Mechanisms*

and Methods 2011; 21(1): 53-62. http://dx.doi.org/10.3109/15376516.2010.529190

213. Raveh L, Grunwald J, Marcus D, Papier Y, Cohen E, Ashani Y. Human Butyrylcholinesterase as a General Prophylactic Antidote for Nerve Agent Toxicity - Intro and in-Vivo Quantitative Characterization. *Biochemical Pharmacology* 1993; 45(12): 2465-74. http://dx.doi.org/10.1016/0006-2952(93)90228-O
214. Sun W, Doctor B, Saxena A. Safety and Pharmacokinetics of Human Serum Butyrylcholinesterase in Guinea Pigs. *Chemico-Biological Interactions* 2005; 157(Sp. Iss. SI): 428-29. http://dx.doi.org/10.1016/j.cbi.2005.10.090
215. Saxena A, Sun W, Luo CY, Doctor BP. Human Serum Butyrylcholinesterase: In Vitro and in Vivo Stability, Pharmacokinetics, and Safety in Mice. *Chemico-Biological Interactions* 2005; 157: 199-203. http://dx.doi.org/10.1016/j.cbi.2005.10.028
216. Rowland M, Tozer TN. Protein Drugs *Clinical Pharmacokinetics and Pharmacodynamics: Concepts and Applications*. 4th ed: Lippincott Williams and Wilkins; 2010. pp 633-62.
217. Vugmeyster Y, Xu X, Theil FP, Khawli LA, Leach MW. Pharmacokinetics and Toxicology of Therapeutic Proteins: Advances and Challenges. *World journal of biological chemistry* 2012; 3(4): 73-92. http://dx.doi.org/10.4331/wjbc.v3.i4.73
218. Rowland M, Tozer TN. Membranes and Distribution *Clinical Pharmacokinetics and Pharmacodynamics: Concepts and Applications*. 4th ed: Lippincott Williams and Wilkins; 2010. pp 73-110.
219. John H, Balszuweit F, Kehe K, Worek F, Thiermann H. Toxicokinetics of Chemical Warfare Agents: Nerve Agents and Vesicants. In: Gupta RC (ed.)

Handbook of Toxicology of Chemical Warfare Agents. 1st ed: Academic Press; 2009. pp 755-90.

220. Mason H. The Recovery of Plasma Cholinesterase and Erythrocyte Acetylcholinesterase Activity in Workers after over-Exposure to Dichlorvos. *Occupational Medicine-Oxford* 2000; 50(5): 343-47. http://dx.doi.org/10.1093/occmed/50.5.343

221. Edmondson PW, Wyburn JR. The Erythrocyte Life-Span, Red Cell Mass and Plasma Volume of Normal Guinea-Pigs as Determined by the Use of ^{51}chromium, ^{32}phosphorus Labelled Di-Iso-Propyl Fluorophosphonate and ^{131}iodine Labelled Human Serum Albumin. *British Journal of Experimental Pathology* 1963; 44(1): 72-80. http://www.ncbi.nlm.nih.gov/pmc/articles/PMC2095176/pdf/brjexppathol00343-0092.pdf

222. Lintern MC, Wetherell JR, Smith ME. Differential Recovery of Acetylcholinesterase in Guinea Pig Muscle and Brain Regions after Soman Treatment. *Human & Experimental Toxicology* 1998; 17(3): 157-62. http://dx.doi.org/10.1177/096032719801700306

223. Langenberg JP, van Dijk C, Sweeney RE, Maxwell DM, Dejong LPA, Benschop HP. Development of a Physiologically Based Model for the Toxicokinetics of C(+/-)P(+/-)-Soman in the Atropinized Guinea Pig. *Archives of Toxicology* 1997; 71(5): 320-31. http://dx.doi.org/10.1007/s002040050393

224. Raveh L, Grauer E, Grunwald J, Cohen E, Ashani Y. The Stoichiometry of Protection against Soman and Vx Toxicity in Monkeys Pretreated with Human Butyrylcholinesterase. *Toxicology and Applied Pharmacology* 1997; 145: 43-53. http://dx.doi.org/10.1006/taap.1997.8160

225. Chu Y, Wang X, Guo J, Li W, Ma X, Zhu Y. Pharmacokinetic Study of Unbound Forsythiaside in Rat Blood and Bile by Microdialysis Coupled with Hplc Method. *European Journal of Drug Metabolism and Pharmacokinetics* 2012; 37(3): 173-77. http://dx.doi.org/10.1007/s13318-012-0084-y

226. Lu C-M, Hou M-L, Lin L-C, Tsai T-H. Development of a Microdialysis System to Monitor Lamivudine in Blood and Liver for the Pharmacokinetic Application in Herbal Drug Interaction and the Gene Expression in Rats. *Journal of Pharmaceutical and Biomedical Analysis* 2014; 96(0): 231-40. http://dx.doi.org/10.1016/j.jpba.2014.04.001

227. Nirogi R, Ajjala DR, Kandikere V, Aleti R, Pantangi HR, Srikakolapu SR, Benade V, Bhyrapuneni G, Vurimindi H. Lc-Ms/Ms Method for the Quantification of Almotriptan in Dialysates: Application to Rat Brain and Blood Microdialysis Study. *Journal of Pharmaceutical and Biomedical Analysis* 2013; 81-82(0): 160-67. http://dx.doi.org/10.1016/j.jpba.2013.04.008

228. Sweeney RE, Langenberg JP, Maxwell DM. A Physiologically Based Pharmacokinetic (Pb/Pk) Model for Multiple Exposure Routes of Soman in Multiple Species. *Archives of Toxicology* 2006; 80(11): 719-31. http://dx.doi.org/10.1007/s00204-006-0114-0

229. Gabrielsson J, Weiner D. Design Elements *Pharmacokinetic & Pharmacodynamic Data Analysis: Concepts and Applications*. 4th ed: Swedish Pharmaceutical Press; 2007. pp 464-90.

230. Rajman I. Pk/Pd Modelling and Simulations: Utility in Drug Development. *Drug Discovery Today* 2008; 13(7-8): 341-46. http://dx.doi.org/10.1016/j.drudis.2008.01.003

231. Derendorf H, Lesko LJ, Chaikin P, Colburn WA, Lee P, Miller R, Powell R, Rhodes G, Stanski D, Venitz J. Pharmacokinetic/Pharmacodynamic Modeling in Drug Research and Development. *Journal of Clinical Pharmacology* 2000; 40(12): 1399-418. http://dx.doi.org/10.1177/009127000004001211

232. Food and Drug Administration. *Guidance for Industry: Exposure-Response Relationships - Study Design, Data Analysis and Regulatory Applications.* Food and Drug Administration, 2003.

233. Aurbek N, Thiermann H, Szinicz L, Eyer P, Worek F. Application of Kinetic-Based Computer Modelling to Evaluate the Efficacy of Hi 6 in Percutaneous Vx Poisoning. *Toxicology* 2006; 224(1-2): 74-80. http://dx.doi.org/10.1016/j.tox.2006.04.031

234. Rowland M, Tozer TN. Constant-Rate Input *Clinical Pharmacokinetics and Pharmacodynamics: Concepts and Applications*. 4th ed: Lippincott Williams and Wilkins; 2010. pp 259-91.

235. Armstrong SJ, Wetherell J, Greig NHs. How Does Physostigmine Work When Used as a Nerve Agent Therapy? In: USAMRICD *Bioscience Review* Hunt Valley, Maryland, USA.; 6th - 10th June 2006.

236. Triggle DJ, Mitchell JM, Filler R. The Pharmacology of Physostigmine. *CNS Drug Reviews* 1998; 4(2): 87-135. http://dx.doi.org/10.1111/j.1527-3458.1998.tb00059.x

237. Men Y, Venitz J. In Vitro Inhibition of Rbc Acetylcholinesterase (Ache) Activity by Physostigmine (Phys), Pyridostigmine (Pyr), and Neostigmine (Neo). *Clinical Pharmacology & Therapeutics* 2002; 71(2): 87. http://dx.doi.org/10.1038/clpt.2002.13

238. Obach RS, Baxter JG, Liston TE, Silber BM, Jones BC, Macintyre F, Rance DJ, Wastall P. The Prediction of Human Pharmacokinetic Parameters from

Preclinical and in Vitro Metabolism Data. *Journal of Pharmacology and Experimental Therapeutics* 1997; 283(1): 46-58. http://jpet.aspetjournals.org/content/283/1/46.abstract

239. Herkert NM, Thiermann H, Worek F. In Vitro Kinetic Interactions of Pyridostigmine, Physostigmine and Soman with Erythrocyte and Muscle Acetylcholinesterase from Different Species. *Toxicology Letters* 2011; 206(1): 41-46. http://dx.doi.org/10.1016/j.toxlet.2011.03.004
240. Dawson RM. Rate Constants of Carbamylation and Decarbamylation of Acetylcholinesterase for Physostigmine and Carbaryl in the Presence of an Oxime. *Neurochemistry International* 1994; 24(2): 173-82. http://dx.doi.org/10.1016/0197-0186(94)90104-X
241. Dawson RM. Oxime Effects on the Rate Constants of Carbamylation and Decarbamylation of Acetylcholinesterase for Pyridostigmine, Physostigmine and Insecticidal Carbamates. *Neurochemistry International* 1995; 26(6): 643-54. http://dx.doi.org/10.1016/0197-0186(94)00161-M
242. Okumura T, Hisaoka T, Yamada A, Naito T, Isonuma H, Okumura S, Miura K, Sakurada M, Maekawa H, Ishimatsu S, Takasu N, Suzuki K. The Tokyo Subway Sarin Attack Lessons Learned. *Toxicology and Applied Pharmacology* 2005; 207(2, Supplement): 471-76. http://dx.doi.org/10.1016/j.taap.2005.02.032
243. Okumura T, Takasu N, Ishimatsu S, Miyanoki S, Mitsuhashi A, Kumada K, Tanaka K, Hinohara S. Report on 640 Victims of the Tokyo Subway Sarin Attack. *Annals of Emergency Medicine* 1996; 28(2): 129-35. http://dx.doi.org/10.1016/S0196-0644(96)70052-5
244. Reiter G, Müller S, Koller M, Thiermann H, Worek F. In Vitro Toxicokinetic Studies of Cyclosarin: Molecular Mechanisms of Elimination. *Toxicology*

Letters 2014; 227(1): 1-11. http://dx.doi.org/10.1016/j.toxlet.2014.03.003

245. De Jong LPA, van Dijk C, Berhitoe D, Benschop HP. Hydrolysis and Binding of a Toxic Stereoisomer of Soman in Plasma and Tissue Homogenates from Rat, Guinea Pig and Marmoset, and in Human Plasma. *Biochemical Pharmacology* 1993; 46(8): 1413-19. http://dx.doi.org/10.1016/0006-2952(93)90106-7
246. Due AH, Trap HC, Langenberg JP, Benschop HP. Toxicokinetics of Soman Stereoisomers after Subcutaneous Administration to Atropinized Guinea-Pigs. *Archives of Toxicology* 1994; 68(1): 60-63. http://dx.doi.org/10.1007/BF03035709
247. Price M, Armstrong S, Mumford H, Wetherell J. *Future Oximes for the Treatment of Nerve Agent Poisoning in the Guinea Pig - 1.* Dstl report number: Unpublished - CR 16309, 2009.
248. Poole SJ, Rudall SR. *Determination of Atropine Doses for Use in Triple Therapy (Containing Hi-6 Dms, Atropine and Avizafone) in in Vivo Efficacy Studies.* Dstl report number: Unpublished - CR59614, 2011.
249. Miles S. *Some Effects of Injection of Atropine Sulphate in Healthy Young Men.* Dstl report number: Unpublished - PTP 514, 1955.
250. Cullumbine H, McKee WHE, Cruickshank JD, Lacon HW, Wybergh JGM. *The Effect of Atropine Sulphate on Military Efficiency.* Dstl report number: Unpublished - PTP 310, 1952.
251. Rowland M, Tozer TN. Prediction and Refinement of Human Kinetics from in Vitro, Preclinical, and Early Clinical Data *Clinical Pharmacokinetics and Pharmacodynamics: Concepts and Applications*. 4th ed: Lippincott Williams and Wilkins; 2010. pp 663-86.

252. Merrill E, Ruark C, Gearhart J, Robinson P. Physiologically Based Pharmacokinetic/Pharmacodynamic Modeling of Countermeasures to Nerve Agents. In: Gupta RC (ed.) *Handbook of Toxicology of Chemical Warfare Agents*. 1st ed. San Diego: Academic Press; 2009. pp 951-64.

253. Sterner TR, Ruark CD, Covington TR, Yu KO, Gearhart JM. A Physiologically Based Pharmacokinetic Model for the Oxime Tmb-4: Simulation of Rodent and Human Data. *Archives of Toxicology* 2013; 87(4): 661-80. http://dx.doi.org/10.1007/s00204-012-0987-z

254. Gueorguieva I, Aarons L, Rowland M. Diazepam Pharamacokinetics from Preclinical to Phase I Using a Bayesian Population Physiologically Based Pharmacokinetic Model with Informative Prior Distributions in Winbugs. *Journal of Pharmacokinetics and Pharmacodynamics* 2006; 33(5): 571-94. http://dx.doi.org/10.1007/s10928-006-9023-3

255. Igari Y, Sugiyama Y, Sawada Y, Iga T, Hanano M. Prediction of Diazepam Disposition in the Rat and Man by a Physiologically Based Pharmacokinetic Model. *Journal of Pharmacokinetics and Biopharmaceutics* 1983; 11(6): 577-93. http://dx.doi.org/10.1007/bf01059058

256. Moriya H, Takagi Y, Nakanishi T, Hayashi M, Tani T, Hirotsu I. Affinity Profiles of Various Muscarinic Antagonists for Cloned Human Muscarinic Acetylcholine Rectepto (Machr) Subtypes and Machrs in Rat Heart and Submandibular Gland. *Life Sciences* 1999; 64(25): 2351 - 58. http://dx.doi.org/10.1016/S0024-3205(99)00188-5

257. Dalton CH, Hattersley IJ, Rutter SJ, Chilcott RP. Absorption of the Nerve Agent Vx (O-Ethyl-S- 2(Di-Isopropylamino)Ethyl Methyl Phosphonothioate) through Pig, Human and Guinea Pig Skin in Vitro. *Toxicology in Vitro* 2006; 20(8): 1532-36. http://dx.doi.org/10.1016/j.tiv.2006.06.009

258. Reiter G, Mikler J, Hill I, Weatherby K, Thiermann H, Worek F. Simultaneous Quantification of Vx and Its Toxic Metabolite in Blood and Plasma Samples and Its Application for in Vivo and in Vitro Toxicological Studies. *Journal of Chromatography B-Analytical Technologies in the Biomedical and Life Sciences* 2011; 879(26): 2704-13. http://dx.doi.org/10.1016/j.jchromb.2011.07.031

259. Parker PJ. Casualty Evacuation Timelines: An Evidence-Based Review. *Journal of the Royal Army Medical Corps* 2007; 153(4): 274-77. http://dx.doi.org/10.1136/jramc-153-04-11

260. North Atlantic Treaty Organization. *Allied Joint Doctrine for Medical Evacuation.* report number: AJMedP-2 (STANAG 2546), 2008. http://nsa.nato.int/nsa/zPublic/ap/ajmedp-2.pdf

261. Eddleston M, Bateman DN. Pesticides. *Medicine* 2007; 35(12): 646-48. http://dx.doi.org/10.1016/j.mpmed.2007.09.020

262. Eddleston M, Buckley NA, Eyer P, Dawson AH. Management of Acute Organophosphorus Pesticide Poisoning. *Lancet* 2008; 371(9612): 597-607. http://dx.doi.org/10.1016/S0140-6736(07)61202-1

263. Eddleston M. The Pathophysiology of Organophosphorus Pesticide Self-Poisoning Is Not So Simple. *The Netherlands Journal of Medicine* 2008; 66(4): 146-48. http://www.njmonline.nl/getpdf.php?id=10000299

264. Kassa J. Review of Oximes in the Antidotal Treatment of Poisoning by Organophosphorus Nerve Agents. *Journal of Toxicology-Clinical Toxicology* 2002; 40(6): 803-16. http://dx.doi.org/10.1081/CLT-120015840

265. Suzuki J, Kohno T, Tsukagosi M, Furuhata T, Yamazaki K. Eighteen Cases Exposed to Sarin in Matsumoto, Japan. *Internal Medicine* 1997; 36(7): 466-70. http://dx.doi.org/10.2169/internalmedicine.36.466

266. Mann T. *Efficacy of Sustained Release Formulations of Therapy Drugs for Percutaneous Poisoning.* Dstl report number: Unpublished - CR 71183, 2013.

267. Armstrong RB, Dmochowski RR, Sand PK, MacDiarmid S. Safety and Tolerability of Extended-Release Oxybutynin Once Daily in Urinary Incontinence: Combined Results from Two Phase 4 Controlled Clinical Trials. *International Urology and Nephrology* 2007; 39(4): 1069-77. http://dx.doi.org/10.1007/s11255-006-9157-7

268. Pavanetto F, Conti B, Giunchedi P, Genta I, Conte U. Polylactide Microspheres for the Controlled-Release of Diazepam. *European Journal of Pharmaceutics and Biopharmaceutics* 1994; 40(1): 27-31.

269. Florea-Spiroiu M, Olteanu M, Stanescu V, Peretz S. Biopolymeric Microcapsules for Controlled Release of Pralidoxime Chloride. *Materiale Plastice* 2009; 46(3): 295-99. http://www.revmaterialeplastice.ro/pdf/FLOREA%20SPIROIU%20M%203.pdf

270. Dixon H, MacNaughton MG. *Sustained Release Therapy for Treating Percutaneous Poisoning.* SwRI® report number: Unpublished - 01 17316, 2013.

271. Mann T, Mumford, Tattersall JEHs. Protecting against Percutaneous Vx Poisoning with Sustained Deliveries of Medical Countermeasures In: *19th Biennial Medical Defense Bioscience Review*, Baltimore, Maryland, USA; 11th - 15th May. 2014

272. Brown RP, Delp MD, Lindstedt SL, Rhomberg LR, Beliles RP. Physiological Parameter Values for Physiologically Based Pharmacokinetic Models. *Toxicology and Industrial Health* 1997; 13(4): 407-84. http://dx.doi.org/10.1177/074823379701300401

273. Lenz DE, Clarkson ED, Schulz SM, Cerasoli DM. Butyrylcholinesterase as a Therapeutic Drug for Protection against Percutaneous Vx. *Chemico-Biological Interactions* 2010; 187(SI): 249-52. http://dx.doi.org/10.1016/j.cbi.2010.05.014

274. Mumford H, Troyer JK. Post-Exposure Therapy with Recombinant Human Buche Following Percutaneous Vx Challenge in Guinea-Pigs. *Toxicology Letters* 2011; 206(1): 29-34. http://dx.doi.org/10.1016/j.toxlet.2011.05.1016

275. Cerasoli DM, Robison CL, D'Ambrozio JA, Nwaneri IY, McDonough JH, Lenz DE, Lumley LA. Pretreatment with Pegylated Protexia Protects against Exposure to the Nerve Agents Vx and Soman. *Society for Neuroscience Abstracts* 2005; 31(337.19). http://www.sfn.org/index.cfm?pagename=abstracts_archive&task=view&controlID=5856&year=2005

276. Allon N, Raveh L, Gilat E, Cohen E, Grunwald J, Ashani Y. Prophylaxis against Soman Inhalation Toxicity in Guinea Pigs by Pretreatment with Human Serum Butyrylcholinesterase. *Toxicological Sciences* 1998; 43(2): 121-28. http://dx.doi.org/10.1006/toxs.1998.2463

277. Castle N, Owen R, Hann M, Clark S, Reeves D, Gurney I. Impact of Chemical, Biological, Radiological, and Nuclear Personal Protective Equipment on the Performance of Low- and High-Dexterity Airway and Vascular Access Skills. *Resuscitation* 2009; 80: 1290-95. http://dx.doi.org/10.1016/j.rescuscitation.2009.08.001

278. Murray DB, Eddleston M, Thomas S, Jefferson RD, Thompson A, Dunn M, Vidler DS, Clutton RE, Blain PG. Rapid and Complete Bioavailability of Antidotes for Organophosphorus Nerve Agent and Cyanide Poisoning in Minipigs after Intraosseous Administration. *Annals of Emergency*

Medicine 2012; 60(4): 424–

30. http://dx.doi.org/10.1016/j.annemergmed.2012.05.013